Publishing House ASV

begell house, inc. publishers

Scientific coordination is carried out by the Russian Academy of Architecture and Construction Sciences (RAACS)

Volume 15 • Issue 4 • 2019

ISSN 2588-0195 (Online)
ISSN 2587-9618 (Print) Continues ISSN 1524-5845

International Journal for

Computational Civil and Structural Engineering

Международный журнал по расчету гражданских и строительных конструкций

http://raasn.ru/public.php

http://ijccse.iasv.ru/

DOI: 10.22337/2587-9618

GICID: 71.0000.1500.2830

EXECUTIVE EDITOR

Vladimir I. Travush,
Full Member of RAACS, Professor, Dr.Sc.,
Vice-President of the Russian Academy
of Architecture and Construction Sciences;
Urban Planning Institute
of Residential and Public Buildings;
24, Ulitsa Bolshaya Dmitrovka, 107031, Moscow, Russia

EDITOR-IN-CHIEF

Vladimir N. Sidorov,
Corresponding Member of RAACS, Professor, Dr.Sc.,
Russian University of Transport (RUT – MIIT);
Russian University of Friendship of Peoples;
Moscow Institute of Architecture (State Academy);
Perm National Research Polytechnic University;
Kielce University of Technology (Poland);
9b9, Obrazcova Street, Moscow, 127994, Russia

EDITORIAL DIRECTOR

Valery I. Telichenko,
Full Member of RAACS, Professor, Dr.Sc.,
The First Vice-President of the Russian Academy
of Architecture and Construction Sciences;
National Research Moscow State University
of Civil Engineering;
24, Ulitsa Bolshaya Dmitrovka, 107031, Moscow, Russia

MANAGING EDITOR

Nadezhda S. Nikitina,
Professor, Ph.D.,
Director of ASV Publishing House;
National Research Moscow State University
of Civil Engineering;
26, Yaroslavskoe Shosse, 129337, Moscow, Russia

ASSOCIATE EDITORS

Pavel A. Akimov,
Full Member of RAACS, Professor, Dr.Sc.,
Executive Scientific Secretary of the Russian Academy
of Architecture and Construction Sciences;
Scientific Research Center "STADYO";
Tomsk State University of Architecture and Building;
Russian University of Friendship of Peoples;
24, Ul. Bolshaya Dmitrovka, 107031, Moscow, Russia

Alexander M. Belostotsky,
Corresponding Member of RAACS, Professor, Dr.Sc.,
Research & Development Center "STADYO";
Russian University of Transport (RUT – MIIT);
Russian University of Friendship of Peoples;
Perm National Research Polytechnic University;
Tomsk State University of Architecture and Building;
Irkutsk National Research Technical University;
8th Floor, 18, ul. Tretya Yamskogo Polya,
125040, Moscow, Russia

Vladimir Belsky, Ph.D.,
Dassault Systèmes Simulia;
1301 Atwood Ave Suite 101W
02919 Johnston, RI, United States

Mikhail Belyi, Professor, Dr.Sc.,
Dassault Systèmes Simulia;
1301 Atwood Ave Suite 101W
02919 Johnston, RI, United States

Vitaly Bulgakov, Professor, Dr.Sc.,
Micro Focus;
Newbury, United Kingdom

Nikolai P. Osmolovskii, Professor, Dr.Sc.,
Systems Research Institute, Polish Academy of
Sciences; Kazimierz Pulaski University
of Technology and Humanities in Radom;
29, ul. Malczewskiego, 26-600, Radom, Poland

Gregory P. Panasenko, Professor, Dr.Sc.,
Equipe d'Analise Numerique; NMR CNRS 5585
University Gean Mehnet;
23 rue. P.Michelon 42023, St.Etienne, France

Leonid A. Rozin, Professor, Dr.Sc.,
Peter the Great Saint-Petersburg
Polytechnic University;
29, Ul. Politechnicheskaya,
195251 Saint-Petersburg, Russia

Scientific coordination is carried out by the Russian Academy of Architecture and Construction Sciences (RAACS)

PUBLISHER

ASV Publishing House
(ООО «Издательство АСВ»)
19/1,12, Yaroslavskoe Shosse, 120338, Moscow, Russia
Tel. +7(925)084-74-24; E-mail: iasv@iasv.ru; Интернет-сайт: http://iasv.ru/

ADVISORY EDITORIAL BOARD

Robert M. Aloyan,
Corresponding Member
of RAACS, Professor, Dr.Sc.,
Russian Academy of Architecture
and Construction Sciences;
24, Ul. Bolshaya Dmitrovka,
107031, Moscow, Russia

Vladimir I. Andreev,
Full Member of RAACS,
Professor, Dr.Sc.,
National Research Moscow State
University of Civil Engineering;
Yaroslavskoe Shosse 26,
Moscow, 129337, Russia

Mojtaba Aslami, Ph.D,
Fasa University; Daneshjou blvd,
Fasa, Fars Province, Iran

Klaus-Jurgen Bathe, Professor
Massachusetts Institute
of Technology;
Cambridge, MA 02139, USA

Yuri M. Bazhenov,
Full Member of RAACS,
Professor, Dr.Sc.,
National Research Moscow State
University of Civil Engineering;
Yaroslavskoe Shosse 26,
Moscow, 129337, Russia

Alexander T. Bekker,
Corresponding Member
of RAACS, Professor, Dr.Sc.,
Far Eastern Federal University;
Russian Academy of Architecture
and Construction Sciences;
8, Sukhanova Street, Vladivostok,
690950, Russia

Tomas Bock, Professor, Dr.-Ing.,
Technical University of Munich,
Arcisstrasse 21, D-80333
Munich, Germany

Jan Buynak, Professor, Ph.D.,
University of Žilina;
1, Univerzitná, Žilina, 010 26,
Slovakia

Evgeniy M. Chernishov,
Full Member of RAACS,
Professor, Dr.Sc.,
Voronezh State Technical
University; 14, Moscow Avenue,
Voronezh, 394026, Russia

Vladimir T. Erofeev,
Full Member of RAACS,
Professor, Dr.Sc.,
Ogarev Mordovia State
University; 68, Bolshevistskaya
Str., Saransk 430005, Republic of
Mordovia, Russia

Victor S. Fedorov,
Full Member of RAACS,
Professor, Dr.Sc.,
Russian University of Transport
(RUT – MIIT);
9b9 Obrazcova Street, Moscow,
127994, Russia

Sergey V. Fedosov,
Full Member of RAACS,
Professor, Dr.Sc.,
Russian Academy of Architecture
and Construction Sciences;
24, Ul. Bolshaya Dmitrovka,
107031, Moscow, Russia

Sergiy Yu. Fialko,
Professor, Dr.Sc.,
Cracow University of
Technology;
24, Warszawska Street, Kraków,
31-155, Poland

Vladimir G. Gagarin,
Corresponding Member
of RAACS, Professor, Dr.Sc.,
Research Institute of Building
Physics of Russian Academy
of Architecture and Construction
Sciences;
21, Lokomotivny Proezd,
Moscow, 127238, Russia

Alexander S. Gorodetsky,
Foreign Member of RAACS,
Professor, Dr.Sc.,
LIRA SAPR Ltd.;
7a Kiyanovsky Side Street
(Pereulok), Kiev, 04053, Ukraine

Vyatcheslav A. Ilyichev,
Full Member of RAACS,
Professor, Dr.Sc.,
Russian Academy of Architecture
and Construction Sciences;
Podzemproekt Ltd.;
24, Ulitsa Bolshaya Dmitrovka,
Moscow, 107031, Russia

Marek Iwański,
Professor, Dr.Sc.,
Kielce University of Technology;
7, al. Tysiąclecia Państwa
Polskiego Kielce, 25 – 314,
Poland

Sergey Yu. Kalashnikov,
Advisor of RAACS,
Professor, Dr.Sc.,
Volgograd State Technical
University; 28, Lenin avenue,
Volgograd, 400005, Russia

Semen S. Kaprielov,
Corresponding Member
of RAACS, Professor, Dr.Sc.,
Research Center of Construction;
6, 2nd Institutskaya St., Moscow,
109428, Russia

Nikolay I. Karpenko,
Full Member of RAACS,
Professor, Dr.Sc.,
Research Institute of Building
Physics of Russian Academy
of Architecture and Construction
Sciences; Russian Academy of
Architecture and Construction
Sciences; 21, Lokomotivny
Proezd, Moscow, 127238, Russia

Vladimir V. Karpov,
Professor, Dr.Sc.,
Saint Petersburg State University
of Architecture and Civil
Engineering;
4, 2-nd Krasnoarmeiskaya Steet,
Saint Petersburg, 190005, Russia

Galina G. Kashevarova,
Corresponding Member
of RAACS, Professor, Dr.Sc.,
Perm National Research
Polytechnic University;
29 Komsomolsky pros., Perm,
Perm Krai, 614990, Russia

John T. Katsikadelis,
Professor, Dr.Eng, PhD, Dr.h.c.,
National Technical University of
Athens; Zografou Campus
9, Iroon Polytechniou str
15780 Zografou, Greece

Vitaly I. Kolchunov,
Full Member of RAACS,
Professor, Dr.Sc.,
Southwest State University;
Russian Academy of Architecture
and Construction Sciences;
94, 50 let Oktyabrya, Kursk,
305040, Russia

Markus König, Professor
Ruhr-Universität Bochum;
150, Universitätsstraße, Bochum,
44801, Germany

Sergey B. Kositsin,
Advisor of RAACS,
Professor, Dr.Sc.,
Russian University of Transport
(RUT – MIIT); 9b9 Obrazcova
Street, Moscow, 127994, Russia

Sergey B. Krylov,
Corresponding Member
of RAACS, Professor, Dr.Sc.,
Research Center of Construction;
6, 2nd Institutskaya St., Moscow,
109428, Russia

Sergey V. Kuznetsov,
Professor, Dr.Sc.,
Ishlinsky Institute for Problems
in Mechanics of the Russian
Academy of Sciences;
101-1, Prosp. Vernadskogo,
Moscow, 119526, Russia

Vladimir V. Lalin,
Professor, Dr.Sc.,
Peter the Great Saint-Petersburg
Polytechnic University;
29, Ul. Politechnicheskaya,
Saint-Petersburg, 195251, Russia

Leonid S. Lyakhovich,
Full Member of RAACS,
Professor, Dr.Sc.,
Tomsk State University
of Architecture and Building;
2, Solyanaya Sq., Tomsk,
634003, Russia

Rashid A. Mangushev,
Corresponding Member
of RAACS, Professor, Dr.Sc.,
Saint Petersburg State University
of Architecture and Civil
Engineering;
4, 2-nd Krasnoarmeiskaya Steet,
Saint Petersburg, 190005, Russia

Ilizar T. Mirsayapov,
Advisor of RAACS,
Professor, Dr.Sc., Kazan State
University of Architecture and
Engineering; 1, Zelenaya Street,
Kazan, 420043, Republic
of Tatarstan, Russia

Vladimir L. Mondrus,
Corresponding Member
of RAACS, Professor, Dr.Sc.,
National Research Moscow State
University of Civil Engineering;
Yaroslavskoe Shosse 26,
Moscow, 129337, Russia

Valery I. Morozov,
Corresponding Member
of RAACS, Professor, Dr.Sc.,
Saint Petersburg State University
of Architecture and Civil
Engineering;
4, 2-nd Krasnoarmeiskaya Steet,
Saint Petersburg, 190005, Russia

Anatoly V. Perelmuter,
Foreign Member of RAACS,
Professor, Dr.Sc., SCAD Soft;
Office 1,2, 3a Osvity street,
Kiev, 03037, Ukraine

Alexey N. Petrov,
Advisor of RAACS, Professor,
Dr.Sc., Petrozavodsk State
University; 33, Lenina Prospect,
Petrozavodsk, 185910,
Republic of Karelia, Russia

Vladilen V. Petrov,
Full Member of RAACS,
Professor, Dr.Sc.,
Yuri Gagarin State Technical
University of Saratov;
77 Politechnicheskaya Street,
Saratov, 410054, Russia

Jerzy Z. Piotrowski,
Professor, Dr.Sc.,
Kielce University of Technology;
al. Tysiąclecia Państwa Polskiego
7, Kielce, 25 – 314, Poland

Chengzhi Qi, Professor, Dr.Sc.,
Beijing University of Civil
Engineering and Architecture;
1, Zhanlanlu, Xicheng District,
Beijing, China

Vladimir P. Selyaev,
Full Member of RAACS,
Professor, Dr.Sc., Ogarev
Mordovia State University;
68, Bolshevistskaya Str., Saransk
430005, Republic of Mordovia,
Russia

Eun Chul Shin,
Professor, Ph.D.,
Incheon National University;
(Songdo-dong)119 Academy-ro,
Yeonsu-gu, Incheon, Korea

D.V. Singh,
Professor, Ph.D,
University of Roorkee;
Roorkee, India, 247667

Wacław Szcześniak,
Foreign Member of RAACS,
Professor, Dr.Sc.,
Lublin University of Technology;
Ul. Nadbystrzycka 40,
20-618 Lublin, Poland

Tadatsugu Tanaka,
Professor, Dr.Sc.,
Tokyo University; 7-3-1 Hongo,
Bunkyo, Tokyo, 113-8654, Japan

Josef Vican,
Professor, Ph.D,
University of Žilina;
1, Univerzitná, Žilina, 010 26,
Slovakia

Zbigniew Wojcicki,
Professor, Dr.Sc.,
Wroclaw University
of Technology;
11 Grunwaldzki Sq., 50-377,
Wrocław, Poland

Artur Zbiciak, Ph.D.,
Warsaw University of
Technology;
Pl. Politechniki 1, 00-661
Warsaw, Poland

Segrey I. Zhavoronok, Ph.D.,
Institute of Applied Mechanics of
Russian Academy of Sciences;
Moscow Aviation Institute
(National Research University);
7, Leningradsky Prt.,
Moscow, 125040, Russia

Askar Zhussupbekov,
Professor, Dr.Sc.,
Eurasian National University;
5, Munaitpassov street, Astana,
010000, Kazakhstan

TECHNICAL EDITOR

Taymuraz B. Kaytukov,
Advisor of RAACS,
Associate Professor, Ph.D.,
Deputy Executive Scientific
Secretary of the Russian
Academy of Architecture and
Construction Sciences;
24, Ul. Bolshaya Dmitrovka,
107031, Moscow, Russia

EDITORIAL TEAM

Vadim K. Akhmetov, Professor, Dr.Sc., National Research Moscow State University of Civil Engineering; 26, Yaroslavskoe Shosse, 129337 Moscow, Russia

Pavel A. Akimov, Full Member of RAACS, Professor, Dr.Sc., Executive Scientific Secretary of the Russian Academy of Architecture and Construction Sciences; Scientific Research Center "STADYO"; Tomsk State University of Architecture and Building; Russian University of Friendship of Peoples; 24, Ul. Bolshaya Dmitrovka, 107031, Moscow, Russia

Alexander M. Belostotsky, Corresponding Member of RAACS, Professor, Dr.Sc., Research & Development Center "STADYO"; Russian University of Transport (RUT – MIIT); Russian University of Friendship of Peoples; Perm National Research Polytechnic University; Tomsk State University of Architecture and Building; Irkutsk National Research Technical University; 8th Floor, 18, ul. Tretya Yamskogo Polya, 125040, Moscow, Russia

Vladimir Belsky, Ph.D., Dassault Systèmes Simulia; 1301 Atwood Ave Suite 101W 02919 Johnston, RI, United States

Mikhail Belyi, Professor, Dr.Sc., Dassault Systèmes Simulia; 1301 Atwood Ave Suite 101W 02919 Johnston, RI, United States

Vitaly Bulgakov, Professor, Dr.Sc., Micro Focus; Newbury, United Kingdom

Charles El Nouty, Professor, Dr.Sc., LAGA Paris-13 Sorbonne Paris Cite; 99 avenue J.B. Clément, 93430 Villetaneuse, France

Natalya N. Fedorova, Professor, Dr.Sc., Novosibirsk State University of Architecture and Civil Engineering (SIBSTRIN); 113 Leningradskaya Street, Novosibirsk, 630008, Russia

Darya Filatova, Professor, Dr.Sc., Probability, Assessment, Reasoning and Inference Studies Research Group, EPHE Laboratoire CHART (PARIS) 4-14, rue Ferrus, 75014 Paris

Vladimir Ya. Gecha, Professor, Dr.Sc., Research and Production Enterprise All-Russia Scientific-Research Institute of Electromechanics with Plant Named after A.G. Iosiphyan; 30, Volnaya Street, Moscow, 105187, Russia

Taymuraz B. Kaytukov, Advisor of RAACS, Ph.D, Deputy Executive Scientific Secretary of the Russian Academy of Architecture and Construction Sciences; 24, Ul. Bolshaya Dmitrovka, 107031, Moscow, Russia

Amirlan A. Kusainov, Foreign Member of RAACS, Professor, Dr.Sc., Kazakh Leading Architectural and Civil Engineering Academy; Kazakh-American University, 9, Toraighyrov Str., Almaty, 050043, Republic of Kazakhstan

Marina L. Mozgaleva, Professor, Dr.Sc., National Research Moscow State University of Civil Engineering; 26, Yaroslavskoe Shosse, 129337 Moscow, Russia

Nadezhda S. Nikitina, Professor, Ph.D., Director of ASV Publishing House; National Research Moscow State University of Civil Engineering; 26, Yaroslavskoe Shosse, 129337 Moscow, Russia

Nikolai P. Osmolovskii, Professor, Dr.Sc., Systems Research Institute Polish Academy of Sciences; Kazimierz Pulaski University of Technology and Humanities in Radom; 29, ul. Malczewskiego, 26-600, Radom, Poland

Gregory P. Panasenko, Professor, Dr.Sc., Equipe d'Analise Numerique NMR CNRS 5585 University Gean Mehnet; 23 rue. P.Michelon 42023, St.Etienne, France

Leonid A. Rozin, Professor, Dr.Sc., Peter the Great Saint-Petersburg Polytechnic University; 29, Ul. Politechnicheskaya, 195251 Saint-Petersburg, Russia

Marina V. Shitikova, Advisor of RAACS, Professor, Dr.Sc., Voronezh State Technical University; 14, Moscow Avenue, Voronezh, 394026, Russia

Igor L. Shubin, Corresponding Member of RAACS, Professor, Dr.Sc., Research Institute of Building Physics of Russian Academy of Architecture and Construction Sciences; 21, Lokomotivny Proezd, Moscow, 127238, Russia

Vladimir N. Sidorov, Corresponding Member of RAACS, Professor, Dr.Sc., Russian University of Transport (RUT – MIIT); Russian University of Friendship of Peoples; Moscow Institute of Architecture (State Academy); Perm National Research Polytechnic University; Kielce University of Technology (Poland); 9b9 Obrazcova Street, Moscow, 127994, Russia

Valery I. Telichenko, Full Member of RAACS, Professor, Dr.Sc., The First Vice-President of the Russian Academy of Architecture and Construction Sciences; National Research Moscow State University of Civil Engineering; 24, Ulitsa Bolshaya Dmitrovka, 107031, Moscow, Russia

Vladimir I. Travush, Full Member of RAACS, Professor, Dr.Sc., Vice-President of the Russian Academy of Architecture and Construction Sciences; Urban Planning Institute of Residential and Public Buildings; 24, Ulitsa Bolshaya Dmitrovka, 107031, Moscow, Russia

INVITED REVIEWERS

Akimbek A. Abdikalikov, Professor, Dr.Sc.,
Kyrgyz State University of Construction, Transport and Architecture n.a. N. Isanov;
34 Maldybayeva Str., Bishkek, 720020, Biskek, Kyrgyzstan

Vladimir N. Alekhin, Advisor of RAACS, Professor, Dr.Sc.,
Ural Federal University named after the first President of Russia B.N. Yeltsin;
19 Mira Street, Ekaterinburg, 620002, Russia

Irina N. Afanasyeva, Ph.D.,
University of Florida; Gainesville, FL 32611, USA

Ján Čelko, Professor, PhD, Ing.,
University of Žilina; Univerzitná 1, 010 26, Žilina, Slovakia

Tatyana L. Dmitrieva, Professor, Dr.Sc.,
Irkutsk National Research Technical University; 83, Lermontov street, Irkutsk, 664074, Russia

Petr P. Gaidzhurov, Advisor of RAACS, Professor, Dr.Sc.,
Don State Technical University; 1, Gagarina Square, Rostov-on-Don, 344000, Russia

Jacek Grosel, Associate Professor, Dr inz.
Wroclaw University of Technology; 11 Grunwaldzki Sq., 50-377, Wrocław, Poland

Stanislaw Jemioło, Professor, Dr.Sc.,
Warsaw University of Technology; 1, Pl. Politechniki, 00-661, Warsaw, Poland

Konstantin I. Khenokh, M.Ing., M.Sc.,
General Dynamics C4 Systems; 8201 E McDowell Rd, Scottsdale, AZ 85257, USA

Christian Koch, Dr.-Ing.,
Ruhr-Universität Bochum;
Lehrstuhl für Informatik im Bauwesen, Gebäude IA, 44780, Bochum, Germany

Gaik A. Manuylov, Professor, Ph.D.,
Moscow State University of Railway Engineering; 9, Obraztsova Street, Moscow, 127994, Russia

Alexander S. Noskov, Professor, Dr.Sc.,
Ural Federal University named after the first President of Russia B.N. Yeltsin;
19 Mira Street, Ekaterinburg, 620002, Russia

Grzegorz Świt, Professor, Dr.hab. Inż.,
Kielce University of Technology; 7, al. Tysiąclecia Państwa Polskiego, Kielce, 25 – 314, Poland

AIMS AND SCOPE

The aim of the Journal is to advance the research and practice in structural engineering through the application of computational methods. The Journal will publish original papers and educational articles of general value to the field that will bridge the gap between high-performance construction materials, large-scale engineering systems and advanced methods of analysis.

The scope of the Journal includes papers on computer methods in the areas of structural engineering, civil engineering materials and problems concerned with multiple physical processes interacting at multiple spatial and temporal scales. The Journal is intended to be of interest and use to researches and practitioners in academic, governmental and industrial communities.

ОБЩАЯ ИНФОРМАЦИЯ О ЖУРНАЛЕ

International Journal for Computational Civil and Structural Engineering

(Международный журнал по расчету гражданских и строительных конструкций)

Международный научный журнал "International Journal for Computational Civil and Structural Engineering (Международный журнал по расчету гражданских и строительных конструкций)" (IJCCSE) является ведущим научным периодическим изданием по направлению «Инженерные и технические науки», издаваемым, начиная с 1999 года (ISSN 2588-0195 (Online); ISSN 2587-9618 (Print) Continues ISSN 1524-5845). В журнале на высоком научно-техническом уровне рассматриваются проблемы численного и компьютерного моделирования в строительстве, актуальные вопросы разработки, исследования, развития, верификации, апробации и приложений численных, численно-аналитических методов, программно-алгоритмического обеспечения и выполнения автоматизированного проектирования, мониторинга и комплексного наукоемкого расчетно-теоретического и экспериментального обоснования напряженно-деформированного (и иного) состояния, прочности, устойчивости, надежности и безопасности ответственных объектов гражданского и промышленного строительства, энергетики, машиностроения, транспорта, биотехнологий и других высокотехнологичных отраслей.

В редакционный совет журнала входят известные российские и зарубежные деятели науки и техники (в том числе академики, члены-корреспонденты, иностранные члены, почетные члены и советники Российской академии архитектуры и строительных наук). Основной критерий отбора статей для публикации в журнале − их высокий научный уровень, соответствие которому определяется в ходе высококвалифицированного рецензирования и объективной экспертизы, поступающих в редакцию материалов.

Журнал входит в Перечень ВАК РФ ведущих рецензируемых научных изданий, в которых должны быть опубликованы основные научные результаты диссертаций на соискание ученой степени кандидата наук, на соискание ученой степени доктора наук по научным специальностям и соответствующим им отраслям науки:

- 01.02.04 – Механика деформируемого твердого тела (технические науки),
- 05.13.18 – Математическое моделирование численные методы и комплексы программ (технические науки),
- 05.23.01 – Строительные конструкции, здания и сооружения (технические науки),
- 05.23.02 – Основания и фундаменты, подземные сооружения (технические науки),
- 05.23.05 – Строительные материалы и изделия (технические науки),
- 05.23.07 – Гидротехническое строительство (технические науки),
- 05.23.17 – Строительная механика (технические науки).

В Российской Федерации журнал индексируется Российским индексом научного цитирования (РИНЦ).

Журнал входит в базу данных Russian Science Citation Index (RSCI), полностью интегрированную с платформой Web of Science. Журнал имеет международный статус и высылается в ведущие библиотеки и научные организации мира.

Издатели журнала – *Издательство Ассоциации строительных высших учебных заведений /АСВ/* (Россия, г. Москва) и до 2017 года *Издательский дом Begell House Inc.* (США, г. Нью-Йорк). Официальными партнерами издания является *Российская академия архитектуры и строительных наук* (*РААСН*), осуществляющая научное курирование издания, и *Научно-исследовательский центр СтаДиО* (ЗАО НИЦ СтаДиО).

Цели журнала – демонстрировать в публикациях российскому и международному профессиональному сообществу новейшие достижения науки в области вычислительных ме-

тодов решения фундаментальных и прикладных технических задач, прежде всего в области строительства.

Задачи журнала:

- предоставление российским и зарубежным ученым и специалистам возможности публиковать результаты своих исследований;
- привлечение внимания к наиболее актуальным, перспективным, прорывным и интересным направлениям развития и приложений численных и численно-аналитических методов решения фундаментальных и прикладных технических задач, совершенствования технологий математического, компьютерного моделирования, разработки и верификации реализующего программно-алгоритмического обеспечения;
- обеспечение обмена мнениями между исследователями из разных регионов и государств.

Тематика журнала. К рассмотрению и публикации в журнале принимаются аналитические материалы, научные статьи, обзоры, рецензии и отзывы на научные публикации по фундаментальным и прикладным вопросам технических наук, прежде всего в области строительства. В журнале также публикуются информационные материалы, освещающие научные мероприятия и передовые достижения Российской академии архитектуры и строительных наук, научно-образовательных и проектно-конструкторских организаций.

Тематика статей, принимаемых к публикации в журнале, соответствует его названию и охватывает направления научных исследований в области разработки, исследования и приложений численных и численно-аналитических методов, программного обеспечения, технологий компьютерного моделирования в решении прикладных задач в области строительства, а также соответствующие профильные специальности, представленные в диссертационных советах профильных образовательных организациях высшего образования.

Редакционная политика. Политика редакционной коллегии журнала базируется на современных юридических требованиях в отношении авторского права, законности, плагиата и клеветы, изложенных в законодательстве Российской Федерации, и этических принципах, поддерживаемых сообществом ведущих издателей научной периодики.

За публикацию статей плата с авторов не взымается. Публикация статей в журнале бесплатная. На платной основе в журнале могут быть опубликованы материалы рекламного характера, имеющие прямое отношение к тематике журнала.

Журнал предоставляет непосредственный открытый доступ к своему контенту, исходя из следующего принципа: свободный открытый доступ к результатам исследований способствует увеличению глобального обмена знаниями.

Индексирование. Публикации в журнале входят в системы расчетов индексов цитирования авторов и журналов. «Индекс цитирования» — числовой показатель, характеризующий значимость данной статьи и вычисляющийся на основе последующих публикаций, ссылающихся на данную работу.

Авторам. Прежде чем направить статью в редакцию журнала, авторам следует ознакомиться со всеми материалами, размещенными в разделах сайта журнала (интернет-сайт Российской академии архитектуры и строительных наук (http://raasn.ru); подраздел «Издания РААСН» или интернет-сайт Издательства АСВ (http://iasv.ru); подраздел «Журнал IJCCSE»): с основной информацией о журнале, его целями и задачами, составом редакционной коллегии и редакционного совета, редакционной политикой, порядком рецензирования направляемых в журнал статей, сведениями о соблюдении редакционной этики, о политике авторского права и лицензирования, о представлении журнала в информационных системах (индексировании), информацией о подписке на журнал, контактными данными и пр. Журнал рабо-

тает по лицензии Creative Commons типа cc by-nc-sa (Attribution Non-Commercial Share Alike) – Лицензия «С указанием авторства – Некоммерческая – Копилефт».

Рецензирование. Все научные статьи, поступившие в редакцию журнала, проходят обязательное двойное слепое рецензирование (рецензент не знает авторов рукописи, авторы рукописи не знаю рецензентов).

Заимствования и плагиат. Редакционная коллегия журнала при рассмотрении статьи проводит проверку материала с помощью системы «Антиплагиат». В случае обнаружения многочисленных заимствований редакция действует в соответствии с правилами COPE.

Подписка. Журнал зарегистрирован в Федеральном агентстве по средствам массовой информации и охраны культурного наследия Российской Федерации. Индекс в общероссийском каталоге РОСПЕЧАТЬ − 18076.

По вопросам подписки на международный научный журнал “International Journal for Computational Civil and Structural Engineering (Международный журнал по расчету гражданских и строительных конструкций)” обращайтесь в Агентство «Роспечать» (Официальный сайт в сети Интернет: http://www.rosp.ru/) или в издательство Ассоциации строительных вузов (АСВ) в соответствии со следующими контактными данными:

ООО «Издательство АСВ»

Юридический адрес: 129337, Россия, г. Москва, Ярославское ш., д. 26, офис 705;

Фактический адрес: 129337, Россия, г. Москва, Ярославское ш., д. 19, корп. 1, 5 этаж, офис 12 (ТЦ Соле Молл);

Телефоны: +7 (925) 084-74-24, +7 (926) 010-91-33;

Интернет-сайт: www.iasv.ru. Адрес электронной почты: iasv@iasv.ru.

Контактная информация. По всем вопросам работы редакции, рецензирования, согласования правки текстов и публикации статей следует обращаться к главному редактору журнала члену-корреспонденту РААСН *Сидорову Владимиру Николаевичу* (адреса электронной почты: sidorov.vladimir@gmail.com, sidorov@iasv.ru, iasv@iasv.ru, sidorov@raasn.ru) или к техническому редактору журнала советнику РААСН *Кайтукову Таймуразу Батразовичу* (адреса электронной почты: tkaytukov@gmail.com; kaytukov@raasn.ru). Кроме того, по указанным вопросам, а также по вопросам размещения в журнале рекламных материалов можно обращаться к генеральному директору ООО «Издательство АСВ» *Никитиной Надежде Сергеевне* (адреса электронной почты: iasv@iasv.ru, nsnikitina@mail.ru, ijccse@iasv.ru).

Журнал становится технологичнее. Издательство АСВ с сентября 2016 года является членом Международной ассоциации издателей научной литературы (Publishers International Linking Association (PILA)), осуществляющей свою деятельность на платформе CrossRef. Оригинальным статьям, публикуемым в журнале, будут присваиваться уникальные номера (индексы DOI – Digital Object Identifier), что значительно облегчит поиск метаданных и местонахождение полнотекстового произведения. DOI – это система определения научного контента в сети Интернет.

С октября 2016 года стал возможен прием статей на рассмотрение и рецензирование через онлайн систему приема статей Open Journal Systems на сайте журнала (электронная редакция): http://ijccse.iasv.ru/index.php/IJCCSE.

Автор имеет возможность следить за продвижением статьи в редакции журнала в личном кабинете Open Journal Systems и получать соответствующие уведомления по электронной почте.

В феврале 2018 года журнал был зарегистрирован в Directory of open access journals (DOAJ) (это один из самых известных поисковых сервисов в мире, который предоставляет открытый доступ к материалам и индексирует не только заголовки журналов, но и научные статьи), в сентябре 2018 года включен в продукты EBSCO Publishing.

International Journal for
Computational Civil and Structural Engineering
(Международный журнал по расчету гражданских и строительных конструкций)
Volume 15, Issue 4 ***2019***

Scientific coordination is carried out by the Russian Academy of Architecture and Construction Sciences (RAACS)

CONTENTS

About "Legitimization" of Numerical Modelling of Wind Impacts on Buildings and Structures in Design Codes 14
Alexander M. Belostotsky, Pavel A. Akimov, Irina N. Afanasyeva

Stability of Three-Layer Rods with Allowance for Initial Imperfections and Shear Deformation 25
Viacheslav S. Chepurnenko, Batyr M. Yazyev

The Analysis of Thermal Properties of a Wall Fragment Made with 3D Construction Technology 34
Valery A. Ezersky, Pavel V. Monastyrev , Ivan A. Ivanov

Multi-Agent Simulation for Self-Healing Mechanisms of Damaged Geotechnical Structures 48
Darya Filatova

Optimization of Simply Supported Castellated I-Beams Loaded by a Uniformly Distributed Load 58
Oleg S. Goryachevskiy

The Second Stage of Stressed-Deformed Condition of Reinforced Concrete Structures When Turning with Bending (Case 2) 66
Vladimir I. Kolchunov, Aleksey I. Demyanov, Nikolay V. Naumov

Analysis of Combined Plates With Allowance for Contact With Elastic Foundation 83
Elena B. Koreneva

Assessment Criteria of Optimal Solutions for Creation of Rods With Piecewise Constant Cross-Sections With Stability Constraints or Constraints for Value of the First Natural Frequency Part 1: Theoretical Foundations 88
Leonid S. Lyakhovich, Pavel A. Akimov, Boris A. Tukhfatullin

Assessment Criteria of Optimal Solutions for Creation of Rods With Piecewise Constant Cross-Sections With Stability Constraints or Constraints for Value of the First Natural Frequency Part 2: Numerical Examples 101
Leonid S. Lyakhovich, Pavel A. Akimov, Boris A. Tukhfatullin

Modelling of Blast Effects on Underground Structure 111
Oleg V. Mkrtychev, Anton Y. Savenkov

Superelement Simulation Technique of Dynamics for Large-Size System "Base – Reinforced Concrete Structures – Metal Structures". Verification and Approbation 123
Alexander I. Nagibovich

Solution of the Problem of Thermoelasticity for Nonlinear Elastic Inhomogeneous Thick-Wall Cylindrical Shell 133
Lyudmila S. Polyakova, Vladimir I. Andreev

Design and Construction of Footings of Buildings and Structures on Permafrost Soils in Conjunction With Environmental Requirements 143
Igor I. Sakharov, Nadezda S. Nikitina, S. Nyamdorzh, E.S. Shin

Determination of Strain-Stress Parameters of a Multi-Storey Reinforced Concrete Building on an Elastic Foundation With Allowance for Different Resistance of Materials and Cracking 150
Alexander A. Treschev, Victor G. Telichko, Nikita V. Zolotov

Stress-Strain Relation for Concrete in Nonuniform Tension 164
Michael L. Zak

International Journal for
Computational Civil and Structural Engineering
(Международный журнал по расчету гражданских и строительных конструкций)
Volume 15, Issue 4 ***2019***

Scientific coordination is carried out by the Russian Academy of Architecture and Construction Sciences (RAACS)

СОДЕРЖАНИЕ

О «легитимизации» в строительных нормах и правилах численного моделирования ветровых воздействий на здания и сооружения 14
А.М. Белостоцкий, П.А. Акимов, И.Н. Афанасьева

Устойчивость трехслойных стержней при ползучести с учетом начальных несовершеств и деформаций сдвига 25
В.С. Чепурненко, Б.М. Язьев

Анализ теплотехнических качеств фрагмета стены здания, возводимого в 3D технологии 34
В.А. Езерский, П.В. Монастырев, И.А. Иванов

Многоагентное моделирование механизмов самовосстановления поврежденных геотехнических сред 48
Д. Филатова

Оптимизация свободно опертых развитых двутавров, нагруженных равномерно распределенной нагрузкой 58
О.С. Горячевский

Вторая стадия напряженно-деформированного состояния железобетонных конструкций при кручении с изгибом (Случай 2) 66
Вл.И. Колчунов, А.И. Демьянов, Н.В. Наумов

Расчет комбинированных плит с учетом их контакта с упругим основанием 83
Е.Б. Коренева

Критерии оценки оптимальных решений при формировании стержней с кусочно-постоянным изменением поперечных сечений при органичениях по устойчивости или на величину первой собственной частоты. Часть 1: Теоретические основы 88
Л.С. Ляхович, П.А. Акимов, Б.А. Тухфатуллин

Критерии оценки оптимальных решений при формировании стержней с кусочно-постоянным изменением поперечных сечений при органичениях по устойчивости или на величину первой собственной частоты. Часть 2: Примеры расчета 101
Л.С. Ляхович, П.А. Акимов, Б.А. Тухфатуллин

Моделирование воздействия ударной волны на подземное сооружение 111
О.В. Мкртычев, А.Ю. Савенков

Методика суперэлементного моделирования динамики большеразмерных систем «основание – железобетонные конструкции – металлические конструкции». Верификация и апробация 123
А.И. Нагибович

Решение задачи термоупругости для нелинейно неоднородной толстостенной цилиндрической оболочки
Л.С. Полякова, В.И. Андреев 133

Проектирование и строительство фундаментов зданий и сооружений на вечномерзлых грунтах в увязке с требованиями экологии 143
И.И. Сахаров, Н.С. Никитина, С. Нямдорж, Е.С. Шин

Определение параметров напряженно-деформированного состояния многоэтажного железобетонного здания на упругом основании с учетом разносопротивляемости и трещинообразования 150
А.А. Трещев, В.Г. Теличко, Н.В. Золотов

Соотношение «напряжения – деформации» для бетона при неоднородном растяжении 164
М.Л. Зак

DOI:10.22337/2587-9618-2019-15-4-14-24

ABOUT "LEGITIMIZATION" OF NUMERICAL MODELLING OF WIND IMPACTS ON BUILDINGS AND STRUCTURES IN DESIGN CODES

Alexander M. Belostotsky [1, 2, 3, 4, 5, 6]***, Pavel A. Akimov*** [1, 2, 3, 7]***, Irina N. Afanasyeva*** [1, 8]

[1] Scientific Research Center "StaDyO", Moscow, RUSSIA
[2] Tomsk State University of Architecture and Civil Engineering, Tomsk, RUSSIA
[3] Peoples' Friendship University of Russia, Moscow, RUSSIA
[4] Russian University of Transport (MIIT), Moscow, RUSSIA
[5] Perm National Research Polytechnic University, Perm, RUSSIA
[6] Irkutsk National Research Technical University, Irkutsk, RUSSIA
[7] Russian Academy of Architecture and Building Sciences, Moscow, RUSSIA
[8] University of Florida, Gainesville, USA

Abstract: The distinctive paper is detoded to problem of "legitimization" of numerical modelling of wind loads and impacts on buildings and structures. General information about computational fluid dynamics (CFD) and its development prospects is presented. The main advantages and disadvantages of numerical simulation compared with tests in wind tunnels (wind tunnel tests) are considered. Besides, information about the second modification of corresponding Russian design codes (SP 20.13330.2016 "SNiP 2.01.07-85* Loads and effects") is provided. Prospects for the further development of numerical modelling and its applications for solution of problems of construction aerodynamics are given.

Keywords: numerical modelling, wind loads, wind impacts, wind tunnels, construction aerodynamics, computational fluid dynamics, design codes

О «ЛЕГИТИМИЗАЦИИ» В СТРОИТЕЛЬНЫХ НОРМАХ И ПРАВИЛАХ ЧИСЛЕННОГО МОДЕЛИРОВАНИЯ ВЕТРОВЫХ ВОЗДЕЙСТВИЙ НА ЗДАНИЯ И СООРУЖЕНИЯ

А.М. Белостоцкий [1, 2, 3, 4, 5, 6]***, П.А. Акимов*** [1, 2, 3, 7]***, И.Н. Афанасьева*** [1, 8]

[1] Научно-исследовательский центр СтаДиО, г. Москва, РОССИЯ
[2] Томский государственный архитектурно-строительный университет, г. Томск, РОССИЯ
[3] Российский университет дружбы народов, г. Москва, РОССИЯ
[4] Российский университет транспорта (МИИТ), г. Москва, РОССИЯ
[5] Пермский национальный исследовательский политехнический университет, г. Пермь, РОССИЯ
[6] Иркутский национальный исследовательский технический университет, г. Иркутск, РОССИЯ
[7] Российская академия архитектуры и строительных наук, г. Москва, РОССИЯ
[8] Университет Флориды, г. Гейнсвилл, США

Аннотация: Настоящая статья посвящена актуальным вопросам, связанным с «легитимизацией» численного моделирования ветровых нагрузок и воздействий. В работе приводятся некоторые общие сведения о развитии методов вычислительной аэродинамики и их приложений в строительной сфере. Рассмотрены основные преимущества и недостатки численного моделирования по сравнению с испытаниями в аэродинамических трубах. Кроме того, приведены сведения об изменении №2 свода правил (СП) 20.13330.2016 «СНиП 2.01.07-85* Нагрузки и воздействия». В заключение указаны перспективы дальнейшего развития численного моделирования для решения задач строительной аэродинамики.

Ключевые слова: численное моделирование, ветровые нагрузки, ветровые воздействия, аэродинамические трубы, строительная аэродинамика, вычислительная аэрогидродинамика, строительные нормы и правила

1. GENERAL INFORMATION

Analysis and design of unique buildings, structures and complexes is traditionally complicated, in particular, by the fact that the current design codes do not contain recommendations on the determination of values of aerodynamic coefficients for original in shape and large-sized construction objects (including majority of high-rise buildings) [1-8]. In addition to the substantially approximate nature of the corresponding engineering approaches, both Russian and a number of foreign design codes do not consider options for the location of such buildings and structures in buildings and the interference of buildings and structures. In other words, these approaches are suitable only for buildings and structures with a relatively simple shape, low and medium height, located in conditions of sparse development. For unique buildings, structures and complexes (especially located in conditions of relatively dense development) more accurate (refined, high-presicion) methods are needed. In such cases, in Russian and some foreign design codes it was proposed to use the results of tests of large-scale models in specialized wind tunnels, allowing reproducing the atmospheric boundary layer. At the same time, in accordance with numerous research works of Russian and foreign scientists published in recent years, it was noted that computational fluid dynamics (CFD) [1], which has been developing rapidly in recent decades, in the future can be considered as an effective alternative of tests in wind tunnels for solution of problems of determination of wind loads and impacts on buildings and structures, assessment of pedestrian comfort and analysis of air pollution. A certain confidence in such assessments was also given by the continuous rapid development of corresponding hardware and software.

Application of methods of computational aerodynamics methods (numerical modeling) allows researcher obtaining results with an accuracy equal to or greater than accuracy, provided by tests in wind tunnels, associated, as a rule, with the need to attract significant resources (including financial resources). Corresponding modern software is characterized by advanced user interface, powerful and convenient preprocessor and postprocessor, sophisticated tools for monitoring and analysis of results.

2. THE MAIN ADVANTAGES OF NUMERICAL SIMULATION IN COMPARISON WITH TESTS IN WIND TUNNELS

2.1. Automatic determination of computational parameters at specified subdomains of the computational domain.

As is known, when testing in a wind tunnel, it is necessary to place measuring equipment to determine the wind speed at a specific point. Application of methods of computational aerodynamics methods allows computing of velocity values within numerical modelling.

2.2. The relative simplicity of making changes to design solutions.

The software that implements the methods of computational aerodynamics allows efficient interaction with CAD applications; modifications of design solutions can be introduced as soon as possible. Obviously, within physical modelling, the same changes are associated with significantly larger time and labor costs, especially in situations when changes to design solutions are made after a considerable time and after the initial tests in wind tunnel or in conditions when the corresponding wind tunnel is busy in other projects.

2.3. Economic efficiency.

Application of method of computational aerodynamics is normally associated with significantly lower financial costs and time expenditures in comparison to conducting tests in wind tunnels.

2.4. Visual clarity of results.

Software that implements computational aerodynamics methods allows researcher simply and

clearly visualize corresponding results. Photos of tests in wind tunnels, on the contrary, are not so informative.

2.5. Universality.
It is rather complicated to solve problems dealing with determination of the wind direction, the level of concentration of pollutants, radiation level, etc. by the tests in wind tunnels. Methods of computational aerodynamics are more flexible and therefore more convenient in this connection.

2.6. The disadvantages of wind tunnels.
As is known, testing in wind tunnels requires large-sized expensive equipment, which is produced by a relatively small number of multinational firms and foreign research and educational centers. Numerical modelling can be performed by a large number of firms, research and educational centers, which in many cases have deeper and more reliable values dealing with the meteorological situation in the construction area.

3. THE MAIN DISADVANTAGES OF NUMERICAL SIMULATION IN COMPARISON WITH TESTS IN WIND TUNNELS

3.1. Lack of standard approach status.
Numerical modelling is a relatively new, constantly improving approach to solving the problems of construction aerodynamics, which is currently used, first of all, by advanced scientific and educational centers equipped with sophisticated software.

3.2. Possible inaccuracy of the results.
According to the results of corresponding research works, it was found that the results of numerical modelling in some cases may be incorrect. However, problem areas of the application are quite well known, and the corresponding error of the results, as a rule, are small and uncritical, taking into account the hypotheses introduced on the safe side (it is quite typical for engineering approaches). In addition, multi-parameter verification analysis (accuracy assessments of numerical solutions in comparison with known solutions) and validation analysis (accuracy assessments of computer modelling in comparison with experimental data), including using the results of field measurements and / or wind tunnel tests.

3.3. High qualification requirements for research groups.
Numerous studies of recent years clearly show that the results of knowledge-based modelling carried out by different research groups can vary significantly, even if using the same software. Stages dealing with setting of initial data (in particular, defining parameters specifying the state of the atmosphere), boundary conditions, the choice of an approximation mesh and mathematical models (primarily turbulence models) are of paramount importance. In other words, the results of numerical modelling can be very sensitive with respect to some computational user-defined parameters of the corresponding software. In this regard, the task of development of appropriate methodological recommendations and descriptions of best practices for the application of computational aerodynamics methods in construction is particularly urgent. Besides, the practice of formal use of corresponding software (without deep knowledge of theoretical foundations of corresponding methods and algorithm, without any doubt about the correctness of the results obtained) is extremely dangerous.

3.4. Limitations on the complexity of objects of modelling.
The maximum dimension of the considering type of problems of numerical modelling depends on the productivity and available resources of the used hardware and software. A large wind tunnel is less limited in terms of size and complexity of models. Obviously, this drawback becomes less critical as the computer technology, universal and specialized software improve and develop.

3.5. Higher accuracy of results for less complex objects.

It should be noted that the accuracy of the results of tests in a wind tunnel does not depend on the complexity of the geometry of the considering object. High accuracy of results of numerical modelling, for complex objects requires significant time and computational costs. Moreover, for some approaches to modelling turbulence it is not at all currently achievable.

3.6. A significant amount of computational work associated with computing of pulsating component solutions.

The resulting distribution of the average components of wind loads can be used for a number of practical applications, including solution of problems of pedestrian comfort analysis and air pollution analysis (when the kinetic energy of turbulence is used to analyze wind gusts). The pulsating components of the loads are important for determining the most critical locations and times.

4. THE SECOND MODIFICATION OF CORRESPONDING RUSSIAN DESIGN CODES (SP 20.13330.2016 “SNIP 2.01.07-85 * LOADS AND EFFECTS”)

The second modification of corresponding Russian design codes (SP 20.13330.2016 “SNiP 2.01.07-85 * Loads and effects”) was approved by the order of the Ministry of Construction and Housing and Communal Services of the Russian Federation dated January 28, 2019 No. 49 / pr.

In accordance with the third paragraph of item 11.1.7 [8] of this document [9] we have the revised corresponding text version:

“For structures with increased level of responsibility, which are specified in [1, item 48.1, part 2] or in note 2, as well as in all cases not specified in B.1 (other shapes of structures, reasonable allowance for other directions of the wind flow or components of the total resistance of the body in other directions, the need to take into account the influence of nearby buildings and structures, terrain and similar cases), aerodynamic coefficients are specified in recommendations developed with allowance for item 4.7 and based on the results of

1) physical (experimental) modelling - tests in wind tunnels (appendices “G” and “I”);
2) mathematical (numerical) modelling of wind aerodynamics based on numerical schemes for solution of three-dimensional equations of motion of liquid and gas with adequate turbulence models implemented in modern advanced verified licensed software systems of computational fluid dynamics”.

It should be noted that the link [1] in the citation is the link [10] in this paper.

In accordance to [9], the last paragraph (before the note) of item 11.2 is formulated in the new edition:

“Aerodynamic coefficients and are computed on the basis of the results of model tests of structures in wind tunnels, numerical simulation or taking into account data published in the technical literature. For separate rectangular buildings in plan terms, the values of these coefficients are specified in B.1.17”.

These changes were the result of a corresponding initiative of the authors of the distinctive paper, due to the fact that recent years are associated with a fairly rapid development of computational aerohydrodynamics (computational fluid dynamics (CFD)), modification and refinement of computational technology and steadily increasing perfofmance of computers. Leading foreign research and design organizations have also increasingly begun to combine tests in wind tunnels and “numerical” experiments. In the future, the role of mathematical modelling, as experience in related fields (for example, aerospace engineering) and problems (structural mechanics) shows, will only increase.

5. PROSPECTS FOR THE FURTHER DEVELOPMENT OF NUMERICAL MODELLING FOR SOLUTION OF PROBLEMS OF CONSTRUCTION AERODYNAMICS

In accordance with the recommendations of Russian and foreign researchers, numerical modelling and tests in wind tunnels can be applied for solution of problems of construction aerodynamics. Besides, in the future, the role of numerical modelling, as shown by experience in related fields (for example, aerospace) and problems (structural mechanics)) will only increase. At the same time, high qualification of research team is a necessary condition for obtaining reliable results of numerical modelling.

It should be noted that currently researches in the field of analysis of errors in the results of numerical and physical modelling, sensitivity analysis of results, verification and validation are relevant.

It is necessary to continue the development and updating of design codes and methodological documents based on best practices in the application of methods of computational aerodynamics in the field of construction. It should be noted that such work has so far been done for steady RANS approaches to modelling turbulence based on Reynolds averaged unsteady Navier-Stokes equations, and to a much lesser extent for the large vortex modelling method (LES method). Corresponding research works will have highest priority in the future [11-49].

REFERENCES

1. **Belostotsky A.M., Akimov P.A., Afanasyeva I.N.** Vychislitel'naja ajerodinamika v zadachah stroitel'stva [Computational aerodynamics for problems of construction]. Moscow, ASV Publishing House, 2017, 720 pages.
2. **Popov N.A.** Nacional'noe prilozhenie k EN 1991 Evrokod 1 **[**National Annex to EN 1991 Eurocode 1]. Moscow, JSC Research Center of Construction, Research Institute of Building Constructions (TSNIISK) named after V. A. Koucherenko, 2011, 99 pages.
3. **Popov N.A.** Rekomendacii po utochnennomu dinamicheskomu raschetu zdanij i sooruzhenij na dejstvie pul'sa-cionnoj sostavljajushhej vetrovoj nagruzki [Recommendations on the refined dynamic structural analysis with allowance for effect of the pulsation component of the wind load]. Moscow, Research Institute of Building Constructions (TSNIISK) named after V. A. Koucherenko, 2000, 45 pages.
4. **Popov N.A., Bogachev D.S.** Vozdejstvie vetra na vysotnye zdanija v uslovijah plotnoj gorodskoj zastrojki [The impact of wind on high-rise buildings in dense urban areas]. // *Vestnik of JSC Research Center of Construction*, 2011, No. 3-4, pp. 189-198.
5. **Popov N.A., Lebedeva I.V.** Izmenenie №1 k SP 20.13330.2011 “Nagruzki i vozdejstvija”, Aktualizirovannoj redakcii SNiP 2.01.07-85 [The first modification to SP 20.13330.2011 “Loads and Impacts”, Updated version of SNiP 2.01.07-85]. // *Structural Mechanics and Analysis of Constructions*, 2014, No. 2(253), pp. 67-70.
6. **Popov N.A., Lebedeva I.V.** Razrabotka nacional'nyh prilozhenij k Evrokodam EN 1990, EN 1991 s uchetom trebovanij rossijskih normativnyh dokumentov [Development of national annexes to Eurocodes EN 1990, EN 1991, with allowance for requirements of the Russian design codes. // *BST: Bulletin of construction equipment*, 2013, No. 2(942), pp. 37-41.
7. **Popov N.A., Lebedeva I.V.** Sravnitel'nyj analiz Evrokodov EN 1991 i aktualizirovannoj redakcii SNiP “Nagruzki i vozdejstvija” [Comparative analysis of Eurocodes EN 1991 and the updated edition of SNiP “Loads and Impacts”]. // *Earthquake engineering. Constructions safety*, 2011, No. 6, pp. 17-21.
8. SP 20.13330.2016 Nagruzki i vozdejstvija. Aktualizirovannaja redakcija SNiP 2.01.07-

85* (s Izmeneniem No. 1) [SP 20.13330.2016 Loads and effects. Updated version of SNiP 2.01.07-85 * (with the First Modification 1). Moscow, JSC “Kodeks”, 2017.
9. Izmenenie No. 2 k SP 20.13330.2016 “SNIP 2.01.07-85* Nagruzki i vozdejstvija” [The Second Modification to SP 20.13330.2016 “SNIP 2.01.07-85* Loads and impacts”]. Approved by order of the Ministry of Construction and Housing and Communal Services of the Russian Federation dated January 28, 2019 No. 49 / pr. Moscow, 2019, 21 pages.
10. Federal'nyj zakon ot 29 dekabrja 2004 g. №190-FZ “Gradostroitel'nyj kodeks Rossijskoj Federacii” [Federal Law of December 29, 2004 No. 190-FZ “Town Planning Code of the Russian Federation”].
11. **Ai Z.T., Mak C.M.** CFD Simulation of Flow and Dispersion Around Anisolated Building: Effect of Inhomogeneous ABL and Near-Wall Treatment. // *Atmos. Environ.*, 2003, Vol. 77, pp. 568-578.
12. **Antipin A.A., Alekhin V.N., Gorodilov S.N., Khramtsov S.V., Noskov A.S.** Numerical Simulation of Wind Loads on High-Rise Buildings. // *19th Australasian Fluid Mechanics Conference*, Melbourne, Australia 8-11 December 2014, 4 pages.
13. **Baker C.J.** Wind Engineering – Past, Present and Future. // *J. Wind Eng. Ind. Aerodyn*., 2007, Vol. 95(9-11), pp. 843-870.
14. **Blocken B.** 50 years of Computational Wind Engineering: Past, present and future. // *J. Wind Eng. Ind. Aerodyn*., 2014, Vol. 129, pp. 69-102.
15. **Blocken B., Carmeliet J.** On the Errors Associated with the Use of Hourly Data in Wind-Driven Rain Calculations on Building Facades. // *Atmos. Environ.*, 2007, Vol. 41 (11), pp. 2335–2343.
16. British Standard, Loadings for Buildings – Part 2: Code of Practice for Wind Loads, Building and Civil Engineering Sector Board, UK, 1995.
17. **Castro I.P., Graham J.M.R.** Numerical Wind Engineering: the Way Ahead? // *Proc. Inst. Civil Eng. – Struct. Build*., 1999, Vol. 134(3), pp. 275-277.
18. **Cochran L., Derickson R.** Aphysical Modeler's View of Computational Wind Engineering. // *J. Wind Eng. Ind. Aerodyn.*, 2011, Vol. 99(4), pp. 139-153.
19. **Cowan, Ian R. Castro, Ian P. Robins, Alan G.** Numerical Considerations for Simulations of Flow and Dispersion around Buildings. // *J. of Wind Eng. and Ind. Aerodynamics*, 1997, Vols. 67 & 68, pp. 535-545.
20. **Davenport A.G.** The Missing Links. // In: *Proceedings of the10th International Conference on Wind Engineering*, Copenhagen, 1999, pp. 3-15.
21. **Di Sabatino S., Buccolieri R., Salizzoni P.** Recent Advancements in Numerical Modelling of Flow and Dispersion in Urban Areas: A Short Review. // *Int. J. Environ. Pollut.*, 2013, Vol. 52(3-4), pp. 172-191.
22. Eurocode 1: Basis design and action on structures. Part 1: “Basis design”. ENV 1991 1, // CEN, 1994, 232 pages.
23. **Ferziger J.H.** Approaches to Turbulent Flow Computation: Applications to Flow over Obstacles. // *J. Wind Eng. Ind. Aerodyn.*, 1990, Vol. 35, pp. 1-19.
24. **Ferziger J.H.** Estimation and Reduction of Numerical Error. // FED vol. 158, In: *Proceedings of the Symposium on Quantification of Uncertainty in Computational Fluid Dynamics*, ASME Fluid Engineering Division, Summer Meeting, Washington DC, June20-24, 1993, pp. 1-8.
25. **Ferziger J.H., Peric M.** Computational Methods for Fluid Dynamics. Springer, Berlin, 1996, 356 pages.
26. **Fothergill C.E., Roberts P.T.** Flow and Dispersion Around Storage Tanks: A Comparison Between Numerical and Wind Tunnel Studies. // *Wind & Structures*, 2002, Vol. 5, No.2-4, pp. 89-100.
27. **Hanna S.R.** Plume Dispersion and Concentration Fluctuations in the Atmosphere. //

Encyclopedia of Environmental Control Technology. Air Pollution Control, 1989, Vol. 2, Gulf Publishing Company, Houston, TX, pp. 547-582.

28. **Hargreaves D.M., Wright N.G.** On the Use of the k–ε Model in Commercial CFD Software to Model the Neutral Atmospheric Boundary Layer. // *J. Wind Eng. Ind. Aerodyn.*, 2007, Vol. 95(5), pp. 355-369.
29. **Hanjalic K.** Will RANS Survive LES? A View of Perspectives. // *J. Fluids Eng. – Trans. ASME*, 2004, Vol. 127(5), pp. 831-839.
30. **Huber A.** Development and applications of CFD simulations in support of air quality studies involving buildings. // *13th Conf. on the App. of Air Poll. Met./5th AWMA Conf. on the Urban Env.*, August 25th, 2004.
31. **Leschziner M.A.** Modelling Engineering Flows with Reynolds Stress Turbulence Closure. // *J. Wind Eng. Ind. Aerodyn.*, 1990, Vol. 35, pp. 21-47.
32. **Leschziner M.A.** Computational Modelling of Complex Turbulent Flow – Expectations, Reality and Prospects. // *J. Wind Eng. Ind. Aerodyn.*, 1993, Vols. 46-47, pp. 37-51.
33. **Leitl B.M., Meroney R.N.** Car Exhaust Dispersion in a Street Canyon. // Numerical Critique of a Wind Tunnel Experiments. // *J.Wind Eng. Ind. Aerodyn.*, 1997, Vols. 67&68, pp. 293-304.
34. **Meroney R.N.** Wind Tunnel and Numerical Simulation of Pollution Dispersion: A Hybrid Approach. // *Paper for Invited Lecture at the Croucher Advanced Study Institute*, Hong Kong University of Science and Technology, 6-10 December 2004.
35. **Murakami S.** Current Status and Future Trends in Computational Wind Engineering. // *J. Wind Eng. Ind. Aerodyn.*, 1997, Vols. 67-68, pp. 3-34.
36. **Mochida A., Iizuka S., Tominaga Y., Lun I.Y.F.** Up-scaling CWE Models to Include Mesoscale Meteorological Influences. // *J. Wind Eng. Ind. Aerodyn.*, 2011, Vol. 99(4), pp. 187-198.
37. **Murakami S.** Numerical Simulation of Turbulent Flow Field around Cubic Model: Current Status and Applications of k–e model and LES. // *J. Wind Eng. Ind. Aerodyn.*, 1990, Vol. 33(1-2), pp. 139-152.
38. **Murakami S., Ooka R., Mochida A.,Yoshida S., Kim S.** CFD Analysis of Wind Climate from Human Scale to Urban Scale. // *J. Wind Eng. Ind. Aerodyn.*, 1999, Vol. 81(1-3), pp. 57-81.
39. **Oberkampf W.L., Trucano T.G., Hirsch C.** Verification, Validation and Predictive Capability in Computational Engineering and Physics. // *Appl. Mech. Rev.*, 2004, Vol. 57(5), pp. 345-384.
40. **Richards P.J., Hoxey R.P.** Appropriate Boundary Conditions for Computational Wind Engineering Models Using the k–ε Turbulence Model. // *J. Wind Eng. Ind. Aerodyn*., 1993, Vols. 46&47, pp. 145-153.
41. **Richards P.J., Norris S.E.** Appropriate Boundary Conditions for Ccomputational Wind Engineering Models Revisited. // *J. Wind Eng. Ind. Aerodyn.*, 2011, Vol. 99(4), pp. 257-266.
42. **Roache P.J.** Quantification of Uncertainty in Computational Fluid Dynamics. // *Annu. Rev. Fluid Mech.*, 1997, Vol. 29, pp. 123-160.
43. **Schatzmann M., Leitl B.** Issues with Validation of Urban flow and Dispersion CFD models. // *J. Wind Eng. Ind. Aerodyn.*, 2011, Vol. 99, pp. 169-186.
44. **Schatzmann M., Rafailidis S., Pavageau M.** Some Remarks on the Validation of Small-Scale Dispersion Models with Field and Laboratory Data. // *J. Wind Eng. Ind. Aerodyn.*, 1997, Vols. 67-68, pp. 885-893.
45. **Stathopoulos T.** Computational Wind Engineering: Past Achievements and Future Challenges. /// *J. Wind Eng. Ind. Aerodyn.*, 1997, Vols. 67-68, pp. 509-532.
46. **Stathopoulos T.** The Numerical Wind Tunnel for Industrial Aerodynamics: Real or Virtual in the New Millennium? // *Wind & Structures*, 2002, Vol. 5, No. 2-4, pp. 193-208.

47. **Tamura T.** Towards Practical Use of LES in Wind Engineering. // *J. Wind Eng. Ind. Aerodyn.*, 2008, Vol. 96(10-11), pp. 1451–1471.
48. **Tominaga Y., Iizuka S., Imano M., Kataoka H., Mochida A., Nozu T., Ono Y., Shirasawa T., Tsuchiya N., Yoshie R.** Cross Comparisons of CFD Results of Wind and Dispersion Fields for MUST Experiment: Evaluation Exercises by AIJ. // *J. Asian Archit. Building Eng.*, 2013, Vol. 12(1), pp. 117-124
49. **Xie Z.-T., Castro I.P.** Efficient Generation of Inflow Conditions for Large Eddy Simulation of Street-Scale Flows. // *Flow, Turbul. Combust.*, 2008, Vol. 81, pp. 449-470.

СПИСОК ЛИТЕРАТУРЫ

1. **Белостоцкий А.М., Акимов П.А., Афанасьева И.Н.** Вычислительная аэродинамика в задачах строительства. – М.: АСВ, 2017. – 720 с.
2. **Попов Н.А.** Национальное приложение к EN 1991 Еврокод 1. ОАО «НИЦ Строительство». – М.: ЦНИИСК им. В.А. Кучеренко, 2011. – 99 с.
3. **Попов Н.А.** Рекомендации по уточненному динамическому расчету зданий и сооружений на действие пульсационной составляющей ветровой нагрузки. Госстрой России. – М.: ГУП ЦНИИСК им. В.А. Кучеренко, 2000. – 45 с.
4. **Попов Н.А., Богачев Д.С.** Воздействие ветра на высотные здания в условиях плотной городской застройки. // *Вестник НИЦ Строительство*, 2011, №3-4, с. 189-198.
5. **Попов Н.А., Лебедева И.В.** Изменение №1 к СП 20.13330.2011 «Нагрузки и воздействия», Актуализированной редакции СНиП 2.01.07-85. // *Строительная механика и расчет сооружений*, 2014, №2(253), с. 67-70.
6. **Попов Н.А., Лебедева И.В.** Разработка национальных приложений к Еврокодам EN 1990, EN 1991 с учетом требований российских нормативных документов. // *БСТ: Бюллетень строительной техники*, 2013, №2(942), с. 37-41.
7. **Попов Н.А., Лебедева И.В.** Сравнительный анализ Еврокодов EN 1991 и актуализированной редакции СНиП «Нагрузки и воздействия». // *Сейсмостойкое строительство. Безопасность сооружений*, 2011, №6, с. 17-21.
8. СП 20.13330.2016 Нагрузки и воздействия. Актуализированная редакция СНиП 2.01.07-85* (с Изменением №1). – М.: АО «Кодекс», 2017.
9. Изменение №2 к СП 20.13330.2016 «СНИП 2.01.07-85* Нагрузки и воздействия». Утверждено приказом Министерства строительства и жилищно-коммунального хозяйства Российской Федерации от 28 января 2019 г. №49/пр. – М., 2019. – 21 с.
10. Федеральный закон от 29 декабря 2004 г. №190-ФЗ «Градостроительный кодекс Российской Федерации».
11. **Ai Z.T., Mak C.M.** CFD Simulation of Flow and Dispersion Around Anisolated Building: Effect of Inhomogeneous ABL and Near-Wall Treatment. // *Atmos. Environ.*, 2003, Vol. 77, pp. 568-578.
12. **Antipin A.A., Alekhin V.N., Gorodilov S.N., Khramtsov S.V., Noskov A.S.** Numerical Simulation of Wind Loads on High-Rise Buildings. // *19th Australasian Fluid Mechanics Conference*, Melbourne, Australia 8-11 December 2014, 4 pages.
13. **Baker C.J.** Wind Engineering – Past, Present and Future. // *J. Wind Eng. Ind. Aerodyn*., 2007, Vol. 95(9-11), pp. 843-870.
14. **Blocken B.** 50 years of Computational Wind Engineering: Past, present and future. // *J. Wind Eng. Ind. Aerodyn*., 2014, Vol. 129, pp. 69-102.
15. **Blocken B., Carmeliet J.** On the Errors Associated with the Use of Hourly Data in Wind-Driven Rain Calculations on Building Facades. // *Atmos. Environ.*, 2007, Vol. 41 (11), pp. 2335–2343.

16. British Standard, Loadings for Buildings – Part 2: Code of Practice for Wind Loads, Building and Civil Engineering Sector Board, UK, 1995.
17. **Castro I.P., Graham J.M.R.** Numerical Wind Engineering: the Way Ahead? // *Proc. Inst. Civil Eng. – Struct. Build*., 1999, Vol. 134(3), pp. 275-277.
18. **Cochran L., Derickson R.** Aphysical Modeler's View of Computational Wind Engineering. // *J. Wind Eng. Ind. Aerodyn.*, 2011, Vol. 99(4), pp. 139-153.
19. **Cowan, Ian R. Castro, Ian P. Robins, Alan G.** Numerical Considerations for Simulations of Flow and Dispersion around Buildings. // *J. of Wind Eng. and Ind. Aerodynamics*, 1997, Vols. 67 & 68, pp. 535-545.
20. **Davenport A.G.** The Missing Links. // In: *Proceedings of the10th International Conference on Wind Engineering*, Copenhagen, 1999, pp. 3-15.
21. **Di Sabatino S., Buccolieri R., Salizzoni P.** Recent Advancements in Numerical Modelling of Flow and Dispersion in Urban Areas: A Short Review. // *Int. J. Environ. Pollut.*, 2013, Vol. 52(3-4), pp. 172-191.
22. Eurocode 1: Basis design and action on structures. Part 1: "Basis design". ENV 1991 1, // CEN, 1994, 232 pages.
23. **Ferziger J.H.** Approaches to Turbulent Flow Computation: Applications to Flow over Obstacles. // *J. Wind Eng. Ind. Aerodyn.*, 1990, Vol. 35, pp. 1-19.
24. **Ferziger J.H.** Estimation and Reduction of Numerical Error. // FED vol. 158, In: *Proceedings of the Symposium on Quantification of Uncertainty in Computational Fluid Dynamics*, ASME Fluid Engineering Division, Summer Meeting, Washington DC, June20-24, 1993, pp. 1-8.
25. **Ferziger J.H., Peric M.** Computational Methods for Fluid Dynamics. Springer, Berlin, 1996, 356 pages.
26. **Fothergill C.E., Roberts P.T.** Flow and Dispersion Around Storage Tanks: A Comparison Between Numerical and Wind Tunnel Studies. // *Wind & Structures*, 2002, Vol. 5, No.2-4, pp. 89-100.
27. **Hanna S.R.** Plume Dispersion and Concentration Fluctuations in the Atmosphere. // *Encyclopedia of Environmental Control Technology. Air Pollution Control*, 1989, Vol. 2, Gulf Publishing Company, Houston, TX, pp. 547-582.
28. **Hargreaves D.M., Wright N.G.** On the Use of the k–ε Model in Commercial CFD Software to Model the Neutral Atmospheric Boundary Layer. // *J. Wind Eng. Ind. Aerodyn.*, 2007, Vol. 95(5), pp. 355-369.
29. **Hanjalic K.** Will RANS Survive LES? A View of Perspectives. // *J. Fluids Eng. – Trans. ASME*, 2004, Vol. 127(5), pp. 831-839.
30. **Huber A.** Development and applications of CFD simulations in support of air quality studies involving buildings. // *13th Conf. on the App. of Air Poll. Met./5th AWMA Conf. on the Urban Env.*, August 25th, 2004.
31. **Leschziner M.A.** Modelling Engineering Flows with Reynolds Stress Turbulence Closure. // *J. Wind Eng. Ind. Aerodyn.*, 1990, Vol. 35, pp. 21-47.
32. **Leschziner M.A.** Computational Modelling of Complex Turbulent Flow – Expectations, Reality and Prospects. // *J. Wind Eng. Ind. Aerodyn.*, 1993, Vols. 46-47, pp. 37-51.
33. **Leitl B.M., Meroney R.N.** Car Exhaust Dispersion in a Street Canyon. // Numerical Critique of a Wind Tunnel Experiments. // *J.Wind Eng. Ind. Aerodyn.*, 1997, Vols. 67&68, pp. 293-304.
34. **Meroney R.N.** Wind Tunnel and Numerical Simulation of Pollution Dispersion: A Hybrid Approach. // *Paper for Invited Lecture at the Croucher Advanced Study Institute*, Hong Kong University of Science and Technology, 6-10 December 2004.
35. **Murakami S.** Current Status and Future Trends in Computational Wind Engineering. // *J. Wind Eng. Ind. Aerodyn.*, 1997, Vols. 67-68, pp. 3-34.
36. **Mochida A., Iizuka S., Tominaga Y., Lun I.Y.F.** Up-scaling CWE Models to Include

Mesoscale Meteorological Influences. // *J. Wind Eng. Ind. Aerodyn.*, 2011, Vol. 99(4), pp. 187-198.

37. **Murakami S.** Numerical Simulation of Turbulent Flow Field around Cubic Model: Current Status and Applications of k–e model and LES. // *J. Wind Eng. Ind. Aerodyn.*, 1990, Vol. 33(1-2), pp. 139-152.
38. **Murakami S., Ooka R., Mochida A.,Yoshida S., Kim S.** CFD Analysis of Wind Climate from Human Scale to Urban Scale. // *J. Wind Eng. Ind. Aerodyn.*, 1999, Vol. 81(1-3), pp. 57-81.
39. **Oberkampf W.L., Trucano T.G., Hirsch C.** Verification, Validation and Predictive Capability in Computational Engineering and Physics. // *Appl. Mech. Rev.*, 2004, Vol. 57(5), pp. 345-384.
40. **Richards P.J., Hoxey R.P.** Appropriate Boundary Conditions for Computational Wind Engineering Models Using the k–ε Turbulence Model. // *J. Wind Eng. Ind. Aerodyn*., 1993, Vols. 46&47, pp. 145-153.
41. **Richards P.J., Norris S.E.** Appropriate Boundary Conditions for Ccomputational Wind Engineering Models Revisited. // *J. Wind Eng. Ind. Aerodyn.*, 2011, Vol. 99(4), pp. 257-266.
42. **Roache P.J.** Quantification of Uncertainty in Computational Fluid Dynamics. // *Annu. Rev. Fluid Mech.*, 1997, Vol. 29, pp. 123-160.
43. **Schatzmann M., Leitl B.** Issues with Validation of Urban flow and Dispersion CFD models. // *J. Wind Eng. Ind. Aerodyn.*, 2011, Vol. 99, pp. 169-186.
44. **Schatzmann M., Rafailidis S., Pavageau M.** Some Remarks on the Validation of Small-Scale Dispersion Models with Field and Laboratory Data. // *J. Wind Eng. Ind. Aerodyn.*, 1997, Vols. 67-68, pp. 885-893.
45. **Stathopoulos T.** Computational Wind Engineering: Past Achievements and Future Challenges. /// *J. Wind Eng. Ind. Aerodyn.*, 1997, Vols. 67-68, pp. 509-532.
46. **Stathopoulos T.** The Numerical Wind Tunnel for Industrial Aerodynamics: Real or Virtual in the New Millennium? // *Wind & Structures*, 2002, Vol. 5, No. 2-4, pp. 193-208.
47. **Tamura T.** Towards Practical Use of LES in Wind Engineering. // *J. Wind Eng. Ind. Aerodyn.*, 2008, Vol. 96(10-11), pp. 1451–1471.
48. **Tominaga Y., Iizuka S., Imano M., Kataoka H., Mochida A., Nozu T., Ono Y., Shirasawa T., Tsuchiya N., Yoshie R.** Cross Comparisons of CFD Results of Wind and Dispersion Fields for MUST Experiment: Evaluation Exercises by AIJ. // *J. Asian Archit. Building Eng.*, 2013, Vol. 12(1), pp. 117-124
49. **Xie Z.-T., Castro I.P.** Efficient Generation of Inflow Conditions for Large Eddy Simulation of Street-Scale Flows. // *Flow, Turbul. Combust.*, 2008, Vol. 81, pp. 449-470.

Alexander M. Belostotsky, Corresponding Member of the Russian Academyof Architecture and Construction Sciences, Professor, Dr.Sc.; Director of Scientific Research Center «StaDyO»; Professor of Department of Structures, Buildings and Facilities, Russian University of Transport» (RUT –MIIT); Professor of Department of Architecture and Construction, Peoples' Friendship University; Professor of Department of Building Structures and Computational Mechanics, Peoples' Friendship University of Russia; Professor of Irkutsk National Research Technical University; office 810, 18, 3ya Ulitsa Yamskogo Polya, Moscow, 125040, Russia; phone +7 (499) 706-88-10;
E-mail: amb@stadyo.ru.

Pavel A. Akimov, Full Member of the Russian Academy of Architecture and Construction Sciences (RAACS), Professor, Dr.Sc.; Executive Scientific Secretary of Russian Academy of Architecture and Construction Sciences; Vice-Director for Science Activities, Scientific Research Center "StaDyO"; Professor of Department of Architecture and Construction, Peoples' Friendship University of Russia; Professor of Department of Structural Mechanics, Tomsk State University of Architecture and Building; 24, Ul. Bolshaya Dmitrovka, 107031, Moscow, Russia;
phone +7(495) 625-71-63; fax: +7 (495) 650-27-31;
E-mail: akimov@raasn.ru, pavel.akimov@gmail.com.

Irina N. Afanasyeva, Ph.D., Senior Engineer of Scientific Research Center "StaDyO"; Master's Degree Student, University of Florida (USA); office 810, 18, 3ya Ulitsa Yamskogo Polya, Moscow, 125040, Russia;

phone +7 (499) 706-88-10,
E-mail: irina.n.afanasyeva@gmail.com.

Белостоцкий Александр Михайлович, член-корреспондент РААСН, профессор, доктор технических наук; генеральный директор ЗАО «Научноисследовательский центр СтаДиО»; профессор кафедры «Строительные конструкции, здания и сооружения» Российского университета транспорта (МИИТ); профессор Департамента архитектуры и строительства Российского университета дружбы народов; профессор кафедры строительных конструкций и вычислительной механики Пермского национального исследовательского политехнического университета; профессор Иркутского национального исследовательского технического университета; 125040, Россия, Москва, ул. 3-я Ямского Поля, д.18, офис 810;
тел. +7 (499) 706-88-10; e-mail: amb@stadyo.ru.

Акимов Павел Алексеевич, академик Российской академии архитектуры и строительных наук (РААСН), профессор, доктор технических наук; главный ученый секретарь Российской академии архитектуры и строительных наук; заместитель генерального директора по науке ЗАО «Научно-исследовательский центр СтаДиО»; профессор Департамента архитектуры и строительства Российского университета дружбы народов; профессор кафедры строительной механики Томского государственного архитектурно-строительного университета; 107031, г. Москва, ул. Большая Дмитровка, д. 24, стр. 1; тел. +7(495) 625-71-63;
факс +7 (495) 650-27-31; E-mail: akimov@raasn.ru,
pavel.akimov@gmail.com.

Афанасьева Ирина Николаевна, кандидат технических наук, ведущий инженер-расчетчик ЗАО «Научно-исследовательский центр СтаДиО» (ЗАО НИЦ «СтаДиО»); магистрант Университета Флориды (США); 125040, Россия, г. Москва, ул. 3-я Ямского Поля, д.18, 8 этаж, офис 810, тел. +7 (495) 706-88-10,
E-mail: irina.n.afanasyeva@gmail.com.

DOI:10.22337/2587-9618-2019-15-4-25-33

STABILITY OF THREE-LAYER RODS WITH ALLOWANCE FOR INITIAL IMPERFECTIONS AND SHEAR DEFORMATIONS

Viacheslav S. Chepurnenko, Batyr M. Yazyev
Don State Technical University, Rostov-on-Don, Russia

Abstract: The article presents the derivation of equations describing the pre-buckling behavior of three-layer rods in the presence of shear deformation and creep of the middle layer. The test problem for a rod with a filler made of polyurethane foam is solved. A technique has been developed for calculating the critical time under loads which values exceed the long critical ones.

Keywords: three-layer beams, stability, shear, creep, numerical methods

УСТОЙЧИВОСТЬ ТРЕХСЛОЙНЫХ СТЕРЖНЕЙ ПРИ ПОЛЗУЧЕСТИ С УЧЕТОМ НАЧАЛЬНЫХ НЕСОВЕРШЕНСТВ И ДЕФОРМАЦИЙ СДВИГА

В.С. Чепурненко, Б.М. Язьев
Донской государственный технический университет, г. Ростов-на-Дону, РОССИЯ

Аннотация: В статье приводится вывод уравнений, описывающих докритическое поведение трёхслойных стержней при наличии сдвиговых деформаций и ползучести среднего слоя. Решается тестовая задача для стержня с заполнителем из пенополиуретана. Разработана методика вычисления критического времени при нагрузках, значения которых превышают длительные критические.

Ключевые слова: трехслойные балки, устойчивость, сдвиг, ползучесть, численные методы

1. INTRODUCTION

When solving the problems of stability of rods, in many cases it is necessary to take into account shear deformations: for example, when considering elements made of anisotropic fibrous materials with a shear modulus significantly smaller than the elastic modulus or when calculating three-layer rods consisting of two thin metal outer layers and a lightweight, much less rigid filler. Taking into account the shear force in deformable elements of this type leads to obtaining lower critical loads than without taking it into account. There is a formula in [1] derived analytically to calculate the critical force, acting on central-compressed three-layer rod. It is important to note that the polymer filler is subjected to creep, accordingly, the actual values of the loads leading to buckling will be lower than those obtained in the book [1], which should be taken into account in the calculations and structural analysis.

2. DERIVATION OF RESOLVING EQUATIONS

We consider the element shown in Figure 1, subject to longitudinal bending. In deriving the equations, we take the Timoshenko's model as a model of rod deformation, which includes shear deformations in the calculations.

In Figure 1 the following notation is accepted: γ_{xz} – shear strain (it is equal to the angle between the plane, normal to the median surface and the cross section plane), φ – the angle of cross section rotation relative to the initial position,

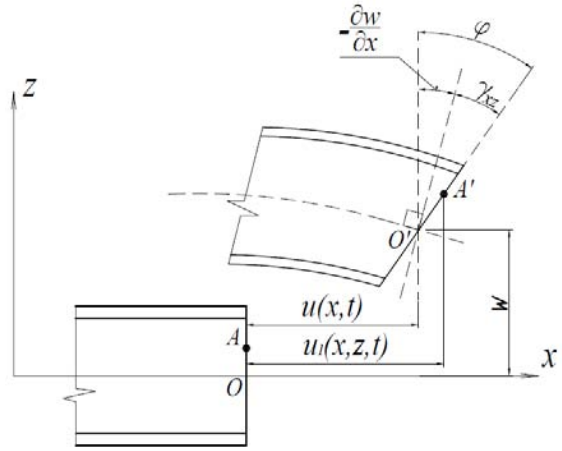


Figure 1. Element of rod subject to longitudinal bending.

$u_1(x,z,t)$ – the displacement of a certain point A of the cross section in the x direction.
As follows from Figure 1:

$$\gamma_{xz} = \varphi + \frac{\partial w}{\partial x}, \quad (1)$$

$$u_1(x,z,t) = u(x,t) + z\varphi(x,t). \quad (2)$$

We take into account the initial imperfection, defined by some function $w_0(x)$, according to the method, mentioned in [2], assuming that the displacements of the points along the z axis are:

$$u_3 = w_0(x) + w(x,t), \quad (3)$$

and then eliminating from the terms of the Green strain tensor components those, that contain only $w_0(x)$, since they correspond only to the initial imperfections, when the stresses in the rod are equal to zero. Neglecting the terms of large order of smallness, we thus obtain:

$$\varepsilon_{11} = \varepsilon_{xx} = \frac{\partial u_1}{\partial x_1} + \frac{1}{2}\left(\frac{\partial u_3}{\partial x_1}\right)^2 = \frac{\partial u}{\partial x} + z\frac{\partial \varphi}{\partial x} + \frac{1}{2}\left(\frac{\partial w}{\partial x}\right)^2 + \frac{\partial w}{\partial x}\frac{\partial w_0}{\partial x}, \quad (4)$$

$$\varepsilon_{xy} = \varepsilon_{xz} = \varepsilon_{yz} = \varepsilon_{zz} = \varepsilon_{yy} = 0, \quad (5)$$

According to the generalized Hooke's law for the isotropic material of filler with creep strain taken into account:

$$\begin{cases} \varepsilon_{xx} = \varepsilon_{xx}^{el} + \varepsilon_{xx}^{*} = \dfrac{1}{E_f}\sigma_{xx} + \varepsilon_{xx}^{*} \\ \gamma_{xz} = \gamma_{xz}^{el} + \gamma_{xz}^{*} = \dfrac{1}{G_f}\sigma_{xz} + \gamma_{xz}^{*} \end{cases}, \quad (6)$$

the symbol «*» indicates creep strain, ε_{xx}^{el}, γ_{xz}^{el} - elastic strains, E_f, G_f – filler characteristics.
We write the expression of the variational principle of the minimum total potential energy [3]:

$$\Pi = \delta(U+V) = \delta U + \delta V = 0, \quad (7)$$

U – potential elastic strain energy, V – external forces potential;

$$\delta U = \int_V (\sigma_{xx}\delta\varepsilon_{xx}^{el} + \sigma_{xz}\delta\gamma_{xz}^{el})dV = \int_V \left(\sigma_{xx}\delta(\varepsilon_{xx} - \varepsilon_{xx}^{*}) + \sigma_{xz}\delta(\gamma_{xz} - \gamma_{xz}^{*})\right)dV = \int_L\int_A (\sigma_{xx}\delta\varepsilon_{xx} + \sigma_{xz}\delta\gamma_{xz})\,dAdx. \quad (8)$$

In equation (8) the variations of creep strains are equal to zero, as is in subsequent numerical calculation step method at a small interval of time Δt the creep strains will depend only on the components of the stress tensor, obtained in the points of the rod in the previous step.
In the case of joint support of the rod (Figure 2), compressed by the force P, with one movable joint in the x direction and one stationary joint, the variation of the external forces potential will be equal to:

$$\delta V = -P\delta u(x=0). \quad (9)$$

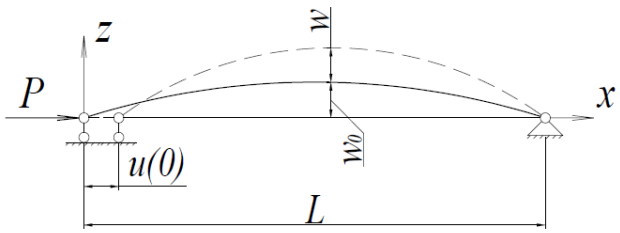


Figure 2. Loading model.

We denote the axial, shear forces and bending moment as:

$$N_x = \int_A \sigma_{xx} dA,\ Q = \int_A \sigma_{xz} dA,\ \ M = \int_A \sigma_{xx} z dA. \quad (10)$$

Substituting in (8) and varying the components of the strains given in (1), (4), we obtain the expression:

$$\delta U = \int_L \Big(N_x \Big(\frac{\partial \delta u}{\partial x} + \frac{\partial \delta w}{\partial x}\frac{\partial w}{\partial x} + \frac{\partial \delta w}{\partial x}\frac{\partial w_0}{\partial x}\Big) + M\frac{\partial \delta \varphi}{\partial x} + Q\Big(\delta\varphi + \frac{\partial \delta w}{\partial x}\Big)\Big) dx \quad (11)$$

Applying integration by parts and grouping the terms with factors $\delta u,\ \delta w,\ \delta\gamma_{xz}$ in expression (11) and substituting it together with (9) in (7), we get the following result:

$$N_x(L)\delta u(L) - (N_x(0)\delta u(0) + P\delta u(0)) + \Big(N_x\frac{\partial w_0}{\partial x} + N_x\frac{\partial w}{\partial x} + Q\Big)\delta w\Big|_0^L + M\delta\varphi\Big|_0^L + \int_L \Big(\Big(-\frac{\partial N_x}{\partial x}\Big)\delta u + \Big(-\frac{\partial}{\partial x}\Big(N_x\Big(\frac{\partial w}{\partial x} + \frac{\partial w_0}{\partial x}\Big)\Big) - \frac{\partial Q}{\partial x}\Big)\delta w + \Big(-\frac{\partial M}{\partial x} + Q\Big)\delta\varphi \Big) dx = 0. \quad (12)$$

In accordance with the main lemma of the variational calculus, we obtain the system:

$$\begin{cases} -\dfrac{\partial N_x}{\partial x} = 0 \\ -\dfrac{\partial}{\partial x}\Big(N_x\Big(\dfrac{\partial w}{\partial x} + \dfrac{\partial w_0}{\partial x}\Big)\Big) - \dfrac{\partial Q}{\partial x} = 0,\ x \in (0; L). \\ -\dfrac{\partial M}{\partial x} + Q = 0 \end{cases} \quad (13)$$

From the fixing conditions for the rod we have:

$$w(0,t) = w(L,t) = u(L,t) = 0 \Rightarrow \delta w(0,t) = \delta w(L,t) = \delta u(L,t) = 0 \quad (14)$$

at an arbitrary point of time. For convenience, we omit the time t during subsequent writing in the notation of time-dependent functions. We get the final set of six boundary conditions:

$$\begin{cases} w(0) = w(L) = u(L) = 0 \\ N_x(0) + P = 0 \\ M(0) = M(L) = 0 \end{cases}, \quad (15)$$

Using dependencies (13), (15), we transform (13) to a system of two differential equations:

$$\begin{cases} P\Big(\dfrac{\partial^2 w}{\partial x^2} + \dfrac{\partial^2 w_0}{\partial x^2}\Big) = \dfrac{\partial Q}{\partial x} \\ Q = \dfrac{\partial M}{\partial x} \end{cases}. \quad (16)$$

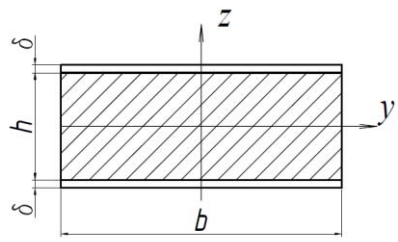


Figure 3. Rod cross section.

We substitute the formulas for strains and Hooke's law (6) in expressions (10) for the stresses, taking into account the cross sectional parameters with the dimensions shown in Fig. 3. We obtain:

$$M = \int_A E(z)(\frac{\partial u}{\partial x} + z\frac{\partial \varphi}{\partial x} + \frac{1}{2}\left(\frac{\partial w}{\partial x}\right)^2 + \\ + \frac{\partial w}{\partial x}\frac{\partial w_0}{\partial x} - \varepsilon_{xx}^*)zdA = \int_A E(z^2\frac{\partial \varphi}{\partial x} - \varepsilon_{xx}^* z)dA = \quad (17)$$
$$= (E_s I_s + E_f I_f)\frac{\partial \varphi}{\partial x} - E_f \int_{A_f} \varepsilon_{xx}^* zdA,$$

E_s – modulus of elasticity of the metal sheathings,

I_s, I_f – moments of inertia of the metal and polymer cross section parts,

$$I_s \approx (h\delta^2 + \frac{\delta h^2}{2})b, \quad I_f = \frac{bh^3}{12}. \quad (18)$$

$$Q = \int_{A_f} \sigma_{xz} dA = \int_{A_f} G_f(\gamma_{xz} - \gamma_{xz}^*)dA = \\ = K_s G_f \gamma_{xz} A_f - G_f \int_{A_f} \gamma_{xz}^* dA. \quad (19)$$

Integration in expression (19) is performed over the filler area due to the insignificant thickness of metal plates that work only on compression, K_s is a coefficient that takes into account the irregular distribution of shear stresses over the section height (It is assumed in the Timoshenko model that γ_{xz} is constant in height). According to [4], the coefficient value for a rectangular section takes the form:

$$K_s = \frac{10(1+\nu_f)}{12+11\nu_f}.$$

For convenience, we introduce the notation for integrals containing components of creep strains:

$$M^* = E_f \int_{A_f} \varepsilon_{xx}^* zdA, \; Q^* = G_f \int_{A_f} \gamma_{xz}^* dA, \quad (20)$$

We substitute (17), (19) into (16), taking into account the previously introduced notation:

$$\begin{cases} P\left(\frac{\partial^2 w}{\partial x^2} + \frac{\partial^2 w_0}{\partial x^2}\right) = K_s G_f A_f \left(\frac{\partial \varphi}{\partial x} + \frac{\partial^2 w}{\partial x^2}\right) - \frac{\partial Q^*}{\partial x} \\ K_s G_f A_f(\varphi + \frac{\partial w}{\partial x}) - Q^* = \\ = (E_s I_s + E_f I_f)\frac{\partial^2 \varphi}{\partial x^2} - \frac{\partial M^*}{\partial x} \end{cases}$$

Transferring all terms with w and φ to the left side of the system and dividing by $K_s G_f A_f$, we obtain the final system of resolving partial differential equations (21):

$$\begin{cases} \frac{\partial^2 w}{\partial x^2}\left(1 - \frac{P}{K_s G_f A_f}\right) + \frac{\partial \varphi}{\partial x} = \frac{P}{K_s G_f A_f}\frac{\partial^2 w_0}{\partial x^2} + \\ + \frac{1}{K_s G_f A_f}\frac{\partial Q^*}{\partial x} \\ \frac{\partial w}{\partial x} + \varphi - \frac{E_s I_s + E_f I_f}{K_s G_f A_f}\frac{\partial^2 \varphi}{\partial x^2} = -\frac{1}{K_s G_f A_f}\frac{\partial M^*}{\partial x} \end{cases} \quad (21)$$

with boundary conditions (22):

$$\begin{cases} w(0) = 0 \\ w(L) = 0 \\ (E_s I_s + E_f I_f)\frac{\partial \varphi}{\partial x}(0) = M^*(0) \\ (E_s I_s + E_f I_f)\frac{\partial \varphi}{\partial x}(L) = M^*(L) \end{cases} \quad (22)$$

As a law describing the creep process of a polymer filler, we accept the Maxwell-Gurevich equation [5]:

$$\frac{\partial \varepsilon_{ij}^*}{\partial t} = \left(\frac{3}{2}(\sigma_{ij} - p\delta_{ij}) - E_\infty \varepsilon_{ij}^*\right)\frac{1}{\eta^*} = \frac{f_{ij}}{\eta^*}, \quad (23)$$

η^* – invariant relaxation viscosity coefficient, $p = \frac{\sigma_{xx}}{3}$, δ_{ij} – Kronecker delta, E_∞ – modulus of viscoelasticity.

$$\eta^* = \eta_0^* \exp\left(-\frac{1}{m^*}(|\frac{3}{2}(\sigma_{rr} - p) - E_\infty \varepsilon_{rr}^* |_{\max}) \right), \quad (24)$$

the index r denotes the principle directions for stresses, η_0^* – initial relaxation viscosity, m^* – velocity module.

3. METHOD OF CALCULATION

The system (21) of nonlinear differential equations will be solved by the finite difference method. Formulas for partial derivatives with respect to x used in solving with accuracy $O(\Delta x^2)$ for i-th point [6]:

$$\frac{\partial f(x_i)}{\partial x} \approx \frac{f(x_{i+1}) - f(x_{i-1})}{2\Delta x}, \quad (25)$$

$$\frac{\partial^2 f(x_i)}{\partial x^2} \approx \frac{f(x_{i-1}) - 2f(x_i) + f(x_{i+1})}{\Delta x^2}, \quad (26)$$

here Δx – is the distance between adjacent points of the FDM grid.

The system of differential equations (21) with boundary conditions (22) is transformed to a system of linear equations for each time moment t. In calculating the creep strain components (23) at different time moments, the Euler's method [7] is used.

We write the system in the form:

$$[A]\{X\} = \{B\}, \quad (27)$$

$$[A] = \begin{bmatrix} a_{1,1} & a_{1,2} & \dots & a_{1,2n} \\ a_{2,1} & a_{2,2} & \dots & a_{2,2n} \\ \vdots & \vdots & \ddots & \vdots \\ a_{2n,1} & \cdots & \cdots & a_{2n,2n} \end{bmatrix} -$$

matrix containing elements that are constant in time with $2n \times 2n$ dimensions.

$\{X\} = [w_1\ \varphi_1\ w_2\ \varphi_2\ \dots w_n\ \varphi_n]^T$ – column vector of unknown displacements, n – number of nodes of the FDM grid, including 2 fictitious ones that go on Δx beyond the length of the rod L and are used to write expressions for partial derivatives with respect to x at the points of the rod with coordinates $x = 0,\ x = L$.

$\{B\} = [b_1\ b_2\ \cdots\ b_{2n}]^T$ – column vector of free terms with $2n \times 1$ dimensions.

4. RESULTS AND DISCUSSION

When solving a test problem, we use the following data:

rod axis is initially curved according to the equation

$$w_0 = f \cdot \sin(\frac{\pi x}{L}),\ L = 3 \text{ m},\ b = 0.15 \text{ m},$$
$$h = 0.05 \text{ m},\ \delta = 1 \text{ mm},$$

sheathings material is aluminum with $E_s = 0.7 \cdot 10^5$ MPa, the filler material is polyurethane foam with the following characteristics:

$$G_f = 5 \text{ MPa},\ \nu_f = 0.3,\ E_\infty = 27.38 \text{ MPa},$$
$$m^* = 0.0218 \text{ MPa},\ \eta_0^* = 1.43 \cdot 10^4 \text{ MPa} \cdot \text{h}.$$

According to [1], the critical force for a rod without taking into account the rheological characteristics of the filler material is:

$$P_{cr} = \frac{P_{cr}^0}{1 + \frac{P_{cr}^0}{G_f A_f}} = 10.71 \text{ kN}, \quad (28)$$

where $P_{cr}^0 = \frac{\pi^2 (E_s I_s + E_f I_f)}{L^2} = 15$ kN

– Euler critical force (excluding shear deformations). When a coefficient K_s is added to formula (28), the value of the critical force will be equal to:

$$P_{cr} = \frac{P_{cr}^0}{1+\frac{P_{cr}^0}{K_s G_f A_f}} = 10.195 \text{ kN}. \quad (29)$$

When calculating the stability of the rod without taking into account the effect of viscoelasticity by the finite element method, a critical load $P_{cr} = 10.49$ kN was obtained in the LIRA-SAPR software, the form of stability loss is shown in Figure 4



Figure 4. The first form of buckling.

The number of three-dimensional (3D) solid elements when modeling along the height of the filler section is 8, along the length is 100. From the ends, the axial load is transferred to the section using the installed additional aluminum plate. From the modeling by 3D and plate elements in the software package it follows that local loss of stability in thin metal sheathings does not occur.

Next, we perform the calculation taking into account creep effect in accordance with the procedure described in this article using the MATLAB software package.

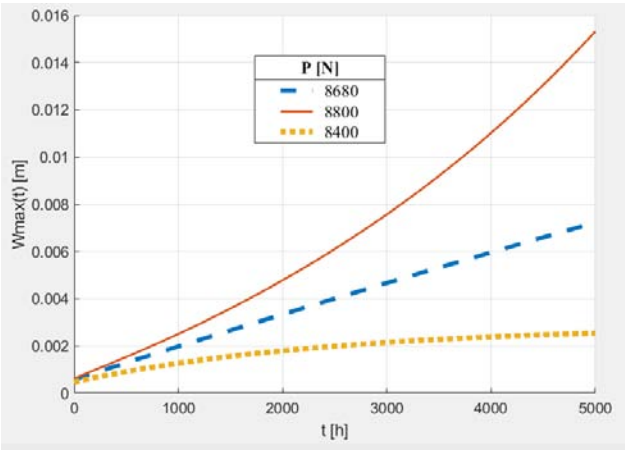


Figure 5. Displacements along z axis versus time for various loads.

In the calculation, the initial deflection parameter was taken to be equal to $f = 0.1$ mm, number of sectors between nodes along the length of the rod – 50, the number of time steps – 100. An increase in the number of accepted steps and sections leads to negligible changes in the results, the solutions are stable.

In [8, 9], when analyzing the stability of viscoelastic rods and beams using the Maxwell-Gurevich equation, the value of the long-term critical load is introduced by replacing the instantaneous elastic constants E and G of the filler by long ones determined by the formulas:

$$G_{f,l} = \frac{G_\infty G_f}{G_\infty + G_f}, \quad (30)$$

$$E_{f,l} = \frac{E_\infty E_f}{E_\infty + E_f}, \quad (31)$$

here $G_\infty = \frac{E_\infty}{3}$, the long-term Poisson's ratio of the material used in calculating the coefficient K_s [10]:

$$\nu_{f,l} = \frac{\alpha^*}{\beta^*}, \quad (32)$$

where $\alpha^* = \frac{1}{E_f} + \frac{1}{E_\infty}$, $\beta^* = \frac{\nu_f}{E_f} + \frac{1}{2E_\infty}$.

Using this technique, we write down the long-term critical force in the form:

$$P_l = \frac{P_l^0}{1+\frac{P_l^0}{K_{s,l} G_{f,l} A_f}} = 8.683 \text{ kN}, \quad (33)$$

where $P_l^0 = \frac{\pi^2 (E_s I_s + E_{f,l} I_f)}{L^2}$.

As can be seen from the graphs shown in Figure 5 when $P_l \approx 8680$ N the creep process is steady,

the deflection grows at a constant speed. This result with a high degree of accuracy corresponds to the value obtained in expression (33). At loads lower than P_l, the deflection growth gradually slows down, at loads $P > P_l$ the deflection growth accelerates. Note that the nature of the curves does not change for various parameters of the initial imperfections *f*, which affect only the final value of the deflection during decreasing creep, as well as the critical time during buckling. We demonstrate this in Fig. 6, showing the influence of the parameter of initial imperfections *f* on the critical time at a load $P = 8900$ N $> P_l$. In the general case, the initial imperfections of real structures are arbitrary and have a wide range of values, due to both technological and operational reasons, respectively, the actual values of long-term loads under which the presented structure works must be less than P_l.

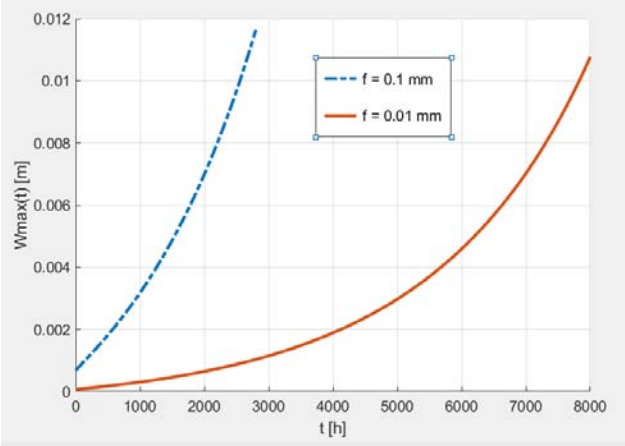


Figure 6. The influence of the initial imperfection on the critical time, P = 8900 N.

Thus, in the presence of complete data on the characteristics of the materials and the initial imperfections, it seems possible to calculate the critical time.

In order to simplify the solution, normal stresses in the filler can be neglected if its elastic modulus is low, assuming that all normal stress is perceived by metal sheathings. The effect of taking into account normal stresses in the filler on the critical time is shown in Figure 7.

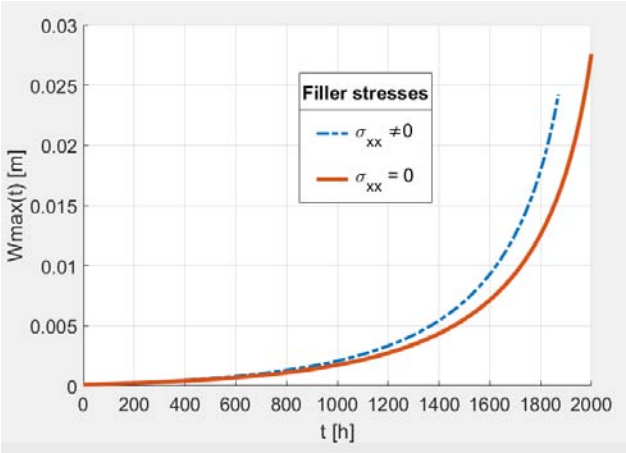


Figure 7. The effect of taking into account normal stresses in the filler on the critical time, P=9400 N.

Obviously, when using a polymer filler with greater rigidity, the difference between the critical time obtained without taking into account the normal stresses in it and taking them into account will increase significantly.

6. CONCLUSIONS

In the article, resolving equations are obtained that describe the process of rod buckling taking into account shear deformations and creep effects, and a method for numerically solving them is given. The presented algorithm for solving the problem allows us to determine the critical load leading to loss of stability, the critical time in the presence of data on the initial imperfections of the compressed structure, and also to trace the history of its deformation in time. The test problem is solved under various loads.

For the initial data corresponding to part 3 of this article, the difference in critical loads when taking into account creep and without considering it is equal to:

$$\frac{10.2-8.68}{10.2}\cdot 100\% = 14.9\%,$$

which is important to consider when designing such three-layer elements in schemes that allow their work under compression forces.

REFERENCES

1. **Alfutov N.A.** Osnovy raschyota na ustojchivost' uprugih sistem [Basics of calculating the stability of elastic systems]. Moscow, Mashinostroyenie, 1978, 312 pages (in Russian).
2. **Amabili M.** Nonlinear mechanics of shells and plates in composite, soft and biological materials. New York, Cambridge University Press, 2018, 568 pages.
3. **Reddy J.N.** Energy principles and variational methods in applied mechanics. 2nd Edition. New York, John Wiley, 2002, 608 pages.
4. **Wang, C.M., Wang, C.Y., Reddy, J.N**. Exact solutions for buckling of structural members. Florida, CRC Press LLC, 2004, 224 pages.
5. **Goldman A.Y.** Prochnost' konstrukcionnyh plastmass [Strength of structural plastics]. Leningrad, Mashinostroyenie, 1979, 320 pages (in Russian).
6. **Esfandiari R.S.** Numerical methods for engineers and scientists using MATLAB. 2nd edition. Florida, CRC Press LLC, 2017, 417 pages.
7. **Yazyev B.M., Chepurnenko A.S., Litvinov S.V., Kozel'skaya M.Yu.** Napryazhenno-deformirovannoe sostoyanie predvaritel'no napryazhennogo zhelezobetonnogo tsilindra s uchetom polzuchesti betona [Stress-strain state of a prestressed reinforced concrete cylinder with the consideration of concrete creep] // *Nauchnoe obozrenie,* 2014, No. 11, part 3, pp. 759-763 (in Russian).
8. **Zotov I.M., Chepurnenko A.S., Yazyev S.B.** Raschet na ustoychivost' ploskoy formy izgiba balok pryamougol'nogo secheniya s uchetom polzuchesti [Calculation of the flat bending shape stability of rectangular cross section beams with regard to creep] // *Herald of Dagestan State Technical University. Technical Sciences*, 2019, Vol. 46(1), pp. 169-176 (in Russian).
9. **Nikora N.I., Chepurnenko A.S., Litvinov S.V.** Opredelenie dlitelnyh kriticheskih nagruzok dlya szhatyh polimernyh sterzhnej pri nelinejnoj polzuchesti [Determination of long-term critical loads for compressed polymer rods with nonlinear creep] // *Inzhenernyj vestnik Dona*, 2015, no 1, part 2. URL: ivdon.ru/ru/magazine/archive/n1p2y2015/2796 (in Russian).
10. **Litvinov S.V., Danilova-Volkovskaya G. M., Dudnik A. E., Chepurnenko A. S.** Napryazhenno-deformirovannoe sostoyanie mnogosloynykh polimernykh trub s uchetom polzuchesti materiala [Stress-strain state of multilayer polymer pipes taking into account the creep of material] // *Sovremennaya nauka i innovatsii,* 2015, no 3 (11), pp. 71-78 (in Russian).

СПИСОК ЛИТЕРАТУРЫ

1. **Алфутов Н.А.** Основы расчета на устойчивость упругих систем. – М.: Машиностроение, 1978. – 312 с.
2. **Amabili M.** Nonlinear mechanics of shells and plates in composite, soft and biological materials. New York, Cambridge University Press, 2018, 568 pages.
3. **Reddy J.N.** Energy principles and variational methods in applied mechanics. 2nd Edition. New York, John Wiley, 2002, 608 pages.
4. **Wang, C.M., Wang, C.Y., Reddy, J.N**. Exact solutions for buckling of structural members. Florida, CRC Press LLC, 2004, 224 pages.
5. **Гольдман А.Я.** Прочность конструкционных пластмасс. – Л.: Машиностроение, 1979. – 320 с.

6. **Esfandiari R.S.** Numerical methods for engineers and scientists using MATLAB. 2nd edition. Florida, CRC Press LLC, 2017, 417 pages.
7. **Язьев Б.М., Чепурненко А.С., Литвинов С.В., Козельская М.Ю.** Напряженно-деформированное состояние предварительно напряженного железобетонного цилиндра с учетом ползучести бетона. // *Научное обозрение*, №11, часть 3, 2014, с. 759-763.
8. **Зотов И.М., Чепурненко А.С., Язьев С.Б.** Расчет на устойчивость плоской формы изгиба балок прямоугольного сечения с учетом ползучести. // *Вестник Дагестанского государственного технического университета. Технические науки*, №46(1), 2019, с. 169-176.
9. **Никора Н.И., Чепурненко А.С., Литвинов С.В.** Определение длительных критических нагрузок для сжатых полимерных стержней при нелинейной ползучести. // *Инженерный вестник Дона*, №1, часть 2, 2015.
11. **Литвинов С.В., Данилова-Волковская Г.М., Дудник А.Е., Чепурненко А.С.** Напряженно-деформированное состояние многослойных полимерных труб с учетом ползучести материала. // *Современная науки и инновации,* №3(11), 2015, с. 71-78 (in Russian).

Язьев Батыр Меретович, советник Российской академии архитектуры и строительных наук (РААСН), доктор технических наук, профессор кафедры «Сопротивление материалов» Донского государственного технического университета, 344022, Россия, Ростов-на-Дону, ул. Социалистическая, 162; тел.: +7(863)201-91-36; e-mail: ps62@yandex.ru; http://orcid.org/0000-0002-5205-1446

Чепурненко Вячеслав Сергеевич, студент Донского государственного технического университета, 344022, Россия, Ростов-на-Дону, ул. Социалистическая, 162; тел.: +7(919)888-09-24;
E-mail: chepurnenkoviacheslav@gmail.com;
https://orcid.org/0000-0001-6033-2603.

Yazyev Batyr Meretovich, Advisor of the Russian Academy of Architecture and Construction Sciences (RAACS), Doctor of Technical Sciences, Professor of the Department “Strength of Materials”, Don State Technical University, 344022, Russia, Rostov-on-Don, Sotcialisticheskaya st., 162; phone: +7 (863) 201-91-36;
E-mail: ps62@yandex.ru;
https://orcid.org/0000-0002-5205-1446.

Chepurnenko Viacheslav Sergeevich, student, Don State Technical University, 344022, Russia, Rostov-on-Don, Sotcialisticheskaya st., 162; phone: +7(919)888-09-24;
E-mail: chepurnenkoviacheslav@gmail.com;
https://orcid.org/0000-0001-6033-2603.

DOI:10.22337/2587-9618-2019-15-4-34-47

THE ANALYSIS OF THERMAL PROPERTIES OF A WALL FRAGMENT MADE WITH 3D CONSTRUCTION TECHNOLOGY

Valery A. Ezersky [1], Pavel V. Monastyrev [2], Ivan A. Ivanov [2]
[1] Bialystok University of Technology, Bialystok, Poland
[2] Tambov State Technical University, Tambov, Russian Federation

Abstract: The article presents the results of the analysis of the effect of the parameters of the external wall of a building, constructed using 3D technology on its heat engineering propertis.The dependence of the heat penetration coefficient Λ (function Y) of the wall on the followig factors has been constructed: the thickness of the outer walls d_1 (factor X_1), the thickness of telongitudinal partitions between the voids d_2(factor X_2), the number of voids in the wall cross section in the transverse direction m (factor X_3), the number of voids in the wall section per 1 rm in the longitudinal direction n (factor X_4), the thermal conductivity coefficient of the heat-insulating material in the voids λ_1 (factor X_5), provided that the cross-sectional area of the bearing part of the wall, taken under the condition of ensuring strength. The data set foranalysis was obtained by implementing a computational experiment. The analysis and optimi-zation of the parameters was performed on the basis of a deterministic mathematical model that describes the presented dependence for the selected void formation scheme in the wall. The information may be useful for scientists, designers and technologists involved in the development of structural solutions of buildings using 3D printing technology.

Keywords: buildings in 3D technology, outer wall, air voids, heat engineering properties, heat penetration coefficient, heat conductivity coefficient, optimization, deterministic mathematical model

АНАЛИЗ ТЕПЛОТЕХНИЧЕСКИХ КАЧЕСТВ ФРАГМЕТА СТЕНЫ ЗДАНИЯ, ВОЗВОДИМОГО В 3D ТЕХНОЛОГИИ

В.А. Езерский [1], П.В. Монастырев [2], И.А. Иванов [2]
[1] Белостокский технический университет, г. Белосток, ПОЛЬША
[2] Тамбовский государственный технический университет, г. Тамбов, РОССИЯ

Аннонтация: В статье представлены результаты оригинального исследования по анализу влияния параметров наружной стены здания, возводимого в 3D технологии, на теплозащитные качества. Построена зависимость коэффициента теплопередачи стены U (функция Y) от следующих факторов: толщины внутренних стенок несущей части сечения стены d (фактор X_1), количества пустот в сечении стены в поперечном направлении m (фактор X_2), количества пустот в сечении стены на 1 мп в продольном направлении n (фактор X_3), коэффициента теплопроводности материала несущей части сечения стены U_1 (фактор X_4) и коэффициента теплопроводности изоляционного материала в пустотах U_2 (фактор X_5) при постоянной площади сечения несущей части стены, принимаемой по условию обеспечения прочности. Совокупность данных для анализа получена путем реализации вычислительного эксперимента. Анализ и оптимизация параметров выполнены на основе детерминистических математических моделей, описывающих представленную зависимость для двух вариантов конфигурации сечения. Информация может быть полезна для научных работников, проектировщиков и технологов, занимающихся развитием решений зданий в относительно новой 3D технологии.

Ключевые слова: здания в 3D технологии, наружная стена, теплотехнические качества, коэффициент теплопередачи, коэффициент теплопроводности, детерминистическая математическая модель

INTRODUCTION

A fundamentally new approach to the design of buildings is becoming more and more popular across the globe. It is based on the creation of an information (computer) model of a building that has a numerical description and organized information about the object, which is used not only at the stage of its design and construction, but throughout the entire life cycle of the building. This approach is called Building Informational Modeling or BIM for short. At present, digital models of buildings are being integrated with the construction industry, where 3D printers are used in the construction of buildings, which apply the concrete mixture layer by layer according to the programmed contour of the building structure, thereby making building structures of the building or "printing" the building.

The trend for digitalization refers to the construction industry in the Russian Federation, which has been moving towards the development and implementation of an information modeling approach for buildings since the beginning of the century [1-3]. Currently, digital models of buildings are being integrated in the construction industry, where 3D printers are used in the construction of buildings, which apply concrete mixture layer by layer, reproducing the process of "printing" the building in reality [4-6].

Information on the materials used for 3D printing of buildings is extremely limited. However, it is known that the developers of the Chinese company WinSun [7, 8] use a cement-sand mixture with waste from demolition of buildings, fiberglass and special additives in their technologies. When using products of processing building materials and micro-reinforcing, the density of the resulting mixture was from 2000 to 2200 kg/m^3, the flexural strength of the concrete mixture was 8.2 MPa, and the compressive strength was 34.5 MPa. The width of the printed layer ranged from 30-60 mm [7,8].

One of the Russian companies, SPETSAVIA, [9] offers high-strength cement mix, fiberglass concrete, M300 sand concrete, kaolin mixture as a material for 3D printing. The density of the material is 2200-2350 kg/m^3, the compressive strength is from 30 MPa. The layer width is 20-50 mm, the thickness is 5-10mm.

The company "Loughborough University" in the UK, when creating 3D printer designs, uses high strength cement concrete (with compressive strength of 100-110 MPa, the density of which varies between 2250-2350 kg/m^3. The width of the printed layer is 25 mm, the thickness is 25 mm [10].

As it is known, the outer walls of heated buildings must have the required heat-shielding qualities. The analysis of fragments of the horizontal section of walls erected in 3D technology in several firms [11-13] showed that this problem remains unsolved. The thickness of the outer walls is most often taken equal to 300mm. The walls have a hollow structure. The placement of voids forms a far from optimal configuration from the point of view of thermal protection. The wall thicknesses of the bearing part of the section vary within 30-50 mm for external walls, and 15-30 mm for internal walls. As an example, discussed further in the authors' study, we present a fragment of a section of the wall of the company Contour Crafting (Figure 1) [14]. Using the AutoCAD software package, the authors calculated the area of the bearing part, which amounted to 0.186 m^2, for a fragment of this section 0,3×1 m^2 in size. The proportion of the bearing part in the total section area was 62.0%.

It is known [15] that the heat transfer resistance of a hollow product is significantly affected by the heat flux path length in the partitions between voids from the base material. Analyzing the Contour Crafting wall [14], one can notice that the path length of the heat flux in the partitions was not analyzed. It is not the best from this point of view, although the partitions of the sinusoidal voids somewhat extend the heat flow path. In this study, the authors of the article considered it appropriate to return to the orthogonal pattern of the placement of voids, in particular, with the placement of longitudinal voids in the wall and the displacement of their centers in adjacent rows by half the length (Figure 2).

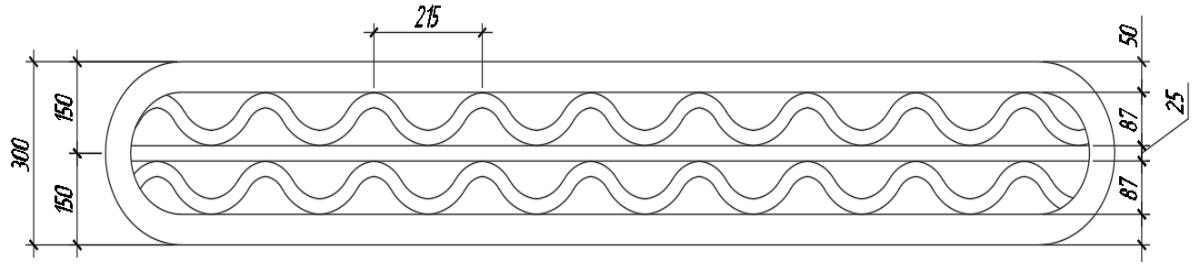


Figure 1. Contour Crafting Wall [14].

The authors assumed that by operating the number of voids in the section, as well as the thickness of the partitions between them, it is possible to provide a large number of options for the configuration of voids, which will allow installing a variant of a fragment of the wall with improved thermal properties.

The use of a large number of closed non-vented voids in the wall section is always complicated by the unequal conditions of their work, which affect the stability of their heat-shielding properties. The point is that with an increase in the thickness of voids inside them, the convective heat transfer increases, which does not increase, and sometimes reduces, the heat-shielding properties of voids [15, 16]. If cracks or damage occur in the wall sheath and the voids become ventilated, their heat-shielding properties are sharply reduced. On the other hand, the location of voids in the wall (in its outer or inner part) forms uneven temperatures on their surfaces, which affects the intensity of radiation heat transfer [15,16]. In the authors' opinion, in order to increase the thermal engineering reliability of walls with voids constructed in 3D technology, it is necessary fill the voids with various modern effective heat-insulating materials, which will not greatly complicate the technological part of the construction process [17-19].

The purpose of this study is to analyze the influence of the selected parameters of the external wall of the building, constructed in 3D technology, namely: the thickness of the external walls of the external wall d_1 (factor X_1), the thickness of the longitudinal partitions between the voids d_2 (factor X_2), the number of voids in the cross section of the wall in the transverse direction m (factor X_3), the number of voids in the wall section per 1 rm in the longitudinal direction n (factor X_4), the thermal conductivity coefficient of the heat-insulating material in the voids λ_1 (factor X_5) by the heat penetration coefficient of the wall fragment Λ (function Y) under the condition of constant cross-sectional area of the supporting walls, under the condition of ensuring the strength. The analysis is based on the deterministic mathematical model developed by the authors, which describes the studied dependence for the selected void formation scheme in the wall section. Using the model, the optimization procedure of parameters was carried out.

1. DESCRIPTION OF THE WALL FRAGMENTS UNDER STUDY

A fragment of the outer wall of a building constructed in 3D technology with a length l_w=1.00 m and a thickness d_w=0.30 m was selected as the object under study. The fragment variants differed in configuration and in the geometric parameters of voids in the section. First of all, a diagram of the configuration of voids in the wall was selected. Considering the data [15] on the influence of the heat flux path length in the partitions on the heat transfer resistance of a hollow product, in this study we adopted a scheme with orthogonal placement of longitudinal voids and a shift of their centers in adjacent rows by half their length (Figure 2). In order to increase the thermotechnical reliability of the wall in the fragments under study, it was also decided to fill the air voids with effective

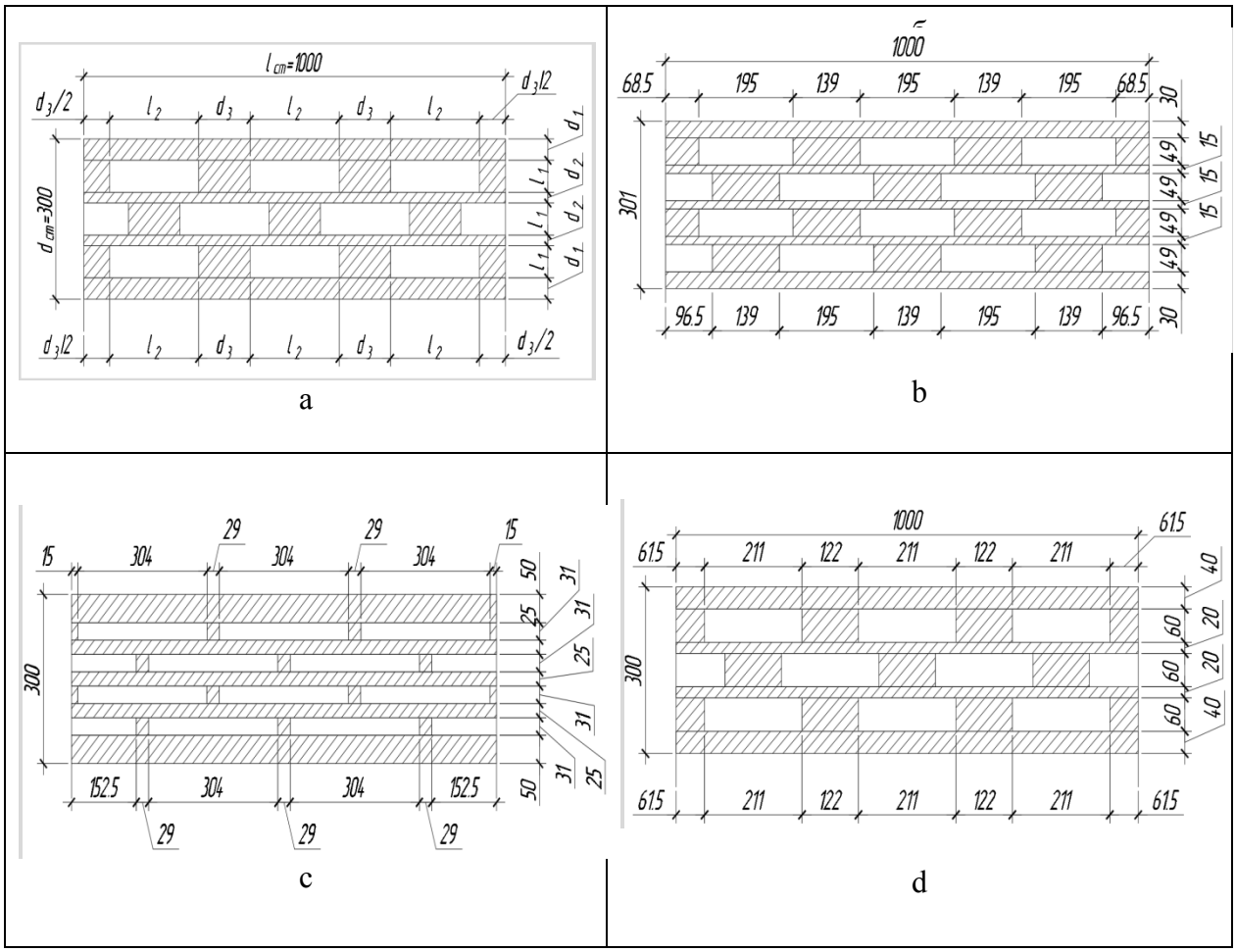


Figure 2. Options of a wall fragment in 3D technology with various configurations of voids in sections: a-general scheme; b-option # 5; option #8; option # 23 (numbering according to the plan in Table 1).

heat-insulating materials with a wide range of changes in the coefficient of thermal conductivity of the material of the liners.

The initial condition for all considered configuration options is the constancy of the cross-sectional area of the load-bearing part of the wall for each of the variants of void formation, adopted by the condition of ensuring strength and comprising 62% of the total cross-sectional area of the wall fragment, as recommended in [14]. This condition put forward the task of cutting voids in the wall with equally balanced configuration options, i.e. options with different configuration of voids, but with the same cross-sectional areas of the bearing part, comprising 0.30x0.62=0.186 m^2. For cutting voids, the authors' program implemented in Exel was used.

2. METHOD OF CALCULATING HEAT PENETRATION COEFFICIENT *Λ* OF THE WALL FRAGMENTS WITH HETEROGENEOUS INCLUSIONS

Heat penetration coefficient of wall fragments *Λ*, W/(m^2 ^{O}C) was calculated using the formula for the amount of heat Q, transferred by the wall [16]:

$$Q=\Lambda(\tau_в - \tau_н) Fz, \quad (1)$$

where: τ_{in} is temperature of the inner surface of the wall, ^{O}C; τ_{out} is temperature of the outer

1. Entering independent variables d_1 , d_2 , m , n , λ_1
2. Entering stabilized variables d_w , l_w , t_{out} , t_{in} , α_{out} , α_{in} , λ_2
3. Calculating geometric parameters of the configuration of voids $S_{нч}$, $S_{из}$, d_3 , l_1 , l_2
4. Calculating temperatures and heat flux in the fragment under study τ_{in} , τ_{out}, q
5. Calculating thermal permeability coefficient of a wall fragment Λ

Figure 3. Block diagram of the calculation of the heat penetration coefficient of the wall fragment Λ with heterogeneous inclusions.

surface of the wall, ^{O}C; F is the area of the wall, m^2; z is heat transfer duration, s.

If we assume F =1 m^2 and z =1 s, then we obtain the formula for the heat flux q, that simplifies fining of the value Λ:

$$\Lambda = q / (\tau_{in} - \tau_{out}) \qquad (2)$$

Previously, with the help of the authors' program, in Exel we generated possible and valid options for cutting voids for wall fragments. Then, geometric calculation models of wall fragments, reduced to 1 rm, were imported from Autodesk AutoCAD 2016 in the R12/LT2 DXF file extension.

Further, for each variant of wall fragments, using the Elcut software package, two-dimensional temperature fields were calculated. The calculations were performed for the climatic conditions of the city of Tambov. The boundary conditions were taken as follows: outdoor temperature $t_{out} = -28$℃; heat transfer coefficient of the outer surface of the wall α_{out}=23 W/(m^2 ^{O}C); indoor temperature $t_{in} = 20$℃; heat transfer coefficient of the inner surface α_{in}=8.7 W/(m^2 ^{O}C); for end parts of the structure heat flux q=0 W/m^2. The results of the calculations were the temperatures on the inner τ_{in} and outer τ_{out} surfaces of the wall, as well as the heat flux q along the inner surface of the wall. These values served as data for calculating the heat penetration coefficient of wall fragments Λ. Figure 3 presents a simplified block diagram of the complete calculation of the heat penetration coefficient.

3. MATHEMATICAL MODEL OF HEAT PENETRATION COEFFICIENT OF WALL FRAGMENTS WITH HETEROGENEOUS INCLUSIONS

to achieve the stated goal a scientific method of mathematical modeling was used, which allows using mathematical dependencies to describe the functioning of the object under study, determine the output parameters, and search for the optimal values of the object parameters. Using mathematical modeling makes it possible to avoid physical modeling, reduce the process of pilot testing and reduce the complexity of the study. The main component in this formulation is the mathematical model [20].

To ensure the practical usefulness of the model and its effectiveness, it is recommended to develop short models that use the most important factors that describe the properties being studied and provide information that consumers are interested in. Factors in the models must be controllable, compatible, unique, mutually independent and directly affect the properties studied [20].

In accordance with the purpose of the study, the heat penetration coefficient Λ of a wall fragment, [W/(m^{2}K)] is adopted as a function of the target Y, which was studied depending on five factors: the thickness of the outer walls of the outer wall d_1, [m] (factor X_1), thickness of longitudinal partitions between voids d_2, [m] (factor X_2), the number of voids in the cross section of the wall in the transverse direction m, [pcs] (factor X_3), the number of voids in the wall section per 1 rm in the longitudinal direction n, [pcs] (factor X_4), coefficient of thermal conductivity of thermal insulation material in voids λ_1, [W/(m K)] (factor X_5) with a constant cross-sectional

area of the supporting part of the wall, under the condition of ensuring strength in the amount of 62% of the total area of the fragment.

It was assumed that the desired dependence $Y=f(X_1,X_2,X_3,X_4,X_5)$ can be described by an algebraic polynomial of the second degree. In order to obtain data to describe this dependence, a five-factor computational experiment was performed according to a second-order plan (Table 1). A composite symmetric three-level plan, including 26 experiments, was used [21]. To calculate the values of Y_i in 26 lines of the plan, the Elcut software package was used.

When choosing ranges of factors, the data on structural solutions of the external walls of buildings erected in 3D technology, taken from several foreign and domestic companies, which are presented by the authors in the overview part of the article, were taken into account. So for factor X_1 (thickness of the outer walls of the outer wall d_1), the following levels were accepted: 0.030 (-1) - 0.040 (0) - 0.050 (+1) m.

Factor X_2 (the thickness of the longitudinal partitions between the voids d_2) was adopted at the levels: 0.015 (-1) - 0.020 (0) - 0.025 (+1) m. The thickness of the transverse partitions between the voids d_3, exactly like the sizes of voids l_1, l_2, were not were controlled, because otherwise it was impossible to fulfill the condition of constant cross-sectional area of the bearing part of the wall, adopted under the condition of ensuring strength. However, the minimum value of d_3 for the corresponding options for technological reasons was taken as not less than the thickness d_2 at the lower level, i.e. equal to 0.015 m. The maximum thickness d_3 was determined by the results of cutting the section into voids. The values of d_3, l_1, l_2 were required to calculate the heat penetration coefficient Λ of the wall fragment and they are given in Table 1.

Factor X_3 (the number of voids in the cross section of the wall in the transverse direction m) ranged between: 2(-1) - 3(0) - 4(+1). Factor X_4 (the number of voids in the wall section per 1 rm in the longitudinal direction n) considered in the range of variation: 3 (-1) - 5(0) - 7(+1). It was taken into account that factors X_3 and X_4 were integer and cannot take fractional values. The last factor X_5 (thermal conductivity coefficient of the insulating material in voids λ_1) was considered in a wide range of changes: 0.028(-1) – 0.070 (0) – 0.112(+1) W/(m^{2}K).

The integer values of the listed above factors $\dot{X}_1,\dot{X}_2,\dot{X}_3,\dot{X}_4,\dot{X}$ and the corresponding coded values in brackets X_1,X_2,X_3,X_4,X_5 are presented in Table1. Transition from natural values $\dot{X}_i$ to coded values X_i was carried out according to the formula [22]:

$$X_i=[2\dot{X}_i - (\dot{X}_{imax}+\dot{X}_{imin})]/(\dot{X}_{imax}- \dot{X}_{imin}) \qquad (3)$$

where: $\dot{X}_i$, $\dot{X}_{imax}$, $\dot{X}_{imin}$ are current, maximum and minimum natural values of the i-factor, respectively.

Accepted levels of selected factors allowed for the wall section under consideration to generate 3x3x3x3=81 configuration option for voids subject to the initial conditions. The remaining input parameters are taken at a constant level. The wall thickness is taken equal d_w=0.300 m; the estimated length of the wall section l_w=1.000 m. Given the fact that firms most often use dense (2200 kg/m^3) and strong concrete for the bearing part of the wall section, the thermal conductivity coefficient of the material of the bearing section is assumed to be constant and equal to λ_2 = 1.650 W/(m K).

Based on the calculation results (Table 1) using the least squares method [22], a dependency model $Y=f(X_1,X_2,X_3,X_4,X_5)$ is constructed in the form of a second-order regression equation:

$$\hat{Y} = 1.815 - 0.198X_1 - 0.027X_2 - 0.433X_3 + 0.336X_4 + 0.199X_5 - 0.018X_1X_2 + 0.004X_1X_3 - 0.033X_1X_4 + 0.005X_1X_5 - 0.044X_2X_3 - 0.032X_2X_4 - 0.042X_2X_5 - 0.037X_3X_4 + 0.029X_3X_5 - 0.064X_4X_5 - 0.007X_1^2 - 0.015X_2^2 + 0.060X_3^2 - 0.088X_4^2 - 0.008X_5^2. \qquad (4)$$

When assessing the adequacy of the model, it was taken into account that deterministic models are characterized by a one-to-one correspondence between external influence and reaction to this effect. In this regard, only one calcu-

lation is performed at each point in the plan. For testing, Fisher's criterion F was used, which showed how many times the scattering decreased with respect to the obtained regression equation compared with the scattering with respect to the mean [20,22]:

$$F = \frac{S_y^2(f_1)}{S_r^2(f_2)}$$

where: S^2_y is variance of the mean; S^2_r is residual variance;
f_1, f_2 are degrees of a system;

$$f_1 = (N\text{-}1)=26\text{-}1=25;\ f_2 = (N\text{-}N_b)=26\text{-}21=5.$$

N is the number of experiments in a plan;
N_b is the number of coefficients in the regression equation.
The regression equation describes the experimental results adequately if the value F exceeds the tabular F_t at a significance level of p and degrees of freedom f_1 and f_2. As calculations showed, F=0.2834/0.0020=141.9716; tabular value Ft=$F_{0,05;\ 25;\ 5}$ =2,60 [22]. Therefore, the value F is many times higher than F_t, which confirms the adequacy of the model and its suitability for further analysis. The determination coefficient R^2=0.9986 also confirms the high efficiency of the model.

4. ANALYSIS OF RESEARCH RESULTS BASED ON MATHEMATICAL MODEL

The influence of the studied factors on the heat penetration coefficient Λ of a wall fragment was analyzed on a mathematical model (4). For convenience and a better understanding, a discussion of the results was carried out using the natural values of the variables. Of greatest interest were the parameters of the wall fragment, which provided the smallest value of the thermal penetration coefficient Λ. From this point of view, the factors comprised two groups that gave beneficial effects if the coefficient Λ decreased with their increase and useless (negative) effects if the coefficient Λ increased with their increase.
Analyzing the constructed model, it was revealed that in the center G_p of the factor space, which is characterized by coordinates d_1=0.040 m; d_2=0.020 m; m =3; n=5; λ_1=0.070 W/(m K), the coefficient Λ is 1.815 W/(m^{2}K). Using the Gp point as a reference point, the influence of individual factors was estimated. It turned out that, taking into account the selected intervals of variation, the factor m (X_3) has the most powerful and useful effect on Λ. When the value m changed from 2 to 4 voids in the transverse direction (the other factors in the analysis are characterized by coordinates for the Gp point), the value Λ decreased from 2.308 to 1.442 W/(m^{2}K), i.e. there was a decrease of 37.6%. Moreover, due to the small quadratic effect of this factor, an increase in the number of voids m from 2 to 3 reduced Λ by 21.4%, but when m increased from 3 to 4, the value Λ decreased by 16.2%. The uneven nature of the change in Λ is due to the fact that with an increase in the number of voids in the wall section at a constant thickness, the thickness of voids filled with a heat insulator decreased, and thus their thermal resistance decreased.
Factor d_1 (X_1) had a weaker beneficial effect when the thickness of the outer walls of the outer wall changed from 0.030 to 0.050 m, Λ decreased from 2.006 to 1.610 W/(m^{2}K), i.e. by 19.7%, with a slight quadratic effect. The weakest beneficial effect was achieved by factor d_2 (X_2) - with a change in the thickness of the longitudinal partitions between voids from 0.015 to 0.025 m, a decrease in Λ from 1.827 to 1.773 W/(m^{2}K) was observed, i.e. by 3.0%.
Other factors had a negative effect - with their increase, Λ increased. So, when n (X_3) changed from 3 to 7 voids in the longitudinal direction, Λ grew from 1.391 to 2.063 W/(m^{2}K), i.e. increases by 48.3%. Due to the significant quadratic effect, this growth was uneven: when n varied from 3 to 5 voids, Λ increased by 30.5%, and when n changed from 5 to 7 voids, Λ increased by 17.8%. This influence of factor n was due to the fact that with the increase in its value, the number of thermal bridges in the form

Table 1. Plan of a computational experiment for five factors if N = 26 experiments.

Nr	*(X_1)* d_1	*(X_2)* d_2	*(X_3)* m	*(X_4)* n	*(X_5)* λ_1	Λ, W/(m^{2}K)	l_1 / l_2	d_3
1	-1 0.030	-1 0.015	-1 2	-1 3	+1 0.112	2.198	0.113/0.169	0.164
2	+1 0.050	-1 0.015	-1 2	-1 3	-1 0.028	1.344	0.093/0.205	0.128
3	-1 0.030	+1 0.025	-1 2	-1 3	-1 0.028	1.868	0.108/0.177	0.157
4	+1 0.050	+1 0.025	-1 2	-1 3	+1 0.112	1.880	0.088/0.217	0.116
5	-1 0.030	-1 0.015	+1 4	-1 3	-1 0.028	0.893	0.049/0.195	0.139
6	+1 0.050	-1 0.015	+1 4	-1 3	+1 0.112	1.272	0.039/0.245	0.088
7	-1 0.030	+1 0.025	+1 4	-1 3	+1 0.112	1.417	0.041/0.230	0.103
8	+1 0.050	+1 0.025	+1 4	-1 3	-1 0.028	0.562	0.031/0.304	0.029
9	-1 0.030	-1 0.015	-1 2	+1 7	-1 0.028	2.644	0.113/0.072	0.071
10	+1 0.050	-1 0.015	-1 2	+1 7	+1 0.112	2.506	0.093/0.088	0.055
11	-1 0.030	+1 0.025	-1 2	+1 7	+1 0.112	2.848	0.108/0.076	0.067
12	+1 0.050	+1 0.025	-1 2	+1 7	-1 0.028	2.217	0.088/0.093	0.050
13	-1 0.030	-1 0.015	+1 4	+1 7	+1 0.112	2.133	0.049/0.084	0.059
14	+1 0.050	-1 0.015	+1 4	+1 7	-1 0.028	1.307	0.039/0.105	0.038
15	-1 0.030	+1 0.025	+1 4	+1 7	-1 0.028	1.642	0.041/0.099	0.044
16	+1 0.050	+1 0.025	+1 4	+1 7	+1 0.112	1.397	0.031/0.130	0.013
17	-1 0.030	0 0.020	0 3	0 5	0 0.070	2.015	0.067/0.114	0.086
18	+1 0.050	0 0.020	0 3	0 5	0 0.070	1.602	0.053/0.143	0.058
19	0 0.040	-1 0.015	0 3	0 5	0 0.070	1.808	0.063/0.120	0.080
20	0 0.040	+1 0.025	0 3	0 5	0 0.070	1.792	0.057/0.134	0.066
21	0 0.040	0 0.020	-1 2	0 5	0 0.070	2.331	0.100/0.114	0.086
22	0 0.040	0 0.020	+1 4	0 5	0 0.070	1.419	0.040/0.143	0.058
23	0 0.040	0 0.020	0 3	-1 3	0 0.070	1.332	0.060/0.211	0.122
240	0 0.040	0 0.020	0 3	+1 7	0 0.070	2.122	0.060/0.091	0.052
25	0 0.040	0 0.020	0 3	0 5	-1 0.028	1.604	0.060/0.0127	0.073
26	0 0.040	0 0.020	0 3	0 5	+1 0.112	2.011	0.060/0.127	0.073

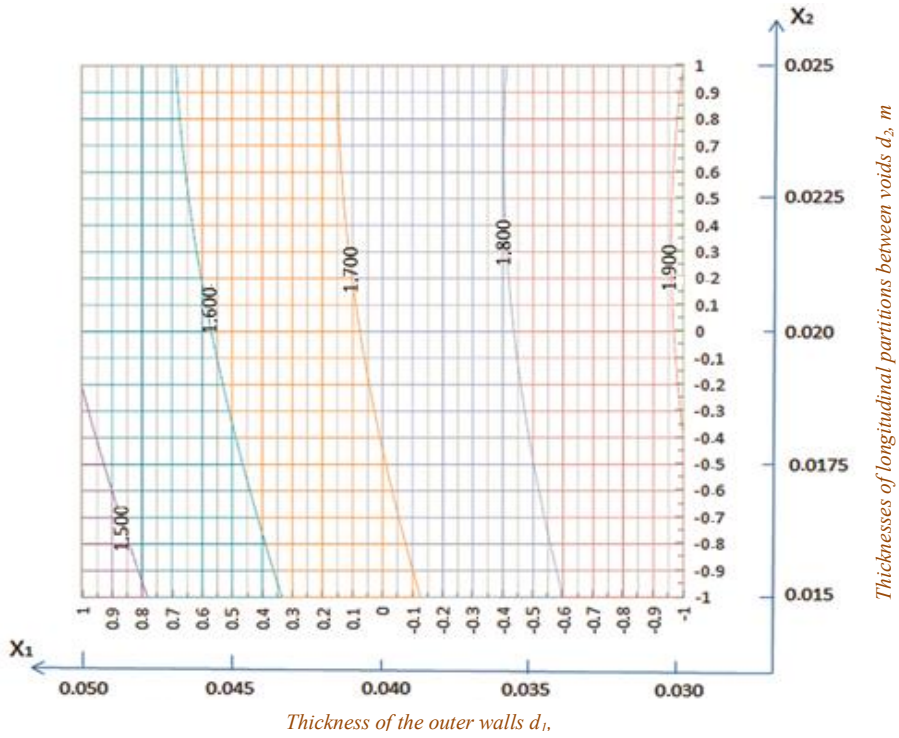


Figure 4. Correlation of heat penetration coefficient Λ, W/(m²K) (Y) of the wall fragment and the thickness of the outer walls d_1, m (X_1) and thicknesses of longitudinal partitions between voids d_2, m (X_2) if: the number of voids in the cross section of the wall in the transverse direction m=3 pcs. (X_3), the number of voids in the wall section per 1 rm in the longitudinal direction n=5 pcs. (X_4), thermal conductivity coefficient of thermal insulation material in voids λ_1=0.070 [W/(m K)] (X_5) and a constant proportion of the cross-sectional area of the bearing part of the wall 62% of the total area of the fragment.

of partitions between the ends of the voids increased and the path length of the heat flux decreased.

A weaker negative effect was revealed by factor $\lambda_1(X_5)$. When the thermal conductivity coefficient λ_1 of the heat-insulating material in the voids changed from 0.028 to 0.112 W/(m K), the value Λ increased from 1.608 to 2.006 W/(m²K), i.e. increased by 24.8% with a small quadratic effect.

The nature of the influence of factors is also shown in Figure 4 for correlation $Y=f(X_1,X_2)$ and Figure 5 for correlation $Y=f(X_2,X_5)$.

Based on model (4), the optimization procedure was performed and the extreme values of the heat penetration coefficient Λ of the wall fragment were determined, and the optimal values of the studied factors providing extrema were established. It turned out that the maximum value of the heat penetration coefficient Λ equal to 2.938 W/(m²K), is achieved at d_1=0.030 m; d_2=0.015 m; m =2; n=7; λ_1=0,112 W/(m K). On the contrary, the minimum value of Λ we are interested in, equal to 0.552 W/(m²K), is provided at d_1 = 0.050 m; d_2 = 0.025 m; m=4; n=3; λ_1=0.028 W/(m K). These parameters should be considered optimal and recommended for solving the wall in 3D technology, since they provide the highest level of thermal protection. The range of values of the heat penetration coefficient Λ with varying factors was 2.938-0.552 = 2.386 W/(m²K), which was 432.3% with respect to the minimum value of the heat penetration coefficient.

Thus, as a result of the study, it was revealed that for a constant area of the bearing part of the wall section constructed in 3D technology, by changing the configuration parameters of voids, namely,

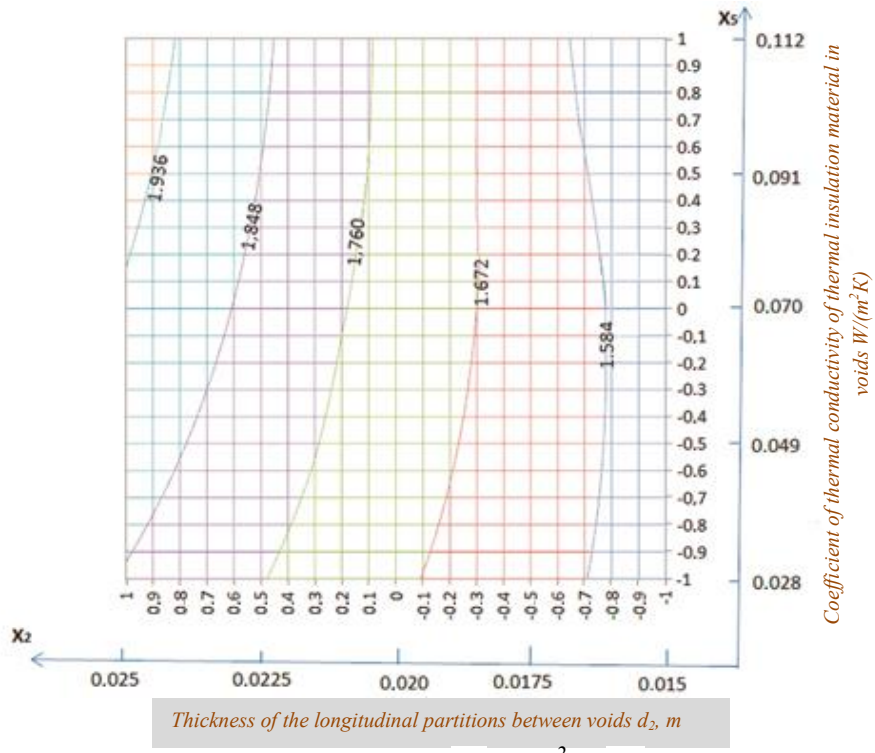


Figure 5. Correlation of heat penetration coefficient Λ, W/(m²K) (Y) of the wall fragment and the thickness of the longitudinal partitions between voids d_2, m (X_2) and coefficient of thermal conductivity of thermal insulation material in voids λ_1, [W/(m K)] (X_5) if: the thickness of the outer walls d_1=0.040 m (X_1), the number of voids in the cross section of the wall in the transverse direction m=3 pcs. (X_3), the number of voids in the wall section per 1 rm in the transverse direction n=5 pcs. (X_4) a constant proportion of the cross-sectional area of the bearing part of the wall 62% of the total area of the fragment.

the number of voids in the transverse and longitudinal directions and the thickness of the partitions, as well as the corresponding choice of material for thermal liners in voids, it is possible to significantly reduce the value of the penetration coefficient *Λ* of the wall. This indicates the potential of the proposed method for improving the heat-shielding qualities of walls with voids constructed in 3D technology.

CONCLUSIONS

1. The proposed deterministic mathematical model made it possible to assess the nature and degree of influence of the selected parameters of the wall constructed in 3D technology on the heat penetration coefficient *Λ* of the wall fragment.
2. The heat penetration coefficient *Λ* of the wall fragment decreases with an increase in the number of voids *m* in the transverse direction of the wall section, the thickness d_1 of the outer walls and the thickness d_2 of the longitudinal partitions between the voids, as well as with a decrease in the number of voids *n* in the longitudinal direction and the thermal conductivity coefficient λ_1 of the thermal insulation material in voids.
3. The minimum value of the heat penetration coefficient *Λ* of the studied wall fragment is 0.552 W/(m²K) and is achieved at d_1=0.050 m; d_2=0.025 m; *m*=4; *n*=3; λ_1=0.028 W/(m K). These parameters provide the highest level of thermal protection and are optimal for

solving the problem of constructing the wall in 3D technology.

REFERENCES

1. **Akimov P.A., Chernyshov E.M., Monastyrev P.V.** Nauchnye issledovaniya i razrabotki Rossijskoj akademii arhitektury i stroitel'nyh nauk: sostoyanie, napravleniya i perspektivy razvitiya [Research and development of the Russian Academy of Architecture and Building Sciences: state, directions and development prospects]. // Materialy 4-j mezhdunarodnoj nauchno-prakticheskoj konferencii "Ustojchivoe razvitie regiona: arhitektura, stroitel'stvo, transport". Tambov, TGTU, 15-16 ijunya 2017 [Proceedings of the 4th international research practical conference "Sustainable development of the region: architecture, construction, transport", TGTU. 15-16 June 2017]. Izdatelstvo Pershina R.V., pp. 12-28 (in Russian).
2. **Mishchenko E.S., Monastyrev P.V., Evdokimtsev O.V.** Aspekty razrabotki obrazovatel'nyh programm v oblasti BIM-tekhnologij s uchetom rabotodatelej [Aspects of developing educational programs in the field of BIM-technologies with regard to employer requirements]. // Materialy 5-j mezhdunarodnoj nauchno-prakticheskoj konferencii "Ustojchivoe razvitie regiona: arhitektura, stroitel'stvo, transport". Tambov, TGTU. 24-25 maya 2018 [Proc. of the 5th international research practical conference "Sustainable development of the region: architecture, construction, transport". Tambov, TSTU, May 24-25, 2018]. Izdatelstvo Pershina R.V. Pp. 385-392 (in Russian).
3. **Mishchenko E.S., Monastyrev P.V., Evdokimtsev O.V.** Improving the Quality of Training in Building Information Modeling. // ICL 2018; Kos Island; Greece; 25 September 2018 до 28 September 2018; 2020, Volume 916, pp. 453-459, Code 224239.
4. **Monastyrev P.V., Ezersky V.A., Ivanov I.A., Baltozar A.D.** Analiz tekhnologij 3D-pechati sten maloetazhnyh zdanij i ih klassifikaciya [Analysis of 3D printing technologies for walls of low-rise buildings and their classification]. // Sbornik nauchnyh statej Mezhdunarodnoj nauchno- prakticheskoj konferencii (22 maya 2019 g.) [Collection of scientific articles of the International Scientific and Practical Conference (May 22, 2019)], Yugo-Zap. gos. un-t, Kursk, Iz-vo YUgo-Zap. gos. un-t, 2019, pp. 70-80 (in Russian).
5. **Monastyrev P.V., Ezersky V.A., Ivanov I.A., Azaui Dubla B.** Additivnye tekhnologii vozvedeniya sten maloetazhnyh zdanij i ih klassifikaciya [Additive technologies for the erection of walls of low-rise buildings and their classification]. // Fundamental'nye, poiskovye i prikladnye issledovaniya RAASN po nauchnomu obespecheniyu razvitiya arhitektury, gradostroitel'stva i stroitel'noj otrasli Rossijskoj Federacii v 2018 godu. Nauchnye trudy RAASN. Tom 2 [Fundamental, search and applied researches of RAASN on scientific support of development of architecture, town planning and construction branch of the Russian Federation in 2018. Collection of papers RAASN. Volume 2]. Moscow, Izdatel'stvo ASV, 2019, pp. 368-379 (in Russian).
6. **Monastyrev P.V., Mishchenko E.S., Balthazar A.D., Ovsiannikova V.A., Ovsiannikov O.A.** Analysis of technologies of buildings 3D printing and their classification. // 21st General Assembly of the International Experts and Symposium Heritage as a Builder of Peace. Florence (Italy), Fondazione Romualdo Del Bianco Istituto Internazionale Life Beyond Tourism, 2019, pp. 363-369.

7. Website WinSun. URL: http://webcache.googleusercontent.com/search?q=cache:http://www.winsun3d.com/En/About/ (Accessed 08.03.2019).
8. Winsun. Future of Construction. URL:https://futureofconstruction.org/case/winsun/.
9. Website SPECAWIA. URL: https://specavia.pro/articls/pervyj-v-evrope-zhiloj-dom-napechatannyj-na-3d-printere-predstavili-v-yaroslavle/ (Accessed 09.03.2019).
10. **Inozemtsev A.S., Korolev E.V., Zyong Thang Kui.** Analiz sushchestvuyushchih tekhnologicheskih reshenij 3D-pechati v stroitel'stve [Analysis of existing 3D printing technology solutions in construction]. // *Vestnik MGSU*, 2018, Volume 13, No. 7 (118), pp. 863-876 (in Russian).
11. Apis Cor. We print buildings. [Электронный ресурс]. URL: http://apis-cor.com/. (Accessed 09.03.2019).
12. Betabram — visitreport. URL: http://3dprintetbyggeri.dk/pdf/bes%C3%B8gsrapporter/BetAbram.pdf (Accessed 16.03.2019).
13. **Lim S., Buswell R.A., Le T.T. et al.** Development in construction-scale additive manufacturing processes. // *Automation in Construction*, 2012, Volume 21, No. 1, pp. 262-268.
14. Website Contour Crafting URL: http://contourcrafting.com (Accessed 29.04.2019).
15. **Lykov A.V.** Teoreticheskie osnovy stroitel'noj teplofiziki [Theoretical foundations of building thermophysics]. Minsk, AN BSSR, 1961, 520 pages (in Russian).
16. **Fokin K.F.** Stroitel'naya teplotekhnika ograzhdayushchih chastej zdanij [Construction heat engineering of enclosing parts of buildings]. Ed. Yu.A. Tabunshchikov & V.G. Gagarin. Moscow, AVOK-Press, 2006, 256 pages (in Russian).
17. **Gusev B.V., Yezersky V.A., Monastyrev P.V.** Teploprovodnost' mineralovatnyh plit v uslovijah ekspluatacionnyh vozdejstvij [Heat-conductivity of mineral wool slabs when subjected to operation effects]. // *Promyshlennoe i Grazhdanskoe Stroitel'stvo*, 2005, No. 1, pp. 48-49 (in Russian).
18. **Gusev B.V., Yezersky V.A., Monastyrev P.V.** Izmenenie linejnyh razmerov mineralovatnyh plit v uslovijah ekspluatacionnyh vozdejstvij [Change in the linear dimensions of mineral wool slabs subjected to operation effects]. // *Promyshlennoe i Grazhdanskoe Stroitel'stvo*, 2004, No. 8, pp. 32-34 (in Russian).
19. **Erofeev A.V., Yartsev V.P., Monastyrev P.V.** Dekorativno-zashhitnye plity fasadnoj otdelki zdanij [Decorative and protective plates for facade decoration of buildings]. // *Izvestiya Vysshikh Uchebnykh Zavedenii, Seriya Teknologiya Tekstil'noi Promyshlennosti*, 2017, No. 1(367), pp. 101-104 (in Russian).
20. **Tarasik V.P.** Matematicheskoe modelirovanie tekhnicheskih system [Mathematical modeling of technical systems]. Minsk, Izd-vo DizajnPRO, 640 pages (in Russian).
21. **Brodsky V.Z., Brodsky L.I., Golikova T.I., Nikitina E.P., Panchenko L.A.** Tablicy planov eksperimenta dlya faktornyh i polinomial'nyh modelej (spravochnoe izdanie) [Tables of experimental designs for factorial and polynomial models (reference book.]. Moscow, Izdatelstvo Metallurgiya, Moskva 1982, 752 pages (in Russian).
22. **Krasovsky G.I., Filaretov G.F.** Planirovanie eksperimenta [Experiment planning]. Minsk, Izdatelstvo BGU, 1982, 302 pages (in Russian).

СПИСОК ЛИТЕРАТУРЫ

1. **Акимов П.А., Чернышов Е.М., Монастырев П.В.** Научные исследования и разработки Российской академии архитектуры и строительных наук: состоя-

ние, направления и перспективы развития. // Сборник трудов «Устойчивое развитие региона: архитектура, строительство, транспорт». Материалы 4-й Международной научно-практической конференции Института архитектуры, строительства и транспорта Тамбовского государственного технического университета (Тамбов, 15-16 июня 2017 года), 2017, с. 12-28.

2. **Мищенко Е.С., Монастырев П.В., Евдокимцев О.В.** Аспекты разработки образовательных программ в области BIM-технологий с учетом работодателей. // Сборник трудов «Устойчивое развитие региона: архитектура, строительство, транспорт». Материалы 5-й Международной научно-практической конференции Института архитектуры, строительства и транспорта Тамбовского государственного технического университета (Тамбов, 24-25 мая 2018 года), 2018, с. 385-391.
3. **Mishchenko E.S., Monastyrev P.V., Evdokimtsev O.V.** Improving the Quality of Training in Building Information Modeling. // ICL 2018; Kos Island; Greece; 25 September 2018 до 28 September 2018; 2020, Volume 916, pp. 453-459, Code 224239.
4. **Монастырев П.В., Езерский В.А., Иванов И.А., Бальтозар А.Д.** Анализ технологий 3D-печати стен малоэтажных зданий и их классификация. // Сборник «Современные проблемы в строительстве: постановка задач и пути их решения». Сборник научных статей Международной научно-практической конференции (Курск, 22 мая 2019 года). Юго-Западный государственный университет, 2019, С. 70-80.
5. **Монастырев П.В., Езерский В.А., Иванов И.А., Азауи Дубла Б.** Адаптивные технологии возведения стен малоэтажных зданий и их классификация. // Сборник трудов «Фундаментальные, поисковые и прикладные исследования Российской академии архитектуры и строительных наук по научному обеспечению развития архитектуры, градостроительства и строительной отрасли Российской Федерации в 2018 году». – М.: Российская академия архитектуры и строительных наук, 2019, с. 368-379.
6. **Monastyrev P.V., Mishchenko E.S., Balthazar A.D., Ovsiannikova V.A., Ovsiannikov O.A.** Analysis of technologies of buildings 3D printing and their classification. // 21st General Assembly of the International Experts and Symposium Heritage as a Builder of Peace. Florence (Italy), Fondazione Romualdo Del Bianco Istituto Internazionale Life Beyond Tourism, 2019, pp. 363-369.
7. Website WinSun. URL: http://webcache.googleusercontent.com/search?q=cache:http://www.winsun3d.com/En/About/ (Accessed 08.03.2019).
8. Winsun. Future of Construction. URL:https://futureofconstruction.org/case/winsun/.
9. Website SPECAWIA. URL: https://specavia.pro/articls/pervyj-v-evrope-zhiloj-dom-napechatannyj-na-3d-printere-predstavili-v-yaroslavle/ (Accessed 09.03.2019).
10. **Иноземцев А.С., Королев Е.В., Зыонг Тхань Куй.** Анализ существующих технологических решений 3D-печати в строительстве. // *Вестник МГСУ*, 2018, Том 13, №7(118), с. 863-876.
11. Apis Cor. We print buildings. [Электронный ресурс]. URL: http://apis-cor.com/. (Accessed 09.03.2019).
12. Betabram — visitreport. URL: http://3dprintetbyggeri.dk/pdf/bes%C3%B8gsrapporter/BetAbram.pdf (Accessed 16.03.2019).
13. **Lim S., Buswell R.A., Le T.T. et al.** Development in construction-scale additive manufacturing processes. // *Automation in Construction*, 2012, Volume 21, No. 1, pp. 262-268.

14. Website Contour Crafting URL: http://contourcrafting.com (Accessed 29.04.2019).
15. **Лыков А.В.** Теоретические основы строительной теплофизики. – Минск: Издательство Академии наук БССР, 1961. – 525 с.
16. **Фокин К.Ф.** Строительная теплотехника ограждающих частей зданий (под редакцией Ю.А. Табунщикова, В.Г. Гагарина). – М.: Авок-пресс, 2006. – 256 с.
17. **Гусев Б.В., Езерский В.А., Монастырев П.В.** Теплопроводность минераловатных плит в условиях эксплуатационных воздействий. // *Промышленное и гражданское строительство*, 2005, №1, с. 48-49.
18. **Гусев Б.В., Езерский В.А., Монастырев П.В.** Изменение линейных размеров минераловатных плит в условиях эксплуатационных воздействий. // *Промышленное и гражданское строительство*, 2004, №8, с. 32-34.
19. **Ерофеев А.В., Ярцев В.П., Монастырев П.В.** Декоративно-защитные плиты фасадной отделки зданий. // *Известия высших учебных заведений. Технология текстильной промышленности*, 2017, №1 (367), с. 101-104.
20. **Тарасик В.П.** Математическое моделирование технических систем. – Минск: Дизайн-ПРО, 2004. – 640 с.
21. **Бродский В.З., Бродский Л.И., Голикова Т.И., Никитина Е.П., Панченко Л.А.** Таблицы планов эксперимента (для факторных и полиномиальных моделей). – М.: Металлургия, 1982. – 752 с.
22. **Красовский Г.И., Филаретов Г.Ф.** Планирование эксперимента. – Минск: БГУ, 1982. – 302 с.
23. **Krasovsky G.I., Filaretov G.F.** Planirovanie eksperimenta [Experiment planning]. Mn.: Izd-vo BGU, 1982. - 302 p.

Valery A. Ezersky, Professor, Dr.Sc., Bialystok University of Technology; 45A, Wiejska Street, 15-351 Bialystok, Poland; phone: 85 746 90 00; fax: 85 746 90 15;
E-mail: wiz75micz@rambler.ru.

Pavel V. Monastyrev, Advisor of the Russian Academy of Architecture and Construction Sciences (RAACS), Professor, Dr.Sc., Tambov State Technical University; 106 Sovetskaya St, Tambov, 392000, Russia;
phone: +7(4752) 63-10-19;
E-mail: monastyrev68@mail.ru.

Ivan A. Ivanov, Ph.D. Student, Tambov State Technical University; 106 Sovetskaya St, Tambov, 392000, Russia;
phone: +7(4752) 63-10-19;
E-mail: ivan.ov-tambov@list.ru.

Езерский Валерий Александрович, член-корреспондент Международной инженерной академии (МИА), профессор, доктор технических наук, Белостокский технический университет; Wiejska 45A, 15-351 Białystok, Польша; тел. 85 746 90 00;
факс: 85 746 90 15; e-mail: wiz75micz@rambler.ru.

Монастырев Павел Владиславович, советник Российской академии архитектуры и строительных наук (РААСН), профессор, доктор технических наук, Тамбовский государственный технический университет; 392000, Россия, г. Тамбов, ул. Советская, д.106;
тел. +7 (4752) 63-10-19; факс: 63-06-43;
E-mail: monastyrev68@mail.ru.

Иванов Иван Александрович, аспирант, Тамбовский государственный технический университет; 392000, Россия, г. Тамбов, ул. Советская, д.106;
тел. +7 (4752) 63-10-19; факс: 63-06-43;
E-mail: ivan.ov-tambov@list.ru.

DOI:10.22337/2587-9618-2019-15-4-48-57

MULTI-AGENT SIMULATION FOR SELF-HEALING MECHANISMS OF DAMAGED GEOTECHNICAL STRUCTURES

Darya Filatova
Belarusian State University of Informatics and Radioelectronics, Minsk, BELARUS

Abstract: The paper is devoted to the task of multi-agent modeling of self-healing mechanisms for the damaged surface of an abstract geotechnical structure using biotechnology. We consider two-component self-healing mechanism. The first one is presented as a dynamic stochastic model of the aggregated behavior of agents. The second one is described by the "game-of-life" principle. The principals of numerical modeling of both mechanisms are discussed and illustrated by different scenarios.

Keywords: multi-agent simulation, Gaussian process, self-healing mechanism, geotechnical structures, biotechnology

МНОГОАГЕНТНОЕ МОДЕЛИРОВАНИЕ МЕХАНИЗМОВ САМОВОССТАНОВЛЕНИЯ ПОВРЕЖДЕННЫХ ГЕОТЕХНИЧЕСКИХ СРЕД

Дарья Филатова
Белорусский государственный университет информатики и радиоэлектроники, г. Минск, БЕЛАРУСЬ

Аннотация: Работа посвещена задаче многоагентного моделирования механизмов самовосстановления поврежденной поверхности некоторой абстрактной геотехнической среды с использованием агломерации бактерии. В качестве механизма предложено использование динамической стохастической модели агрегированного поведения агентов и модели передачи сигнала по принципу игры «жизнь». Представлены алгоритмы численного моделирования разработанных механизмов, а так же результаты их работы для разных сценариев.

Ключевые слова: многоагентное моделирование, гауссовский процесс, механизм самовосстановления, геотехнические структуры, биотехнология

1. INTRODUCTION

It is well-known, that concrete, being the most world common building materials, as all composite materials, despite its strength, collapses over time. Therefore, the proper engineering and maintenance as well as enhance the durability and serviceability of technical structures become crucial conditions. Under external environmental uncertainty, constructions' reliability still is one of the most important factors during all stages of project development. Lately, the conception of self-healing materials in construction attracts special attention. Named Materials for Life (M4L) and inspired by self-regeneration properties and sustainable development of biological organisms and systems these last find applications in buildings foundations, selected types of cement, grouts and concrete, asphalt and many other geo-environmental and geotechnical structures [1].

Motivated by reliability from one side and by substantial savings maintenance costs of geostructures, the first significant achievements were made in the development of composite materials by adding stabilizing bio-chemical agents to concrete or asphalt. In simple way the self-healing mechanism can be explained as follows [2].

To improve the autogenous healing property of

concrete, some encapsulated healing agents (usually bacteria) are added to the composite [1–3]. Crack formation and interaction with the external environment instigate metabolic activities of agents and, in consequence, the production of limestone clogging the cracks. The feasibility of this solution was checked in different ways: the influence of capsules' size, the influence of nutrition, dosage etc. [3]. Despite the progress made in this field, there are many non-solved problems concerning self-healing mechanisms of named composites. One of them relates to the complex environmental behavior of living organisms' agglomerates and has to be also taken into account by biotechnology.

Biotechnology aims to use biological systems to make or modify products or processes for specific purposes of medicine, food production, agriculture, or mentioned engineering problems. Taking into account the complexity of biotechnological processes related to bioengineering, biomedical and molecular engineering, or biomanufacturing, one can expect that integrated multiple biological experiments, as a method of new technology development, are expensive and difficult to conduct. Hence, mathematical modeling and computer simulation via a well-defined set of assumptions can be performed to conduct desired experiments and, in a consequence, to test alternative hypotheses, theories, technologies, production and exploitation methods, etc. The quality of the modeling and the simulation depends on the model selection. This last one can be achieved by different approaches. Analyzing the tendencies of the selection of the mathematic models for the tasks of image and sequences recognition, in signal processing, in biomass dynamic prediction or epidemic spread (where signals contain white, rose or black noises or mixed noises) one can note that due to various heterogeneities the stochastic models give "better" and "richer" results than deterministic ones. It becomes particularly evident when the contact network is analyzed. Contact processes are assumed to be Poisson, Marcovian or non-Marcovian (see [6], [7] – pair approximation model, [8] – [10] – message passing model, or [11] – edge based model). However, to study the propagation mechanisms and dynamics of considered phenomenon, the models have also to reflect complex correlation structures (self-similarity, short-range or long-range dependences, stationarity or non-stationarity) [12]. Thus, due to the complexity of mathematical backgrounds the practical usage of these models is still limited [13].

The goal of this work is ***the development of a model of self-healing mechanism such that it could serve for the expansion of biotechnology***. Since, in general, the technology is based on the metabolic activity of biomass, we will focus our attention on the description of its activity with respect to the single elements as independent agents.

The rest of this paper is organized in the following manner. In Section 2, we propose two models that reflect an individual and aggregated behavior of the agents. For both models, the simulation algorithms are discussed in Section 3. The special attention is focused on the advantages of the mixed fractional Brownian motion application for the transition mechanism. Section 4 contains some illustrations and recommendations on the methodology application and its further development.

2. THE MODELS OF HEALING MECHANISM

By the self-healing mechanism, we mean the transition of a bacterium from a state of hibernation (for example, interaction with the environment arising from damage) to a state of metabolic activity in which the bacterium produces a substance that allows filling the crack[1]. The mechanism stops working at the moment of exhaustion of nutrients, as a result of which the bacterium goes into a state of hibernation. Bac-

[1]The ideas of this methodology were discussed by the author of this paper in the presentation "Mixed fractional Brownian motion: some perspectives of mathematical modeling for biotechnology" on NANOMED/11th ITMED 2018, Manchester, UK, 26-28 June 2018.

teria transmit signals to each other determining the behavior. We introduce a model of this mechanism, considering two problems, namely: the transition from state to state (*dynamic model*) for aggregated behavior and the principle of transmitting alerts about environmental changes of one bacterium (*message-passing model*).

2.1. The aggregated behavior model

Let $N = \{1, 2, ..., n\}$ denote a universe of encapsulated bacteria (we will call them agents) belonging to the same population. For the simplicity, we suppose that vital dynamics of the population is negligible and that with respect to a certain environmental conditions each agent can stay in one of three states, namely [14]:

- dormancy (the state of those who have the potential and feed for the physiological activity, but not activated yet);
- metabolic activity (the state of those who have been activated by exogenous factors);
- hibernation (the state of those who have been isolated due to lack of the feed or those who have used all the feed and as a consequence were forced to stop the physiological activity).

This subdivision gives three classes of agents according to their activity status. At some moment of time t, $t \in [t_0, t_1]$, $S(t)$, $I(t)$, and $R(t)$ represent the cardinalities of dormant, active, and hibernated classes correspondingly. The total population is

$$\forall t \quad S(t) + I(t) + R(t) \equiv n,$$

where $S(t) \geq 0$, $I(t) \geq 0$, $R(t) \geq 0$.

It is proved that bacteria actively exchange some kinds of chemical signals, coordinating their co-existence. The limited volume of nutrition does not allow on the unlimited growth of the encapsulated population. Moreover, when a lack of nutrition occurs, the agent secretes an appropriate substance, which allows the neighborhood to prepare for the transition to hunger and quickly adjust their metabolic processes.

Following to the ideas of [13], we allow all possible transitions between the states as it shown in Fig.1. Since at any time moment t for each agent, there exist the possibilities of the metabolic changing, there also exist the switching intensities, which depend on individual physiological parameters and on other exogenous factors concerning the population.

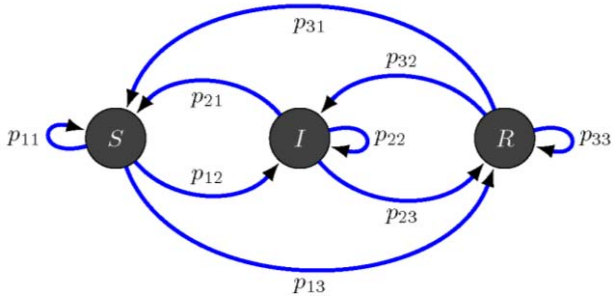


Figure 1. Three-state propagation mechanism (S –dormancy, I – metabolic activity, R – hibernation, $p_{jk}(t)$, $j,k \in \{1,2,3\}$ – the transition intensities).

Moreover, the passage of an agent from state to state occurs on the one hand due to contacts among individuals, on the other due to time-varying exogenous and endogenous factors which cannot be discovered or measured. Therefore, it is possible to assume that these intensities are randomly time-varying, we denote them as $p_{jk}(t)$ ($p_{jk} \geq 0$, $\forall j \quad 0 < \sum_k p_{jk} \leq 1$, $j,k \in \{1,2,3\}$, $t \in [t_0, t_1]$). Choosing values of the intensities one can get different classical deterministic compartmental models. That is to say if $p_{13} = p_{31} = p_{23} = p_{32} = 0$, then one get a well-known in biology "SI"-model, if $p_{13} = p_{21} = p_{32} = 0$, then it becomes a "SIRS"-model, and etc. (see e.g. [15]).

Without loss of generality, we limit our considerations and put $p_{21} = p_{32} = 0$. Moreover, we allow the time-varying stochastic state-to-state transition. Taking into account all the aforesaid, the dynamical model of the spread of the chemical signals, corresponding to the tree-state propagation mechanism (see Fig. 2), takes a form of the following system:

$$\begin{cases} \dfrac{dS(t)}{dt} = -x_1(t)S(t)I(t) + x_3(t)R(t) \\ \qquad\qquad -x_4(t)S(t), \\ \dfrac{dI(t)}{dt} = x_1(t)S(t)I(t) - x_2(t)I(t), \\ \dfrac{dR(t)}{dt} = x_2(t)I(t) - x_3(t)R(t) \\ \qquad\qquad +x_4(t)S(t), \end{cases} \quad (1)$$

where $x_1(t)$, $x_2(t)$, $x_3(t)$, and $x_4(t)$ are the transition rates between states such that x_1 stands for the transition from the state "S" to the state "I", x_2 – from "I" to "R", x_3 – from "R" to "S", and x_4 – from "S" to "R"; $S(t_0) = s_0$, $I(t_0) = i_0$, and $R(t_0) = r_0$. The equilibrium of the system (1) means the loose of the self-healing ability of the structure.

Let us comment the parameters of (1). Firstly, these parameters should be smooth enough in order to fulfill the conditions for the existence and uniqueness of the solution.

Secondly, if the time-varying parameters are deterministic, the model (1) displays "mean" behavior. Unlikely, all microorganisms will have the same reactions and, therefore, the same ability to transmit and/or to receive. To reflect the stochastic nature of phenomenon, the transitions rates should be driven by some continuous stochastic processes. Taking into account the ideas of [16] for all i one can put the parameters as

$$\tilde{x}_i(t) = \left(\tilde{x}_{i0}^{1-m_i} - a_i(m_i - 1)\tilde{B}_i(t)\right)^{\frac{1}{(1-m_i)}}, \quad (2)$$

where $\tilde{x}_i(t_0) = x_{i0}$ is the initial value, a_i and m_i are calibration parameters, $\tilde{B}_i(t)$ is some continuous stochastic process, defined as in [17] such that $B_i(t_0) = b_{i0}$ ($i = 1,...,4$). It seems natural to substitute the parameters (2) into (1) and to get the dynamics of (1), however, the theoretical properties and global behavior of this model are hardly possible to study. The alternative usage of (2) is the application of multi-agent modeling, i.e. the transition rates are unique for each agent, the evolution of these rates follows (2), the "global" behavior of (1) is estimated with respect to the cardinal numbers of each class.

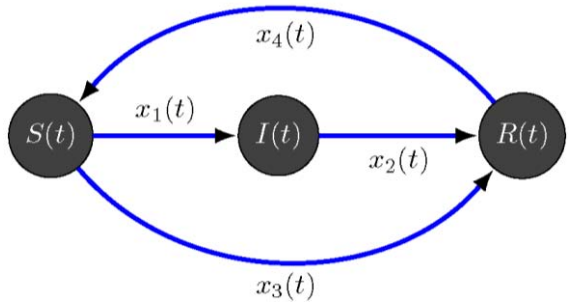


Figure 2. Dynamics of three-state propagation mechanism for the spread of the chemical signals ($S(t)$ – dormancy, $I(t)$ – metabolic activity, $R(t)$ – hibernation, $x_i(t)$, $i = 1,...,4$ the signal transition rates).

2.2. The message-passing model.

Now following the same reasoning as in [18], we suppose that the universe of N agents is an two-dimensional orthogonal grid (it can be easy compared with the damaged surface of an abstract geotechnical structure). Each agent is associated with one square cell of this grid and could interact with its eight neighbors (Moore's model, see Figure 3).

NW	N	NE
W	**C**	E
SW	S	SE

Figure 3. Moore neighborhood (C – active agent who transmits the signal in the directions N – north, E – east, S – south, W – west, NW – north-west, NE – north-east, SW – south-west and SE – south-east).

Each agent can be dormant, metabolically active, or hibernated forming so-called "configuration" at instant of time τ, $\tau \in [t_0, t_1]$. Each agent has its own endogenous characteristics, which allow it to send and receive signals as well as make the transitions from state to state. At the initial moment t_0 say n_0 agents ($n_0 << n$) are randomly activated (it can be considered as an epicenter of the crack on the surface of the geotechnical structure), the rest stay dormant. This configuration leads to a new one at instant of time $\tau + \Delta$ ($\Delta > 0, \tau + \Delta \in [t_0, t_1]$) according to the set of the following rules:

(i) the active agent transmits a signal to the nearest neighbors by Moore scheme with time-varying intensity,
(ii) if the signal is received, the neighbor becomes (with some probability) metabolically active (each agent is characterized by own threshold value for the signal acceptance);
(iii) if the metabolically active agent has two active-neighbor agents at the time τ, then it remains in its state at the time $\tau + \Delta$;
(iv) if the metabolically active agent has less than two active neighbors or more than three, its goes into the hibernation state;
(v) if at some instant in time none of the agents changes state, a universe of agents has the equilibrium, indicating the loss of the ability to self-healing.

3. SIMULATION ALGORITHM AND SOME RELATED QUESTIONS

3.1. The transition rates as the sample paths of the stochastic processes.

Let $(W_t)_{t \in \mathbb{R}_+}$ and $\left(W_t^H\right)_{t \in \mathbb{R}_+}$ be two independent stochastic processes (say a Brownian motion (Bm) and a fractional Brownian motion (fBm) of Hurst parameter $H \in (0,1)$) defined on the same probability space $(\Omega, F, \mathbb{P})$. A process

$$B^H = B^H(b_1, b_2) = b_1 W_t + b_2 W_t^H \qquad (3)$$

is called mixed fractional Brownian motion (mfBm) of parameters b_1, b_2 (b_1 and b_2 are two real constants such that $(b_1, b_2) \neq (0,0)$). The generalized properties of this process were studied and presented in [19, 21, 22]. In our case, we name among others the following properties:

- B^H is a centered Gaussian process and $B_0^H = 0$ a.s.;
- for any $t, s \in \mathbb{R}_+$ the covariance function of B_t^H and B_s^H is given by

$$\begin{aligned} Cov(t,s) &= \tfrac{1}{2} b_1^2 \left(t + s - |t - s|\right) \\ &+ \tfrac{1}{2} b_2^2 \left(t^{2H} + s^{2H} - |t - s|^{2H}\right); \end{aligned} \qquad (4)$$

- for any $\Delta > 0$ the increments of B^H are stationary and mixed-self-similar

$$\left\{B_{\Delta t}^H(b_1, b_2)\right\} \overset{D}{=} \left\{B_t^H\left(b_1 \Delta^{\frac{1}{2}}, b_2 \Delta^H\right)\right\}, \qquad (5)$$

where $\overset{D}{=}$ means "to have the same law";

- the increments of B^H are positively correlated if $\frac{1}{2} < H < 1$ (long-range dependence), uncorrelated if $H = \frac{1}{2}$ and negatively correlated if $0 < H < \frac{1}{2}$ (short-range dependence).

The sample paths of (3) can be simulated by different methods. We refer to the methodology developed by [20] for the fBm sample paths simulation. This method, based on the fast Fourier transform of the covariance function of the process allows on the multiple simulations of the uncorrelated sample paths of fBm. Moreover, the paper [20] contains the detailed description of the simulation algorithm, therefore we omit it here. The example of several sample paths of (3) for different values of Hurst parameters and $b_1 = b_2 = 1$ are listed on Figure 4. As it

is possible to notice, the mfBm sample paths give the characteristic mixed-colored noise that is the hallmark of this process.

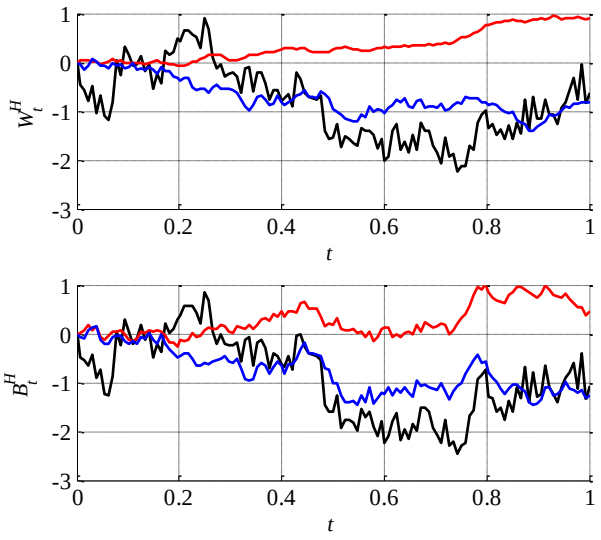


Figure 4. The sample paths of the Bm and fBm (W_t^H) and the mfBm (B_t^H) for different values of Hurst parameter ($H = 0.25$ – red trajectory, $H = 0.50$ – blue trajectory, $H = 0.75$ – black trajectory).

Further, replacing the process $\tilde{B}$ in (2) by the process (3) for $t \in [t_0, t_1]$

$$x(t) = \left(x_0^{1-m} - a(m-1) B^H(t) \right)^{\frac{1}{(1-m)}}, \quad (6)$$

fixing the initial value $x_{i0} = 0.5$, and taking different values of the scaling parameters a and m, we conclude as follows on the behavior of the stochastic process driven by (6). Several examples of the sample paths are presented on Figure 5 and Figure 6.

The mean value of the process (6) oscillates around the initial value (in this case it is 0.5), the variation on the scaling parameters is a convenient way to change the square-mean behavior of the transmission functions between 0 and 1. Therefore, the each agent transmits an activation signal with random intensity such that it can or can not be strong enough to activate neighbors.

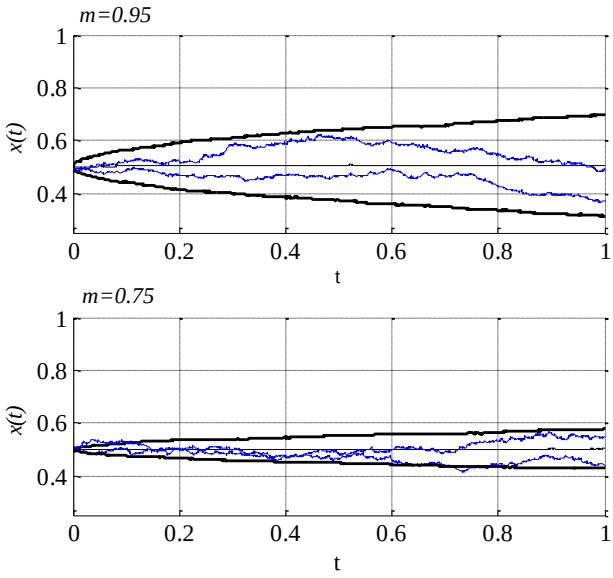


Figure 5. The sample paths of (6) and the confidential interval for $H = 0.75$ and $a = 0.125$.

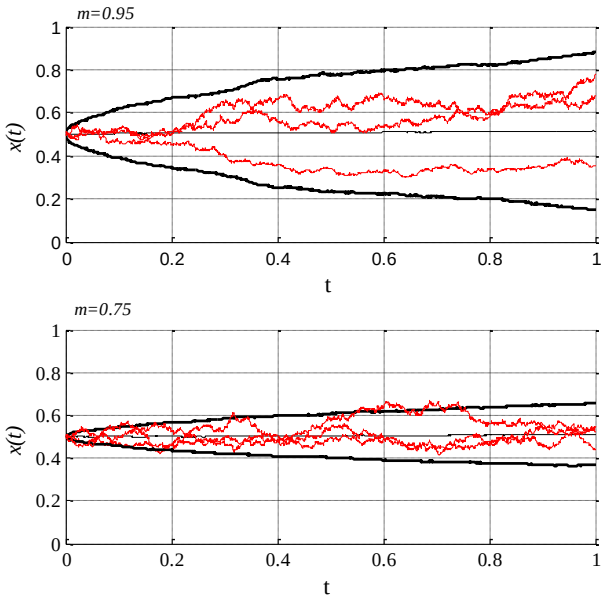


Figure 6. The sample paths of (6) and the confidential interval for $H = 0.75$ and $a = 0.250$.

3.2. The simulation algorithm for self-healing mechanism.

To illustrate the work of the self-healing mechanism, the following algorithm based on the multi-agent simulation method is proposed, namely:

I. Initialization - general settings of the artificial environment

- set the initial grid $M \times M$ and get the number of the agents $n = M^2$, initially each cell is associated with one non-activated anent;
- set the evolution time period $[t_0, t_1]$;
- define the m-stages equidistant discretization of the evolution time period $[t_0, t_1]$, such that $\tau_j = \tau_{j-1} + \Delta$, $\Delta = \frac{t_1 - t_0}{m}$, $\tau_0 = t_0$, $j = 1, 2, ..., m$;
- the initial cardinalities of groups: $I(\tau_0) = n_0$, $S(\tau_0) = n - n_0$, and $R(\tau_0) = 0$;
- the "mean" ability of the transmitted signal acceptance β,
- the initial values of transitions rates x_{i0}, values of parameters a_i and m_i, $i \in \{1, 2, 3, 4\}$.

II. Initialization - agent's and transmission characteristics:

- for each agent generate the set of the mfBm sample paths with the same values of b_1, b_2 and H using the m-stages equidistant discretization of the evolution time period,
- for each agent calculate the transmission characteristics (6) with respect to the set of the mfBm sample paths.

III. Processing – step evolution over time line $[t_0, t_1]$:

- activate the agents who will transmit the signal (select circle in the center of the grid with a radius of $r << M$ cells and consider the agents inside this circle as the activated one – we will call it as Protocol I – or activate the agents in randomly selected cells – we will call it as Protocol II);
- define the rules for the Moore neighborhood for the eight nearest neighbors (see Fig. 3);
- for each step of the evolution iterate over all cells in grid the spread of activation signal;
- if the agent is active, check the activity of the neighbors according to the rules (i) – (iv) and update the status of the agent;
- count the cardinality number of each group, check the rule (v), if the rule (v) is fulfilled stop the evolution.

IV. Aggregating behavior:

- complete the parametric identification of aggregate model (1) and its analysis.

4. SIMULATION RESULTS

We run several numerical experiments under Protocol I and Protocol II excluding the last step of the algorithm from the simulations. The interested reader can find all the details for the identification of the aggregated behavior and to get qualitative characteristics of the system (1) (for the details see [23]). In this work, the general settings of the artificial environment are the following, namely: $M = 100$, $t_0 = 0$, $t_1 = 1$, $m = 500$, $r = 4$ (for Protocol I), $n_0 = 50$ (for Protocol II), $x_{10} = 0.5$, $x_{20} = 0.4$, $x_{30} = 0.55$, $x_{40} = 0.45$; $H_i = 0.75$, $a_i = 0.025$ and $m_i = 0.85$, $i \in \{1, 2, 3, 4\}$; $b_1 = 0.7$, $b_2 = 0.3$; the update rules for the Moore neighborhood are given in matrix form

$$\begin{pmatrix} (1\ \text{-}1) & (1\ 0) & (1\ 1) \\ (0\ \text{-}1) & (0\ 0) & (0\ 1) \\ (\text{-}1\ \text{-}1) & (\text{-}1\ 1) & (\text{-}1\ 0) \end{pmatrix}.$$

The results of simulations are listed on Fig. 7 – 10 (blue, green, or red color refers to the dormant, metabolically active, or hibernated agent correspondently).

As one can see the initial placement of the active agents and relation between the mean ability of the transmitted signal acceptance and the initial values of transition rates have the crucial role in self-healing dynamics (compare Figure 7 with Figure 9 and Figure 8 with Figure 10). That is to say, for $\beta = x_{01} = 0.5$ the equilibrium is reached faster if the activated agents are randomly distributed on the damaged surface.

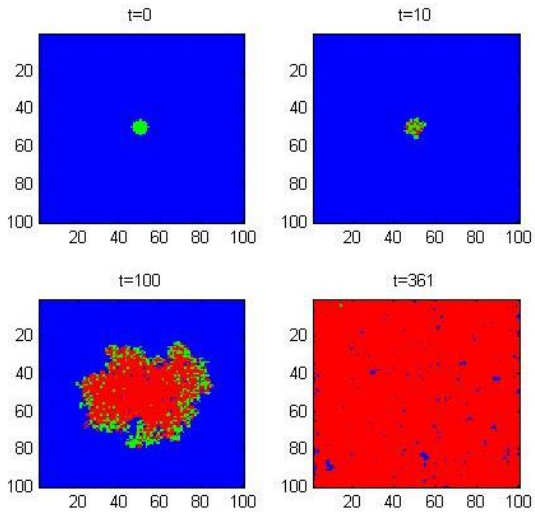


Figure 7. Protocol I ($\beta = 0.5$).

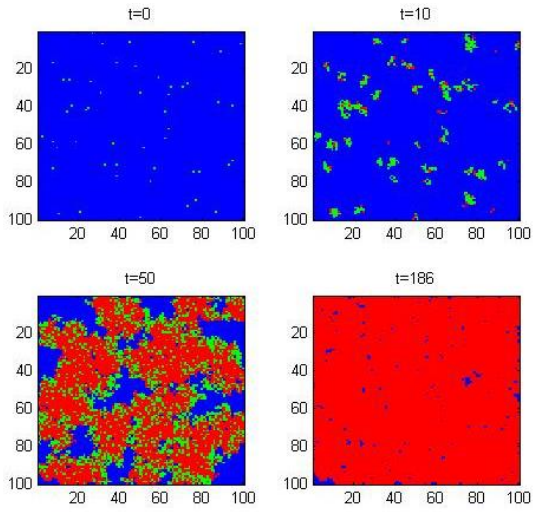


Figure 9. Protocol II ($\beta = 0.5$).

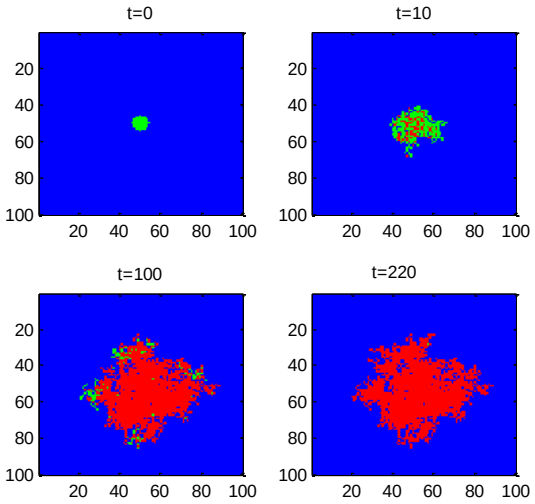


Figure 8. Protocol I($\beta = 0.1$).

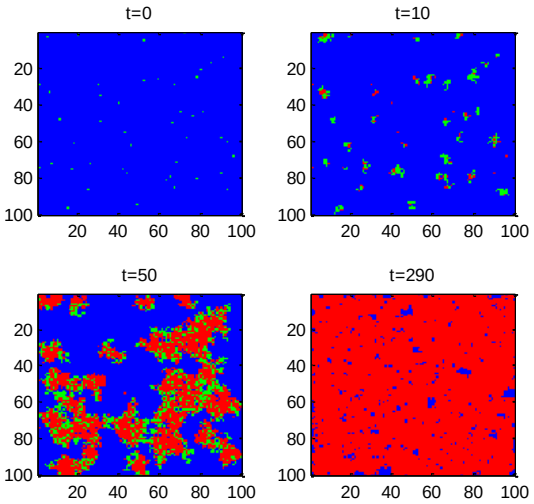


Figure 10. Protocol II ($\beta = 0.1$).

Moreover, the "repaired" surfaces can be compared by quantities of hibernated and dormant agents. In the case for $\beta < x_{01}$ the equilibrium is reached faster for the case when agents are concentratedly placed. This means that the transmission of the activation signal stops faster too (compare all the figures). Therefore, varying the parameters of the simulation model one can study different phenomena of the signals' transmissions.

5. CONCLUSIONS

The self-healing mechanisms for the damaged surface of an abstract geotechnical structure using biotechnology attract much attention of many scientists from different fields. Multi-agent modeling can help to solve numerous problems arising during new technology development. Proposed in this paper the two-component model of self-healing mechanism allows on the imitation of one or several cracks on a surface and on the estimation of life cycle of the material. In further investigation the 3D model of cracks as well as the parameters of the biologically active elements of the composites will be considered.

REFERENCES

1. **Gardner D., Lark R., Tony J., Davies R.** A survey on problems encountered in current concrete construction and the potential benefits of self-healing cementitious materials. // *Case Studies in Construction Materials*, 2018, Volume 8, pp. 238-247.
2. **Wiktor V., Jonkers H. M.** Quantification of crack-healing in novel bacteria-based self-healing concrete. // *Cement and Concrete Composites*, 2011, Volume 33 (7), pp. 763-770.
3. **Hilloulin B., Hilloulin D., Grondin F., Loukili A., De Belie N.**, Mechanical regains due to self-healing in cementitious materials: Experimental measurements and micro-mechanical model. // *Cement and Concrete Research*, 2016, Volume 80, pp. 21-32.
4. **Ahn T. , Kim H., Ryou J.** New Surface-Treatment Technique of Concrete Structures Using Crack Repair Stick with Healing Ingredients. // *Materials*, 2016, No. 9(8), pp. 654.
5. **Huang H., Ye G., Shui Z.**, Feasibility of self-healing in cementitious materials – By using capsules or a vascular system? // *Construction and Building Materials*, 2014, Volume 63, pp. 108-118.
6. **Sharkey K.J.** Deterministic epidemiological models at the individual level. // *Journal of Mathematical Biology*, 2008, Volume 57, Issue 3, pp. 311-331.
7. **Kiss I. Z., Rost G., Vizi Z.** Generalization of pairwise models to non-markovian epidemics on networks. // *Physical Review Letters*, 2015, Volume 115 (7), pp. 078701.
8. **Karrer B., Newman M.E.J.** Message passing approach for general epidemic models. // *Physical Review E*, 2010, Volume 82(1), pp. 016101.
9. **Simon P., Taylor M., Kiss I.**, Exact epidemic models on graphs using graph-automorphism driven. // *Journal of Mathematical Biology*, 2011, Volume 62(4), pp. 479-508.
10. **Wilkinson R.R., Ball F.G., Sharkey K.J.** The relationships between message passing, pairwise, kermack-mckendrick and stochastic SIR epidemic models. // *Journal of Mathematical Biology*, 2017, Volume 75, Issue 6, pp. 1563-1590.
11. **Miller J.C.** Spread of infectious disease through clustered populations. // *Journal of the Royal Society Interface*, 2009, Volume 6(41), pp. 1121-1134.
12. **Angstmann C., Henry B., McGann A.** A fractional-order infectivity sir model. // *Physica A: Statistical Mechanics and its Applications*, 2018, Volume 452, pp. 86-93.
13. **Lu J., Yu X., Chen G., Yu W.** Complex Systems and Networks: Dynamics, Controls and Applications. Springer-Verlag Berlin Heidelberg, 2016.
14. **Evdokimova N.V., Tchernenkaya T.V.** Persister Microbial Cells: a Novel View on the Old Problem. // Clinical Microbiology and Antimicrobial Chemotherapy, 2013, Volume 15(3), pp. 192-197.
15. **Edelstein-Keshet L.** Mathematical models in biology. SIAM, 2005.
16. **Galleani L.** Time-Frequency Characterization of Stochastic Differential Equations. In Rodino L., Wong M., Zhu H. (Eds.) *Pseudo-Differential Operators: Analysis, Applications and Computations. Operator Theory: Advances and Applications*, 2011, Volume 213, Springer, Basel, pp. 265-274.
17. **Samorodnitsky G., Taqqu M.S.** Stable non-Gaussian random processes. Chapman & Hall, 1994.
18. **Chu G., Karen K.E., Yorke-Smith N.**, Constraint Programming to Solve Maximal Density Still Life. In: Adamatzky A. (Ed.) Game of Life Cellular Automata, Springer London, pp. 167-175, 2010.
19. **El-Nouty C.** The fractional mixed fractional Brownian motion. // *Statistics & Probability Letters*, 2003, No. 65(2), pp. 111-120.
20. **Stoev S., Taqqu M.S.** Simulation methods for linear fractional stable motion and FARIMA using the fast Fourier transform. // *Fractals*, 2004, No. 12(1), pp. 95-121.

21. **El-Nouty C., Journé J-L.** Upper classes of the bifractional Brownian motion. // *Studia Sci. Math. Hungar*, 2011, Volume 48, pp. 371-407.
22. **El-Nouty C.** On approximately stationary Gaussian processes. // *International Journal for Computational Civil and Structural Engineering*, 2015, Volume 11, pp. 15-26.
23. **Filatova D.V., Baratgin J.** Multi-agent social choice model and some related questions. // 11th International Conference on Human System Interaction, 2018, pp. 425-431.
24. **Filatova D., Bourgeois-Gironde S., Baratgin J., Jamet F., Shao J.** Cycles of maximin and utilitarian policies under the veil of ignorance. // *Mind and Society*, 2016, No. 15(1), pp. 105-116.

Филатова Дарья, профессор, доктор физико-математических наук, кафедра информатики факультета компьютерных систем и сетей Белорусского государственного университета информатики и радиоэлектроники; Ассоциированный член Лаборатории человеческого и искусственного познания Практической школы высших исследований; 220013, Республика Беларусь, г. Минск, ул. П. Бровки, д. 6;
E-mail: filatova@bsuir.by;
orcid.org/0000-0001-9434-7993.

Darya Filatova, Professor, Dr.hab., Informatics Department, Faculty of Computer Systems and Networks, Belarusian State University of Informatics and Radioelectronics, Minsk, Belarus and associated member of CHART EPHE, Paris, France; BSUIR, Gikalo 9, 220005 Minsk, Belarus; E-mail: filatova@bsuir.by.

DOI:10.22337/2587-9618-2019-15-4-58-65

OPTIMIZATION OF SIMPLY SUPPORTED CASTELLATED I-BEAMS LOADED BY A UNIFORMLY DISTRIBUTED LOAD

Oleg S. Goryachevskiy
National Research Moscow State University of Civil Engineering, Moscow, RUSSIA
Scientific Research Center «StaDyO», Moscow, RUSSIA
Russian University of Transport (MIIT), Moscow, RUSSIA

Abstract: The paper discusses the problem of optimizing the geometric parameters of simply supported I-beams in order to maximize their load carrying capacity. Numerical simulation of various types of failure of castellated I-beams with ideal elastic-plastic steel is carried out. The stability of the wall, the strength of the welds and flanges, depending on the geometric parameters investigated. Using the coordinate descent method, the optimization problem is solved for nine design schemes with respect to the section height and the weld length. It was revealed that in short beams the section height should be less and the weld length longer, in contrast to long beams.

Keywords: castellated I-beam, numerical simulation, optimization, ideal elastic-plastic material

ОПТИМИЗАЦИЯ СВОБОДНО ОПЕРТЫХ РАЗВИТЫХ ДВУТАВРОВ, НАГРУЖЕННЫХ РАВНОМЕРНО РАСПРЕДЕЛЕННОЙ НАГРУЗКОЙ

О.С. Горячевский
Национальный исследовательский Московский государственный строительный университет, г. Москва, РОССИЯ
Научно-исследовательский центр СтаДиО, г. Москва, РОССИЯ
Российский университет транспорта (МИИТ), г. Москва, РОССИЯ

Аннотация: В статье рассматривается проблема оптимизации геометрических параметров развитых двутавров с перфорированной стенкой с целью максимизации их несущей способности. Проведено численное моделирование различных типов разрушения развитых двутавров в идеальной упругопластической постановке. Исследована устойчивость стенки, прочность швов и полок в зависимости от геометрических параметров. Используя метод покоординатного спуска, решена проблема оптимизации для девяти расчетных схем относительно двух параметров: высоты сечения и длины сварного шва. Выявлено, что в коротких балках высота сечения должна быть меньше, а длина шва больше, чем в длинных балках.

Ключевые слова: развитые двутавры, численное моделирование, оптимизация, идеальный упругопластический материал

INTRODUCTION

Existing analytical methods for calculating strength, rigidity and stability of castellated I-beams give a very approximate result [1-2]. These methods bad take in account a complexity of the geometric shape of the castellated I-beams and plastic deformation steel in angles of holes. These factors can be taken account with sufficient accuracy only by experiment and numerical methods. Of practical interest is the question of choosing such geometric parameters zigzag cutting I-beam that will provide maximum load carrying capacity of castellated I-beam. But experiment methods are too expensive and time-consuming for their application in full optimization problem.

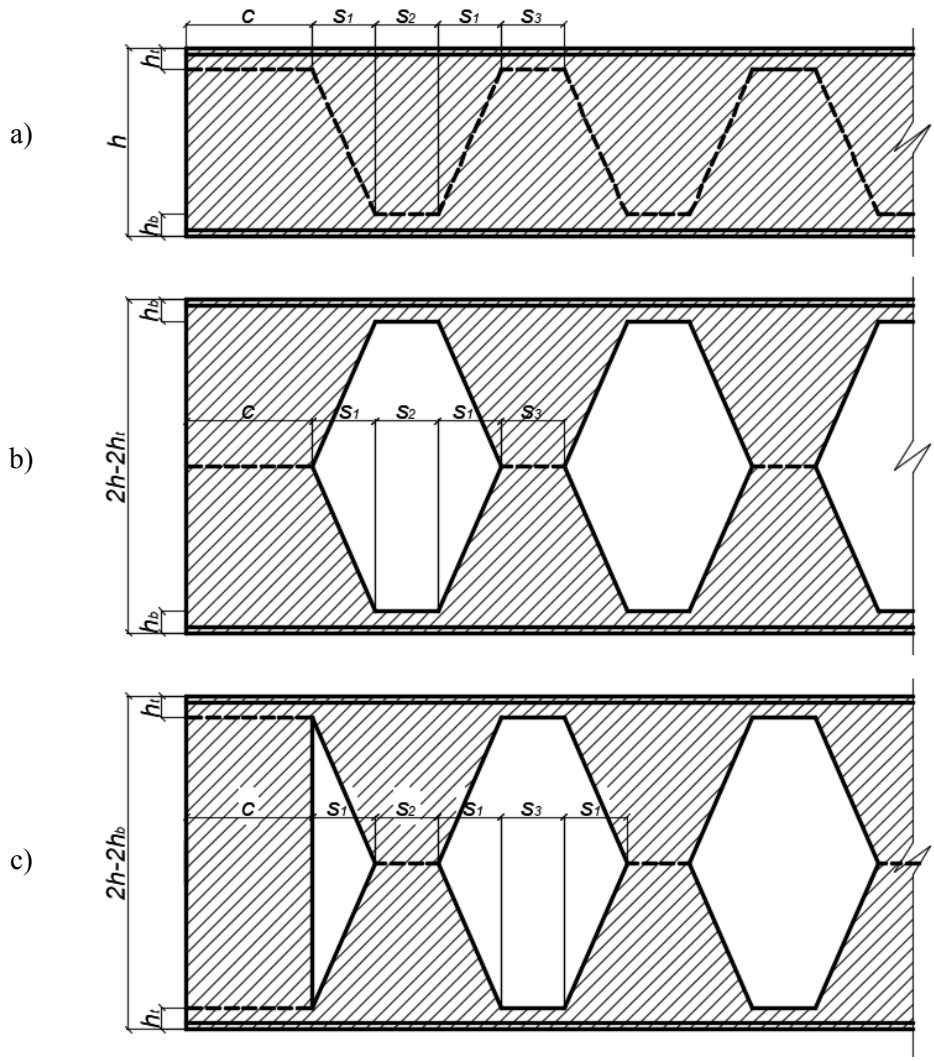


Figure 1. Scheme method for cutting (a) and subsequent welding of halves (b, c) of the original I-beam.

In this paper, to solve the nonlinear optimization problem, numerical methods are used. Stress-strain state and buckling is calculated by the finite element method. Using FEM analysis results, the ultimate load on the castellated I-beam is calculated according to several criteria (more about the criteria will be further in the text). To search the optimal geometric parameters, the coordinate descent method is used.

ANSYS Mechanical is used to solve the problem. APDL macros allow automated load carrying capacity calculation and use powerful capabilities of ANSYS in the finite element analysis [3].

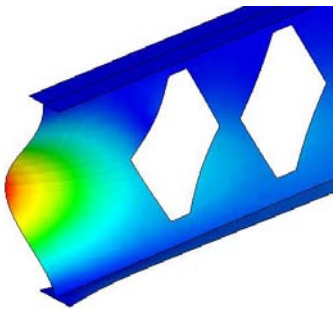
There are several methods for cutting and subsequent welding of halves of the I-beam. Different methods give different relationship between geometric parameter. The paper adopts the method illustrated in the Figure 1.

The article discusses the optimization of the load carrying capacity of the castellated I-beam composed of the lower halves of the original I-beams (Figure 1a). In order for the holes to be the same in both versions of the castellated I-beam (Figure 1b, 1c)

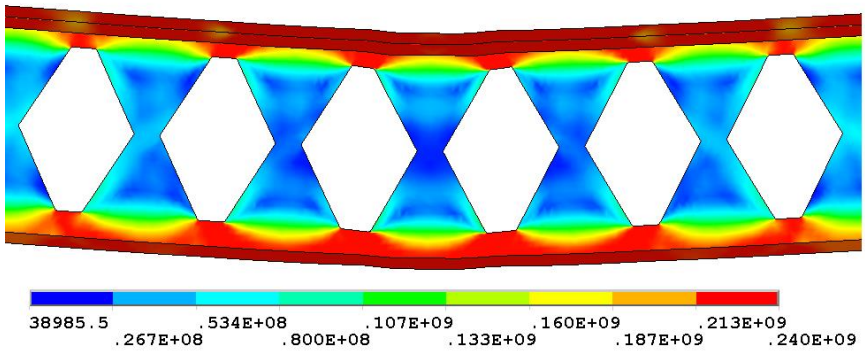
$$s_2 = s_3.$$

Radius of fillet in the corners due to cutting – $r = 1cm$.

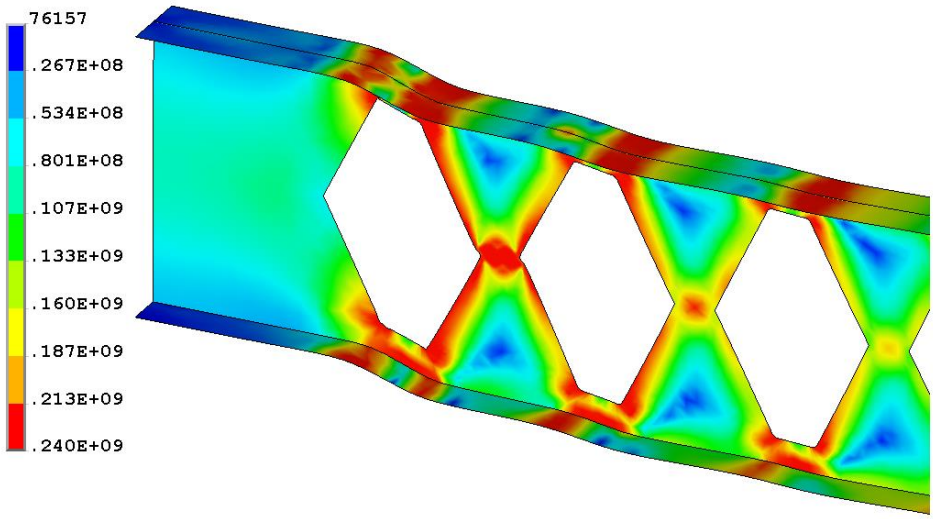
The design scheme: beam supported at its ends and loaded by a uniformly distributed load Q.



a) web buckling



b) failure of the flange and web in the centre of span (von Mises stress field on picture)



c) failure of the weld and the flange near support (von Mises stress field on picture)

Figure 2. Types of failure of the castellated I-beams.

The material model (steel): ideal elastic-plastic (stress-strain curve with elastic modulus $E = 206\ GPa$, yield strength $\sigma_y = 240\ MPa$, Poisson's ratio $v = 0.3$).

Geometric parameters of the original I-beams are taken according to GOST 8239-89 [4].

1. LOAD CARRYING CAPACITY PARAMETERS

There are 4 types of failure of the castellated I-beam supported at its ends and loaded by a uniformly distributed load:

1. Web buckling (Figure 2a).
2. Failure of the flange and web in the field of angles in the centre of span (Figure 2b).
3. Failure of the flange and web in the field of angles near support (Figure 2c).
4. Failure of the weld (Figure 2c).

For all types of failure, three parameters can be introduced:

1. $F_b = F_{cr}/1.5$, where F_{cr} – the first critical load, 1.5 – safety factor [1].
2. F_f – load at which plastic strain completely fills the section of the flange.
3. F_w – load at which plastic strain completely fills the weld between two holes.

To automatic calculate the F_b, a buckling analysis (by the Block Lanczos method, linear material model) was first performed. Then the first critical load F_{cr} devided by safety factor 1.5, due to the possible eccentricity of the load and the initial imperfections of the castellated I-beam.

The top flange was fixed against possible lateral movement and rotation around the longitudinal axis, thereby simulating the mounting of the castellated I-beam to overlying structures. The top flange boundary condition us used only in buckling analysis, since it strongly affects the forms of buckling.

To automatic calculate the F_f and F_w, a linear static calculation (linear material model) was initially performed to determine the load F_p at which plastic appears in the castellated I-beam flange. Then a load equal $1.2F_p$ was applied and the static calculation was performed with a nonlinear material with a load step of *0.01*. The load $1.2F_p$ is likely to lead to the failure of the I-beam, because according to analytical decisions, $\approx 1.18F_p$ is enough. Then, in the Postprocessor, a special algorithm at each load step checks for plastic strain in the nodes of the flange and nodes of the weld. If at some load step in a some section of the flange or in the weld in all nodes there are plastic strain, then this load step is recognized as the moment of failure. So,

$$F_f = 1.2F_p[i/100+(i-1)/100]/2,$$
$$F_w = 1.2F_w[j/100+(j-1)/100]/2,$$

where i – load step is recognized as the moment of failure flange, j – load step is recognized as the moment of failure weld.

Ideal elastoplastic material behaves unphysically in the support zone. If fix the beam pointwise on the edge, then near the fastening large plastic strain will quickly develop and the solution will fall apart. Therefore, in a nonlinear analysis at the edges of the beam, all nodes in the section were fixed in the direction of deflection. This avoids problems with the boundary effects.

2. FINITE ELEMENT MODELS

Geometric and finite element model are created automatically using developed APDL macros [3]. In the area between the last holes, and also above them and central holes, the mesh is more detailed. Failure occurs in these areas. Only the top flange for searching for plastic strain is considered, as it does not have boundary effect of supports (Figure 3).

The weld does not differ geometrically and in properties from the steel of original I-beam.

Elements type – *Shell 181*. In the buckling analysis, to combat non-physical buckling forms, full integration in the wall elements was used. Also, a coarser grid was used in the linear and buckling analyses.

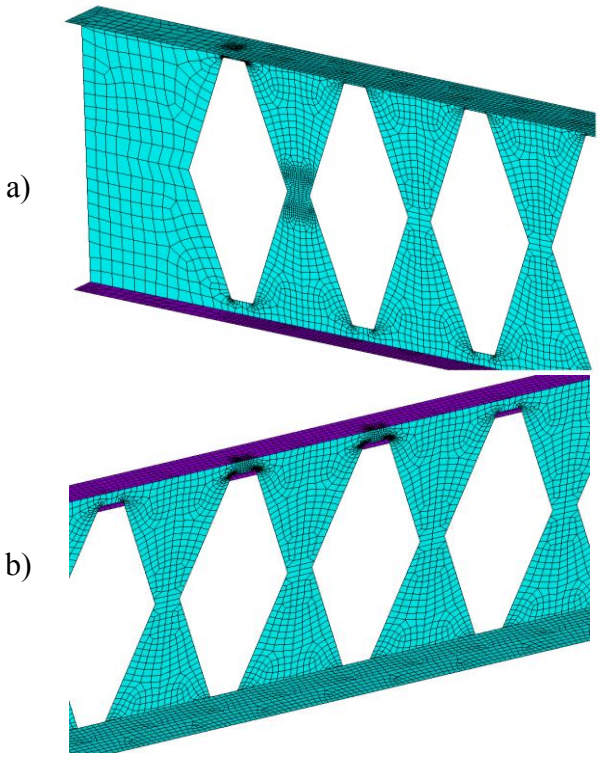


Figure 3. Fragments of the finite element model. Number of elements: ~15-40 thousands depending on the length of the beam and the number of holes.

3. DEPENDENCE OF F_b, F_f AND F_w ON GEOMETRUC PARAMETERS

The important points to make about F_w and F_f calculations:

- if $F_f < F_w$ (much), then F_w cannot be calculated correctly. The fact is that with the destruction of the flange of the castellated I-

beam, the entire structure suffers a collapse – a sharp increase in deflections and plastic strain. In such conditions, the solution loses stability and cannot give correct results;

- if weld length s_2 is large enough, then the weld failure does not occur under load $1.2F_p$. In this case, F_w is not calculated.
- if F_w and F_f changed less than 1%, when changing the argument, then curve F_w and F_f may contain some fluctuations, because load step is also 1%.

The geometric parameters of cutting significantly affect both the magnitude of the F_b, F_f and F_w and the types of failure. For example, large values of c and h_b increase stability (F_b), small values s_2 decreases weld strength (F_w). However, many other dependencies are not obvious and require preliminary study (figure 4).

Figure 4a shows the dependence of F_b, F_f and F_w on c. F_b is obviously increasing, F_f increasing as the failure of the flange at the support is moving away from the support, F_w decreases as reduced weld length s_2 (s_1 is fixed). The reasonable change c does not reveal the presence of extrema.

The number of holes N affects the weld length s_2 (if s_1 is fixed), so F_w decreases (figure 4b). Stability almost independent of hole count N. Flange strength decreases after weld failure – two holes merge into one and the span of the flange increases.

4. STATEMENT OF OPTIMIZATION PROBLEM OF THE CASTELLATED I-BEAM

The problem of maximizing the load carrying capacity can be defined as follow [5-6]:

$$F = \min\left(F_b, F_f, F_w\right) \to \max$$

Objective function F depends on the geometric parameters, type of load and support condition.

For the selected cutting method (Figure 1), the uniformly distributed load and supported at its ends:

$$F = F\left(I, L, c, r, N, s_1, s_2 = s_3, h_b = h_t\right),$$

where L – length of beam, I – number of profile, which defines a number of geometric parameters of section, r – radius of fillet in the corners due to cutting.

Parameter s_1 is not independent:

$$s_1 = \left(L - 2c - \left(2N-1\right)s_2\right)/2N\,.$$

Parameters I and L do not change during of one optimization problem. $r=10mm$ for all schemes.

In the article, we will determine c and N ourselves, and we will optimize only for two parameters s_2 and h_b. Thus, for each design scheme:

$$F = F\left(s_2, h_b\right).$$

Only geometrically inequality constraints:

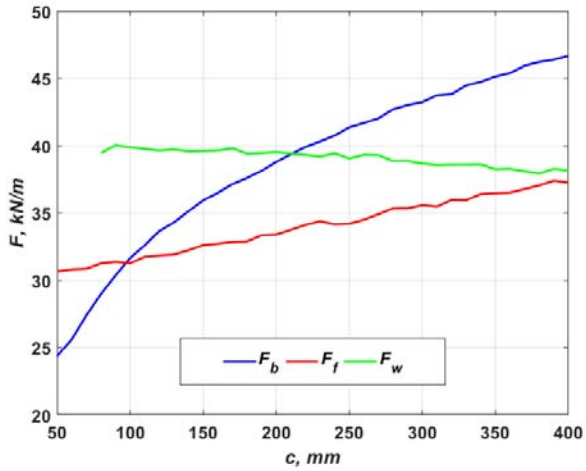
$$0 < s_2 < \left(L - 2c\right)/\left(2N-1\right),$$
$$t < h_b < h/2,$$

where t – thickness of flange, h – height of original I-beam.

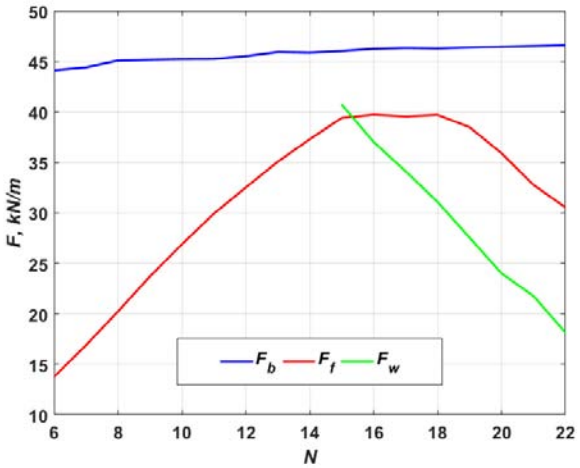
From a technical point of view, we can narrow the conditions without risking losing the optimal point:

$$20mm \le s_2 \le \left(L - 2c\right)/\left(2N-1\right) - 10mm,$$
$$2t \le h_b \le 2h/5$$

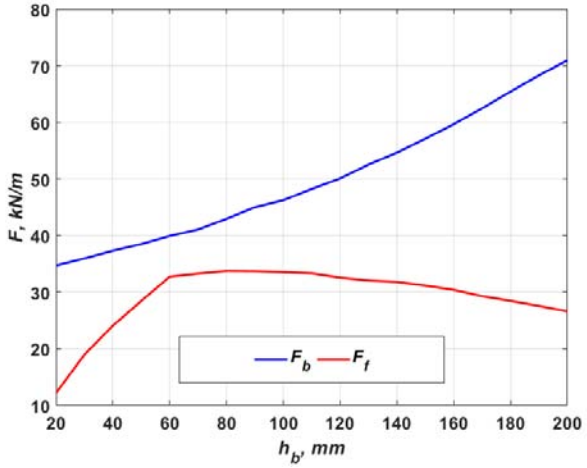
Computation the objective function using the finite element method has some problems. Nonlinear material properties and a difference in the mesh at different points introduce a small noise into the objective function. The presence of noise does not allow the use of derivative-based optimization methods and impairs convergence [7-8].



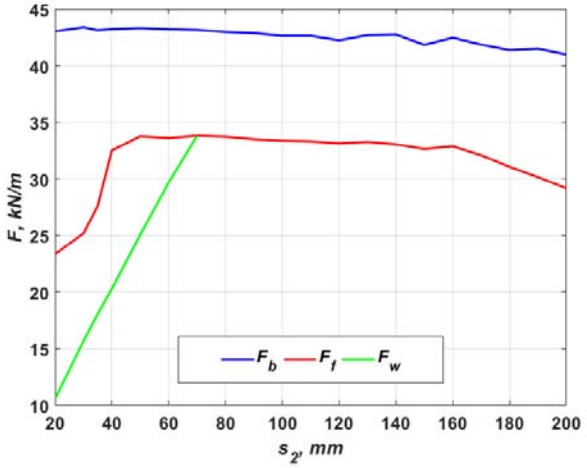
a) Dependence of F_b, F_f and F_w on the c
$c \in [50; 400] mm$, step $10\,mm$
$I30$, $L = 6m$, $N = 16$, $s_1 = 100mm$, $h_b = 50mm$



b) Dependence of F_b, F_f and F_w on the N
$N \in [6; 22]$, step 1 pc
$I30$, $L = 6m$, $c = 300mm$, $s_1 = 100mm$, $h_b = 60mm$



c) Dependence of F_b, F_f on the h_b
$h_b \in [20; 200] mm$, step $10\,mm$
$I50$, $L = 12m$, $N = 24$, $c = 400mm$, $s_2 = 85.1mm$



d) Dependence of F_b, F_f and F_w on the s_2
$s_2 \in [20; 200] mm$, step $10\,mm$
$I50$, $L = 12m$, $N = 24$, $c = 400mm$, $h_b = 80mm$

Figure 4. Dependence of F_b, F_f and F_w for some configuration of castellated I-beam.

5. OPTIMIZATION RESULTS

To search the optimal point (s_2^*, h_b^*), the coordinate descent method was used. At each iteration, the golden-section search was used as the linear search method. The optimal point was calculated with sufficient accuracy after two iterations of the coordinate descent method.
Initial point:

$$(s_2^0, h_b^0) = \left(\frac{s_2^{\min} + s_2^{\min}}{2}; \frac{h_b^{\min} + h_b^{\min}}{2} \right).$$

Tolerance of golden-section search

$$\Delta s_2 \le 2.5mm; \quad \Delta h_b \le 2.5mm.$$

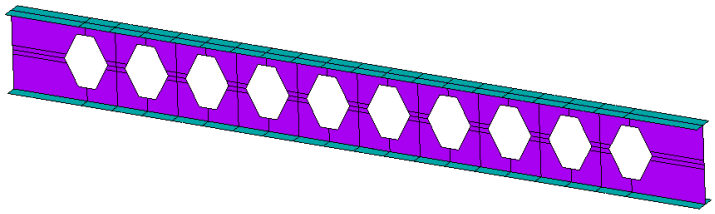
The optimization results are presented in Table 1 and Figure 6.
An important non-dimensional parameter of castellated I-beams – height increase ratio (Table 2).

Table 1. Optimization results.

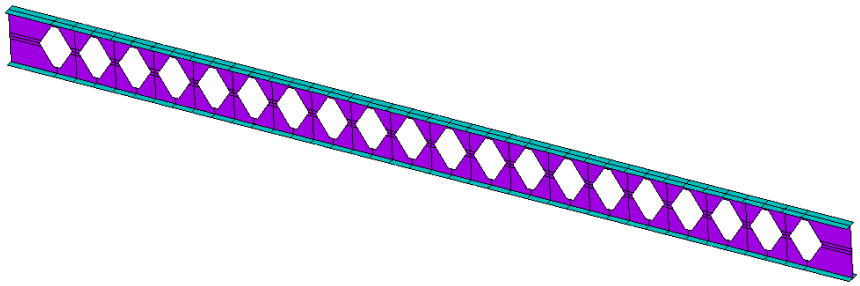
No.	I	L, m	c, mm	N	s2, mm			hb, mm			F, kN	
					min	max	opt	min	max	opt	min	max
1	30	4	300	10	20.0	168.9	99.6	20.4	120.0	77.5	59.73	70.70
2		6	300	16	20.0	164.2	79.1	20.4	120.0	67.4	28.61	39.33
3		8	300	20	20.0	179.7	93.3	20.4	120.0	57.4	19.10	22.53
4	40	5	350	12	20.0	177.0	107.2	26.0	160.0	117.2	78.04	98.90
5		8	350	16	20.0	225.5	94.9	26.0	160.0	80.9	32.57	44.96
6		10	350	20	20.0	228.5	80.0	26.0	160.0	78.1	26.25	29.19
7	50	6	400	12	20.0	216.1	122.7	30.4	200.0	156.4	89.59	115.83
8		9	400	20	20.0	200.3	92.7	30.4	200.0	99.9	46.35	59.11
9		12	400	20	20.0	277.2	89.6	30.4	200.0	96.3	19.74	33.78

Table 2. Height increase ratio.

No.	1	2	3	4	5	6	7	8	9
k	1.48	1.55	1.61	1.41	1.60	1.61	1.37	1.60	1.61



a) *I30, L=4m, c=300mm, N=10*



b) *I40, L=10m, c=350mm, N=20*

Figure 5. Several optimized castellated I-beams: No. 1 (a) and No. 6 (b) from Table 1.

$$k = 2\left(h - h_b\right)/h = 2\left(1 - h_b/h\right).$$

6. CONCLUSIONS

Castellated I-beam load carrying capacity has maximum for many design schemes. However, for some geometric parameters, not all schemes have extrema. Nevertheless, the task of increasing the carrying capacity remains relevant.

Section height and weld length always have a maximum point, therefore, in this work, the problem of optimizing these parameters was solved.

Based on the 9 considered design schemes (Table 1), some conclusions can be drawn:

- the optimal height increase ratio of castellated I-beams increases with increasing span (Table 2)
- the relative length of the weld decreases with increasing span.

The first conclusion is explained by the fact that in short beams, destruction occurs in the zone of

supports. Wall height is a determining factor in its stability. However, stability can be ensured by installing stiffeners. It can be expected that when using stiffeners, the optimal solution will change. In long beams, destruction occurs in the middle of the span from the action of a bending moment. In such type of failure, an increase in the inertia moment by increasing the section height gives the greatest increase in the carrying capacity.
The second conclusion is also related to the type of failure. Welds between end holes have the highest stresses. Therefore, the cause of the loss of load-carrying ability may be the failure of the weld. Increasing the weld length solves this problem.

REFERENCES

1. SP 16.13330.2011 Stal'nye konstrukcii [Steel constructions]. Moscow, Minregion Rossii, 2011.
2. **Pritykin A.I.** Razrabotka metodov rascheta i konstruktivnyh reshenij balok s odnoryadnoj i dvuryadnoj perforaciej stenki [Development of calculation methods and design solutions for beams with single and double row wall perforations]. Diss. na soiskanie uchenoj stepeni d.t.n. Kaliningrad: KGTU, 2011, 331 pages.
3. ANSYS Mechanical 19.2 Tutorials. Canonsburg, 2019.
4. **GOST 8239-89** Hot-rolled steel flange beams. Rolling products. Moscow, IPK Izdatel'stvo standartov, 2003.
5. **Haug E.J., Arora J.S.** Prikladnoe optimal'noe proektirovanie: Mehanicheskie sistemy i konstrukcii [Applied optimal design: Mechanical and structural systems]. Moscow, Mir, 1983, 478 pages
6. **Malkov V.I., Ugodchikov A.G.** Optimizaciya uprugih system [Optimization of elastic systems]. Moscow, Nauka, 1981, 288 pages.
7. **Kochenderfer M.J., Wheeler T.A.** Algorithm for optimization. Cambridge, Massachusetts, The MIT Press, 2019, 500 pages.
8. **Vasil'ev F.P.** Metody optimizacii [Optimization methods]. Moscow, Izdatel'stvo “Faktorial Press”, 2002, 824 pages.

СПИСОК ЛИТЕРАТУРЫ

1. СП 16.13330.2011 Стальные конструкции. – М.: Минрегион России, 2011.
2. **Притыкин А.И.** Разработка методов расчета и конструктивных решений балок с однорядной и двурядной перфорацией стенки. Диссертация на соискание ученой степени доктора технических наук по специальности 05.23.01 – «Строительные конструкции, здания и сооружения». – Калининград: КГТУ, 2011. – 331 с.
3. ANSYS Mechanical 19.2 Tutorials. Canonsburg, 2019.
4. ГОСТ 8239-89 Двутавры стальные горячекатаные. Сортамент. М.: ИПК Издательство стандартов, 2003.
5. **Хог Э., Арора Я.** Прикладное оптимальное проектирование: Механические системы и конструкции. – М.: Мир, 1983. – 478 с.
6. **Малков В.И., Угодчиков А.Г.** Оптимизация упругих систем. – М.: 1981. – 288 с.
7. **Kochenderfer M.J., Wheeler T.A.** Algorithm for optimization. Cambridge, Massachusetts, The MIT Press, 2019, 500 pages.
8. **Васильев Ф.П.** Методы оптимизации. – М.: Издательство «Факториал Пресс», 2002. – 824 с.

Oleg G. Goryachevskiy, Lecturer at the Department of Applied Mathematics, National Research Moscow State University of Civil Engineering, Senior Engineer of Scientific Research Center “StaDyO”, Director of Center of Computer Simulation, Russian University of Transport (MIIT); office 810, 18, 3ya Ulitsa Yamskogo Polya, Moscow, 125040, Russia; phone +7 (499) 706-88-10,
E-mail: osgoryachevskij@mail.ru.

Горячевский Олег Сергеевич, преподаватель и аспирант кафедры прикладной математики Национального исследовательского Московского строительного университета, ведущий инженер расчетчик ЗАО «Научно-исследовательский центр СтаДиО» (ЗАО НИЦ «СтаДиО»), директор Центра компьютерного моделирования (ЦКМ) Российского университета транспорта; 125040, Россия, г. Москва, ул. 3-я Ямского Поля, д.18, 8 этаж, офис 810, тел. +7 (495) 706-88-10;
E-mail: osgoryachevskij@mail.ru.

DOI:10.22337/2587-9618-2019-15-4-66-82

THE SECOND STAGE OF STRESSED-DEFORMED CONDITION OF REINFORCED CONCRETE STRUCTURES WHEN TURNING WITH BENDING (CASE 2)

Vladimir I. Kolchunov, Aleksey I. Demyanov, Nikolay V. Naumov
South-Western State University, Kursk, RUSSIA

Abstract. It is proposed a complex resistance computational model of reinforced concrete constructions in buildings and structures under the action torsion with bending. It consists of from the block near the support (formed by a spatial crack and a compressed concrete zone closed by it – a spatial section k) and a second block, which is formed by a vertical cross section I–I passing perpendicularly to the longitudinal axis of the reinforced concrete element along the edge of the compressed zone, which closes the spatial spiral-shaped crack. The case when the greatest influence on the stress-strain state of structures has the effect of torque is considered (case 2). In this case, as the calculated forces are taken into account in the spatial section: normal and tangential forces in the concrete of the compressed zone; components of axial and "dowel" efforts in the working reinforcement, intersected by a spiral spatial crack. The resolving equations are constructed that form a closed system and the Lagrange function is unified. Using the partial derivatives of the constructed function with respect to all the variables entering into it and equating them to zero, an additional system of equations is constructed. The dependence is obtained after the corresponding algebraic transformations, that allows us to search for the projection of a dangerous spatial crack.

Keywords: calculation methodics, torsion, stress-strain state, reinforced concrete constructions, spatial crack, Lagrange function

ВТОРАЯ СТАДИЯ НАПРЯЖЕННО-ДЕФОРМИРОВАННОГО СОСТОЯНИЯ ЖЕЛЕЗОБЕТОННЫХ КОНСТРУКЦИЙ ПРИ КРУЧЕНИИ С ИЗГИБОМ (СЛУЧАЙ 2)

Вл.И. Колчунов, А.И. Демьянов, Н.В. Наумов
Юго-Западный Государственный Университет, г. Курск, РОССИЯ

Аннотация. Предложена расчетная модель сложного сопротивления железобетонных конструкций в зданиях и сооружениях при кручении с изгибом, состоящая из приопорного блока (образованного пространственной трещиной и замыкаемой на нее сжатой зоной бетона, – пространственное сечение k) и второго блока, образуемого вертикальным сечением I–I, проходящим перпендикулярно к продольной оси железобетонного элемента по краю сжатой зоны, замыкающей пространственную спиралеобразную трещину. Рассмотрен случай когда наибольшее влияние на напряженно-деформирванное состояние конструкций оказывает действие крутящего момента (случай 2). При этом в качестве расчетных усилий в пространственном сечении учитываются: нормальные и касательные усилия в бетоне сжатой зоны; составляющие осевых и нагельных усилий в рабочей арматуре, пересекаемой спиралеобразной пространственной трещиной. Составлены разрешающие уравнения, образующие замкнутую систему и записана функция Лагранжа их объединяющая. Используя частные производные построенной функции по всем входящим в нее переменным и приравнивая их нулю, составлена дополнительная система уравнений, из которой после соответствующих алгебраические преобразований, получена зависимость, позволяющая отыскивать проекцию опасной пространственной трещины.

Ключевые слова: методика расчета, кручение, напряженно–деформированное состояние, железобетонные конструкции, пространственная трещина, функция Лагранжа

1. INTRODUCTION

Building computational models of complex resistance - torsion with a bend is becoming increasingly relevant [1, 2], firstly, because there are relatively few such studies [3–9], and secondly, because the urgent need to take into account the spatial work of the majority of original reinforced concrete structures and buildingss that significantly change the architectural appearance of modern cities [10–12]; thirdly, it becomes a generally accepted postulate that there is nothing more practical than a good theory for calculation of reinforced concrete structures [13–23].

That is why the purpose of these studies is to develop a computational model of the resistance of reinforced concrete structures under the action of torsion with bending for a cross section of any shape that most fully reflect the features of their actual work [2, 12, 17].

For the calculated forces, the resolving equilibrium and strain equations are compiled. The projection of a dangerous spatial crack is determined as a function of many variables using Lagrange multipliers [13, 15].

2. METHOD

While solving a direct engineering problem with external forces, their ratio is always given (Q: M: T). Thus, having determined one of them, for example, the support reaction R_{sup}, the other effects, for example, M and T, can be easily found.

From the balance conditions in cross-section I-I and in the spatial cross-section can be sought the following design parameters (Figures 1, 2): the limiting support reaction R_{sup}; height of compressed zone x in section *I-I*; stresses in the longitudinal reinforcement σ_s at the place of its intersection with a spatial crack; the height of the compressed zone of concrete x_b in a vertical plane passing through the end of the front of a spatial crack; running force in the transverse reinforcement located at the lateral faces of the spatial section $q_{sw,Q}$, caused by the transverse force; running force in the transverse reinforcement located at the lateral faces of the spatial section $q_{sw,T}$, caused by the torque; running force in the transverse reinforcement located at the lower edge of the spatial section $q_{sw,\sigma}$, caused by the torque.

Figure 1 shows: a) a support block (formed by a spatial section k) and a block formed by a vertical section I–I, passing perpendicular to the longitudinal axis of the reinforced concrete element at the edge of the compressed zone closing the spatial spiral-shaped crack; b) - vertical section I – I (III – III), passing perpendicular to the longitudinal axis of the reinforced concrete element, stress plots in compressed concrete and tensioned reinforcement, as well as the distribution of torques in this section. Figure 2 shows spatial section k with projections of all the efforts that occur at the site of the section.

The shear stress τ_Q and the shear stress of torsion in compressed concrete τ_T are determined by projecting the $\sigma_i - \varepsilon_i$ diagram onto the $\tau - \gamma$ plane (taking into account the distribution in proportion to the *Q:T* ratio) and onto the *I–I* plane and projecting the components of the stresses of the k plane onto the plane perpendicular to the longitudinal axis of the reinforced concrete element.

To make the calculation equations, we will separate two blocks from the reinforced concrete element using the section method (Figures 1, 2). The first block is separated by a cross section I-I, passing at the end of a spatial crack. This block is in equilibrium under the influence of external forces.

The second scheme (the first block - section 1–1) is realized with the resistance of reinforced concrete elements subject to the joint action of torques and transverse forces.

To make the calculation equations, we will separate two blocks from the reinforced concrete element using the section method (Figures 1, 2). The first block is separated by a cross section I–I, passing at the end of a spatial crack. This block is in equilibrium under the action of ex-

ternal forces from the support and internal forces arising at the section.

The proposed calculation model is based on the following ***prerequisites:***

- the spatial crack on the lower face of the reinforced concrete element forms perpendicular to the direction of the main deformations of the elongation of the concrete, and the location of the end of the front of the spatial crack at the compressed edge of the reinforced concrete element coincides with the direction of the main deformations of the concrete shortening – thus, the spatial crack has a spiral shape with three possible layouts of the compressed zone – Figure 2;
- the calculation scheme is taken as a design consisting of a support block (formed by a spatial crack and a vertical section passing through the end of the front of this crack in compressed concrete) and a second block formed by a vertical section perpendicular to the longitudinal axis of the reinforced concrete element along the edge of the spatial crack – Figures 1, 2;
- in the spatial section for making the calculation equations following forces are taken into account: normal and tangential forces in the concrete of the compressed zone; components of axial forces in the reinforcement located at the face opposite to that in which the compressed zone is located; components of axial forces in the transverse reinforcement located at the side faces of the reinforced concrete element;
- for medium fiber deformations of compressed concrete and tensiled reinforcement in section *I-I*, is fair hypothesis of their proportionality to the heights of the compressed and stretched section zones;
- the relationship between the strain intensity ε_i and the stress intensity σ_i of concrete is taken in the form of a diagram shown in Figures 3 a, b (for practical calculations, the curvilinear diagram of compressive stresses is replaced by a rectangular diagram above a spatial crack in cross-section *k* - see Fig. 3 c, d, and in cross-section *I-I* in site x_b - rectangular, in site x-x_b - triangular).

The curved section of the «σ_i–ε_i» diagram (Figure 3 a) is described by a square parabola:

$$\sigma_i = \frac{R_b - E_b \cdot \varepsilon_{br}}{\varepsilon_{br}^2} \cdot \varepsilon_i^2 + E_b \varepsilon_i \,, \qquad (1)$$

and straightforward as a linear function:

$$\sigma_i = R_b - \frac{R_b(1-\beta)}{\varepsilon_{bu} - \varepsilon_{br}} \cdot (\varepsilon_i - \varepsilon_{br}) \,. \qquad (2)$$

The parameters $R_{crc,0}$ and $R_{crc,v}$ can be calculated by the formulas given in the reference book [19]. Then $\varepsilon_{crc,0}$, $\varepsilon_{crc,v}$. can be determined from the diagrams (Figure 3a). For example,

$$\varepsilon_{crc,v} = \frac{E_b \cdot \varepsilon_{br}^2}{E_b \cdot \varepsilon_{br} - R_b} + \sqrt{\frac{E_b^2 \cdot \varepsilon_{br}^4}{(E_b \cdot \varepsilon_{br} - R_b)^2} + R_{crc,v}} \,. \qquad (3)$$

The value of $\mu(\lambda)$ at point H corresponds to its value at the point (at these points the stresses in concrete are the same):

$$\mu(\lambda) = 0,2 + \frac{0,3 \cdot (\varepsilon_\beta - \varepsilon_{crc,0})}{\varepsilon_{crc,v} - \varepsilon_{crc,0}}, \qquad (4)$$

$$\varepsilon_\beta = \frac{E_b \cdot \varepsilon_{br}^2}{E_b \cdot \varepsilon_{br} - R_b} + \sqrt{\frac{E_b^2 \cdot \varepsilon_{br}^4}{(E_b \cdot \varepsilon_{br} - R_b)^2}} \,. \qquad (5)$$

The formation of cracks in concrete and its destruction is described by various theories of strength, since the cause of cracking is always the main deformation of the separation, and the cause of the destruction can also be shear deformation at the octahedral sites. For the accepted version of the deformation theory of concrete ductility [2], we will give preference to deformation criteria of strength, because for concrete located in structural elements, experimental verification of only deformations is possible. The

requirements are also presented for the possibility of a direct transition of the stress – strain dependences to the strength condition.

The equations above contain the parameters R_q, $\varepsilon_{q,R}$, $\varepsilon_{q,u}$, $R_{b,z}$, $\varepsilon_{b,z}$, whose values are determined by projecting the diagram «σ_i–ε_I» on the corresponding planes, for example, «τ_q–ε_q». Projection is carried out using the obtained formulas and formulas of mechanics of a solid deformable body for continuous sections of concrete [2].

When preparing equilibrium equations, it is also necessary to take into account the angle α associated with the projection of a dangerous spatial crack c and the angle β that determines the direction of the main deformations of concrete shortening in the vertical section k.

To make the calculation equations, we will separate two blocks from the reinforced concrete element using the section method (Fig. 1, 2). The first block is separated by a cross section *I-I*, passing at the end of a spatial crack. This block is in equilibrium under the action of external forces applied to the block from the support side and internal forces arising at the section.

From the equation of equilibrium of moments of internal and external forces in section *I-I* with respect to the *y* axis, with respect to a point O_1 passing through the point of application of the resultant force in the tensiled reinforcement ($\sum M_{O,I}=0$):

$$\begin{aligned}&\sigma_{b,x,\mathrm{I}}\cdot\omega_{b,I}A_{b,\mathrm{I}}[b-\varphi_y\cdot x]\cdot\eta_{\mathrm{ver,s,I}}\cdot h\\&+\eta_{\mathrm{ver,s,I}}\cdot h\cdot R_{\mathrm{sc,I,rig}}\sum\cdot\omega_{rig}\cdot A_{sc,rig}+\\&-\left(0{,}5\mathrm{h}-a'_s+\eta_{\mathrm{s,s,I}}\cdot h\right)\cdot R_{\mathrm{s,I,up}}\cdot\sum\omega_{up}\cdot A_{s,up}+\\&+\left(0{,}5\mathrm{h}-a'_s+\eta_{\mathrm{s,s,I}}\cdot h\right)\cdot R_{\mathrm{sc,I,up}}\sum\cdot\omega_{up}\cdot A_{sc,up}+\\&+\left(0{,}5\mathrm{h}-a_s-\eta_{\mathrm{s,s,I}}\cdot h\right)\cdot R_{\mathrm{s,I,d}}\cdot\sum\omega_d\cdot A_{s,d}\\&-\left(0{,}5\mathrm{h}-a_s-\eta_{\mathrm{s,s,I}}\cdot h\right)\cdot R_{\mathrm{sc,I,d}}\sum\cdot\omega_d\cdot A_{sc,d}-\\&-\mathrm{K_M}K_{pr,M}\cdot R_{\mathrm{sup}}-R_{\mathrm{sup}}a_{\mathrm{m,S}}=0\,.\end{aligned}\qquad(6)$$

Here $\mathrm{K_M}$ – is a numerical coefficient that takes into account the static loading scheme from the position of additional bending moments along the length of the bar; $\mathrm{K_{pr,M}}$ – coefficient, ratio (it is known, is set) between R_{sup} and M; $a_{\mathrm{m,S}}$ – the horizontal distance from the support in the direction of the *y* axis to the center of gravity of the working longitudinal reinforcement in section *I-I* (point O_1); R_{sup} – the support reaction in the first block (Figure 1).

The unknown is found from this equation $\sigma_{b,x,\mathrm{I}}$.

From the equilibrium equation of the projections of all the forces acting in section *I–I* on the *x* axis, the height of the concrete compressed zone x in this section is determined ($\sum X=0$):

$$\begin{aligned}&\sigma_{b,x,\mathrm{I}}\cdot\omega_{b,I}A_{b,\mathrm{I}}[b-\varphi_y\cdot x]-R_{\mathrm{s,I,up}}\cdot\sum\omega_{up}\cdot A_{s,up}\\&+R_{\mathrm{sc,I,up}}\sum\cdot\omega_{up}\cdot A_{sc,up}-\sigma_{\mathrm{s,I,d}}\cdot\sum\omega_d\cdot A_{s,d}\\&+R_{\mathrm{sc,I,d}}\sum\cdot\omega_d\cdot A_{sc,d}=0\,,\end{aligned}\qquad(7)$$

From the equilibrium equation of the projections of internal and external forces acting in the section *I-I* on the *0Z* axis ($\sum Z=0$) (the loading forces in the working reinforcement in the middle section are zero), we obtain:

$$-\tau_{pl,x}\cdot x\cdot h_0-\gamma_{Q,t}\tau_{pl,x}\cdot\psi_{R,Q}\cdot h_0\cdot\left(b-x\right)+K_M\cdot R_{\mathrm{sup}}=0\qquad(8)$$

Here $\tau_{pl,x}$ is the shear stress determined in the second stage of stress-strain state.

From it is determined

$$\gamma_{Q,t}=\frac{K_M\cdot R_{\mathrm{sup}}-\tau_{pl,x}\cdot x\cdot\left(b-x\right)}{\tau_{pl,x}\cdot\psi_{R,Q}\cdot h_0\cdot\left(b-x\right)}\qquad(9)$$

In this case, the transverse force perceived by the concrete of the compressed zone will be equal to:

$$\mathrm{Q_{I,b}}=\tau_{pl,x}\cdot x\cdot h_0\,,\qquad(10),$$

Ehe transverse force perceived by the concrete of the stretched zone will be equal to:

a)

b)

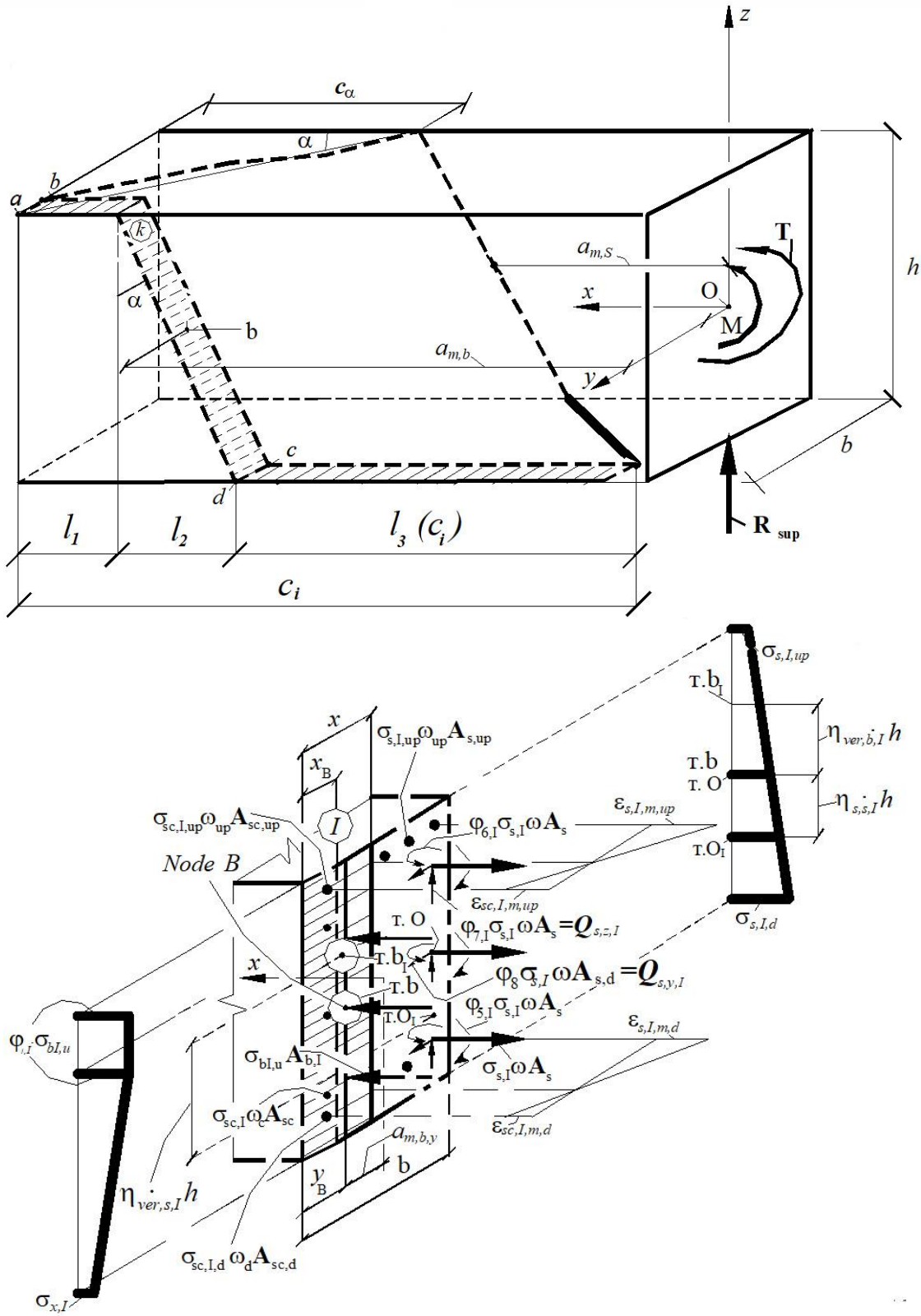


Figure 1. The calculation scheme of the resistance of the reinforced concrete structure under the combined action of bending moment, torque and shear force (case 2): (k) – compressed zone of spatial section; (I) – compressed section zone I–I (III – III).

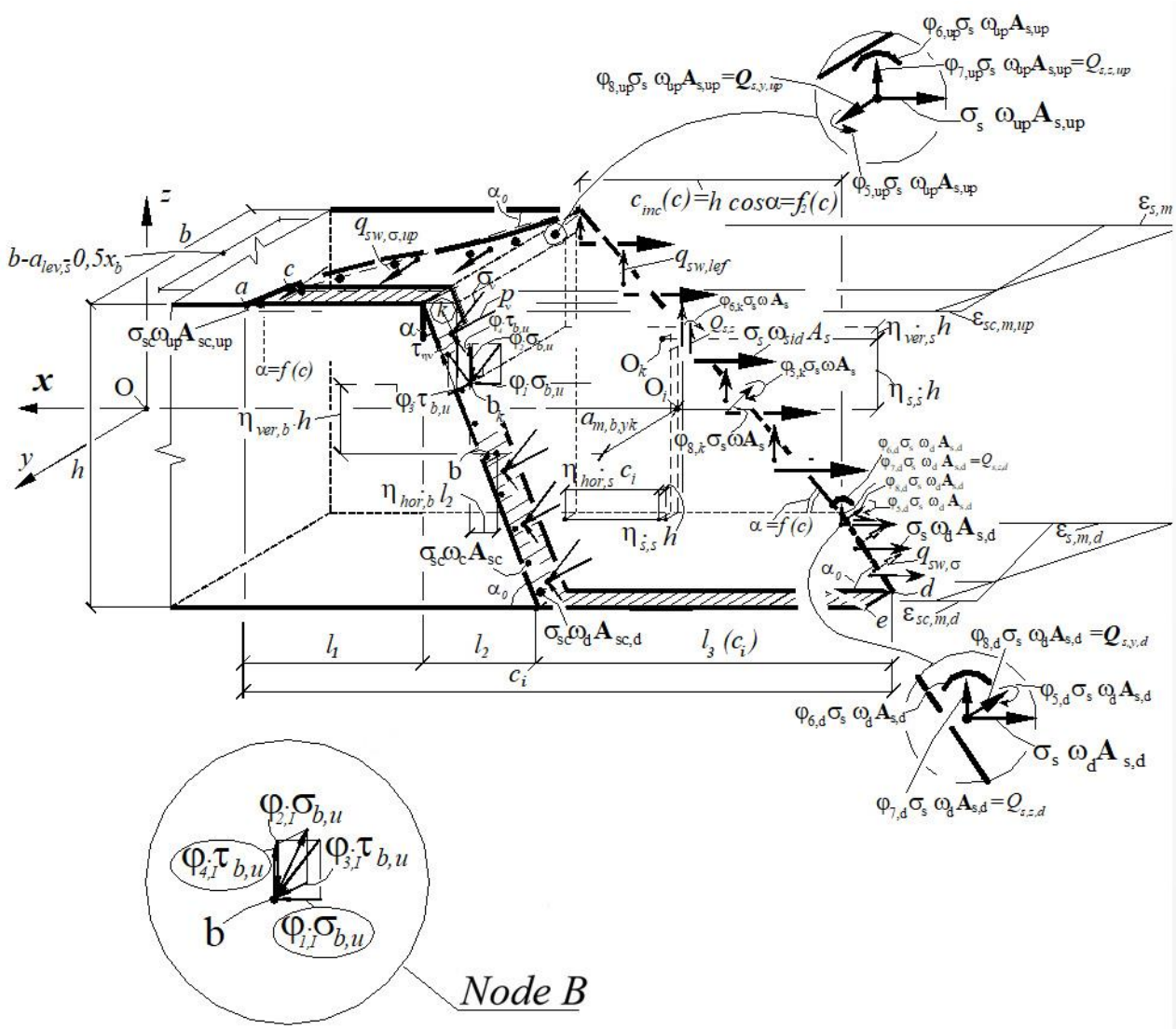


Figure 2. The calculation scheme of the spatial section k: ⓚ *– compressed zone of spatial section.*

$$Q_{I,t} = \gamma_{Q,t}\tau_{pl,x}\cdot\psi_{R,Q}\cdot h_0\cdot(b-x), \quad (11)$$

As unknown, the system of differential equations is set $\gamma_{Q,t}$.

On the other hand:

$$Q_{I,t} = Q - Q_{I,b}. \quad (12)$$

The last equation can be used to determine a parameter $\psi_{R,Q}$ that takes into account the presence of adjacent spatial cracks in the stress-strain state of the extended zone of the middle section *I – I:*

$$\psi_{R,Q} = \frac{Q - Q_{I,b}}{\gamma_{Q,t}\tau_{pl,x}\cdot h_0\cdot(b-x)}. \quad (13)$$

The compilation of the following equations requires some explanation. The upper, lower and lateral longitudinal reinforcement (in the presence of multi-tiered), in Fig. 1 are not shown in order to avoid cumbersome images. Under equilibrium conditions, stresses arising in the marked reinforcement are taken into account. The only exception is the equation of equilibri-

um of the moments of internal and external forces acting in section *I–I* with respect to the *x* axis perpendicular to this section and passing through the point of application of the resultant forces in the compressed zone ($T_{b,I}$=0) (the loading forces in the reinforcement in the middle section *I–I* are taken equal to zero).

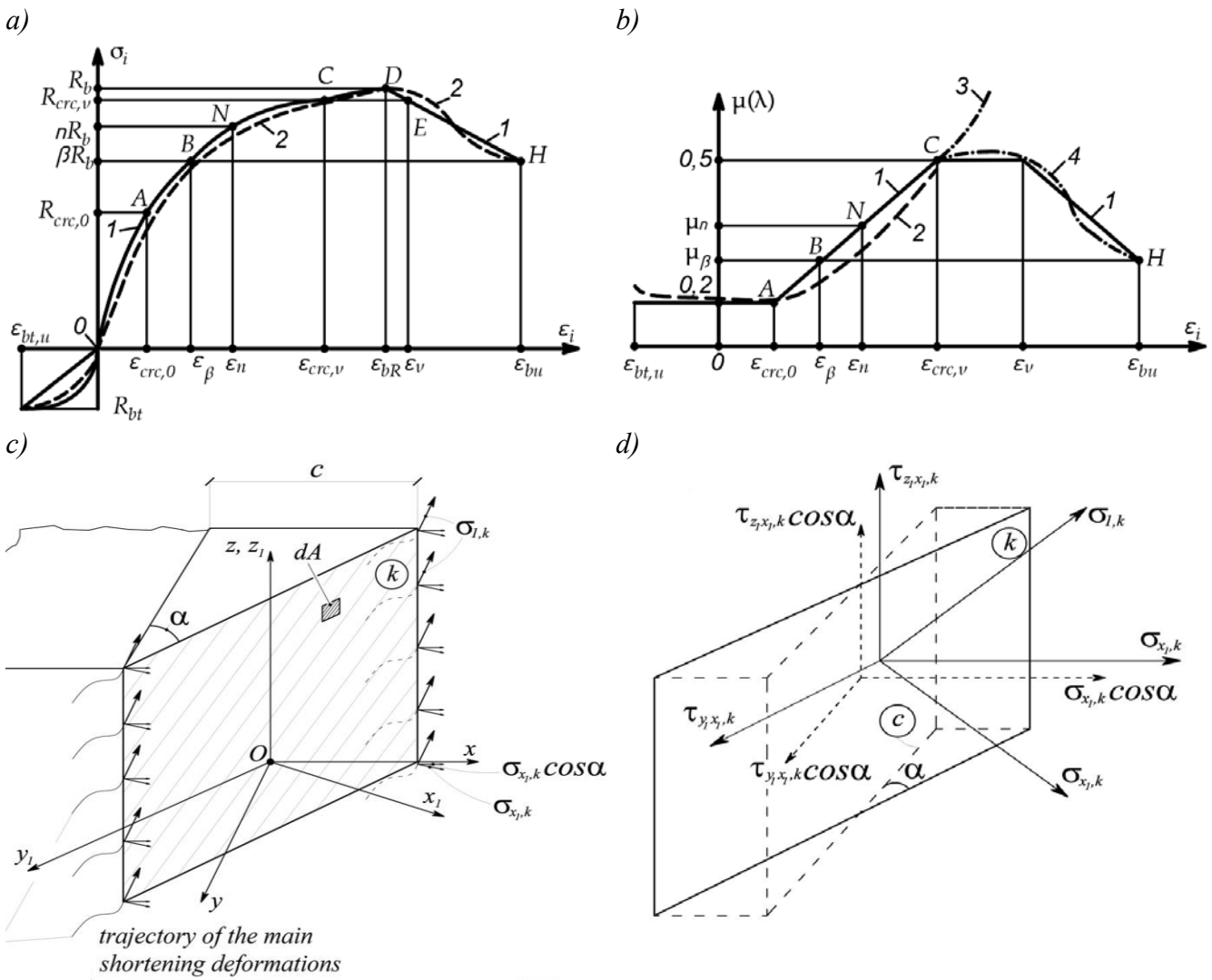


Figure 3. Connection diagrams "stresses – strain" (a), "Transverse strain coefficient" (b) for concrete: 1 - calculated; 2 - built on experimental data; 3 - the same taking into account the main cracks between the pillars; 4 - the same with the measurement of deformations only within the pillars; stresses in the vertical section and the spatial cross-section diagram k passing through the end of the front of the spatial crack (c), components of the stresses at the elementary site of the cross-section k applied to the block from the support side, and internal forces arising at the cross-section location (d).

In the spatial section *k* for block 2, cut off by a complex section passing along a spiral-shaped spatial crack and along the broken section of the compressed zone, all the reinforcement [12, 19] falling into this section are taken into account (Figure 2). Moreover, in the compressed upper longitudinal reinforcement, cut off in sections I – I and III – III, the impact effect is not taken into account, and in the rest of the longitudinal and transverse reinforcement, the components

of the impact effects are taken into account - they are determined using a special second-level model [1, 2, 13, 15]

The need to use a complex broken section of the compressed concrete zone is due to the fact that its destruction occurs (according to the experimental studies) in a certain volume, located not along the entire length between points *A* and *B* (Fig. 1, 2), but only in a certain volume located in the middle part . Moreover, the destruction occurs in the middle part not along the *AB* line, but at an angle close to 45° , located near the upper edge of the reinforced concrete structure, which predetermined the direction of the middle part of the broken section, where the ultimate stress-strain state is reached.

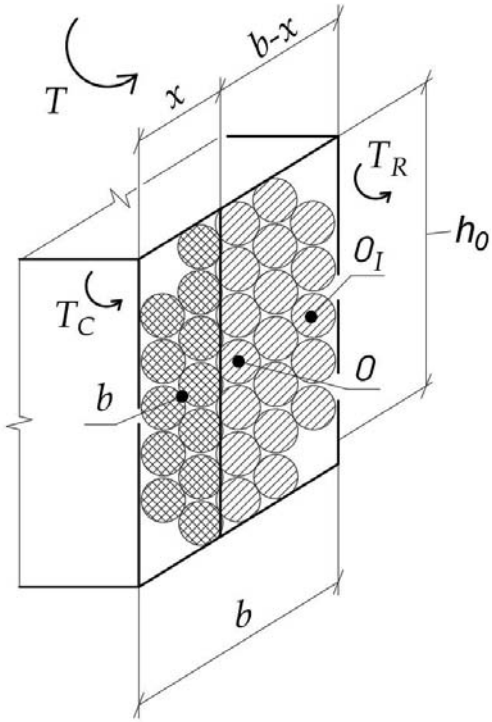


Figure 4. Approximation of a rectangular section I-I (III-III) using squares and circles inscribed in them and the distribution of torques in a compressed and extended zone in the middle section I – I (III-III).

In areas of the compressed zone located at the edges of the broken section, the stress-strain state varies from sections I – I and III – III to the middle zone according to linear dependences, respectively. At the same time, the height of the compressed zone decreases with increasing bending moment (Figure 2). Such a calculation scheme most closely matches the actual resistance, the parameters of which are experimentally confirmed.

The lateral surfaces of the broken section in compressed concrete coincide with the planes of the axis (or "smeared" plane) of the working longitudinal reinforcement. Thus, the angular reinforcement intersects the planes I – I, III – III, respectively, at the end sections of a complex broken section (Figure 5).

The distribution of torques in the compressed and extended zones in the middle section I – I is shown in Figure 4. When assessing the resistance of reinforced concrete structures of rectangular and complex cross sections (consisting of a set of rectangles), the authors use the technique, which is based on the fact that the rectangular section can be divided into a series of squares, which can be subsequently replaced by the circles inscribed in them (Figure 4).

The equation for determining the tangential torsional stresses $\tau_{\text{sum,A}}$ at the corresponding point of the cross section located at a distance from the support is written in a cylindrical and Cartesian coordinate system in accordance with Figure 4:

$$\tau_{\text{sum,A}} = \tau_{\text{t,j,A,cond}} + \tau_{\text{t,i,A,cond}} + \tau_{loc} + \tau_{conc} \pm \tau_{conc,loc} =$$
$$= \frac{M_t}{I_t \cdot \alpha} \cdot r_{j,A} + \frac{M_{t,i}}{I_{t,i} \cdot \alpha} \cdot r_{i,A} + \tau_{loc} + \tau_{conc} \pm \tau_{conc,loc} =$$
$$= \frac{M_t}{I_t \cdot \alpha} \cdot \sqrt{y_{j,A}^2 + z_{j,A}^2} + \frac{M_{t,i}}{I_{t,i} \cdot \alpha} \cdot \sqrt{y_{i,A}^2 + z_{i,A}^2} +$$
$$+ \tau_{loc} + \tau_{conc} \pm \tau_{conc,loc} \le \tau_{t,u}, \quad (14)$$

Here $\tau_{\text{t,j,A,cond}}$ and $\tau_{\text{t,i,A,cond}}$ are the tangential stresses at an arbitrary point A of the large circle described around an arbitrary cross section after "condensation" of the static-geometric characteristics of the section "dissolved" along this circle and the tangential stresses at an arbitrary point A of the small square-circle after "conden-

sation", respectively; $r_{j,A}$, $y_{j,A}$, $z_{j,A}$ – the distances from the center of the large circle described around the cross-section of the rod to an arbitrary point A located in the small j-th circle, in which the values of the tangential torsional stresses τ_t and its coordinates are determined in the common coordinate system YOZ, respectively; M_t – the torque acting in the cross section of the rod; I_t – the polar moment of inertia of the cross section of the rod approximated by small squares - circles; τ_{conc}, $\tau_{conc,loc}$ - shear stresses due to the force, geometric and inter-environment concentration of deformations, as well as components caused by local concentration; $r_{i,A}$, $y_{i,A}$, $z_{i,A}$ – the distances from the center of the small i-th circle to an arbitrary point A located in the small i-th circle, in which the tangential torsional stresses τ_t are determined and its coordinates in the local coordinate system $Y_iO_iZ_i$, respectively; $M_{t,i}$ – torque per i-th small circle into which the cross section of the rod is divided; $I_{t,i}$ – the polar moment of inertia of the i-th small circle into which the cross section of the rod can be divided (consists of its own polar moment of inertia and an additional, equal to $r_j^2 \cdot A_i$); $\tau_{t,u}$ – limit values of tangential torsional stresses.

The torsion moment of inertia in the general case of a complex cross section is equal to the sum of the moment of inertia of the squares into which the section is divided, followed by approximation by circles inscribed in these squares (in this case, one of the superimposed parts of the intersecting sections when summing is entered with a «minus» sign, and angular sections, in view of their insignificant effect on the values of tangential stresses, are not taken into account):

$$I_t = I_{t,1} + I_{t,2} + \ldots + I_{t,j} = \sum I_{t,j}, \quad (15)$$

The torsion moments falling on the inscribed circles are respectively determined:

$$M_{t,1} = M_t \cdot \frac{A_{t,1}}{A_t}; \quad M_{t,2} = M_t \cdot \frac{A_{t,2}}{A_t}$$

$$\ldots M_{t,j} = M_t \cdot \frac{A_{t,j}}{A_t} \quad (16)$$

Here $A_{t,i}$ – the area of the small circle inscribed in the corresponding square; A_t – area of rectangular cross section.

It is important to note that all geometric characteristics are considered relative to the geometric center of a complex section.

In relation to the average section *I–I*, under conditions of complex resistance — torsion with bending (Figure 5), it is advisable to take into account the fact that a significant part of this section is subject to tension. It is known [1, 2, 15] that in a stretched concrete there are a number of adjacent spatial cracks that affect the stress-strain state of the middle section *I–I*. We will take into account this effect of adjacent cracks using the parameter $\psi_{R,T}$:

If the torque changes along the longitudinal axis of the reinforced concrete structure, an additional dependence is introduced, which is a proportional relationship between the torques in section *k* and section *I–I*.

$$\frac{K_T \cdot K_{pr,T} \cdot M_{t,I}}{M_{t,k}} = \frac{a}{c_i - 0,5b \cdot \sin\alpha_0},$$

$$M_{t,I} = \frac{a \cdot M_{t,k}}{K_T \cdot K_{pr,T} \cdot (c_i - 0,5b \cdot \sin\alpha_0)}. \quad (17)$$

Here K_T – a numerical coefficient that takes into account the static loading scheme from the position of additional torques along the length of the rod; $K_{pr,T}$ – coefficient of ratio (it is known, is set) between R_{sup} and T. Here a – the horizontal distance from the center of the support to section *I–I*.

Knowing $\tau_{sum,A}$ from equation (14), you can find the torque per j-th circle of the compressed zone in section *I–I* according to the formula:

$$T_c = M_{t,c} = \frac{\tau_{sum,A} \cdot I_{t,j}}{\sqrt{y^2 + z^2}}. \qquad (18)$$

Performing the summation of all $M_{t,j}$ for all j-th *m* circles, located in the compressed zone of section *I–I*, we will have the total torque perceived by the compressed concrete zone:

$$M_{t,c} = \sum_{j=1}^{m} M_{t,j}. \qquad (19)$$

In turn, the torque perceived by the concrete of the stretched zone will be equal to:

$$T_R = M_{t,R} = \frac{\tau_{sum,A} \cdot \psi_{R,T} \cdot I_{t,j}}{\sqrt{y^2 + z^2}}, \qquad (20)$$

Here $\psi_{R,T}$ – a parameter that takes into account the presence of adjacent spatial cracks in the stress-strain state due to torsion of the extended zone of the middle section *I–I*.

On the other hand, returning to the construction of general resolving equations (Figures 1, 2), here we can use the equation of equilibrium of the moments of internal and external forces acting in section *I–I* relative to the axis perpendicular to this section and passing through the point of application of the resultant forces in the compressed zone ($T_{b,I}$=0):

$$M_{t,R} = M_t - M_{t,c}. \qquad (21)$$

From this equation is determined parameter $\psi_{R,T}$, that takes into account the presence of adjacent spatial cracks in the stress-strain state due to torsion of the stretched zone of the middle section *I–I*:

$$\psi_{R,T} = \frac{\left(M_t - M_{t,c}\right)\sqrt{y^2 + z^2}}{\tau_{sum,A} \cdot I_{t,j}}. \qquad (22)$$

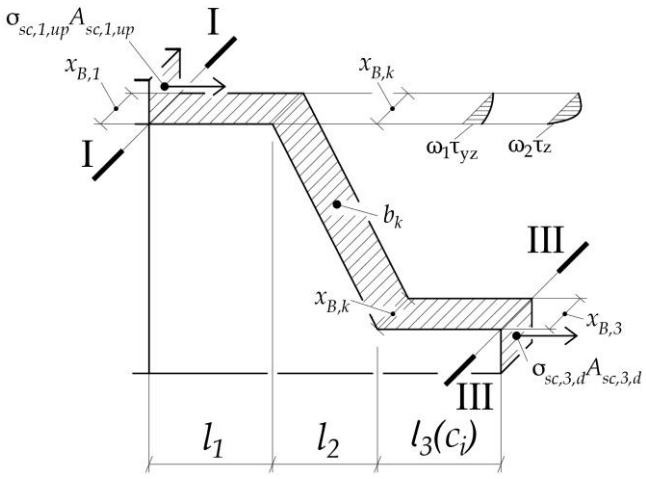


Figure 5. Approximation by a broken section of a compressed zone formed by a spiral-shaped spatial crack, as well as sections I–I and III–III.

From the hypothesis of proportionality of longitudinal strains, we find:

$$\sigma_{s,I} = \frac{\sigma_{b,x,\mathrm{I}} \cdot E_s(\lambda)}{E_b(\lambda)} \cdot \frac{\left(\mathrm{b} - a_s - x\right)}{x} + \sigma_0 \le \mathrm{R_{s,I}}. \qquad (23)$$

Here σ_0 – prestresses in prestressed reinforcement at the moment of decreasing the prestressing value in concrete to zero when the structure is loaded by external forces, taking into account the prestressing losses in prestressed reinforcement corresponding to the considered stage of the construction. If condition (23) is not satisfied, then we set $\sigma_{s,I}$ equal to $R_{s,I}$.

The second support block is separated from the reinforced concrete element by a spatial section formed by a spiral crack and a vertical section passing through the compressed zone of concrete through the end of the front of the spatial crack.

The equilibrium of this block is ensured by the following conditions.

The sum of the moments of all internal and external forces acting in the vertical longitudinal plane with respect to the *y* axis relative to the point of application of the resultant forces in the compressed zone is zero ($\sum M_{b,k}$=0, block *II*).).

$$(0,5h - \mathrm{a}_{s,d} + \eta_{ver,b} h) \cdot \sum \mathrm{R_{s,d}} \cdot \omega_{\mathrm{s,i,d}} \cdot A_{s,i,d}$$

$$-(0,5h-\mathrm{a}_{s,up}-\eta_{ver,b}h)\cdot\sum\mathrm{R}_{\mathrm{s,up}}\cdot\omega_{\mathrm{s,i,up}}\cdot A_{s,i,up}+$$
$$+\varphi_{6,\mathrm{up}}\cdot\sum R_{s,up}\cdot\omega_{s,i,up}\cdot A_{s,i,up}+\varphi_{6,k}\cdot\sum R_{s}\cdot\omega_{s,i}\cdot A_{s,i}$$
$$+\varphi_{6,\mathrm{d}}\cdot\sum R_{s,d}\cdot\omega_{s,i,d}\cdot A_{s,i,d}+$$
$$+\varphi_{7,\mathrm{up}}\cdot\left[\frac{1}{3}\left(\mathrm{b}-\mathrm{a}_{\mathrm{lev,S}}-\frac{0,5x_b}{\sin\alpha}\right)\cos\alpha+0,5l_2-\eta_{\mathrm{hor,b}}\cdot l_2\right]\cdot$$
$$\cdot\sum R_{s,up}\cdot\omega_{s,i,up}\cdot A_{s,i,up}+$$
$$+\varphi_{7,\mathrm{k}}\cdot\left(\eta_{\mathrm{hor,b}}\cdot l_2-\eta_{\mathrm{s,s}}\cdot h\right)\cdot\sum R_{s}\cdot\omega_{s,i}\cdot A_{s,i}+$$
$$+\varphi_{7,\mathrm{d}}\cdot\left[\frac{1}{3}\left(\mathrm{b}-\mathrm{a}_{\mathrm{lev,S}}-\frac{0,5x_b}{\sin\alpha}\right)\cos\alpha+0,5l_2+\eta_{\mathrm{hor,b}}\cdot l_2\right]\cdot$$
$$\cdot\sum R_{s,d}\cdot\omega_{s,i,d}\cdot A_{s,i,d}+$$
$$+(0,5h-\mathrm{a}_{s,d}+\eta_{ver,b}h)\cdot\sum R_{sc,up}\omega_{\mathrm{sc,i,up}}A_{sc,i,up}-$$
$$-(0,5h-\mathrm{a}_{s,up}-\eta_{ver,b}h)\cdot\sum R_{sc,d}\omega_{\mathrm{sc,i,d}}A_{sc,i,d}+$$
$$+\sigma_{\mathrm{s,sid,k}}\cdot\mathrm{z}_{\mathrm{i,up}}\cdot\sum\omega_{\mathrm{s,i,sid}}A_{s,i,sid}-$$
$$-\sigma_{\mathrm{s,sid,k}}\cdot\mathrm{z}_{\mathrm{i,d}}\cdot\sum\omega_{\mathrm{s,i,sid}}A_{s,i,sid}+$$
$$+\mathrm{q}_{\mathrm{sw,lef}}\omega_{\mathrm{sw,i,lef}}\cdot f_2\left(\mathrm{c}\right)\cdot\mathrm{z}_{\mathrm{i,up,sw}}-$$
$$-\mathrm{q}_{\mathrm{sw,lef}}\omega_{\mathrm{sw,i,lef}}\cdot f_2\left(\mathrm{c}\right)\cdot\mathrm{z}_{\mathrm{i,d,sw}}$$
$$-K_M\cdot K_{pr,M}\cdot R_{\mathrm{sup}}-R_{\mathrm{sup}}\cdot\left(a_{m,\mathrm{b}}+\eta_{\mathrm{hor,b}}\cdot l_2\right)=0 \quad (24)$$

here $a_{m,\mathrm{b}}$ – horizontal distance from the support to the center of gravity of the compressed concrete zone in section k; φ_5, $\varphi_{6,\mathrm{up}}$, $\varphi_{6,\mathrm{d}}$, $\varphi_{6,k}$, $\varphi_{7,up}$ $\varphi_{7,\mathrm{d}}$, – parameters that take into account the components of the "indented" effect in the reinforcement (at each step of the iteration, they are taken into account as constants, not as functions, and are determined based on the second-level model); other geometric parameters given in formula (24) are shown in Figures 1, 2; $\mathrm{z}_{\mathrm{i,up}}$ – the distance from the side reinforcement, which is located above point $\mathrm{b_k}$; $\mathrm{z}_{\mathrm{i,d}}$ – the distance from the side reinforcement, which is located below point $\mathrm{b_k}$; $\mathrm{z}_{\mathrm{i,up,sw}}$ – the distance from the center of gravity (found through $\omega_{\mathrm{sw,i,lef}}$) of the linear force in the clamps located on the side face, above point $\mathrm{b_k}$; $\mathrm{z}_{\mathrm{i,d,sw}}$ – the distance from the center of gravity (found through $\omega_{\mathrm{sw,i,lef}}$) of the linear force in the clamps located on the side face, below point $\mathrm{b_k}$. The lateral compressed reinforcement in this equation is not taken into account in view of the smallness of its shoulders relative to the point $\mathrm{b_k}$ (due to the smallness of the parameter x_B);

From equation (24) is determined the unknown $\sigma_{s,sid,k}$ on the left edge.

The sum of the projections of all the forces acting in the spatial section on the x axis is zero ($\sum\mathrm{X}=0$, block II).

$$\sum\mathrm{R}_{\mathrm{s,up}}\cdot\omega_{\mathrm{s,i,up}}\cdot A_{s,i,up}+$$
$$+\sigma_{\mathrm{s,sid,k}}\cdot\sum\omega_{\mathrm{s,i,sid}}A_{s,i,sid}$$
$$+\sum\mathrm{R}_{\mathrm{s,d}}\cdot\omega_{\mathrm{s,i,d}}\cdot A_{s,i,d}-$$
$$-\sum R_{sc,up}\omega_{\mathrm{sc,i,up}}A_{sc,i,up}-$$
$$-\sum R_{sc,d}\omega_{\mathrm{sc,i,d}}A_{sc,i,d}-$$
$$-\sum\mathrm{R}_{\mathrm{sc,rig}}\cdot\omega_{\mathrm{sc,rig}}\cdot A_{\mathrm{sc,rig}}$$
$$-\left(\varphi_{10}\cdot\sigma_{b,x,\mathrm{I}}\cdot\varphi_1\right)\cdot\omega_b\cdot x_B\cdot\sqrt{\mathrm{l}_2^2+\mathrm{h}^2}\ , \quad (25)$$

here ω_b, φ_{10} are accepted at each iteration in the form of constants.

An unknown x_B is found from this equation.

The first case is for the axis of block II ($\sum Y$=0), and for the second case it will be the equation ($\sum Y$=0).

$$-q_{sw,\sigma,\mathrm{up}}\cdot\frac{\left(b-a_{up,s}-x_b\right)}{\sin\alpha_0}\cdot\omega_{up}+$$
$$+q_{sw,\sigma}\cdot\frac{\left(b-a_{d,s}-x_b\right)}{\sin\alpha_0}\cdot\omega$$
$$-\varphi_{8,\mathrm{up}}R_s\sum\omega_{up}A_{s,up}+$$
$$+\varphi_{8,\mathrm{k,sid}}R_{s,sid}\sum\omega_{k,sid}A_{s,sid}$$
$$+\varphi_{8,\mathrm{d}}R_s\sum\omega_d A_{s,d}=0 \quad (26)$$

An unknown $q_{sw,\sigma,\mathrm{up}}$ is found from the equation (26).

The sum of the moments of internal and external forces in the vertical transverse plane rela-

tive to the x axis passing through the point of application of the resultant forces in the compressed zone is equal to zero ($\sum T_{b,k}$=0, block *II*):

$$-\frac{\tau_{sum,A}\cdot I_{t,j}}{\sqrt{y^2+z^2}}\cdot\sin\alpha_0-\frac{\tau_{sum,A}\cdot\psi_{R,T}\cdot I_{t,j}}{\sqrt{y^2+z^2}}\cdot\sin\alpha_0+$$
$$+\varphi_{7,\mathrm{up}}R_s\sum\omega_{up}A_{s,up}\cdot\left(b-a_{s,up}-0,5\cdot x\right)+$$
$$+\varphi_{7,\mathrm{d}}R_s\sum\omega_d A_{s,d}\cdot\left(b-a_{s,d}-0,5\cdot x\right)+$$
$$+\varphi_{7,\mathrm{k}}R_s\sum\omega\cdot A_s\cdot\left(b-a_{s,lef}-0,5\cdot x\right)+$$
$$+\varphi_{8,up}R_s\sum\omega_{up}A_s\cdot(0,5h-\mathrm{a}_{s,up}-\eta_{ver,b}h)+$$
$$+\varphi_{8,\mathrm{k}}R_s\sum\omega\cdot A_s\cdot\eta_{ver,b}h+$$
$$+\varphi_{8,d}R_s\sum\omega_d A_s\cdot(0,5h-\mathrm{a}_{s,up}+\eta_{ver,b}h)+$$
$$+\mathrm{q}_{\mathrm{sw},\sigma,\mathrm{up}}\left(0,5h_0-a_{s,up}-\eta_{ver,b}h\right)+$$
$$+\mathrm{q}_{\mathrm{sw},\sigma}\left(0,5h_0-a_{\mathrm{up,s}}+\eta_{ver,b}h\right)+$$
$$+\mathrm{q}_{\mathrm{sw,lef}}\cdot h\cdot\cos\alpha\cdot\left(b-a_{,lev,s}-0,5x_B\right)-$$
$$-\mathrm{K_T}\cdot\mathrm{K_{pr,T}}\cdot R_{\mathrm{sup}}-\mathrm{R_{sup}}\left(0,5b-0,5x_B\right)=0 \quad (27)$$

here $\mathrm{K_T}$ – a numerical coefficient that takes into account the static loading scheme from the position of additional torques along the length of the rod; $\mathrm{K_{pr,T}}$ – coefficient, ratio (it is known, is set) between R_{sup} and T.

Unknown $q_{sw,\sigma}$ is found from the equation (27).

The sum of the projections of all the forces acting in the spatial section on the y axis is zero ($\sum Z$=0, block II):

$$-\mathrm{q}_{\mathrm{sw,lef}}\cdot h\cdot\cos\alpha-\varphi_{7,d}\mathrm{R_s}\sum\omega_d A_{s,d}-$$
$$-\varphi_{7,up}R_{\mathrm{s}}\sum\omega_{up}A_{s,up}-\varphi_{7,\mathrm{k}}R_s\sum\omega\cdot A_s+$$
$$+\left(\varphi_{10}\cdot\sigma_{b,x,I}\cdot\varphi_1\right)\cdot$$
$$\cdot\omega_b\cdot x_B\cdot\sqrt{\mathrm{l}_2^2+\mathrm{h}^2}+R_{\mathrm{sup}}=0. \quad (28)$$

Here ω_b, φ_{10} are accepted at each iteration in the form of constants. An unknown $\mathrm{q_{sw,lef}}$ is found from the equation (28).

Composing a function of many variables with Lagrange multipliers λ_i

$$F(\sigma_{b,x,I},x,\gamma_{Q,t},\sigma_{s,I},\sigma_{s,sid,k},x_B,q_{sw,\sigma,up},q_{sw,\sigma},$$
$$q_{sw,lef},c,\lambda_1,\lambda_2,\lambda_3,\lambda_4,\lambda_5,\lambda_6,\lambda_7,\lambda_8,\lambda_9),$$

using equations (1)–(23), and equating the partial derivatives with respect to all variables included in it to zero, we obtain an additional system of equations [13, 15]:

$$\left.\begin{array}{l}\frac{\partial f}{\partial x_1}+\lambda_1\frac{\partial\varphi_1}{\partial x_1}+\lambda_2\frac{\partial\varphi_2}{\partial x_1}+\ldots+\lambda_m\frac{\partial\varphi_m}{\partial x_1}=0\\ \frac{\partial f}{\partial x_2}+\lambda_1\frac{\partial\varphi_1}{\partial x_2}+\lambda_2\frac{\partial\varphi_2}{\partial x_2}+\ldots+\lambda_m\frac{\partial\varphi_m}{\partial x_2}=0\\ \ldots\ldots\ldots\ldots\ldots\ldots\ldots\ldots\ldots\ldots\\ \frac{\partial f}{\partial x_n}+\lambda_1\frac{\partial\varphi_1}{\partial x_n}+\lambda_2\frac{\partial\varphi_2}{\partial x_n}+\ldots+\lambda_m\frac{\partial\varphi_m}{\partial x_n}=0\end{array}\right\}. \quad (29)$$

From the system (29) after the corresponding algebraic transformations, for the two cases considered above, it is possible to obtain the equations for the unknown dangerous spatial crack $c_{\mathrm{inc}}(c)$ on the horizontal:

$$c_{inc}(c)=\frac{\sin\alpha(c)+a_4\cdot a_9\cdot\cos\alpha(c)}{a_8\cdot a_{12}\cdot a_9\cdot\sin^2\alpha(c)}, \quad (30)$$

The coefficients

$$a_4,\ a_8,\ a_9,\ a_{12},$$

included in the equation include almost all the calculation parameters

$$\sigma_{b,x,I},x,\gamma_{Q,t},\sigma_{s,I},$$
$$\sigma_{s,sid,k},x_B,q_{sw,\sigma,up},q_{sw,\sigma},q_{sw,lef}$$

of the proposed calculation model (Figure 2).

3. CONCLUSIONS

1. The paper proposes a calculation model of the complex resistance of reinforced concrete structures in buildings and structures under the action of torsion with bending. The structure of the model includes a support block (formed by a spatial crack and a compressed concrete zone closed on it, the spatial section *k*) and a second block formed by a vertical section *I–I* extending perpendicular to the longitudinal axis of the reinforced concrete element along the edge of the compressed zone closing the spiral spiral crack .
2. The case is taken into account when, of the three external influences during torsion with bending (Q, M, T), the greatest influence on the stress-strain state of structures is exerted by the action of the torque T (case 2). In the proposed model, when considering the normal section I – I (III – III) and the spatial section k some parametres are taken into account: the maximum support reaction R_{sup}, the height of the concrete compressed zone in the normal section $x_{B,\mathrm{I}}$, the coefficient for determining the shear force $\gamma_{Q,t}$, the longitudinal reinforcement stress in the normal section $\sigma_{s,I}$, the side reinforcement stress in the spatial section $\sigma_{s,sid,k}$, the height of the compressed zone of the spatial section $x_{B,k}$, the linear force in the transverse reinforcement located at the lateral, upper and lower faces $q_{sw,\sigma,up}, q_{sw,\sigma}, q_{sw,lef}$, normal stresses in concrete $\sigma_{bu,x,\mathrm{I}}$, component axial stresses in the working reinforcement intersected by a spatial crack $\sigma_{\mathrm{s,up}}, \sigma_{\mathrm{sc,up}}, \sigma_{\mathrm{s,d}}, \sigma_{\mathrm{sc,d}}$, tangential forces in concrete $\omega_1\tau_{yz}$, $\omega_2\tau_z$; components of the loading effort in the working reinforcement intersected by a spatial crack *k*, as well as the lengths of the projections of the parts of the spatial crack on the horizontal axis $l_1, l_2, l_3(c_i)$.
3. When assessing the resistance of reinforced concrete structures of rectangular and complex cross sections (consisting of a set of rectangles), the authors use the technique, which is based on the fact that the rectangular section is divided into a series of squares, which are subsequently replaced by the circles inscribed in them.
4. The resolving equations for the proposed model are compiled, forming a closed system and the Lagrange function combining them is written. Using partial derivatives of the constructed function with respect to all variables included in it and equating them to zero, an additional system of equations is compiled, from which, after the corresponding algebraic transformations, a dependence is obtained that allows one to find the projection of a dangerous spatial crack.

REFERENCES

1. **Golyshev A.B., Kolchunov V.I.** Soprotivleniye zhelezobetona [The resistance of reinforced concrete]. Kiev, Basis, 2009, 432 pages (in Russian).
2. **Bondarenko V.M., Kolchunov V.I.** Raschetnye modeli silovogo soprotivleniya zhelezobetona [The computational model of a power resistance of reinforced concrete]. Moscow, ASV, 2004, 472 pages (in Russian).
3. **Vishnu H. Jariwalaa, Paresh V. Patel, Sharadkumar P. Purohit.** Strengthening of RC Beams subjected to Combined Torsion and Bending with GFRP Composites. // *Procedia Engineering*, 2013, Volume 51, pp. 282-289.
4. **Adheena T., Afia S.H.** An Experimental Study On Combined Flexural And Torsional Behaviour Of RC Beams. // *International Research Journal of Engineering and Technology*, 2017, Volume 04, Issue 05, pp. 1367-1370.

5. **Rahal K.** Combined Torsion and Bending in Reinforced and Prestressed Concrete beams Using Simplified Method for Combined Stress-Resultants. // *ACI Structural Journal*, 2007, Volume 104, No. 4, pp. 402-411.
6. **Kolchunov Vl.I., Salnikov A.S.** Eksperimentalnyye issledovaniya treshchinoobrazovaniya zhelezobetonnyye konstruktsiy pri kruchenii s izgibom [Experimental studies of crack formation of reinforced concrete structures under action torsion with bending]. // *Building and Reconstruction*, 2016, No. 65(3), pp. 24-32 (in Russian).
7. **Demyanov A.I., Salnikov A.S.**, **Kolchunov Vl.I.** Eksperimentalnye issledovaniya zhelezobetonnykh konstruktsiy pri kruchenii s izgibom i analiz ikh rezultatov [The experimental investigations of reinforced concrete constructions under the action torsion with bending and analysis of their results]. // *Building and Reconstruction*, 2017, No. 72(4), pp. 17-26 (in Russian).
8. **Demyanov A.I., Pokusaev A.A., Kolchunov V.I.** Eksperimentalnye issledovaniya deformirovaniya zhelezobetonnykh konstruktsiy pri kruchenii s izgibom [The experimental investigations of deformation reinforced concrete structures under the action torsion with bending]. // *Building and Reconstruction*, 2017, No. 73(5), pp. 5-14 (in Russian).
9. **Demyanov A.I., Kolchunov V.I., Pokusaev A.A.** Eksperimentalnye issledovaniya deformirovaniya zhelezobetonnykh konstruktsiy pri kruchenii s izgibom [The experimental investigations of deformation reinforced concrete structures under the action torsion with bending]. // *Structural Mechanics of Engineering Constructions and Buildings*, 2017, No. 6, pp. 37–44 (in Russian).
10. **Santhakumar R., Dhanaraj R., Chandrasekaran E.** Behaviour of retrofitted reinforced concrete beams under combined bending and torsion: A numerical study. // *Electronic Journal of Structural Engineering*, 2007, No. 7, pp. 1-7.
11. **Kalkan I., Kartal S.** Torsional Rigidities of Reinforced Concrete Beams Subjected to Elastic Lateral Torsional Buckling. // *International Journal of Civil and Environmental Engineering*, 2017, Volume 11, No. 7, pp. 969-972.
12. **Salnikov A., Kolchunov Vl., Yakovenko I.** The computational model of spatial formation of cracks in reinforced concrete constructions in torsion with bending. // *Applied Mechanics and Materials*, 2015, Vols. 725-726, pp. 784-789.
13. **Iakovenko I., Kolchunov Vl.** The development of fracture mechanics hypotheses applicable to the calculation of reinforced concrete structures for the second group of limit states. // *Journal of Applied Engineering Science*, 2017, Volume 15, pp. 366-375.
14. **Demyanov A. I., Kolchunov Vl.I., Yakovenko I.A.** Razrabotka universalnogo korotkogo dvukhkonsolnogo elementa k soprotivleniyu zhelezobetonnykh konstruktsiy pri kruchenii s izgibom [The development of universal short double-cantilever element, for resistance of reinforced concrete structures under the action torsion with bending]. // *The News of Higher Educational Institutions Technology of Textile Industry*, 2017, No. 367(4), pp. 258-263 (in Russian).
15. **Iakovenko I., Kolchunov V., Lymar I.** Rigidity of reinforced concrete structures in the presence of different cracks. // *MATEC Web of Conferences*. 6th International Scientific Conference “Reliability and Durability of Railway Transport Engineering Structures and Buildings”. Transbud-2017, Kharkiv, Ukraine, April 19-21, 2017, Volume 0216, 12 pages.
16. **Pettersen J.S.** Non-Linear Finite Element Analyses of Reinforced Concrete with Large Scale Elements: Including a Case Study of a Structural Wall. Norwegian University of Science and Technology, 2014, 85 pages.

17. **Nahvi H., Jabbari M.** Crack detection in beams using experimental modal data and finite element model. // *International Journal of Mechanical Sciences*, 2005, Volume 47, pp. 1477-1497.
18. **Al-Bayati, G., Al-Mahaidi, R., Kalfat, R.** Torsional strengthening of reinforced concrete beams using different configurations of NSM FRP with epoxy resins and cement-based adhesives. // *Composite Structures*, 2016, Volume 168, pp. 569-581.
19. **Golyshev A.B., Bachinskiy V.Ya., Polishchuk V.P., Kharchenko A.V., Rudenko I.V.** Proyektirovaniye zhelezobetonnykh konstruktsiy: Spravochnoye posobiye [Design of reinforced concrete structures: a reference guide]. Kiev, Budivelnyk, 1990, 544 pages.
20. **Shen, K., Wan, S., Mo, Y.L., Jiang, Z.** Theoretical analysis on full torsional behavior of RC beams strengthened with FRP materials. // *Composite Structures*, 2016, No 1(183), pp. 347-357.
21. **Huang, L., Yan, B., Yan, L., Xu, Q., Tan, H., Kasal, B.** Reinforced concrete beams strengthened with externally bonded natural flax FRP plates. // *Composites Part B: Engineering*, 2016, Volume 91, pp. 569-578.
22. **Gunasekaran, K., Ramasubramani, R., Annadurai, R., Prakash Chandar, S.** Study on reinforced lightweight coconut shell concrete beam behavior under torsion. // *Materials and Design*, 2014, Vol. 57, pp. 374-382.
23. **Awadh E.A.** Torsion plus bending and shear on reinforced concrete beams. // *Journal of Engineering and Sustainable Development*, 2016, No. 4, pp. 277-288.

СПИСОК ЛИТЕРАТУРЫ

1. **Голышев А.Б., Колчунов В.И.** Сопротивление железобетона. – Киев: Основа, 2009. – 432 с.
2. **Бондаренко В.М., Колчунов В.И.** Расчетные модели силового сопротивления железобетона. – М.: АСВ, 2004. – 472 с.
3. **Vishnu H. Jariwalaa, Paresh V. Patel, Sharadkumar P.** Purohit. Strengthening of RC Beams subjected to Combined Torsion and Bending with GFRP Composites. // *Procedia Engineering*, 2013, Volume 51, pp. 282-289.
4. **Adheena T., Afia S.H.** An Experimental Study On Combined Flexural And Torsional Behaviour Of RC Beams. // *International Research Journal of Engineering and Technology*, 2017, Volume 04, Issue 05, pp. 1367-1370.
5. **Rahal K.** Combined Torsion and Bending in Reinforced and Prestressed Concrete beams Using Simplified Method for Combined Stress-Resultants. // *ACI Structural Journal*, 2007, Volume 104, No. 4, pp. 402-411.
6. **Колчунов В.И., Сальников А.С.** Экспериментальные исследования трещинообразования железобетонные конструкций при кручении с изгибом. // *Строительство и реконструкция*, 2016, №3(65), с. 24-32.
7. **Демьянов А.И., Сальников А.С., Колчунов Вл.И.** Экспериментальные исследования железобетонных конструкций при кручении с изгибом и анализ их результатов. // *Строительство и реконструкция*, 2017, №4(72), с. 17-26.
8. **Демьянов А.И., Покусаев А.А., Колчунов В.И.** Экспериментальные исследования железобетонных конструкций при кручении с изгибом. // *Строительство и реконструкция*, 2017, №5(73), с. 5-14.
9. **Демьянов А.И., Колчунов В.И., Покусаев А.А.** Экспериментальные исследования деформирования железобетонных конструкций при кручении с изгибом. // *Строительная механика инженерных конструкций и сооружений*, 2017, №6, с. 37-44.

10. **Santhakumar R., Dhanaraj R., Chandrasekaran E.** Behaviour of retrofitted reinforced concrete beams under combined bending and torsion: A numerical study. // *Electronic Journal of Structural Engineering*, 2007, No. 7, pp. 1-7.
11. **Kalkan I., Kartal S.** Torsional Rigidities of Reinforced Concrete Beams Subjected to Elastic Lateral Torsional Buckling. // *International Journal of Civil and Environmental Engineering*, 2017, Volume 11, No. 7, pp. 969-972.
12. **Salnikov A., Kolchunov Vl., Yakovenko I.** The computational model of spatial formation of cracks in reinforced concrete constructions in torsion with bending. // *Applied Mechanics and Materials*, 2015, Vols. 725-726, pp. 784-789.
13. **Iakovenko I., Kolchunov Vl.** The development of fracture mechanics hypotheses applicable to the calculation of reinforced concrete structures for the second group of limit states. // *Journal of Applied Engineering Science*, 2017, Volume 15, pp. 366-375.
14. **Демьянов А.И., Колчунов Вл.И., Яковенко И.А** Разработка универсального короткого двухконсольного элемента к сопротивлению железобетонных конструкций при кручении с изгибом. // *Известия ВУЗов. Технология текстильной промышленности*, 2017, №4(367), с. 258-263.
15. **Iakovenko I., Kolchunov V., Lymar I.** Rigidity of reinforced concrete structures in the presence of different cracks. // *MATEC Web of Conferences*. 6th International Scientific Conference "Reliability and Durability of Railway Transport Engineering Structures and Buildings". Transbud-2017, Kharkiv, Ukraine, April 19-21, 2017, Volume 0216, 12 pages.
16. **Pettersen J.S.** Non-Linear Finite Element Analyses of Reinforced Concrete with Large Scale Elements: Including a Case Study of a Structural Wall. Norwegian University of Science and Technology, 2014, 85 pages.
17. **Nahvi H., Jabbari M.** Crack detection in beams using experimental modal data and finite element model. // *International Journal of Mechanical Sciences*, 2005, Volume 47, pp. 1477-1497.
18. **Al-Bayati, G., Al-Mahaidi, R., Kalfat, R.** Torsional strengthening of reinforced concrete beams using different configurations of NSM FRP with epoxy resins and cement-based adhesives. // *Composite Structures*, 2016, Volume 168, pp. 569-581.
19. **Голышев А.Б., Бачинский В.Я., Полищук В.П.** Проектирование железобетонных конструкций. – Киев: Будивельник, 1990. – 544 с.
20. **Shen K., Wan S., Mo Y.L., Jiang Z.** Theoretical analysis on full torsional behavior of RC beams strengthened with FRP materials. // *Composite Structures*, 2016, No. 1(183), pp. 347-357.
21. **Huang, L., Yan, B., Yan, L., Xu, Q., Tan, H., Kasal, B.** Reinforced concrete beams strengthened with externally bonded natural flax FRP plates. // *Composites Part B: Engineering*, 2016, Volume 91, pp. 569-578.
22. **Gunasekaran, K., Ramasubramani, R., Annadurai, R., Prakash Chandar, S.** Study on reinforced lightweight coconut shell concrete beam behavior under torsion. // *Materials and Design*, 2014, Vol. 57, pp. 374-382.
23. **Awadh E.A.** Torsion plus bending and shear on reinforced concrete beams. // *Journal of Engineering and Sustainable Development*, 2016, No. 4, pp. 277-288.

Vladimir I. Kolchunov, Dr.Sc., Professor, Department of unique building and structures, South-Western State University, 94, 50 let Oktyabrya street, Kursk, 305040,Russia
phone: +7 (910) 317-93-55; e-mail: vlik52@mail.ru.

Aleksey I. Demyanov, Candidate of Technical Sciences, Associated Professor, Department of unique building and structures, South-Western State University, 94, 50 let Oktyabrya street, Kursk, 305040, Russia;
E-mail: speccompany@gmail.com.

Nikolay V. Naumov, PhD student of Department of unique building and structures, South-Western State University, 94, 50 let Oktyabrya street, Kursk, 305040, Russia;
E-mail: speccompany@gmail.com.

Колчунов Владимир Иванович, доктор технических наук, профессор кафедры «Уникальные здания и сооружения», Юго-Западный государственный университет; 305040, Россия, г. Курск, ул. 50 лет Октября, дом 94;
тел.: +7 (910) 317-93-55; e-mail: vlik52@mail.ru.

Демьянов Алексей Иванович, кандидат технических наук, доцент кафедры «Уникальные здания и сооружения», Юго-Западный государственный университет; 305040, Россия, г. Курск, ул. 50 лет Октября, дом 94; e-mail: speccompany@gmail.com

Наумов Николай Валерьевич, аспирант кафедры «Уникальные здания и сооружения», Юго-Западный государственный университет; 305040, Россия, г. Курск, ул. 50 лет Октября, дом 94;
E-mail: kolua199200@yandex.ru

DOI:10.22337/2587-9618-2019-15-4-83-87

ANALYSIS OF COMBINED PLATES WITH ALLOWANCE FOR CONTACT WITH ELASTIC FOUNDATION

Elena B. Koreneva
Moscow Higher Combined-Arms Command Academy, Moscow, RUSSIA

Abstract: The paper covers the problems of combined plates with circular base and consisting of a few sections with different laws of thickness variation. Analytical methods of analysis of similar structures are not yet developed. The present work suggests the analytical method for solving of the stated problems, the contact with the elastic subgrade is also considered. The above-mentioned approach is shown on the example of the analysis of the bottom of the cylindrical reservoir, resting on the elastic subgrade. The inner part of this construction is represented by the ring plate of variable thickness which increases along the direction from the internal boundary. The outer part is represented by the ring plate of the constant thickness. The influence of the elastic basis and the upper part of the reservoir is taken into consideration. The solutions for stresses and deflections of the combined plate are given in closed form in terms of Bessel functions. The conditions of the plate's sections conjugation are fulfilled.

Keywords: combined plates, bottom of the reservoir, Bessel functions

РАСЧЕТ КОМБИНИРОВАННЫХ ПЛИТ С УЧЕТОМ ИХ КОНТАКТА С УПРУГИМ ОСНОВАНИЕМ

Е.Б. Коренева
Московское высшее общевойсковое командное орденов Жукова, Ленина и Октябрьской Революции Краснознаменное училище, г. Москва, РОССИЯ

Аннотация: В работе изучаются комбинированные плиты, состоящие из двух или нескольких участков с различными законами изменения толщины и имеющие в плане круговую форму. Аналитические методы для расчета подобных конструкций практически еще не разработаны. Ниже предлагается аналитический подход к решению подобных задач, также производится учет контакта изучаемой конструкции с упругим основанием. Подобная методика подробно излагается на примере рассмотрения расчета днища цилиндрического резервуара. Внутренняя часть этой конструкции представляет собой кольцевую плиту, толщина которой увеличивается по направлению от внутреннего контура, наружная часть представляет собой плиту постоянной толщины. Производится учет влияния податливого основания и действия веса верхней части резервуара. Решения для перемещений и усилий внутренней и внешней частей комбинированной плиты получены в замкнутом виде и выражены в функциях Бесселя. Выполняются условия сопряжения отдельных участков.

Ключевые слова: комбинированная плита, днище резервуара, функции Бесселя

1. INTRODUCTION

The work considers analytical calculation of combined plates with circular base and consisting of several sections with different laws of thickness variation. Their thickness may be increasing or decreasing in the direction from the plate's center to the outer boundary. The material of the plates under study is isotropic or orthotropic. The separate sections of the mentioned constructions may be made from different materials with various physical characteristics. In the places of the sections conjugation the construction remains continuous. However, in some cases the plates' thickness can have the break of continuity in these positions. The analytical methods of the such constructions computation are in practice not yet developed. The present work covers this lacuna. As an example we will consider the work of the bottom of the

cylindrical reservoir. The bottom is represented by a ring plate, resting on an elastic foundation and consisting of the two sections. The inner part has the variable thickness increasing in the direction to the external boundary. The outer part of the plate has the constant thickness (Figure 1). The elastic foundation properties are described by Winkler's model.

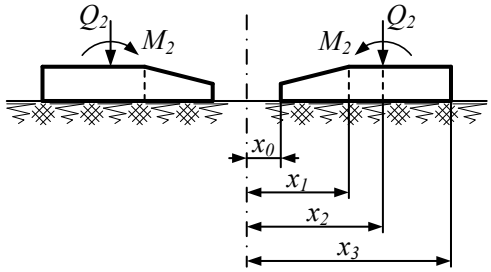


Figure 1. The combined plate on elastic foundation.

The coefficients of foundation under the inner and the outer parts of the plate can be both as different or identical. The loads caused by the upper part of the structure are distributed along the concentric circles. Let us assume that the load is applied to the outer part of the plate and the bottom of the reservoir is made from the isotropic material.

2. THE COMPUTATION OF THE INNER PART OF THE CONSTRUCTION

Let us consider the work of the inner part of the bottom of the cylindrical reservoir when $x_0 \le x \le x_1$, which is represented by a ring plate with varying thickness, resting on an elastic Winkler's foundation. The construction is subjected to an action of the axially symmetric loads. The differential equation describing the similar plate bending has the following form:

$$D\left[\frac{d^4w}{dr^4}+\frac{2}{r}\frac{d^3w}{dr^3}-\frac{1}{r^2}\frac{d^2w}{dr^2}+\frac{1}{r^3}\frac{dw}{dr}\right]+$$
$$+\frac{dD}{dr}\left[2\frac{d^3w}{dr^3}+\frac{(2+\sigma)}{r}\frac{d^2w}{dr^2}-\frac{1}{r^2}\frac{dw}{dr}\right]+ \quad (1)$$
$$+\frac{d^2D}{dr^2}\left[\frac{d^2w}{dr^2}+\frac{\sigma}{r}\frac{dw}{dr}\right]+c_1w=q,$$

where D – cylindrical rigidity, σ – Poisson's ratio, c_1 – coefficient of elastic foundation for the section where $x_0 \le x \le x_1$.

Let us assume that the variable rigidity of the plate to be approximated by the power law

$$D = D_0 r^m, \quad (2)$$

here D_0, m – constants.

Substituting (2) into (1) we get the following equation:

$$r^4\frac{d^4w}{dr^4}+r^3(2m+2)\frac{d^3w}{dr^3}+r^2(-1+m(1+\sigma)+$$
$$+m^2)\frac{d^2w}{dr^2}+r\big((1-m)+\sigma(m^2-m)\big)\frac{dw}{dr}- \quad (3)$$
$$-\frac{c_1w}{D_0n_2}r^{4-m}=\frac{qr^{4-m}}{D_0}.$$

The analysis shows when $m=4$ (3) is Euler's equation integrating in elementary functions. However, it is not possible to obtain the solution of (3) in terms of elementary functions when $m \ne 4$. To receive the result we compare the coefficients of (3) with the coefficients of Nielsen's equation [3]:

$$r^4\frac{d^4w}{dr^4}+A_3r^3\frac{d^3w}{dr^3}+A_2r^2\frac{d^2w}{dr^2}+A_1r\frac{dw}{dr}+ \quad (4)$$
$$+A_0w=0,$$

where we have

$$A_3=6-4a-4c,$$
$$A_2=2(a^2-\mu^2c^2)+4(a+c-1)^2+4(a-1)(c-1)-1,$$
$$A_1=\big[2(\mu^2c^2-a^2)-(2a-1)(2c-1)\big](2a+2c-1),$$
$$A_0=(a^2-\mu^2c^2)(a^2+4ac+4c^2-\mu^2c^2)-b^4c^4r^{4c}.$$

The equation (4) is integrated in terms of Bessel functions. When comparing the coefficients of (3) and (4) we determine that the mentioned equations are similar when the following parameter relations are

$$a = m/4;\ \ c = (4-m)/4;\ \ \mu = -m/(4-m);$$
$$b = \frac{4}{4-m}\sqrt[4]{\frac{c_1 i}{D_0}},\ \ \sigma = \frac{m}{4}. \quad (5)$$

The solution of axially symmetric problem of a circular plate with varying thickness, resting on an elastic Winkler's foundation, can be written in terms of Bessel functions:

$$w = r^{-m/4}\left[C_1 J_\mu\left(br^c\sqrt{i}\right) + C_2 Y_\mu\left(br^c\sqrt{i}\right) + \right.$$
$$\left. + C_3 I_\mu\left(br^c\sqrt{i}\right) + C_4 K_\mu\left(br^c\sqrt{i}\right)\right]. \quad (6)$$

The solution (6) can be written in the form:

$$w = r^{-m/4}\left[B_1 u_\mu\left(br^c\right) + B_2 \upsilon_\mu\left(br^c\right) + \right.$$
$$\left. + B_3 f_\mu\left(br^c\right) + B_4 g_\mu\left(br^c\right)\right]. \quad (7)$$

Since the Poisson's ratio for all materials is

$$0 \le \sigma \le 0.5,$$

the above-mentioned solution (7) may be used only for the cases when $0 \le m \le 2$. This fact corresponds to the case when the thickness increases in the direction from the inner boundary to the outer one (Figure 1). The stresses are determined by the use of the certain formulae [1]. Further we introduce the dimensionless coordinate $x = br^c$.

3. THE CALCULATION OF THE OUTER PART OF THE CONSTRUCTION

We pass to consideration of the outer part of the bottom with the constant thickness. Let us assume that the load caused by the upper part of the structure is subjected along the circumference with the radius x_2. The plate's thickness when $x = x_1$ is continuous and equal to

$$h = h_0 x_1^{m/3} \text{ when } 0 \le m \le 2.$$

Here the conditions of the two parts conjugations are fulfilled; the deflections, angles, bending moments, transverse forces remain continuous. We denote the mentioned values respectively as w_A, ϑ_A, M_A, Q_A.

The solution of the homogeneous differential equation for axially symmetric bending of the similar plate, resting on elastic foundation, is expressed in terms of Bessel functions [4-7] in the following form:

$$w = A_1 u_0(x) + A_2 \upsilon_0(x) + A_3 f_0(x) + A_4 g_0(x), \quad (8)$$

where A_1, A_2, A_3, A_4 – constants;

$$x = \frac{r}{\ell},\ \ \ell = \sqrt[4]{\frac{D}{c_2}},$$

c_2 – modulus of the foundation relevant to the outer part.

To write the expression for the plate's elastic surface we introduce the fundamental functions $w_1(x_1;x)$, $w_2(x_1;x)$, $w_3(x_1;x)$, $w_4(x_1;x)$, which properties are described in [1]. We have

$$w_1(x_1;x) = \frac{\pi x_1}{2}[-u_0'(x_1)g_0(x) - \upsilon_0'(x_1)\times$$
$$\times f_0(x) + f_0'(x_1)\upsilon_0(x) + g_0'(x_1)u_0(x)],$$
$$w_2(x_1;x) = \frac{\pi x_1}{2}[-u_0(x_1)g_0(x) - \upsilon_0(x_1)\times$$
$$\times f_0(x) + f_0(x_1)\upsilon_0(x) + g_0(x_1)u_0(x)],$$
$$w_3(x_1;x) = \frac{\pi x_1}{2}[u_0'(x_1)f_0(x) - \upsilon_0'(x_1)\times$$
$$\times g_0(x) - f_0'(x_1)u_0(x) + g_0'(x_1)\upsilon_0(x)], \quad (9)$$
$$w_4(x_1;x) = \frac{\pi x_1}{2}[u_0(x_1)f_0(x) - \upsilon_0(x_1)\times$$
$$\times g_0(x) - f_0(x_1)u_0(x) + g_0(x_1)\upsilon_0(x)].$$

Thus, when $x \ge x_2$, we can write

$$w = w_{II} = w_A w_1(x_1;x) + \vartheta_A \ell w_2(x_1;x) -$$
$$- M_A \ell^2 w_3(x_1;x) - Q_A \ell^3 w_4(x_1;x). \quad (10)$$

The influence of the construction upper part can be represented by the moments M_2 and forces Q_2 distributed along the circumference with the radius x_2. Then the expression for the deflections of the combined plate by taking into account the inner and the outer parts is:

$$w = w_{\mathrm{I}} + w_{\mathrm{II}} + M_2 \ell^2 w_3(x_2; x) + \\ + Q_2 \ell^3 w_4(x_2; x). \qquad (11)$$

The coefficients incoming in the expression for w_{I} are determined from the boundary conditions and the conditions of the sections conjugation. The values of modulus of subgrade may be either different or similar.

4. CONCLUSION

The analytical method for computation of the combined plate consisting of a few sections with different laws of the thickness variation is proposed. This techniques is stated for the example of the bottom of the cylindrical reservoir examination. The influence of the upper part of the construction under study is considered. The solutions are obtained in the closed form in terms of Bessel functions.

REFERENCES

1. **Koreneva E.B.** Analiticheskie Metody Rascheta Plastin Peremennoj Tolschiny i ih Practicheskije Prilozhenija. [Analylical Methods for Calculation of Plates with Varying Thickness and Their Practical Application]. Moscow, ASV, 2009, 238 pages (in Russian).
2. **Koreneva E.B., Grosman V.R.** Analitycheskoje Reshenije Zadachi ob Izgibe Krugloj Ortotropnoj Plastiny Peremennoj Tolschiny, Lezhazchej na Uprugom Osnovanii. [Analytical Solution of the Flexure of Circular Orthotropic Plate of Variable Thickness, Resting on an Elastic Subgrade]. // *Vestnik MGSU*, 2011, No. 8, pp. 156-159 (in Russian).
3. **Kamke E.** Spravochnik po Obyknovennym Differentsialnym Uravneniyam. [The Handbook for Ordinary Differential Equations]. Moscow, Nauka, 1965, 703 pages (in Russian).
4. **Korenev B.G.** Nekotoryye Zadachi Teorii Uprugosti i Teploprovodnosti, Reshayemyye v Besselevykh Funktsiyakh. [Some Problems of the Theory of Elasticity and Heat Conductivity, Solved in Terms of Bessel Functions]. Moscow, Fizmatgiz, 1960, 458 pages (in Russian).
5. **Koreneva E.B.** Napryazhenno-Deformirovannoje Sostojanie Ledovoj Plity s Polynjej pri Neosesimmetrichnom Zagruzhenii. [Stressed and Strained State of the Ice Slab with the Opening, Subjected to an Action of Unsymmetric Loads]. // *Stroitelnaya Mekhanika i Raschet Sooruzhenij*, 2016, №5, pp. 13-18 (in Russian).
6. **Koreneva E.B.** Raschet Beskonechnoj Ledovoj Plity, Oslablennoj Otverstiem. [Calculation of the Infinite Ice Slab, Relaxed by an Opening] // *International Journal for Computational Civil and Structural Engineering*, 2016, Volume 12, Issue 4, pp. 99-102 (in Russian).
7. **Koreneva E.B.** Metod Kompensirujuschih Nagruzok dlya Reshenija Zadach ob Anizotropnyh Uprugih Sredah. [Method of Compensating Loads for Solving of Anisotropic Medium Problems] // *International Journal for Computational Civil and Structural Engineering*, 2018, Volume 14, Issue 1, pp. 71-77 (in Russian).

СПИСОК ЛИТЕРАТУРЫ

1. **Коренева Е.Б.** Аналитические методы расчета пластин переменной толщины и их практические приложения. – М.: АСВ, 2009. – 238 с.
2. **Коренева Е.Б., Гросман В.Р.** Аналитическое решение задачи об изгибе круг-

лой ортотропной пластины переменной толщины, лежащей на упругом основании. // *Вестник МГСУ*, №8, 2011, с. 156-159.
3. **Камке Э.** Справочник по обыкновенным дифференциальным уравнениям. – М.: Наука, 1965. – 703 с.
4. **Коренев Б.Г.** Некоторые задачи теории упругости и теплопроводности, решаемые в бесселевых функциях. - М.: Физматгиз, 1960. – 458 с.
5. **Коренева Е.Б.** Напряженно-деформированное состояние ледовой плиты с полыньей при неосесимметричном загружении. // *Строительная механика и расчет сооружений*, №5, 2016, с. 13-18.
6. **Коренева Е.Б.** Расчет бесконечной ледовой плиты, ослабленной отверстием. // *International Journal for Computational Civil and Structural Engineering*, Volume 12, Issue 4, 2016, pp. 99-102.
7. **Коренева Е.Б.** Метод компенсирующих нагрузок для решения задач об анизотропных средах. // *International Journal for Computational Civil and Structural Engineering*, Volume 14, Issue 1, 2018, pp. 71-78.

Elena B. Koreneva, Professor, Dr.Sc., Moscow Higher Combined-Arms Command Academy; 2, ul. Golovacheva, Moscow, 109380, Russia,
phone: +7(499)175-82-45;
E-mail: elena.koreneva2010@yandex.ru.

Коренева Елена Борисовна, профессор, доктор технических наук, Московское высшее общевойсковое командное орденов Жукова, Ленина и Октябрьской Революции Краснознаменное училище, 109380, Россия, г. Москва, ул. Головачева, д.2, тел.: +7(499)175-82-45;
E-mail: elena.koreneva2010@yandex.ru.

DOI:10.22337/2587-9618-2019-15-4-88-100

ASSESSMENT CRITERIA OF OPTIMAL SOLUTIONS FOR CREATION OF RODS WITH PIECEWISE CONSTANT CROSS-SECTIONS WITH STABILITY CONSTRAINTS OR CONSTRAINTS FOR VALUE OF THE FIRST NATURAL FREQUENCY PART 1: THEORETICAL FOUNDATIONS

Leonid S. Lyakhovich [1], ***Pavel A. Akimov*** [1, 2, 3, 4], ***Boris A. Tukhfatullin*** [1]
[1] Tomsk State University of Architecture and Building, Tomsk, RUSSIA
[2] Russian Academy of Architecture and Construction Sciences, Moscow, RUSSIA
[3] Scientific Research Center "StaDyO", Moscow, RUSSIA
[4] Peoples' Friendship University of Russia, Moscow, RUSSIA

Abstract: The special properties of optimal systems have been already identified. Besides, criteria has been formulated to assess the proximity of optimal solutions to the minimal material consumption. In particular, the criteria were created for rods with rectangular and I-beam cross-section with stability constraints or constraints for the value of the first natural frequency. These criteria can be used for optimization when the cross sections of a bar change continuously along its length. The resulting optimal solutions can be considered as an idealized object in the sense of the limit. This function of optimal design allows researcher to assess the actual design solution by the criterion of its proximity to the corresponding limit (for example, regarding material consumption). Such optimal project can also be used as a reference point in real design, for example, implementing a step-by-step process of moving away from the ideal object to the real one. At each stage, it is possible to assess the changes in the optimality index of the object in comparison with both the initial and the idealized solution. One of the variants of such a process is replacing the continuous change in the size of the cross sections of the rod along its length with piecewise constant sections. Boundaries of corresponding intervals can be selected based on an ideal feature, and cross-section dimensions can be determined by one of the optimization methods. The distinctive paper is devoted to criteria that allow researcher providing reliable assessment of the endpoint of the optimization process.

Keywords: criterion, optimization, special properties, stability, frequency, critical force, buckling, eigenmode, reduced stresses

КРИТЕРИИ ОЦЕНКИ ОПТИМАЛЬНЫХ РЕШЕНИЙ ПРИ ФОРМИРОВАНИИ СТЕРЖНЕЙ С КУСОЧНО-ПОСТОЯННЫМ ИЗМЕНЕНИЕМ ПОПЕРЕЧНЫХ СЕЧЕНИЙ ПРИ ОГРАНИЧЕНИЯХ ПО УСТОЙЧИВОСТИ ИЛИ НА ВЕЛИЧИНУ ПЕРВОЙ СОБСТВЕННОЙ ЧАСТОТЫ ЧАСТЬ 1: ТЕОРЕТИЧЕСКИЕ ОСНОВЫ

Л.С. Ляхович [1], ***П.А. Акимов*** [1, 2, 3, 4], ***Б.А. Тухфатуллин*** [1]
[1] Томский государственный архитектурно-строительный университет, г. Томск, РОССИЯ
[2] Российская академия архитектуры и строительных наук, г. Москва, РОССИЯ
[3] Научно-исследовательский центр СтаДиО, г. Москва, РОССИЯ
[4] Российский университет дружбы народов, г. Москва, РОССИЯ

Аннотация: Ранее были выявлены особые свойства оптимальных систем и сформулированы критерии, оценивающие близость оптимальных решений к минимально материалоемкому. В частности, были со-

зданы критерии, для стержней с прямоугольным и двутавровым поперечным сечением при ограничениях по устойчивости или на величину первой частоты собственных колебаний. Эти критерии применимы при оптимизации в случаях, когда поперечные сечения стержня непрерывно изменяются по его длине. Полученные при этом оптимальные решения могут рассматриваться как идеализированный объект в смысле предельного. Данная функция оптимального проекта позволяет оценивать реальное конструкторское решение по критерию его близости к предельному (например, по материалоемкости). Такой оптимальный проект также может использоваться и как ориентир при реальном проектировании, например, реализуя поэтапный процесс отхода от идеального объекта к реальному. При этом на каждом этапе появляется возможность оценки изменения показателя оптимальности объекта по сравнению, как с начальным, так и с идеализированным решением. Одни из вариантов такого процесса состоит в замене непрерывного изменения размеров поперечных сечений стержня по его длине соответствующими кусочно-постоянными участками. Границы участков могут выбираться на основе идеального объекта, а размеры поперечных сечений определяться одним из методов оптимизации. В настоящей статье предлагаются критерии, позволяющие надежно оценивать момент окончания процесса такой оптимизации.

Ключевые слова: критерий, оптимизация, особые свойства, устойчивость, частота, критическая сила, формы потери устойчивости, формы собственных колебаний, приведенные напряжения

As is known, there are numerous papers devoted to problem of minimizing the weight of rods under various restrictions. In this connection we should mention pioneer papers of Clausen [1], Lagrange [1], E.L. Nikolai [3], where special properties of optimal constructions were formulated. For example, in paper [4], special criteria were formulated that made it possible to evaluate the proximity of solutions for optimizing rods of rectangular and I-beams to a minimally material-intensive design with limitations on stability or on the value of the first frequency of natural vibrations. The criteria obtained in [4] are applicable for the case when the parameters of the cross sections vary continuously along the length of the rod. Despite the fact that such an optimal project in the overwhelming majority of cases is not directly implemented, it, being the limit, for example, by the minimum material consumption, allows researcher to evaluate the adopted design solution. In addition, the marginal project can be used as the initial stage of the step-by-step process from an ideal object to a technologically acceptable design solution (for example, [4,6]). In particular, such a process may consist of replacing a continuous change in the size of the cross sections of the rod along its length with a corresponding piecewise constant. I order to provide this, sections along the length of the rod are selected, in each of such section the dimensions of the cross-sections do not change. The choice of the boundaries of these sections is determined by technological requirements and objective to approximate to minimally material-intensive solution. After selecting the boundaries of the sections, the dimensions of the cross-sections are determined at each section using one of corresponding optimization methods.

In most optimization methods, the criterion for corresponding the step-by-step process is the state in which at the next search step, the change in the objective function is less than the selected small value in advance.

However, there are cases when, with a small change in the objective function at neighboring steps, the coordinates of the optimum point noticeably change. Obviously, the presence of a criterion that more objectively evaluates the proximity of the solution to the optimum will increase confidence in the result.

Such criteria were formulated in [4] in order to optimize rods of a rectangular and I-shaped cross section under stability restrictions or by the value of the first frequency of natural vibrations, when the parameters of the sections change continuously along the length of the rod. These criteria make it possible to evaluate the proximity of the obtained solution to a minimally demanding project.

The distinctive paper proposes similar criteria for some cases of designing the least weight rods with rectangular or I-shaped piecewise cross-sections continuously varying along the

length of the rod, with limitations on stability or on the value of the first frequency of natural vibrations.

Let us consider the derivation of such a criterion for a rod with a rectangular cross-section. In this case, it is sufficient to formulate a criterion with a limitation of the magnitude of the first frequency of natural oscillations, but taking into account the influence of the longitudinal force. Such a criterion can also be used when only a stability constraint is introduced. In this case, in the expression of the criterion, the value of the natural frequency is assumed to be zero.

The designations of the dimensions of the cross section are shown in Figure 1.

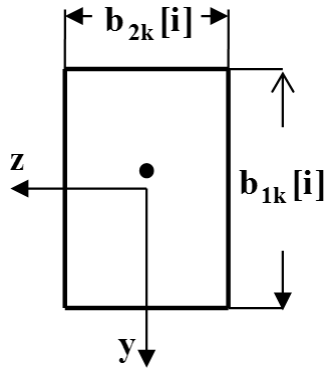


Figure 1. The designations of the dimensions of the cross section.

Rectilinear rods (including multi-span) are considered, bearing mass and loaded with longitudinal force. The rod is divided into sections, within each of which the dimensions of the sections do not change. The designations of the lengths of the sections and the coordinates of their boundaries are shown in Figure 2.

It is required to determine the dimensions of the cross sections of the rod $b_{1k}[i]$ and $b_{2k}[i]$ ($i = 1, 2, .., n$), but provided that the first frequencies in the main planes of inertia ($\omega 1[1]$ and $\omega 2[1]$) are not less than the specified value (ω_0) and that, with the selected boundaries of the rod sections and the constraints, its volume would be minimal.

Thus, the objective function (the volume of the material of the rod) is defined by formula

$$V_0 = \sum_1^n b_{1k}[i] * b_{2k}[i] * l_u[i]. \qquad (1)$$

Restrictions on the magnitude of the lowest frequency of natural vibrations,

$$\omega_0 \le \omega 1[1], \quad \omega_0 \le \omega 2[1]$$

with allowance for vibrations in the two main planes of inertia of the cross section of the rod, can be written as

$$\omega_0 = \omega 1[1] = \omega 2[1]. \qquad (2)$$

It is known that if $\omega 1[1]$ and $\omega 2[1]$ are the first frequencies of natural vibrations in the principal planes of inertia, then the energy functionals must continuously take zero values when the cross sections are continuously changed. Thus, we have

$$\Im_{\omega 1} = \frac{1}{2}\int_0^l \{EI_1(x) * (v''_\omega)^2 - P(x) * (v'_\omega)^2 - \\ - \omega^2 * [m(x) + \rho * F(x)] * v_\omega^2\} dx = 0; \qquad (3)$$

$$\Im_{\omega 2} = \frac{1}{2}\int_0^l \{EI_2(x) * (w''_\omega)^2 - P(x) * (w'_\omega)^2 - \\ - \omega^2 * [m(x) + \rho * F(x)] * w_\omega^2\} dx = 0. \qquad (4)$$

With a piecewise constant change in cross sections, requirements (3) and (4) with allowance for restrictions (2), take the form

$$\Im_{\omega 1} = \frac{1}{2}\sum_{i=1}^n \int_{x[i-1]}^{x[i]} \{EI_1[i] * (v''_\omega)^2 - P[i] * (v'_\omega)^2 - \\ - (\omega 1[1])^2 * [m(x) + \rho * F[i] * v_\omega^2\} dx = 0; \qquad (5)$$

$$\Im_{\omega 2} = \frac{1}{2}\sum_{i=1}^n \int_{x[i-1]}^{x[i]} \{EI_2[i] * (w''_\omega)^2 - P[i] * (w'_\omega)^2 - \\ - (\omega 2[1])^2 * [m(x) + \rho * F[i] * w_\omega^2\} dx = 0. \qquad (6)$$

Here E is the elastic modulus of the material of the rod; $I_1(x)$, $I_1[i]$, $I_2(x)$, $I_2[i]$ are respectively,

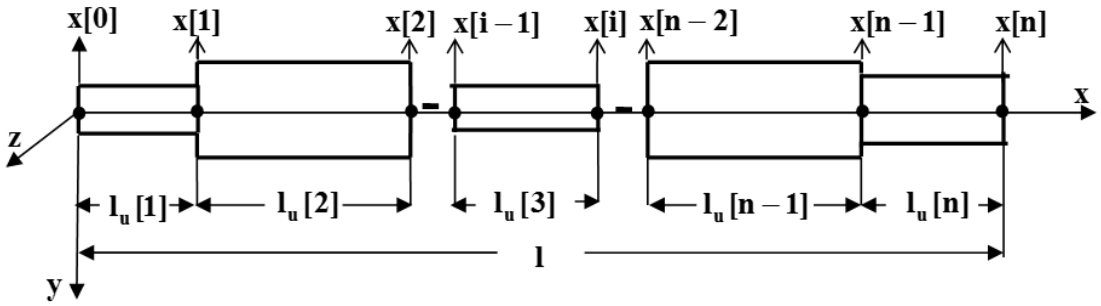


Figure 2. The designations of the lengths of the sections and the coordinates of their boundaries.

the moments of inertia of the cross sections of the rod in the main planes of inertia; v_ω, w_ω are the coordinates of the modes of natural vibrations in the main planes of inertia; ρ is the specific gravity of the material of the rod;

$$F(x) = b_1(x) * b_2(x), \quad F[i] = b_{1k}[i] * b_{2k}[i]$$

is the cross-sectional area of the rod.

Thus, it is required to find the values $b_{1k}[i]$ and $b_{2k}[i]$ that give the function (1) the minimum value when conditions (5), (6) are satisfied.

So, we have to consider corresponding parametric problem.

The expression extremum of which will ensure the minimum of function (1) and the fulfillment of conditions (5), (6), can be written as

$$\begin{aligned} V_{0\omega} &= \sum_{i=1}^{n} b_{1k}[i] * b_{2k}[i] * l_u[i] - \\ &- \sum_{i=1}^{n} \int_{x[i-1]}^{x[i]} \{\lambda_{\omega 1} * [E * \frac{b_{1k}^3[i] * b_{2k}[i]}{12} * (v_\omega'')^2 - \\ &- P[i] * (v_\omega')^2 - \\ &- (\omega 1[1])^2 * (m(x) + \rho * b_{1k}[i] * b_{2k}[i]) * v_\omega^2] - \\ &- \lambda_{\omega 2} * [E * \frac{b_{1k}[i] * b_{2k}^3[i]}{12} * (w_\omega'')^2 - \\ &- P(i) * (w_\omega')^2 - \\ &- (\omega 2[1])^2 * (m(x) + \rho * b_{1k}[i] * b_{2k}[i]) w_\omega^2] \} dx, \end{aligned} \quad (7)$$

where $\lambda_{\omega 1}$ and $\lambda_{\omega 2}$ are arbitrary factors. In the parametric problem, the factors $\lambda_{\omega 1}$ and $\lambda_{\omega 2}$ are constant values.

Obviously, variations of expression (7) with respect to $\lambda_{\omega 1}$ and $\lambda_{\omega 2}$ lead to the fulfillment of conditions (5) and (6), and therefore to constraint (2).

In order to find the minimum of expression (7) under conditions (5), (6) it is necessary to write the system of equations

$$\frac{\partial V_{0\omega}}{\partial b_{1k}[i]} = 0; \quad \frac{\partial V_{0\omega}}{\partial b_{2k}[i]} = 0, \ldots \quad (i = 1, 2, .., n). \quad (7)$$

Let us write i-th couple of equations

$$\begin{aligned} &\frac{\partial V_{0\omega}}{\partial b_{1k}[i]} = b_{2k}[i] * l_u[i] - \\ &- \int_{x[i-1]}^{x[i]} \lambda_{\omega 1} * [E * \frac{b_{1k}^2[i] * b_{2k}[i]}{4} * (v_\omega'')^2 - \\ &- \{(\omega 1[1])^2 * \rho * b_{2k}[i] * v_\omega^2] - \\ &- \lambda_{\omega 2} * [E * \frac{b_{2k}^3[i]}{12} * (w_\omega'')^2 - \\ &- (\omega 2[1])^2 * \rho * b_{2k}[i] * w_\omega^2] \} dx = 0; \\ &\frac{\partial V_{0\omega}}{\partial b_{2k}[i]} = b_{1k}[i] * l_u[i] - \\ &- \int_{x[i-1]}^{x[i]} \{\lambda_{\omega 1} * [E * \frac{b_{1k}^3[i]}{12} * (v_\omega'')^2 - \\ &- (\omega 1[1])^2 * \rho * b_{1k}[i] * v_\omega^2] - \\ &- \lambda_{\omega 2} * [E * \frac{b_{1k}[i] * b_{2k}^2[i]}{4} * (w_\omega'')^2 - \\ &- (\omega 2[1])^2 * \rho * b_{1k}[i] * w_\omega^2 \} dx = 0. \end{aligned} \quad (8)$$

Dividing all the terms of the first equation by $b_{2k}[i]$, and the second by $b_{1k}[i]$ and performing simple transformations, we get

$$\begin{aligned}
&\int_{x[i-1]}^{x[i]} \{\lambda_{\omega 1} * [E * \frac{b_{1k}^2[i]}{4} * (v_\omega'')^2 - \\
&-(\omega 1[1])^2 * \rho * v_\omega^2] + \lambda_{\omega 2} * [E * \frac{b_{2k}^2[i]}{12} * (w_\omega'')^2 - \\
&-(\omega 2[1])^2 * \rho * w_\omega^2]\} dx = l_u[i]; \\
&\int_{x[i-1]}^{x[i]} \{\lambda_{\omega 1} * [E * \frac{b_{1k}^2[i]}{12} * (v_\omega'')^2 - \\
&-(\omega 1[1])^2 * \rho * v_\omega^2] + \lambda_{\omega 2} * [E * \frac{b_{2k}^2[i]}{4} * (w_\omega'')^2 - \\
&-(\omega 2[1])^2 * \rho * w_\omega^2]\} dx = l_u[i].
\end{aligned} \tag{9}$$

Multiplying all terms of the obtained equations by E and taking into account that

$$\begin{aligned}
\sigma_1(x) = \frac{E}{2} * b_1(x) * (v_\omega''); \\
\sigma_2(x) = \frac{E}{2} * b_2(x) * (w_\omega'')
\end{aligned} \tag{10}$$

we can rewrite corresponding equations:

$$\begin{aligned}
&\int_{x[i-1]}^{x[i]} \{\lambda_{\omega 1} * [\sigma_{1\omega}^2(x) - (\omega 1[1])^2 * E * \rho * v_\omega^2] + \\
&+\lambda_{\omega 2} * [\frac{1}{3} * \sigma_{2\omega}^2(x) - \\
&-(\omega 2[1])^2 * E * \rho * w_\omega^2]\} dx = l_u[i] * E; \\
&\int_{x[i-1]}^{x[i]} \{\lambda_{\omega 1} * [\frac{1}{3} * \sigma_{1\omega}^2(x) - (\omega 1[1])^2 * E * \rho * v_\omega^2] + \\
&+\lambda_{\omega 2} * [\sigma_{2\omega}^2(x) - \\
&-(\omega 2[1])^2 * E * \rho * w_\omega^2]\} dx = l_u[i] * E,
\end{aligned} \tag{11}$$

where $\sigma_{1\omega}(x)$ and $\sigma_{2\omega}(x)$ are normal stresses in the extreme fibers of the rod from bending moments arising from natural vibrations in the main planes of inertia. These stresses, as well as displacements, are determined up to a constant factor.

Taking the difference of equations (9), we obtain

$$\begin{aligned}
&\frac{2}{3} * \lambda_{\omega 1} * \int_{x[i-1]}^{x[i]} \sigma_{1\omega}^2(x) dx - \\
&-\frac{2}{3} * \lambda_{\omega 2} * \int_{x[i-1]}^{x[i]} \sigma_{2\omega}^2(x) dx = 0.
\end{aligned} \tag{12}$$

Therefor the following formulas can be obtained:

$$\lambda_{\omega 1} * \int_{x[i-1]}^{x[i]} \sigma_{1\omega}^2(x)\, dx = \lambda_{\omega 2} * \int_{x[i-1]}^{x[i]} \sigma_{2\omega}^2(x)\, dx; \tag{13}$$

$$\lambda_{\omega 1} = \lambda_{\omega 2} * \frac{\int_{x[i-1]}^{x[i]} \sigma_{2\omega}^2\, dx}{\int_{x[i-1]}^{x[i]} \sigma_{1\omega}^2\, dx}; \tag{14}$$

$$\lambda_{\omega 2} = \lambda_{\omega 1} * \frac{\int_{x[i-1]}^{x[i]} \sigma_{1\omega}^2\, dx}{\int_{x[i-1]}^{x[i]} \sigma_{2\omega}^2\, dx}. \tag{15}$$

Based on (13)-(15), equations (11) can be written in the following form

$$\begin{aligned}
&\int_{x[i-1]}^{x[i]} \{\lambda_{\omega 1} * [\sigma_{1\omega}^2(x)\, dx - (\omega 1[1])^2 * E * \rho * v_\omega^2] + \\
&+\lambda_{\omega 2} * \frac{1}{3} * \sigma_{2\omega}^2(x) - \\
&-\lambda_{\omega 2} (\omega 2[1])^2 * E * \rho * w_\omega^2\} dx = l_u[i] * E; \\
&\int_{x[i-1]}^{x[i]} \{\lambda_{\omega 1} * [\frac{1}{3} * \sigma_{1\omega}^2(x) - (\omega 1[1])^2 * E * \rho * v_\omega^2] + \\
&+\lambda_{\omega 2} * \sigma_{2\omega}^2(x) - \\
&-\lambda_{\omega 2} * (\omega 2[1])^2 * E * \rho * w_\omega^2\} dx = l_u[i] * E;
\end{aligned} \tag{16}$$

$$\lambda_{\omega 1}\int_{x[i-1]}^{x[i]}[\sigma_{1\omega}^2(x)\,dx-(\omega 1[1])^2*E*\rho*v_\omega^2]dx+$$
$$+\frac{1}{3}*\lambda_{\omega 1}*\frac{\int_{x[i-1]}^{x[i]}\sigma_{1\omega}^2\,dx}{\int_{x[i-1]}^{x[i]}\sigma_{2\omega}^2\,dx}*\int_{x[i-1]}^{x[i]}\sigma_{2\omega}^2(x)\,dx-$$
$$-\lambda_{\omega 1}\int_{x[i-1]}^{x[i]}\frac{\int_{x[i-1]}^{x[i]}\sigma_{1\omega}^2\,dx}{\int_{x[i-1]}^{x[i]}\sigma_{2\omega}^2\,dx}*\omega 2[1])^2*E*\rho*w_\omega^2\,dx=$$
$$=l_u[i]*E;$$
$$\frac{]}{3}*\lambda_{\omega 2}*\frac{\int_{x[i-1]}^{x[i]}\sigma_{2\omega}^2\,dx}{\int_{x[i-1]}^{x[i]}\sigma_{1\omega}^2\,dx}\int_{x[i-1]}^{x[i]}\sigma_{1\omega}^2(x)\,dx-$$
$$-\int_{x[i-1]}^{x[i]}\lambda_{\omega 1}*(\omega 1[1])^2*E*\rho*v_\omega^2]dx+$$
$$+\lambda_{\omega 2}*\int_{x[i-1]}^{x[i]}[\sigma_{2\omega}^2(x)-(\omega 2[1])^2*E*\rho*w_\omega^2]dx=$$
$$=l_u[i]*E;\qquad(17)$$

$$\lambda_{\omega 1}*\int_{x[i-1]}^{x[i]}\{\frac{4}{3}*\sigma_{1\omega}^2(x)-(\omega 1[1])^2*E*\rho*v_\omega^2-$$
$$-\frac{\int_{x[i-1]}^{x[i]}\sigma_{1\omega}^2\,dx}{\int_{x[i-1]}^{x[i]}\sigma_{2\omega}^2\,dx}*(\omega 2[1])^2*E*\rho*w_\omega^2\}dx=$$
$$=l_u[i]*E;\qquad(18)$$

$$\lambda_{\omega 2}*\int_{x[i-1]}^{x[i]}\{\frac{4}{3}*\sigma_{2\omega}^2(x)-\frac{\int_{x[i-1]}^{x[i]}\sigma_{2\omega}^2\,dx}{\int_{x[i-1]}^{x[i]}\sigma_{1\omega}^2\,dx}*$$
$$*(\omega 1[1])^2*E*\rho*v_\omega^2]-$$
$$-(\omega 2[1])^2*E*\rho*w_\omega^2\}dx=l_u[i]*E.$$

Since $\lambda_{\omega 1},\lambda_{\omega 2},E$ are constant values, we rewrite (18) in the form

$$\frac{1}{l_u[i]}*\int_{x[i-1]}^{x[i]}\{\frac{4}{3}*\sigma_{1\omega}^2(x)-(\omega 1[1])^2*E*\rho*v_\omega^2-$$
$$-\frac{\int_{x[i-1]}^{x[i]}\sigma_{1\omega}^2\,dx}{\int_{x[i-1]}^{x[i]}\sigma_{2\omega}^2\,dx}*(\omega 2[1])^2*E*\rho*w_\omega^2\}dx=$$
$$=E=Const;$$
$$\frac{1}{l_u[i]}*\int_{x[i-1]}^{x[i]}\{\frac{4}{3}*\sigma_{2\omega}^2(x)-\frac{\int_{x[i-1]}^{x[i]}\sigma_{2\omega}^2\,dx}{\int_{x[i-1]}^{x[i]}\sigma_{1\omega}^2\,dx}*$$
$$*(\omega 1[1])^2*E*\rho*v_\omega^2]-$$
$$-(\omega 2[1])^2*E*\rho*w_\omega^2\}dx=E=Const.\qquad(19)$$

Substituting $\omega_0=\omega 1[1]=\omega 2[1]$ and dividing by $4/3$, we obtain

$$\frac{1}{l_u[i]}*\int_{x[i-1]}^{x[i]}[\sigma_{1\omega}^2(x)-\frac{3}{4}*(\omega_0)^2*E*\rho*(v_\omega^2+$$
$$+\frac{\int_{x[i-1]}^{x[i]}\sigma_{1\omega}^2\,dx}{\int_{x[i-1]}^{x[i]}\sigma_{2\omega}^2\,dx}*w_\omega^2)]dx=Const;$$
$$\frac{1}{l_u[i]}*\int_{x[i-1]}^{x[i]}[\sigma_{2\omega}^2(x)-\frac{3}{4}*(\omega_0)^2*E*\rho*\qquad(20)$$
$$*(\frac{\int_{x[i-1]}^{x[i]}\sigma_{2\omega}^2\,dx}{\int_{x[i-1]}^{x[i]}\sigma_{1\omega}^2\,dx}*v_\omega^2+w_\omega^2)]dx=Const.$$

If the boundary conditions in the principal planes of inertia are the same, then

$$v_\omega = w_\omega; \quad \sigma_{1\omega} = \sigma_{2\omega}$$

and (20) take the form

$$\frac{1}{l_u[i]} * \int_{x[i-1]}^{x[i]} [\sigma_{1\omega}^2(x) - 1.5 * (\omega_0)^2 * E * \rho * v_\omega^2] dx = = Const;$$
$$\frac{1}{l_u[i]} * \int_{x[i-1]}^{x[i]} [\sigma_{2\omega}^2(x) - 1.5 * (\omega_0)^2 * E * \rho * w_\omega^2] dx = = Const.$$

(21)

Let us introduce the notation

$$S_1[i] = \frac{1}{l_u[i]} * \int_{x[i-1]}^{x[i]} [\sigma_{1\omega}^2(x) - \frac{3}{4} * (\omega_0)^2 * E * \rho * * (v_\omega^2 + \int_{x[i-1]}^{x[i]} \sigma_{1\omega}^2 dx * \left(\int_{x[i-1]}^{x[i]} \sigma_{2\omega}^2 dx \right)^{-1} * w_\omega^2)] dx;$$
$$S_2[i] = \frac{1}{l_u[i]} * \int_{x[i-1]}^{x[i]} [\sigma_{2\omega}^2(x) - \frac{3}{4} * (\omega_0)^2 * E * \rho * * (\int_{x[i-1]}^{x[i]} \sigma_{1\omega}^2 dx * \left(\int_{x[i-1]}^{x[i]} \sigma_{2\omega}^2 dx \right)^{-1} * v_\omega^2 + w_\omega^2)] dx.$$

(22)

Thus, we can rewrite (20) and (21) in the following form

$$S_1[i] = \frac{1}{l_u[i]} * \int_{x[i-1]}^{x[i]} [\sigma_{1\omega}^2(x) - \frac{3}{4} * (\omega_0)^2 * E * \rho * * (v_\omega^2 + \int_{x[i-1]}^{x[i]} \sigma_{1\omega}^2 dx * \left(\int_{x[i-1]}^{x[i]} \sigma_{2\omega}^2 dx \right)^{-1} * w_\omega^2)] dx = = const$$
$$S_2[i] = \frac{1}{l_u[i]} * \int_{x[i-1]}^{x[i]} [\sigma_{2\omega}^2(x) - \frac{3}{4} * (\omega_0)^2 * E * \rho * * (\int_{x[i-1]}^{x[i]} \sigma_{1\omega}^2 dx * \left(\int_{x[i-1]}^{x[i]} \sigma_{2\omega}^2 dx \right)^{-1} * v_\omega^2 + w_\omega^2)] dx = = const;$$

(23)

$$S_1[i] = \frac{1}{l_u[i]} * \int_{x[i-1]}^{x[i]} [\sigma_{1\omega}^2(x) - \frac{3}{2} * (\omega_0)^2 * E * \rho * v_\omega^2] dx = = const;$$
$$S_2[i] = \frac{1}{l_u[i]} * \int_{x[i-1]}^{x[i]} [\sigma_{2\omega}^2(x) - \frac{3}{2} * (\omega_0)^2 * E * \rho * w_\omega^2] dx = = const.$$

(24)

Both equations (21) become identical. Nevertheless, the conservation of two equations is advisable in order to construct algorithms for the implementation of criterion (16).

If the natural vibrations are considered only in one of the main planes of inertia, then, based on (11), the criteria are presented in the form

$$S_1[i] = \frac{1}{l_u[i]} * \int_{x[i-1]}^{x[i]} [\sigma_{1\omega}^2(x) - (\omega_0)^2 * E * \rho * v_\omega^2] dx = const;$$
$$S_2[i] = \frac{1}{l_u[i]} * \int_{x[i-1]}^{x[i]} [\sigma_{2\omega}^2(x) - (\omega_0)^2 * E * \rho * w_\omega^2] dx = const.$$

(25)

It is advisable to normalize values of $S_1[i]$ and $S_2[i]$. One of the normalization options, for instance for $S_1[i]$ $(i = 1, 2, ..., n)$ includes choosing the highest value in this series and dividing all members of the series into it. Thus, in a row there will be no values of larger than unity. The proximity of the solution to the optimum will be evaluated by the proximity of the values to unity. The series is also normalized.

Let us compare the criteria (23), (24), (25) obtained with a piecewise constant change in rectangular cross sections with similar criteria with

a continuous change. These criteria were obtained in [6] and have the form

$$\begin{aligned}&\sigma_{1\omega}^2(x)-\frac{3}{4}*E*\rho*(\omega_0*k_\omega)^2*\\&\qquad*(v_\omega^2+\frac{\sigma_{1\omega}^2}{\sigma_{2\omega}^2}*w_\omega^2)=const;\\&\sigma_{2\omega}^2(x)-\frac{3}{4}*E*\rho*(\omega_0*k_\omega)^2*\\&\qquad*(\frac{\sigma_{2\omega}^2}{\sigma_{1\omega}^2}*v_\omega^2+w_\omega^2)=const;\end{aligned}\tag{26}$$

or

$$\begin{aligned}&\overline{\sigma}_{1\omega}=\\&=\sqrt{\sigma_{1\omega}^2(x)-\frac{3}{4}*E*\rho*(\omega_0*k_\omega)^2*(v_\omega^2+\frac{\sigma_{1\omega}^2}{\sigma_{2\omega}^2}*w_\omega^2)}=\\&=const\\&\overline{\sigma}_{2\omega}=\\&=\sqrt{\sigma_{2\omega}^2(x)-\frac{3}{4}*E*\rho*(\omega_0*k_\omega)^2*(\frac{\sigma_{2\omega}^2}{\sigma_{1\omega}^2}*v_\omega^2+w_\omega^2)}=\\&=const;\end{aligned}\tag{27}$$

$$\begin{aligned}&\sigma_{1\omega}^2(x)-\frac{3}{2}*(\omega_0*k_\omega)^2*E*\rho*v_\omega^2=const\\&\sigma_{2\omega}^2(x)-\frac{3}{2}*(\omega_0*k_\omega)^2*E*\rho*w_\omega^2=const\end{aligned}\tag{28}$$

or

$$\begin{aligned}&\overline{\sigma}_{1\omega}=\sqrt{\sigma_{1\omega}^2(x)-\frac{3}{2}*(\omega_0*k_\omega)^2*E*\rho*v_\omega^2}=\\&\quad=const;\\&\overline{\sigma}_{2\omega}=\sqrt{\sigma_{2\omega}^2(x)-\frac{3}{2}*(\omega_0*k_\omega)^2*E*\rho*w_\omega^2}=\\&\quad=const;\end{aligned}\tag{29}$$

$$\begin{aligned}&\sigma_{1\omega}^2(x)-(\omega_0*k_\omega)^2*E*\rho*v_\omega^2=const\\&\sigma_{2\omega}^2(x)-(\omega_0*k_\omega)^2*E*\rho*w_\omega^2=const;\end{aligned}\tag{30}$$

$$\begin{aligned}&\overline{\sigma}_{1\omega}=\sqrt{\sigma_{1\omega}^2(x)-(\omega_0*k_\omega)^2*E*\rho*v_\omega^2}=\\&\quad=const;\\&\overline{\sigma}_{2\omega}=\sqrt{\sigma_{2\omega}^2(x)-(\omega_0*k_\omega)^2*E*\rho*w_\omega^2}=\\&\quad=const;\end{aligned}\tag{31}$$

Each of the criteria is presented in two versions. The second versions of presenting the criteria are optional. They were presented only in order to emphasize their connection with the previously formulated criteria (for example, in [3]), where the constant stresses served as a sign of optimality under stability limitations, in the extreme fibers of the rod from bending moments arising from loss of stability.

The use of the second versions of the criteria with restrictions on the value of the lowest frequency of natural oscillations to evaluate the optimization process at the initial stages of the search can lead to negative values of the radical expressions. Therefore, the first criteria presentation options should be used in order to avoid malfunctions in the computing process.

As noted above, the formulated criteria can be used when only a stability constraint is introduced. In this case, in the criteria expressions, the value of the natural frequency is assumed to be zero.

A comparison of the criteria (23), (24), (25) obtained with a piecewise constant change in rectangular cross sections with similar criteria for a corresponding continuous change (26), (28) and (30) shows that under the integrals in (24) and (25) are expressions (28) and (30), respectively, and in (23) the modified expression (26). Criteria $S_1[i]$ and $S_2[i]$ contain a multiplier $1/l_u[i]$. Therefore, the criteria (24) and (25) can be considered on each piecewise constant section as the average value of the criteria (27) and (28), respectively, per unit length of the section; criterion (23) based on the modified criterion (26) is similarly considered. If we use the noted interconnection of criteria for determining the values of $S_1[i]$ and $S_2[i]$, then it is also advisable to normalize these values to assess their proximity to unity.

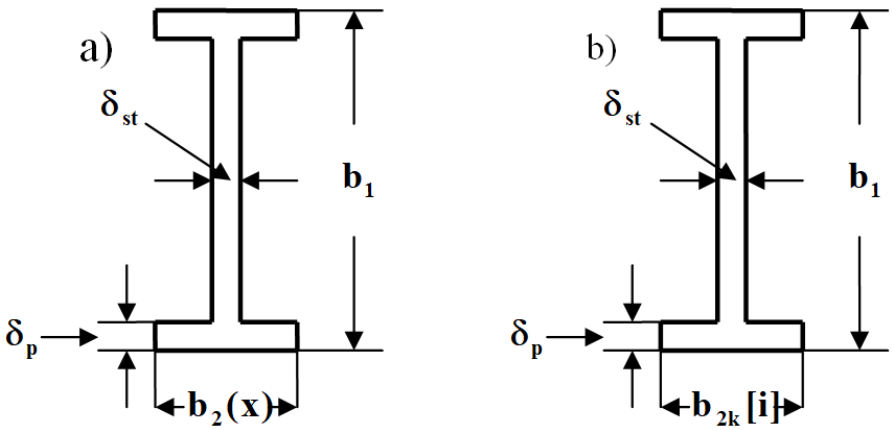


Figure 3. The cross-section of considering rod.

Let us consider criteria similar to those given above for an I-section rod (Figures 3*a*, 3*b*) with stability constraints or constraints for the value of the first natural frequency when the section height (b_1), shelf thickness (δ_p), and wall thickness (δ_{st}) do not vary. Only the dimensions of the width of the shelf ($b_2(x)$) vary with continuous change of dimensions or $b_{2k}[i]$ ($i = 1, 2, ..., n$) with piecewise constant change (Figure 2). Natural oscillations occur in one main plane of inertia $x-o-y$ (Figure 2).

A criterion that allows researcher to evaluate the results of solutions of optimization of the width of a shelf under stability constraints or constraints for the value of the first frequency of natural vibrations, for the case when the width of the shelf varies continuously along the length of the rod, was formulated in [6].

This criterion can be presented in the form of three versions:

$$\sigma_{1\omega}^2(x)*b_1 - \sigma_{1\omega t}^2(x)*(b_1 - 2*\delta_p) - \\ -3*E*(\omega_0*k_\omega)^2*\rho*2*\delta_p*v_\omega^2 = const; \quad (32)$$

$$\sigma_{1\omega}^2(x)*\frac{b_1}{2*\delta_p} - \sigma_{1\omega t}^2(x)*(\frac{b_1}{2*\delta_p} - 1) - \\ -3*E*(\omega_0*k_\omega)^2*v_\omega^2*\rho = const; \quad (33)$$

$$\overline{\sigma}_{1\omega t}(x) = \\ = \sqrt{\sigma_{1\omega}^2(x)*\frac{b_1}{2*\delta_p} - \sigma_{1\omega t}^2(x)*(\frac{b_1}{2*\delta_p} - 1) - \\ -3*E*(\omega_0*k_\omega)^2*v_\omega^2*\rho} = const, \quad (34)$$

where $\sigma_{1\omega}(x)$ and $\sigma_{1\omega t}$ are respectively, normal stresses in the extreme fibers of the I-section and in the fibers at the boundary of the wall and the shelf.

Version (34) was introduced only to emphasize its relationship with the previously formulated criteria. The use of this version of the criteria with constraints for the value of the lowest frequency of natural oscillations for assessments of the process at the initial stages of optimization can lead to negative values of the radical expressions. Therefore, version (34) should not be used in order to avoid malfunctions of the computational process.

Let us formulate a criterion similar to (32) for piecewise-constant changes in the dimensions of the width of the shelf.

The objective function has the form

$$V_0 = \sum_1^n F[i]*l_u[i], \quad (35)$$

where

$$F[i] = 2*b_2k[i]*\delta_p + b_1*\delta_{st} - 2*\delta_p*\delta_{st}. \quad (36)$$

But since only the values $b_{2k}[i]$ vary we have

$$V_0 = \sum_1^n 2*b_{2k}[i]*\delta_p*l_u[i]. \quad (37)$$

Constraints for the value of the lowest frequency of natural oscillations have the form

$$\omega_0 \le \omega 1[1]. \tag{38}$$

Method of searching for a conditional extremum is used in order to identify the criterion of minimum of the objective function with allowance for constraints for the value of the lowest frequency of natural oscillations.

Let us form an integral, the extremum conditions of which should provide minimum of the objective function (37) and the fulfillment of the conditions that the given frequency will be the lowest frequency of natural oscillation in the principal plane of inertia, i.e.

$$\omega_0 = \omega 1[1]. \tag{39}$$

If (39) is satisfied in the form of equality, we have the following condition

$$\begin{aligned}\Im_{\omega 1} = \frac{1}{2}\sum_{i=1}^{n}\int_{x[i-1]}^{x[i]}\{EI_1[i]*(v_\omega'')^2 - P[i]*(v_\omega')^2 - \\ -(\omega 1[1])^2*[m(x)+\rho*F[i]*v_\omega^2\}dx = 0.\end{aligned} \tag{40}$$

The moment of inertia of the section is defined by formula

$$\begin{aligned}I_1[i] = \frac{b_{2k}[i]}{12}*[b_1^3-(b_1-2*\delta_p)^3]+ \\ +\frac{\delta_{st}}{12}*(b_1-2*\delta_p)^3.\end{aligned} \tag{41}$$

An expression whose extremum provides a minimum of function (37) and the fulfillment of conditions (5) can be written as

$$\begin{aligned}V_{0\omega} = \sum_{i=1}^{n}2*b_{2k}[i]*\delta_p*l_u[i] - \\ -\sum_{i=1}^{n}\int_{x[i-1]}^{x[i]}\lambda_{\omega 1}*\{E*[\frac{b_{2k}[i]}{12}* \\ *(b_1^3-(b_1-2*\delta_p)^3)+\frac{\delta_{st}}{12}* \\ *(b_1-2*\delta_p)^3]*(v_\omega'')^2 - P[1]*(v_\omega')^2 - \\ -(\omega_0)^2*[m(x)+\rho*(2*b_{2k}[i]*\delta_p + \\ +b_1*\delta_{st}-2*\delta_p*\delta_{st})]*v_\omega^2]\}dx.\end{aligned} \tag{42}$$

Obviously, the variation of expression (42) by $\lambda_{\omega 1}$ will lead to the fulfillment of condition (5).

Let us write the following system of equations in order to find the minimum of expression (42) under the given conditions (39), (5):

$$\frac{\partial V_{0\omega}}{\partial b_{1k}[i]} = 0, \quad i = 1, 2, .., n. \tag{43}$$

We can write the i-th equation

$$\begin{aligned}\frac{\partial V_{0\omega}}{\partial b_{1k}[i]} = 2*\delta_p*l_u[i] - \\ -\int_{x[i-1]}^{x[i]}\{\lambda_{\omega 1}*\{\frac{E}{12}*[b_1^3-(b_1-2*\delta_p)^3]* \\ *(v_\omega'')^2-(\omega_0)^2*\rho*2*\delta_p*v_\omega^2\}\}dx = 0\end{aligned} \tag{44}$$

or

$$\begin{aligned}\int_{x[i-1]}^{x[i]}\{\frac{E}{12}*[b_1^3-(b_1-2*\delta_p)^3]*(v_\omega'')^2 - \\ -(\omega_0)^2*\rho*2*\delta_p*v_\omega^2\}\}dx = \\ = 2*\delta_p*l_u[i]/\lambda_{\omega 1}.\end{aligned} \tag{45}$$

Taking into account that δ_p and $\lambda_{\omega 1}$ are constant values, we can write

$$\begin{aligned}\frac{1}{l_k[i]}*\int_{x[i-1]}^{x[i]}\{\frac{E}{12}*[b_1^3-(b_1-2*\delta_p)^3]*(v_\omega'')^2 - \\ -(\omega_0)^2*\rho*2*\delta_p*v_\omega^2\}\}dx = const.\end{aligned} \tag{46}$$

As is known, normal stresses in a rod during bending in a fiber that is separated from the neutral layer by a distance y_s are determined by the dependence $\sigma = (M * y_s)/I$.

Since $M = -EI * v''$, we have $\sigma = -E * y_s * v''$.

After simple transformations (46) can be rewritten in the form

$$\frac{1}{l_k[i]} * \int_{x[i-1]}^{x[i]} \{\frac{1}{3*E} * [(\frac{E*b_1*v''_\omega}{2})^2 * b_1 - (\frac{b_1 - 2*\delta_P}{2} * E * v''_\omega)^2 * (b_1 - 2*\delta_p)] - (\omega_0)^2 * \rho * 2 * \delta_p * v_\omega^2\} dx = const. \quad (47)$$

Let us note that

$$(\frac{E*b_1*v''_\omega}{2})^2 = \sigma^2_{1\omega}(x);$$

$$(\frac{b_1 - 2*\delta_P}{2} * E * v''_\omega)^2 = \sigma^2_{1\omega t}(x)$$

are the square of the normal stress in the extreme fibers of the I-section and in the fibers at the boundary of the wall and the shelf.

Thus, (37) can be written as

$$\frac{1}{l_k[i]} * \int_{x[i-1]}^{x[i]} [\sigma^2_{1\omega}(x) * b_1 - \sigma^2_{1\omega t}(x) * (b_1 - 2*\delta_p) - 3*E*(\omega_0)^2 * \rho * 2 * \delta_p * v_\omega^2] dx = const \quad (48)$$

or

$$\frac{1}{l_k[i]} * \int_{x[i-1]}^{x[i]} [\sigma^2_{1\omega}(x) * \frac{b_1}{2*\delta_p} - \sigma^2_{1\omega t}(x) * (\frac{b_1}{2*\delta_p} - 1) - 3*E*(\omega_0)^2 * v_\omega^2(x) * \rho] dx = const. \quad (49)$$

We can rewrite dependencies (48) and (49) in the form

$$S_1[i] = \frac{1}{l_k[i]} * \int_{x[i-1]}^{x[i]} [\sigma^2_{1\omega}(x) * b_1 - \sigma^2_{1\omega t}(x) * (b_1 - 2*\delta_p) - 3*E*(\omega_0)^2 * \rho * 2 * \delta_p * v_\omega^2] dx = const. \quad (50)$$

$$S_1[i] = \frac{1}{l_k[i]} * \int_{x[i-1]}^{x[i]} [\sigma^2_{1\omega}(x) * \frac{b_1}{2*\delta_p} - \sigma^2_{1\omega t}(x) * (\frac{b_1}{2*\delta_p} - 1) - 3*E*(\omega_0)^2 * v_\omega^2(x) * \rho] dx = const. \quad (51)$$

As noted above, the formulated criteria can be used when only a stability constraint is introduced. In this case, in the criteria expressions, the value of the natural frequency is assumed to be zero.

A comparison of the criteria (50), (51) obtained with a piecewise constant change in the width of the shelf with similar criteria for its continuous change (32), (33) and (34) shows that under the integrals in (50) and (51) are respectively the expressions (32) and (33). Criteria $S_1[i]$ and $S_2[i]$ contain a multiplier $1/l_u[i]$. Therefore, criteria (50) and (51) can be considered on each piecewise constant section as the average value of criteria (32) and (33), respectively, per unit length of the section.

When optimizing rods with a rectangular and two-T-shaped cross-section under stability constraints or constraints for the value of the first frequency of natural vibrations, if the cross-sections continuously vary along its length, criteria were formulated to evaluate the proximity of the obtained solutions to the minimum material-intensive [6]. However, in most cases such projects are not directly implemented. At the same time, they allow researcher to evaluate a real design solution by the criterion of its proximity to the limit (for example, by material consumption), and also be used as a guideline in practical (real) design. One of the options for moving from a limiting project to a really acceptable one is to replace continuous change in cross-sectional dimensions with piecewise constant sections. The boundaries of the plots can

be selected on the basis of an ideal object, and the dimensions of the cross sections are determined by one of the optimization methods.
Generally this paper proposes criteria that allow researcher to evaluate (reliably) the end of the process of such optimization.

REFERENCES

1. **Lagrange J.-L.** Sur la figure des collonnes. // *Mescellanea Taurinensia*, 1770-1773, Volume 5, pp. 123.
2. **Clausen T.** Uber die form architektonischer Säulen. // *Bull. cl. physico-raath. Acad. St.-Petersburg*, 1851, Volume 9, pp. 371-380.
3. **Nikolai E.L.** Zadacha Lagranzha o naivygodneishem ochertanii kolonny [The Lagrange problem of the best shape of the column]. // *Bulletin of the St. Petersburg Polytechnic Institute*, 1907, No. 8 (in Russian).
4. **Lyakhovich L.S., Akimov P.A., Tukhfatullin B.A.** O zadachakh poiska minimuma i maksimuma v stroitel'noi mekhanike [About hill-climbing problems in structural mechanics]. // *International Journal for Computational Civil and Structural Engineering*, 2017, Volume 13, Issue 2, pp. 103-124 (in Russian).
5. **Lyakhovich L.S., Malinovsky A.P., Tukhfatullin B.A.** Criteria for Optimal Strengthening of Bar Flange with I-type Cross-section with Stability Constraints on the Value of the First Natural Frequency. // *Procedia Engineering*, 2016. Volume 153, pp. 427-433.
6. **Lyakhovich L.S.** Osobye svoistva optimal'nykh sistem i osnovnye napravleniya ikh realizatsii v metodakh rascheta sooruzhenii [The special properties of optimal systems and the main directions of their implementation in the methods of calculation of structures]. Tomsk, Tomsk State University of Architecture and Building, 2009, 372 pages (in Russian).
7. **Lyakhovich L.S., Perelmuter A.V.** Nekotorye voprosy optimal'nogo proektirovaniya stroitel'nykh konstruktsii [Some problems of building constructions optimal projecting]. // *International Journal for Computational Civil and Structural Engineering*, 2014, Volume 10, Issue 2, pp. 14-23 (in Russian).
8. **Aslami M., Akimov P.A.** Analytical solution for beams with multipoint boundary conditions on two-parameter elastic foundations. // *Archives of Civil and Mechanical Engineering*, 2016, Volume 16, Issue 4, pp. 668-677.
9. **Ludeker J.K., Kriegesmann B.** Fail-safe optimization of beam structures. // *Journal of Computational Design and Engineering*, 2019, Volume 6, Issue 3, pp. 260-268.
10. **Quinteiro G.F.** Beam optimization: improving methodology. // *Annals of Nuclear Energy*, 2004, Volume 31, Issue 4, pp. 399-411.

СПИСОК ПУБЛИКАЦИЙ

1. **Lagrange J.-L.** Sur la figure des collonnes. // *Mescellanea Taurinensia*, 1770-1773, Volume 5, pp. 123.
2. **Clausen T.** Uber die form architektonischer Säulen. // *Bull. cl. physico-raath. Acad. St.-Petersburg*, 1851, Volume 9, pp. 371-380.
3. **Николаи Е.Л.** Задача Лагранжа о наивыгоднейшем очертании колонны. // *Известия Санкт-Петербургского политехнического института*. 1907. №8.
4. **Ляхович Л.С., Акимов П.А., Тухфатуллин Б.А.** О задачах поиска минимума и максимума в строительной механике. // *International Journal for Computational Civil and Structural Engineering*, 2017, Volume 13, Issue 2, pp. 103-124.
5. **Lyakhovich L.S., Malinovsky A.P., Tukhfatullin B.A.** Criteria for Optimal Strengthening of Bar Flange with I-type Cross-section with Stability Constraints on the Value of the First Natural Frequency. //

Procedia Engineering, 2016. Volume 153, pp. 427-433.

6. **Ляхович Л.С.** Особые свойства оптимальных систем и основные направления их реализации в методах расчета сооружений. – Томск: Издательство Томского государственного архитектурно-строительного университета, 2009. – 372 с.
7. **Ляхович Л.С., Перельмутер А.В.** Некоторые вопросы оптимального проектирования строительных конструкций. // *International Journal for Computational Civil and Structural Engineering*, 2014, Volume 10, Issue 2, pp. 14-23.
8. **Aslami M., Akimov P.A.** Analytical solution for beams with multipoint boundary conditions on two-parameter elastic foundations. // *Archives of Civil and Mechanical Engineering*, 2016, Volume 16, Issue 4, pp. 668-677.
9. **Ludeker J.K., Kriegesmann B.** Fail-safe optimization of beam structures. // *Journal of Computational Design and Engineering*, 2019, Volume 6, Issue 3, pp. 260-268.
10. **Quinteiro G.F.** Beam optimization: improving methodology. // *Annals of Nuclear Energy*, 2004, Volume 31, Issue 4, pp. 399-411.

Ляхович Леонид Семенович, академик Российской академии архитектуры и строительных наук (РААСН), профессор, доктор технических наук, профессор кафедры строительной механики, Томский государственный архитектурно-строительный университет; 634003, Россия, г. Томск, Соляная пл. 2;
E-mail: lls@tsuab.ru

Акимов Павел Алексеевич, академик Российской академии архитектуры и строительных наук (РААСН), профессор, доктор технических наук; главный ученый секретарь Российской академии архитектуры и строительных наук; заместитель генерального директора по науке ЗАО «Научно-исследовательский центр СтаДиО»; профессор Департамента архитектуры и строительства Российского университета дружбы народов; профессор кафедры строительной механики Томского государственного архитектурно-строительного университета; 107031, г. Москва, ул. Большая Дмитровка, д. 24, стр. 1; тел. +7(495) 625-71-63;
факс +7 (495) 650-27-31; Email: akimov@raasn.ru, pavel.akimov@gmail.com.

Тухфатуллин Борис Ахатович, доцент, кандидат технических наук, доцент кафедры строительной механики, Томский государственный архитектурно-строительный университет; 634003, Россия, г. Томск, Соляная пл. 2; e-mail: bat9203@gmail.com.

Leonid S. Lyakhovich, Full Member of the Russian Academy of Architecture and Construction Sciences (RAACS), Professor, Dr.Sc., Head of Department of Structural Mechanics, Tomsk State University of Architecture and Building; 634003, Russia, Tomsk, Solyanaya St., 2; e-mail: lls@tsuab.ru

Pavel A. Akimov, Full Member of the Russian Academy of Architecture and Construction Sciences (RAACS), Professor, Dr.Sc.; Executive Scientific Secretary of Russian Academy of Architecture and Construction Sciences; Vice-Director for Science Activities, Scientific Research Center “StaDyO”; Professor of Department of Architecture and Construction, Peoples’ Friendship University of Russia; Professor of Department of Structural Mechanics, Tomsk State University of Architecture and Building; 24, Ul. Bolshaya Dmitrovka, 107031, Moscow, Russia;
phone +7(495) 625-71-63; fax: +7 (495) 650-27-31;
E-mail: akimov@raasn.ru, pavel.akimov@gmail.com.

Boris A. Tukhfatullin, Associate Professor, Ph.D, Associate Professor of Department of Structural Mechanics, Tomsk State University of Architecture and Building; 634003, Russia, Tomsk, Solyanaya St., 2;
E-mail: bat9203@gmail.com.

DOI:10.22337/2587-9618-2019-15-4-101-110

ASSESSMENT CRITERIA OF OPTIMAL SOLUTIONS FOR CREATION OF RODS WITH PIECEWISE CONSTANT CROSS-SECTIONS WITH STABILITY CONSTRAINTS OR CONSTRAINTS FOR VALUE OF THE FIRST NATURAL FREQUENCY PART 2: NUMERICAL EXAMPLES

Leonid S. Lyakhovich [1], Pavel A. Akimov [1, 2, 3, 4], Boris A. Tukhfatullin [1]

[1] Tomsk State University of Architecture and Civil Engineering, Tomsk, RUSSIA
[2] Russian Academy of Architecture and Building Sciences, Moscow, RUSSIA
[3] Scientific Research Center "StaDyO", Moscow, RUSSIA
[4] Peoples' Friendship University of Russia, Moscow, RUSSIA

Abstract: The special properties of optimal systems have been already identified. Besides, criteria has been formulated to assess the proximity of optimal solutions to the minimal material consumption. In particular, the criteria were created for rods with rectangular and I-beam cross-section with stability constraints or constraints for the value of the first natural frequency. These criteria can be used for optimization when the cross sections of a bar change continuously along its length. The resulting optimal solutions can be considered as an idealized object in the sense of the limit. This function of optimal design allows researcher to assess the actual design solution by the criterion of its proximity to the corresponding limit (for example, regarding material consumption). Such optimal project can also be used as a reference point in real design, for example, implementing a step-by-step process of moving away from the ideal object to the real one. At each stage, it is possible to assess the changes in the optimality index of the object in comparison with both the initial and the idealized solution. One of the variants of such a process is replacing the continuous change in the size of the cross sections of the rod along its length with piecewise constant sections. Boundaries of corresponding intervals can be selected based on an ideal feature, and cross-section dimensions can be determined by one of the optimization methods. The distinctive paper is devoted to criteria that allow researcher providing reliable assessment of the endpoint of the optimization process, and the second part of the material presented contains corresponding numerical examples, prepared in accordance with the theoretical foundations given in the first part.

Keywords: criterion, optimization, special properties, stability, frequency, critical force, buckling, eigenmode, reduced stresses, verification

КРИТЕРИИ ОЦЕНКИ ОПТИМАЛЬНЫХ РЕШЕНИЙ ПРИ ФОРМИРОВАНИИ СТЕРЖНЕЙ С КУСОЧНО-ПОСТОЯННЫМИ УЧАСТКАМИ, НА КАЖДОМ ИЗ КОТОРЫХ ПОПЕРЕЧНЫЕ СЕЧЕНИЯ НЕ МЕНЯЮТСЯ, ПРИ ОГРАНИЧЕНИЯХ ПО УСТОЙЧИВОСТИ ИЛИ НА ВЕЛИЧИНУ ПЕРВОЙ СОБСТВЕННОЙ ЧАСТОТЫ ЧАСТЬ 2: ПРИМЕРЫ РАСЧЕТА

Л.С. Ляхович [1], П.А. Акимов [1, 2, 3, 4], Б.А. Тухфатуллин [1]

Аннотация: Ранее были выявлены особые свойства оптимальных систем и сформулированы критерии, оценивающие близость оптимальных решений к минимально материалоемкому. В частности были со-

зданы критерии, для стержней с прямоугольным и двутавровым поперечным сечением при ограничениях по устойчивости или на величину первой частоты собственных колебаний. Эти критерии применимы при оптимизации, когда поперечные сечения стержня непрерывно изменяются по его длине. Полученные при этом оптимальные решения могут рассматриваться как идеализированный объект в смысле предельного. Эта функция оптимального проекта позволяет оценивать реальное конструкторское решение по критерию его близости к предельному (например, по материалоемкости). Такой оптимальный проект также может использоваться и как ориентир при реальном проектировании, например, реализуя поэтапный процесс отхода от идеального объекта к реальному. При этом на каждом этапе появляется возможность оценки изменения показателя оптимальности объекта по сравнению, как с начальным, так и с идеализированным решением. Одни из вариантов такого процесса состоит в замене непрерывного изменения размеров поперечных сечений стержня по его длине кусочно-постоянными участками. Границы участков могут выбираться на основе идеального объекта, а размеры поперечных сечений определяться одним из методов оптимизации. В данной статье предлагаются критерии, позволяющие надежно оценивать момент окончания процесса такой оптимизации, причем представляемая вторая часть материала публикации содержит пример расчета в соответствии с изложенными в первой части теоретическими основами.

Ключевые слова: критерий, оптимизация, особые свойства, устойчивость, частота, критическая сила, формы потери устойчивости, формы собственных колебаний, приведенные напряжения, верификация

EXAMPLE 1

Let us consider a straight cantilever rod (structure), the span of the structure of rectangular cross section is equal to $l = 6\,m$. Let the structure be loaded with a longitudinal force $P = 300000\ N$ and corresponding intensity of distributed mass is equal to $m(x) = 75\ kg/m$. After the transition to corresponding discrete model (including 25 segments), the nodal mass is be equal to $18kg$. Specific mass is equal to $\rho = 2400\ kg/m^3$. The given value of the first circular natural frequency is equal to $\omega_0 = 20\,s^{-1}$, the elastic modulus of the material is equal to $E = 24000\ MPa$ (Figure 4*a*) [8, 9].

Since the boundary conditions in both main planes of inertia are the same, when optimizing the cross-section should be square.

Let us first consider the use of criterion (22) for evaluating optimization stages [1–7, 9, 10] for the case when the cross sections change continuously. Optimization is performed by random search. For the initial approximation, a rod of constant cross-sectional length is taken with the ratio $b_1^0[i]/b_2^0[i] = 1/1$. The values of the desired parameters at the first exit to the boundary of the region of feasible solutions turned out to be equal to $b_1^0[i] = b_2^0[i] = 0.3039\ m$. In this case, the objective function is equal to $V_0 = 0.5543\ m^3$. The results of the three stages of the search are summarized in Table 1. The results of the first stage are obtained after $n = 1000$ attempts of the random search method, the second after $n = 1500$ attempts, the third when $n \succ 2000$. The second column of Table 1 shows the values of the cross-sectional dimensions at the first exit to the boundary of the region of feasible solutions $b_1^0[i] = b_2^0[i] = 0.3039\ m$. The penultimate row of the table shows the values of the objective function V_0 at each stage, and the last one shows its percentage reduction compared to the initial one. Columns 3, 5, 7 show the sizes of the cross sections obtained at each stage, and in columns 4, 6, 8 the values of criterion (22). The table shows that the values of the objective function in comparison with the first stage are almost not reduced. The differences concern only the fourth significant digit. The difference in the size of some sections concerns the third significant digits. However, the values of criterion (22) in the first and second stages indicate that the optimization process is not completed.

The values of criterion (22) at the third stage are close to unity, which allows researcher to confidently make a decision about stopping the optimization process at this stage.

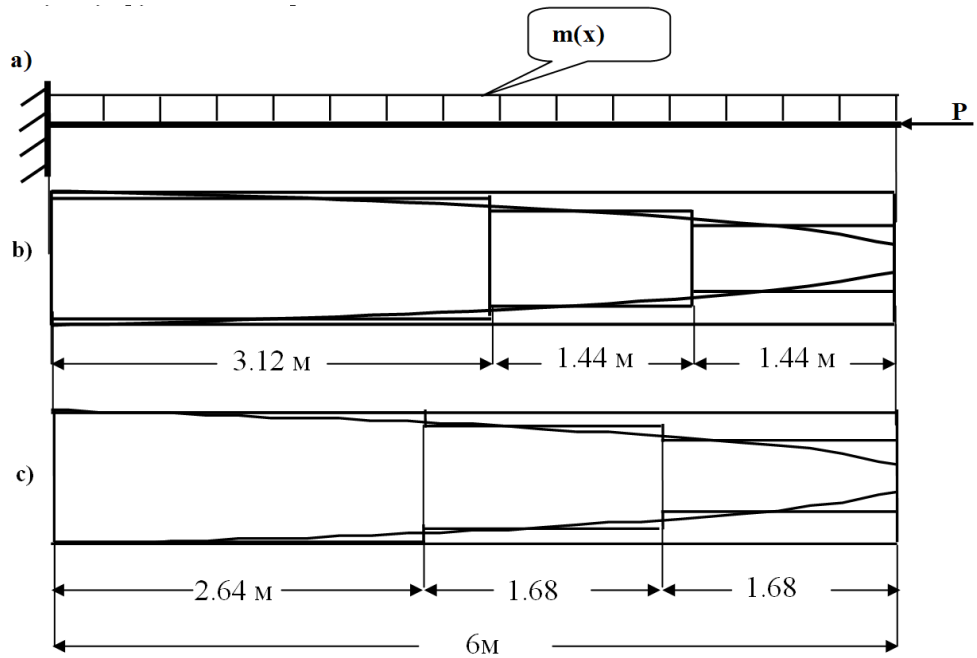


Figure 4. About the first example.

Table 1. Information about solution of the first example.

1	Optimization stages						
	Initial	The first $n=1000$		The second $n=1500$		The third $n \succ 2000$	
No. 1	$b_1^0[i], m$	$b_1[i], m$	$\sigma_{1\omega}^2[i]$	$b_1[i], m$	$\sigma_{1\omega}^2[i]$	$b_1[i], m$	$\sigma_{1\omega}^2[i]$
1	0.3039	0.3072	0.8359	0.3065	0.8414	0.3076	0.9997
2	0.3039	0.3057	0.7926	0.3050	0.8019	0.3038	0.9996
3	0.3039	0.2983	0.8491	0.2986	0.8513	0.2998	0.9997
4	0.3039	0.2995	0.7622	0.2973	0.8012	0.2956	0.9996
5	0.3039	0.2917	0.8206	0.2886	0.8722	0.2912	0.9996
6	0.3039	0.2865	0.8249	0.2883	0.7992	0.2865	0.9996
7	0.3039	0.2815	0.8224	0.2867	0.7404	0.2815	0.9995
8	0.3039	0.2754	0.8447	0.2761	0.8280	0.2762	0.9997
9	0.3039	0.2723	0.7922	0.2693	0.8456	0.2706	0.9996
10	0.3039	0.2653	0.8185	0.2639	0.8354	0.2646	0.9995
11	0.3039	0.2599	0.7917	0.2562	0.8666	0.2582	0.9999
12	0.3039	0.2529	0.7966	0.2515	0.8218	0.2515	0.9997
13	0.3039	0.2425	0.8649	0.2403	0.9168	0.2442	0.9998
14	0.3039	0.2383	0.7819	0.2390	0.7693	0.2364	0.9998
15	0.3039	0.2238	0.9477	0.2265	0.8634	0.2281	0.9996
16	0.3039	0.2217	0.7673	0.2196	0.8155	0.2193	0.9998
17	0.3039	0.2071	0.9186	0.2112	0.7779	0.2097	0.9997
18	0.3039	0.1972	0.9097	0.2022	0.7275	0.1995	0.9996
19	0.3039	0.1885	0.8326	0.1898	0.7655	0.1885	0.9997
20	0.3039	0.1739	0.9330	0.1717	1.0000	0.1765	1.0000
21	0.3039	0.1598	1.0000	0.1636	0.7799	0.1634	0.9996
22	0.3039	0.1486	0.8121	0.1481	0.8078	0.1486	0.9994
23	0.3039	0.1328	0.6891	0.1320	0.7145	0.1315	0.9993
24	0.3039	0.1181	0.1642	0.1134	0.4544	0.1099	0.9988
25	0.3039	0.0964	-0.6147	0.0889	-0.3683	0.0761	0.9994
V_0, m^3	0.5543	0.3397		0.3391		0.3384	
%	0	38.71%		38.83%		38.95%	

Table 2. Information about variants of solution of the first example.

	Вариант 1			Вариант 2		
1	2	3	4	5	6	7
No.	$b_{1k}[i]$, m	$\sigma^2_{1\omega}[i]$	$S_1[i]$	$b_1[i]$, m	$\sigma^2_{1\omega}[i]$	$S_1[i]$
1	0.2901	0.4123	0.9999	0.2956	0.3627	0.9999
2	0.2901	0.3811	0.9999	0.2956	0.3357	0.9999
3	0.2901	0.3502	0.9999	0.2956	0.3090	0.9999
4	0.2901	0.3198	0.9999	0.2956	0.2827	0.9999
5	0.2901	0.2900	0.9999	0.2956	0.2570	0.9999
6	0.2901	0.2609	0.9999	0.2956	0.2319	0.9999
7	0.2901	0.2327	0.9999	0.2956	0.2075	0.9999
8	0.2901	0.2053	0.9999	0.2956	0.1838	0.9999
9	0.2901	0.1790	0.9999	0.2956	0.1610	0.9999
10	0.2901	0.1536	0.9999	0.2956	0.1390	0.9999
11	0.2901	0.1293	0.9999	0.2956	0.1179	0.9999
12	0.2901	0.1060	0.9999	0.2346	0.4226	0.9998
13	0.2901	0.0837	0.9999	0.2346	0.3539	0.9998
14	0.2190	0.4363	1.0000	0.2346	0.2888	0.9998
15	0.2190	0.3496	1.0000	0.2346	0.2275	0.9998
16	0.2190	0.2685	1.0000	0.2346	0.1702	0.9998
17	0.2190	0.1934	1.0000	0.2346	0.1167	0.9998
18	0.2190	0.1242	1.0000	0.2346	0.0670	0.9998
19	0.2190	0.0609	1.0000	0.1570	1.0000	1.0000
20	0.1474	1.0000	0.9998	0.1570	0.6696	1.0000
21	0.1474	0.6081	0.9998	0.1570	0.3794	1.0000
22	0.1474	0.2761	0.9998	0.1570	0.1370	1.0000
23	0.1474	0.0145	0.9998	0.1570	-0.0541	1.0000
24	0.1474	-0.1737	0.9998	0.1570	-0.1948	1.0000
25	0.1474	-0.2925	0.9998	0.1570	-0.2900	1.0000
V_0, m^3	0.3630			0.3645		
%	34.52%			34.24%		

The values of criterion (22) at the third stage are close to unity, which allows researcher to confidently make a decision about stopping the optimization process at this stage.

The results obtained determine the core of minimal material consumption. The shape of the cross-sectional dimensions of this rod ($b_1[i]$) is shown in Figures 3*b* and 3*c*.

If technological requirements do not allow such a law to change the size of cross sections, but allow a piecewise-constant change in cross sections, then the choice of the boundaries of such sections is determined not only by technological requirements knowledge, but also the desire to come closer to a minimally material-intensive solution. Suppose that technological requirements are allowed for the design of the rod from three sections, in each of which the dimensions of the cross sections do not change. Suppose that additional restrictions are also imposed on the length of sections, for example, such as

$$2.8m \le l_u[2] \le 3.8m;$$
$$l_u[1] = l_u[3] = (l - l_u[2])/2.$$

Let us consider two options for the boundaries of the segments. Variants of the boundaries of the segments and the corresponding segment sizes obtained by optimization are shown in Figures 4*b* and 4*c* and are shown in Table 2.

Columns 2 and 5 show the cross-sectional dimensions $b_{1k}[i] = b_{2k}[i]$ of the respective options. Columns 3 and 6 show the values of criterion (28), and columns 4 and 7 of criterion (24).

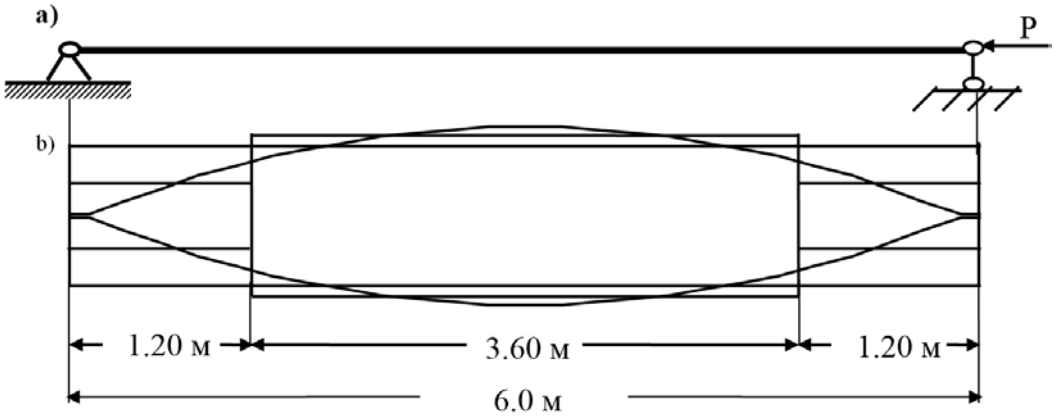


Figure 5. About the second example.

Both criteria are given because, as noted above, in each piecewise constant segment, criterion (24) is implemented as the average value of criterion (28) per unit length of the segment.

The values of criterion (24) in both cases turned out to be close to unity, which indicated the possibility of completing the optimization processes.

The objective function of the minimum material-intensive solution (Table 1, column 7) is equal to $V_0 = 0.3384\ m^3$, which is 38.95% less than the original version, which has $V_0 = 0.5543\ m^3$ (Table 1, column 2). In the first version of the boundaries of piecewise constant resizing, the objective function is equal to $V_0 = 0.3630\ m^3$, which is 34.52% less than the original version. In the second version, the objective function is equal to $V_0 = 0.3645\ m^3$, which is 34.24% less than the original version. Thus, the first option for choosing the boundaries of the plots is less material-intensive. Note that the minimally material-intensive option contributed to the selection of the boundaries of the segments, allowing researcher to choose options that are closest to it.

EXAMPLE 2

Let us consider an example of the use of criterion (50) for the case when stability constraints are introduced.

Particularly let us consider a straight-line simply supported rod of an I-section with a span $l = 6м$ loaded with longitudinal force $P = 9000000\ H$ (Figure 5*a*). The modulus of elasticity of the material is equal to $E = 206000\ MPa$. I-section height is equal to $b_1 = 0.29м$, wall thickness is equal to $\delta_{st} = 0.009м$, shelves thickness is equal to $\delta_p = 0.014м$.

It is required to determine the shape of the shelve of the I-beam in such a way that the critical force would not be greater than the acting force, and the volume of material of the shelf would be minimal.

The stability constraint can be written as

$$P = P_{cr}. \qquad (52)$$

Besides, the objective function has the form (37). We will carry out optimization by a random search method based on a discrete model from 25 segments.

Let's consider three versions. Within the initial version a shelf of constant section length is taken. The values of its sizes are determined at the first exit to the boundary of the region of feasible solutions. They turned out to be equal to $b_2^0[i] = 0.2737м$. In this case, the objective function is equal to $V_0 = 0.0460м^3$. The results of this version are presented in the second column of Table 3 and in Figure 5*b*.

Table 3. Information about variants of solution of the second example.

No.	$b_2^0[i]$, м	$b_{2k}[i]$, m	$\sigma^2_{1\omega}[i]$	$b_{2k}[i]$, m	$\sigma^2_{1\omega}[i]$	$S_1[i]$
1	2	3	4	5	6	7
1	0.2737	0.009	0.7308	0.1233	0.0153	1.0000
2	0.2737	0.0581	0.9994	0.1233	0.1351	1.0000
3	0.2737	0.1075	1.0000	0.1233	0.3596	1.0000
4	0.2737	0.1524	0.9986	0.1233	0.6605	1.0000
5	0.2737	0.1926	0.9976	0.1233	1.0000	1.0000
6	0.2737	0.2277	0.9999	0.3139	0.2564	0.9992
7	0.2737	0.2584	0.9997	0.3139	0.3220	0.9992
8	0.2737	0.2843	0.9994	0.3139	0.3852	0.9992
9	0.2737	0.3057	0.9985	0.3139	0.4426	0.9992
10	0.2737	0.3220	0.9997	0.3139	0.4908	0.9992
11	0.2737	0.3341	0.9976	0.3139	0.5274	0.9992
12	0.2737	0.3412	0.9975	0.3139	0.5501	0.9992
13	0.2737	0.3435	0.9979	0.3139	0.5578	0.9992
14	0.2737	0.3412	0.9975	0.3139	0.5501	0.9992
15	0.2737	0.3341	0.9976	0.3139	0.5274	0.9992
16	0.2737	0.3220	0.9997	0.3139	0.4908	0.9992
17	0.2737	0.3057	0.9985	0.3139	0.4426	0.9992
18	0.2737	0.2843	0.9994	0.3139	0.3852	0.9992
19	0.2737	0.2584	0.9997	0.3139	0.3220	0.9992
20	0.2737	0.2277	0.9999	0.3139	0.2564	0.9992
21	0.2737	0.1926	0.9976	0.1233	1.0000	1.0000
22	0.2737	0.1524	0.9986	0.1233	0.6605	1.0000
23	0.2737	0.1075	1.0000	0.1233	0.3596	1.0000
24	0.2737	0.0581	0.9994	0.1233	0.1351	1.0000
25	0.2737	0.009	0.7308	0.1233	0.0153	1.0000
V_0, $м^3$	0.0460	0.0372		0.0399		
%	0	19.20%		13.18%		

In the second version, a continuous change in the size of the width of the shelf is considered. Here, the criterion for stopping the optimization process is the proximity of the normalized value of criterion (32) to unity. In sections 1 and 25, the criterion is significantly different from unity, which is explained by the achievement of the width of the shelf the size of the wall thickness and the optimization process stopping in these sections. The results of this option are shown in columns 3 and 4 of Table 3 and in Figure 5*b*. The objective function in this version is equal to $V_0 = 0.0372\,м^3$, which is 19.20% less than the original version.

In the third version, a piecewise constant change in the width of the shelf is considered. As noted above, the choice of the boundaries of segments where sizes do not change is determined by both technological requirements and the desire to get as close as possible to a minimally material-intensive solution, in this example, a solution according to the second version. Let us assume that the technological requirements allow the design of the rod from three sections. Since the purpose of the example is to illustrate the criterion (50), then, given the limitation of the size of the paper, we consider only one option for choosing the boundaries of the segments (Figure 5).

The optimization results of this version are shown in columns 5, 6, 7 of Table 3 and in Figure 5*b*. The values of criterion (50) (column 7 of Table 3) in all sections are close to unity, which allows the optimization process to be stopped.

The goal function in this version is equal to $V_0 = 0.0399\,м^3$, which is 13.18% less than the original version.

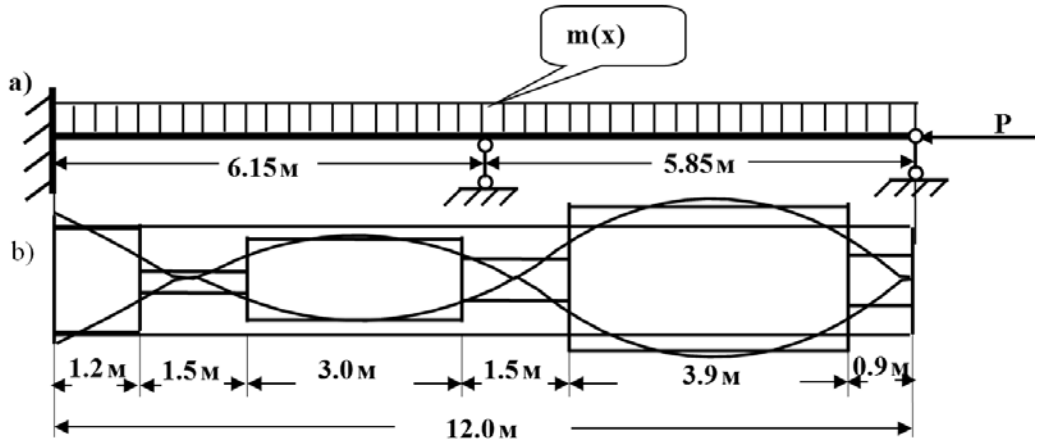


Figure 6. About the third example.

EXAMPLE 3

Let us consider an example illustrating the application of criteria for multi-span rods.

In particular, let us consider a two-span rod of an I-section, loaded with longitudinal force $P = 5000000\ H$ and bearing a distributed mass $m(x) = 200\,kg/m$ (Figure 6*a*).

The modulus of elasticity of the material is equal to $E = 206000\ МПа$, specific gravity is equal to $\rho = 7850\ kg/m^3$. I-section height is equal to $b_1 = 0.29м$, wall thickness is equal to $\delta_{st} = 0.009м$, shelves thickness is equal to $\delta_p = 0.014м$.

It is required to determine the shape of the shelve of the I-beam in such a way that the first frequency of natural vibrations would be no more than a given value $\omega_0 = 90\,\text{sec}^{-1}$, and the volume of material of the shelf would be minimal. Optimization can be done by a random search method based on a discrete model from 40 segments (sections).

Let us consider three versions. For the initial version, a shelf of constant section length is taken. The values of its sizes are determined at the first exit to the boundary of the region of feasible solutions. They turned out to be equal $b_2^0[i] = 0.2934\ м$. In this case, the objective function is equal to. The results of this option are presented in the second column of Table 4 and in Figure 6*b*.

In the second version, a continuous change in the size of the width of the shelf is considered. Here, the criterion for stopping the optimization process is the proximity of the normalized value of criterion (32) to unity. In sections 7 and 22, the criterion differs significantly from unity, which is explained by the achievement of the width of the shelf size close to the wall thickness and the optimization process stopping in these sections. The results of this option are shown in columns 3 and 4 of table 4 and in Figure 6*b*. The objective function in this version is equal to $V_0 = 0.0758\ м^3$, which is 23.10% less than the original version.

In the third version, a piecewise constant change in the width of the shelf is considered. As noted above, the choice of the boundaries of areas where sizes do not change is determined by both technological requirements and the desire to get as close as possible to a minimally material-intensive solution. Given the limitation of the volume of the paper, we consider only one option for choosing the boundaries of the segments (Figure 6).

The optimization results of this option are shown in columns 5, 6, 7 of Table 4 and in Figure 6*b*. The values of criterion (50) (column 7 of Table 4) in all sections are close to unity, which allows the optimization process to be stopped.

Table 4. Information about variants of solution of the third example.

No.	$b_1^0[i]$, m	$b_1[i]$, m	$\sigma_{1\omega}^2[i]$	$b_{1k}[i]$, $м$	$\sigma_{1\omega}^2[i]$	$S_1[i]$
1	2	3	4	5	6	7
1	0.2934	0.3400	0.9962	0.2772	0.6888	0.9994
2	0.2934	0.2842	0.9961	0.2772	0.4922	0.9994
3	0.2934	0.2243	0.9974	0.2772	0.3177	0.9994
4	0.2934	0.1610	0.9948	0.2772	0.1743	0.9994
5	0.2934	0.0939	0.9982	0.0706	0.7387	0.9994
6	0.2934	0.0254	0.9766	0.0706	0.1250	0.9994
7	0.2934	0.0099	0.2779	0.0706	-0.0121	0.9994
8	0.2934	0.0574	1.0000	0.0706	0.2994	0.9994
9	0.2934	0.1116	0.9900	0.0706	0.9401	0.9994
10	0.2934	0.1556	0.9955	0.2199	0.2063	0.9997
11	0.2934	0.1906	0.9971	0.2199	0.3243	0.9997
12	0.2934	0.2168	0.9976	0.2199	0.4317	0.9997
13	0.2934	0.2350	0.9930	0.2199	0.5129	0.9997
14	0.2934	0.2439	0.9950	0.2199	0.5574	0.9997
15	0.2934	0.2451	0.9914	0.2199	0.5605	0.9997
16	0.2934	0.2370	0.9954	0.2199	0.5232	0.9997
17	0.2934	0.2206	0.9963	0.2199	0.4523	0.9997
18	0.2934	0.1958	0.9960	0.2199	0.3589	0.9997
19	0.2934	0.1625	0.9945	0.2199	0.2561	0.9997
20	0.2934	0.1206	0.9986	0.1046	0.5722	0.9989
21	0.2934	0.0722	0.9970	0.1046	0.2569	0.9989
22	0.2934	0.009	0.0091	0.1046	-0.0045	0.9989
23	0.2934	0.0778	0.9993	0.1046	0.2657	0.9989
24	0.2934	0.1657	0.9938	0.1046	1.0000	0.9989
25	0.2934	0.2407	0.9946	0.3908	0.1419	0.9998
26	0.2934	0.3030	0.9947	0.3908	0.2415	0.9998
27	0.2934	0.3528	0.9972	0.3908	0.3473	0.9998
28	0.2934	0.3916	0.9955	0.3908	0.4472	0.9998
29	0.2934	0.4192	0.9959	0.3908	0.5300	0.9998
30	0.2934	0.4364	0.9962	0.3908	0.5868	0.9998
31	0.2934	0.4436	0.9962	0.3908	0.6115	0.9998
32	0.2934	0.4410	0.9962	0.3908	0.6017	0.9998
33	0.2934	0.4281	0.9974	0.3908	0.5588	0.9998
34	0.2934	0.4057	0.9943	0.3908	0.4876	0.9998
35	0.2934	0.3714	0.9967	0.3908	0.3961	0.9998
36	0.2934	0.3264	0.9945	0.3908	0.2946	0.9998
37	0.2934	0.2686	0.9960	0.3908	0.1942	0.9998
38	0.2934	0.1987	0.9944	0.1365	0.8821	1.0000
39	0.2934	0.1163	0.9988	0.1365	0.3351	1.0000
40	0.2934	0.0250	0.9633	0.1365	0.0382	1.0000
V_0, m^3	0.0986	0.0758		0.0813		
%	0	23.10%		17.57%		

The goal function in this version is equal to $V_0 = 0.0813\,м^3$, which is 17.57% less than the original version.

REFERENCES

1. **Lagrange J.-L.** Sur la figure des collonnes. // *Mescellanea Taurinensia*, 1770-1773, Volume 5, pp. 123.

2. **Clausen T.** Uber die form architektonischer Säulen. // *Bull. cl. physico-raath. Acad. St.-Petersburg*, 1851, Volume 9, pp. 371-380.
3. **Nikolai E.L.** Zadacha Lagranzha o naivygodneishem ochertanii kolonny [The Lagrange problem of the best shape of the column]. // *Bulletin of the St. Petersburg Polytechnic Institute*, 1907, No. 8 (in Russian).
4. **Lyakhovich L.S., Akimov P.A., Tukhfatullin B.A.** O zadachakh poiska minimuma i maksimuma v stroitel'noi mekhanike [About hill-climbing problems in structural mechanics]. // *International Journal for Computational Civil and Structural Engineering*, 2017, Volume 13, Issue 2, pp. 103-124 (in Russian).
5. **Lyakhovich L.S., Malinovsky A.P., Tukhfatullin B.A.** Criteria for Optimal Strengthening of Bar Flange with I-type Cross-section with Stability Constraints on the Value of the First Natural Frequency. // *Procedia Engineering*, 2016. Volume 153, pp. 427-433.
6. **Lyakhovich L.S.** Osobye svoistva optimal'nykh sistem i osnovnye napravleniya ikh realizatsii v metodakh rascheta sooruzhenii [The special properties of optimal systems and the main directions of their implementation in the methods of calculation of structures]. Tomsk, Tomsk State University of Architecture and Building, 2009, 372 pages (in Russian).
7. **Lyakhovich L.S., Perelmuter A.V.** Nekotorye voprosy optimal'nogo proektirovaniya stroitel'nykh konstruktsii [Some problems of building constructions optimal projecting]. // *International Journal for Computational Civil and Structural Engineering*, 2014, Volume 10, Issue 2, pp. 14-23 (in Russian).
8. **Aslami M., Akimov P.A.** Analytical solution for beams with multipoint boundary conditions on two-parameter elastic foundations. // *Archives of Civil and Mechanical Engineering*, 2016, Volume 16, Issue 4, pp. 668-677.
9. **Ludeker J.K., Kriegesmann B.** Fail-safe optimization of beam structures. // *Journal of Computational Design and Engineering*, 2019, Volume 6, Issue 3, pp. 260-268.
10. **Quinteiro G.F.** Beam optimization: improving methodology. // *Annals of Nuclear Energy*, 2004, Volume 31, Issue 4, pp. 399-411.

СПИСОК ПУБЛИКАЦИЙ

1. **Lagrange J.-L.** Sur la figure des collonnes. // *Mescellanea Taurinensia*, 1770-1773, Volume 5, pp. 123.
2. **Clausen T.** Uber die form architektonischer Säulen. // *Bull. cl. physico-raath. Acad. St.-Petersburg*, 1851, Volume 9, pp. 371-380.
3. **Николаи Е.Л.** Задача Лагранжа о наивыгоднейшем очертании колонны. // *Известия Санкт-Петербургского политехнического института*. 1907. №8.
4. **Ляхович Л.С., Акимов П.А., Тухфатуллин Б.А.** О задачах поиска минимума и максимума в строительной механике. // *International Journal for Computational Civil and Structural Engineering*, 2017, Volume 13, Issue 2, pp. 103-124.
5. **Lyakhovich L.S., Malinovsky A.P., Tukhfatullin B.A.** Criteria for Optimal Strengthening of Bar Flange with I-type Cross-section with Stability Constraints on the Value of the First Natural Frequency. // *Procedia Engineering*, 2016. Volume 153, pp. 427-433.
6. **Ляхович Л.С.** Особые свойства оптимальных систем и основные направления их реализации в методах расчета сооружений. – Томск: Издательство Томского государственного архитектурно-строительного университета, 2009. – 372 с.
7. **Ляхович Л.С., Перельмутер А.В.** Некоторые вопросы оптимального проектирования строительных конструкций. // *International Journal for Computational Civil and Structural Engineering*, 2014, Volume 10, Issue 2, pp. 14-23.

8. **Aslami M., Akimov P.A.** Analytical solution for beams with multipoint boundary conditions on two-parameter elastic foundations. // *Archives of Civil and Mechanical Engineering*, 2016, Volume 16, Issue 4, pp. 668-677.
9. **Ludeker J.K., Kriegesmann B.** Fail-safe optimization of beam structures. // *Journal of Computational Design and Engineering*, 2019, Volume 6, Issue 3, pp. 260-268.
10. **Quinteiro G.F.** Beam optimization: improving methodology. // *Annals of Nuclear Energy*, 2004, Volume 31, Issue 4, pp. 399-411.

Ляхович Леонид Семенович, академик Российской академии архитектуры и строительных наук (РААСН), профессор, доктор технических наук, профессор кафедры строительной механики, Томский государственный архитектурно-строительный университет; 634003, Россия, г. Томск, Соляная пл. 2;
E-mail: lls@tsuab.ru

Акимов Павел Алексеевич, академик Российской академии архитектуры и строительных наук (РААСН), профессор, доктор технических наук; главный ученый секретарь Российской академии архитектуры и строительных наук; заместитель генерального директора по науке ЗАО «Научно-исследовательский центр СтаДиО»; профессор Департамента архитектуры и строительства Российского университета дружбы народов; профессор кафедры строительной механики Томского государственного архитектурно-строительного университета; 107031, г. Москва, ул. Большая Дмитровка, д. 24, стр. 1; тел. +7(495) 625-71-63;
факс +7 (495) 650-27-31; Email: akimov@raasn.ru, pavel.akimov@gmail.com.

Тухфатуллин Борис Ахатович, доцент, кандидат технических наук, доцент кафедры строительной механики, Томский государственный архитектурно-строительный университет; 634003, Россия, г. Томск, Соляная пл. 2; e-mail: bat9203@gmail.com.

Leonid S. Lyakhovich, Full Member of the Russian Academy of Architecture and Construction Sciences (RAACS), Professor, Dr.Sc., Head of Department of Structural Mechanics, Tomsk State University of Architecture and Building; 634003, Russia, Tomsk, Solyanaya St., 2; e-mail: lls@tsuab.ru

Pavel A. Akimov, Full Member of the Russian Academy of Architecture and Construction Sciences (RAACS), Professor, Dr.Sc.; Executive Scientific Secretary of Russian Academy of Architecture and Construction Sciences; Vice-Director for Science Activities, Scientific Research Center “StaDyO”; Professor of Department of Architecture and Construction, Peoples’ Friendship University of Russia; Professor of Department of Structural Mechanics, Tomsk State University of Architecture and Building; 24, Ul. Bolshaya Dmitrovka, 107031, Moscow, Russia;
phone +7(495) 625-71-63; fax: +7 (495) 650-27-31;
E-mail: akimov@raasn.ru, pavel.akimov@gmail.com.

Boris A. Tukhfatullin, Associate Professor, Ph.D, Associate Professor of Department of Structural Mechanics, Tomsk State University of Architecture and Building; 634003, Russia, Tomsk, Solyanaya St., 2;
E-mail: bat9203@gmail.com.

DOI:10.22337/2587-9618-2019-15-4-111-122

MODELING OF BLAST EFFECTS ON UNDERGROUND STRUCTURE

Oleg V. Mkrtychev, Anton Y. Savenkov
National Research Moscow State University of Civil Engineering, Moscow, RUSSIA

Abstract: Modeling of the impact of a point explosion shock wave on a soil mass and an underground structure at different locations of the explosion epicenter from the ground surface was performed. The study of the stress-strain state of soils was carried out using a nonlinear dynamic method and a fully coupled numerical model, including various models of materials. The result of numerical modeling showed the adequacy of the adopted numerical calculation methods. The findings showed that solving the problem in a nonlinear dynamic formulation allows obtaining the parameters of the shock wave at different depths from the explosion center, as well as obtaining a complete picture of the interaction of the shock wave with the underground structure in surface and underground explosions.

Keywords: explosion loads, shock wave, compression wave, nonlinear dynamics, stress-strain state, underground structure, soil model

МОДЕЛИРОВАНИЕ ВОЗДЕЙСТВИЯ УДАРНОЙ ВОЛНЫ НА ПОДЗЕМНОЕ СООРУЖЕНИЕ

О.В. Мкртычев, А.Ю. Савенков
Национальный исследовательский Московский государственный строительный университет, г. Москва, РОССИЯ

Аннотация: Выполнено моделирование воздействия ударной волны точечного взрыва на грунтовый массив и подземное сооружение при различном расположении эпицентра взрыва от поверхности грунта. Исследование напряженно-деформированного состояния грунтов осуществлялось с использованием нелинейного динамического метода и полностью связанной численной модели, включающей различные модели материалов. Результат численного моделирования показал адекватность принятых численных методик расчета. Сделанные выводы показали, что решение задачи в нелинейной динамической постановке позволяет получить параметры ударной волны на различных глубинах от центра взрыва, а также получить полную картину взаимодействия ударной волны с подземным сооружением при поверхностном и подземном взрыве.

Ключевые слова: взрывные воздействия, ударная волна, волна сжатия, нелинейная динамика, напряженно-деформированное состояние, подземное сооружение, грунтовая модель

1. INTRODUCTION

Currently, various industrial undertakings are being built, relating to oil and gas and space industries, as well to nuclear power facilities, which include underground structures. Such underground structures include repositories, shelters, civil defense shelters, command posts, etc.
The current design standards [1-4] require the calculation of such structures for emergency actions, including explosions. At the same time, the structures located on the surface have been thoroughly studied and there are a sufficient number of approved calculation methods for them, including the explosion triggered progressive collapse, earthquake loads, and fires [5-8]. For example, the most common methods are equivalent-static, linear-spectral, as well as direct dynamic methods of calculation [9-11], while there are not enough methods for under-

ground structures and they are in great demand, in which case the problem is complicated, since it is necessary to take into account the soil surrounding the underground structure. Therefore, there is a need to find and study new approaches to solving the problem of the interaction of shock waves with a structure.

1.1. Work relevance.

The relevance of the work lies in solving the problem of the interaction of a point explosion shock wave with an underground structure using a nonlinear dynamic method of calculation and a fully coupled numerical model, including the model of the soil, air, and an underground structure.

1.2. Study objective.

The primary objective of this study is to investigate the soil strain-stress state and the response of an underground structure soil under various explosion scenarios. To achieve this goal, the specific objectives of the study include:

- analysis of soil behavior under explosive loads;
- analysis of soil models used in the calculation of underground structures for explosive loads;
- a study of the strain-stress state of the soil mass in the propagation of shock and seismic waves; and
- modeling of loads on an underground structure.

2. MATERIALS AND METHODS

2.1. Soil model.

Soils tend to have a complex structure consisting mainly of mineral particles that form the soil skeleton. The space between the solid particles is filled with air and/or water. When the pores between the solid particles are filled with air, the soil is of the dry type. When the pores are filled with water containing a small proportion of air, the soil is called saturated soil. Therefore, in general, soils can be called three-phase soils (Figure 1). Relative volume fractions of the three constituent materials of the soil are usually quantitatively determined by the porosity α and the saturation degree β.

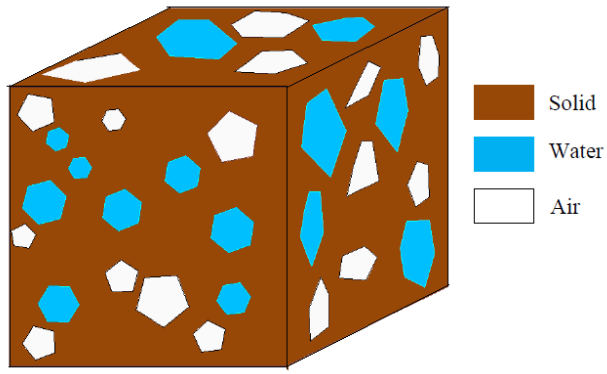


Figure 1. Soil element.

- For many processes with a low loading rate (under static loads), the overall macroscopic behavior of the soil skeleton can be determined within the framework of the principles of continuum mechanics, which makes it possible to simplify modeling and apply theories and methods of continuum mechanics. Under conditions of fast loading, which are typical for explosions, soil models should include constitutive models of three phases necessary for determining the soil behavior; thus, different soil behavior should be taken into account, namely:
- Dilatancy/contraction: Shear strains in soils can lead to volume changes. This determines the relationship between the shear strength of the soil and its strain properties. This effect was first described by Osborne Reynolds in 1885-1886 and was called dilatancy and the decrease in volume is called negative dilatancy or contraction. In dense sand and overcompacted clay, with a displacement, the height of the sample is increased by a certain amount, thereby increasing the soil volume, and in loose sand and normally compacted clay, a decrease in volume can be observed. Thus, the shear stress initially rises rapidly to a peak value with a relatively low displacement value with a corresponding increase in

volume. With this new volume, the blocking is reduced, and, therefore, as the displacement continues, the shear stress decreases and, finally, is aligned with the final residual value.

- Such a nature of strain is explained by the fact that when one part of the soil is displaced relative to another, its shear strength is determined by sliding friction. To overcome the adhesion forces, it is necessary to extend and uplift them to a certain level, in which case loosening occurs in the shear zone, which is accompanied by a decrease in its shear strength. Thus, dense soils become looser, as a result of dilatancy, and loose soils become denser, as a result of contraction.
- Plasticity: An increase in the applied stress usually results in some irreversible strain, with no signs of cracking or failure. Most soils have a very small elastic area and show plasticity from the beginning of loading.
- Hardening/softening (thixotropy): It is the ability of soils to reduce their viscosity (to liquefy), as a result of mechanical damage, and increase the viscosity at rest. Freundlich found that thixotropy is manifested in soils, in which the content of clay particles exceeds 2%. It is suggested that all clay soils are potentially thixotropic, but for a specific manifestation of thixotropy, certain conditions and, first of all, quite intense exposures are necessary (Figure 2).

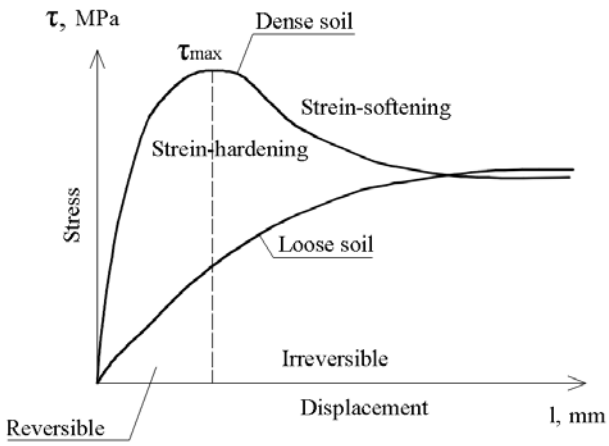


Figure 2. Response of soil with respect to shearing.

- High strain rate behavior: Soils with different water content exhibit different behavior at high strain rates. In experiments with different soils from sands to clays, it was noted that with a decrease in the loading time (an increase in the loading rate), the compressive strength increases. Thus, in clay soils, when comparing experiments with a loading rate of 0.02 s with tests at a loading rate of 10 min, the strength increased by 1.5-2 times and smaller values were obtained for more durable clays. In sandy soils, the effect of loading rate was significantly lower and the strength increment did not exceed 15% of the static value.

  With repeated impulses and vibrations, all observations and experiments show the opposite picture, a significant reduction in the soil shear resistance in some cases.
- Effects of drainage and volume changes: In saturated soils, an increase in the applied compressive stress causes an increase in the pore pressure of water. If drainage is possible, water outflows to the surrounding areas, where the water pore pressure is lower. The outflow rate depends on the soil permeability; in gravel and sand, it is relatively fast and in silts and clays, it is slow. When the excess pressure of the pore water is dissipated, the applied stress is transferred from the pore pressure to the effective stress.

  It should be noted that there are also other characteristics of soil behavior, such as creep and temperature dependence. These aspects are not discussed here, since they are beyond the scope of this study.

  The mechanical behavior of soils can be modeled at many levels. Hooke's law of linear isotropic elasticity can be considered as the simplest of the available stress-strain relations, but, as a rule, it is too rough to grasp the main characteristics of the soil behavior. On the other hand, several researchers have proposed a large number of soil models to describe the soil behavior in various aspects in detail. However, the number of soil models that are suitable for implementation in

advanced software systems using finite element methods is rather limited.

Let us consider the most commonly used soil models that can predict the soil behavior described above. These models include elastic, perfectly plastic soil models, hardening-plastic soil models, elastic-viscous soil models, three-phase soil models, viscoplastic soil models, SFG unsaturated soil model, and unsaturated plasticity models of the bounding surface.

The most commonly used soil models that can predict the soil behavior described above are:

Elastoplastic soil models:

- Mohr-Coulomb model;
- Drucker-Prager model.
- Hardening soil models;
- Cam-clay tent model (for some soils it is required that they were tent-like, so that there would be a limitation on the resulting hydrostatic pressure);
- Three-phase soil models;
- Viscoplastic soil models.

Among them, the most commonly used in practice is the Mohr-Coulomb model. In further work we will accept it as the main one.

A classical Mohr-Coulomb model is described by the following strength conditions, which have a different appearance under different test conditions. The first strength condition:

$$\tau = \sigma_v tg\varphi' + c' \quad (1)$$

– consolidated-drained shear;

$$\tau = (\sigma_v - u)tg\varphi + c \quad (2)$$

– consolidated-undrained shear;

$$\tau = c_u \quad (3)$$

– unconsolidated-undrained shear (for water-saturated soils);

$$\tau = (u_a - u)tg\varphi^b + (\sigma_v - u)tg\varphi' + c' \quad (4)$$

– consolidated-untrained shear, sedentary soils;

$$\tau = \sigma_v tg\varphi'_r + c'_r \quad (5)$$

– in the case of large shear strains.

whereτ is a shear stress, upon reaching which the destruction of the ground will occur; σ_v – is an effective normal stress; φ' – is an effective angle of internal friction; φ – is a drained angle of internal friction; c – are drained specific adhesion forces; c' – is effective specific adhesion forces; u_a – is a pore air pressure; u – is a pore water pressure; φ_b is an angle of internal friction, depending on the magnitude of the matrix suction; φ'_r – is a residual angle of internal friction; c'_r – are residual specific adhesion forces; and c_u – is an undrained strength.

Second strength condition:

$$sin\varphi = \frac{\sigma_1 - \sigma_3}{\sigma_1 + \sigma_3} \quad (6)$$

– for gravel, sandy and coarse soils;

$$\frac{\sigma_1 - \sigma_3}{(\sigma_1 + \sigma_3 + 2cctg\varphi)} = sin\varphi \quad (7)$$

– for clay soils.

With a three-dimensional stress-strain state, the equation takes the following form:

$$\left.\begin{aligned} |\sigma_1 - \sigma_2| &= (2cctg\varphi - \sigma_1 - \sigma_2)sin\varphi \\ |\sigma_2 - \sigma_3| &= (2cctg\varphi - \sigma_2 - \sigma_3)sin\varphi \\ |\sigma_3 - \sigma_1| &= (2cctg\varphi - \sigma_3 - \sigma_1)sin\varphi \end{aligned}\right\} \quad (8)$$

According to this equation, the Mohr-Coulomb yield surface in the space of primary stresses has the form of a hexagonal pyramid (Figure 3), with a vertex at the point with coordinates. $\{cctg\varphi; cctg\varphi; cctg\varphi\}$

As is obvious, this model describes different types of soil, with different water saturation. But in addition to the classical model, there are other modifications of the model used for certain specific tasks.

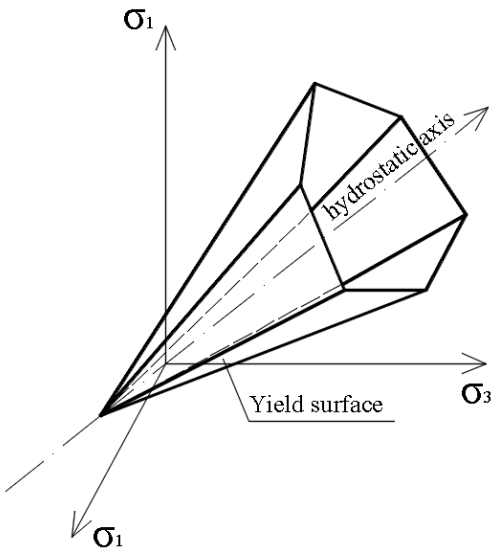


Figure 3. Mohr-Coulomb yield surface in the space of primary stresses.

For example, the Mohr-Coulomb model based on the works of A.J. Abbo and S.W. Sloan performed in 1995 [12,13], taking into account all the above-mentioned soil behaviors, as well as the removal of elements, which is typical for explosive loads [14,15]. Therefore, we will use this version of the Mohr-Coulomb model.
The usual Mohr-Coulomb yield surface is described by the function:

$$F = -Psin\varphi + K(\theta)\sqrt{J_2} - c\cos\varphi = 0 \quad (9)$$

where P is a mean pressure; φ is an angle of internal friction; $K(\theta)$ is a function of the angle θ in the deviator plane; $\sqrt{J_2}$ is a square root of the second invariant of the stress deviator; and C is an adhesion.
The modified yield surface is a hyperboloid "fitted" to the Mohr-Coulomb surface. The modified surface equation has the following form:

$$F = -Psin\varphi + \sqrt{J_2K(\theta)^2 + a^2sin^2\varphi} - c\cos\varphi = 0 \quad (10)$$

where "a" is a parameter that determines the approximation of the modified surface to the ordinary Mohr-Coulomb surface.

2.2. Air model.
The model used in the calculation is described by a polynomial equation:

$$p = C_0 + C_1\mu + C_2\mu^2 + C_3\mu^3 + (C_4 + C_6 + C_7\mu^2)E \quad (11)$$

$$\mu = \frac{1}{V} - 1 \quad (12)$$

where V - relative volume, E - internal energy.

2.3. Model of an explosive.
The explosive model is described by the Jones-Wilkins-Lee (JWL) equation of state:

$$p = A\left(1 - \frac{\omega}{R_1V}\right)e^{-R_1V} + B\left(1 - \frac{\omega}{R_2V}\right)e^{-R_2V} + \frac{\omega E}{V} \quad (13)$$

2.4. Modeling methods.
Since the explosion in the ground has a highly linear character, for this purpose the best option is to apply a numerical calculation method using arbitrary ALE Lagrangian-Eulerian meshes, where Eulerian meshes were used for air, soil, and explosive and Lagrangian meshes were used for an underground structure.
To solve the problem, we will use the LS-DYNA software suite, which allows solving such problems in a nonlinear dynamic formulation, using the central difference method [16-18].
For approximation of the equations in this work, the second-order Godunov method was used. The time integration of the equations was carried out using an explicit second order accuracy scheme (central difference method) with the observance of the scheme stability condition according to the Courant criterion.
A differential equation of motion of a system with a finite number of degrees of freedom:

$$M\ddot{u} + C\dot{u} + Ku = f^a \quad (14)$$

for an explicit scheme, it looks like this:

$$M\ddot{u}_t + C\dot{u}_t + Ku_t = f_t^a \quad (15)$$

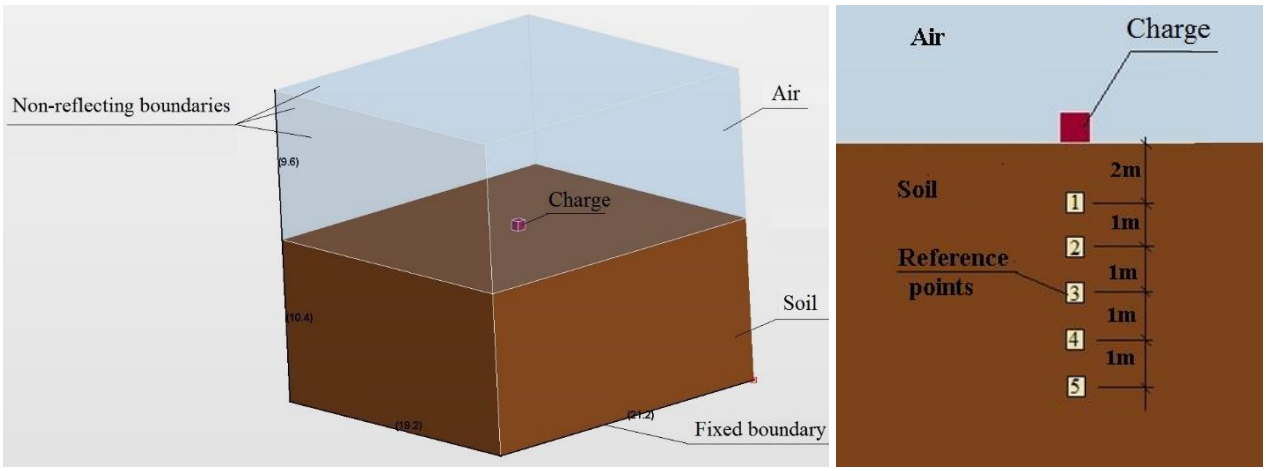


Figure 4. Computational model and layout of reference points.

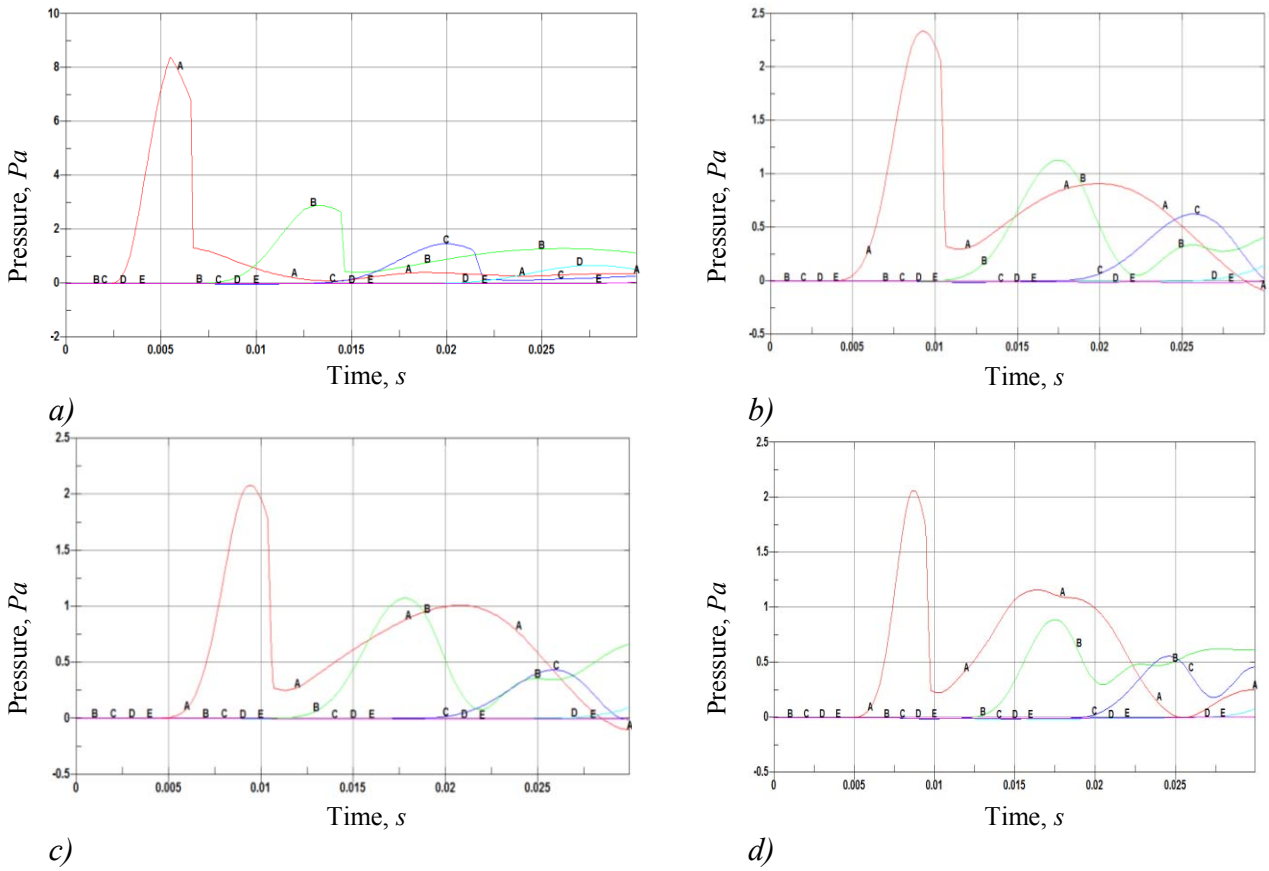


Figure 5. Results of the finite element mesh convergence study with dimensions: a) 0,3 m; b) 0,25 m; c) 0,2 m; d) 0,15 m (where A,B,C,D,E – numbers of reference points).

Acceleration vector:

$$a_t = M^{-1}(f_t^{ext} - f_t^{int}) \quad (16)$$

where f_t^{ext} – external force vector;
f_t^{int} – internal force vector.

Accounting for various types of non-linearities is performed through the internal force vector {F}:

$$f_t^{int} = \sum \left(\int_{\Omega} [B^T]\{\sigma\} d\Omega + \{F^{cont}\} \right) \quad (17)$$

where B – deformation–displacement matrix; σ – displacement vector; F^{cont} – contact force vector. The velocity and displacement vectors in the corresponding step are determined as follows:

$$v_{t+\Delta t/2} = v_{t-\Delta t/2} + a_t \Delta t \quad (18)$$

$$u_{t+\Delta t} = u_t + v_{t+\Delta t/2} \frac{\Delta t_t + \Delta t_{t+\Delta t}}{2} \quad (19)$$

3. STUDY RESULTS

For the analysis of soil strain-stress state, a computational model was created with dimensions of 20.0 x 20.0 x 20 m (h) (Figure 4). In this model, the ground and air areas, as well as an explosive weighing 200 kg were modeled using solid elements.

When using the central difference method, the accuracy of the calculations largely depends on the size of the region to be broken, in other words, in our case, on the size of the solid finite elements. Several computational models with variable size of solid finite elements from 0.3 m to 0.15 m were considered.

The optimal model was chosen with a cell size of 0.2 m, in which the difference with the reference diagram of 0.15 m did not exceed 5%. The structure is located at a depth of 3 m (Figure 5).

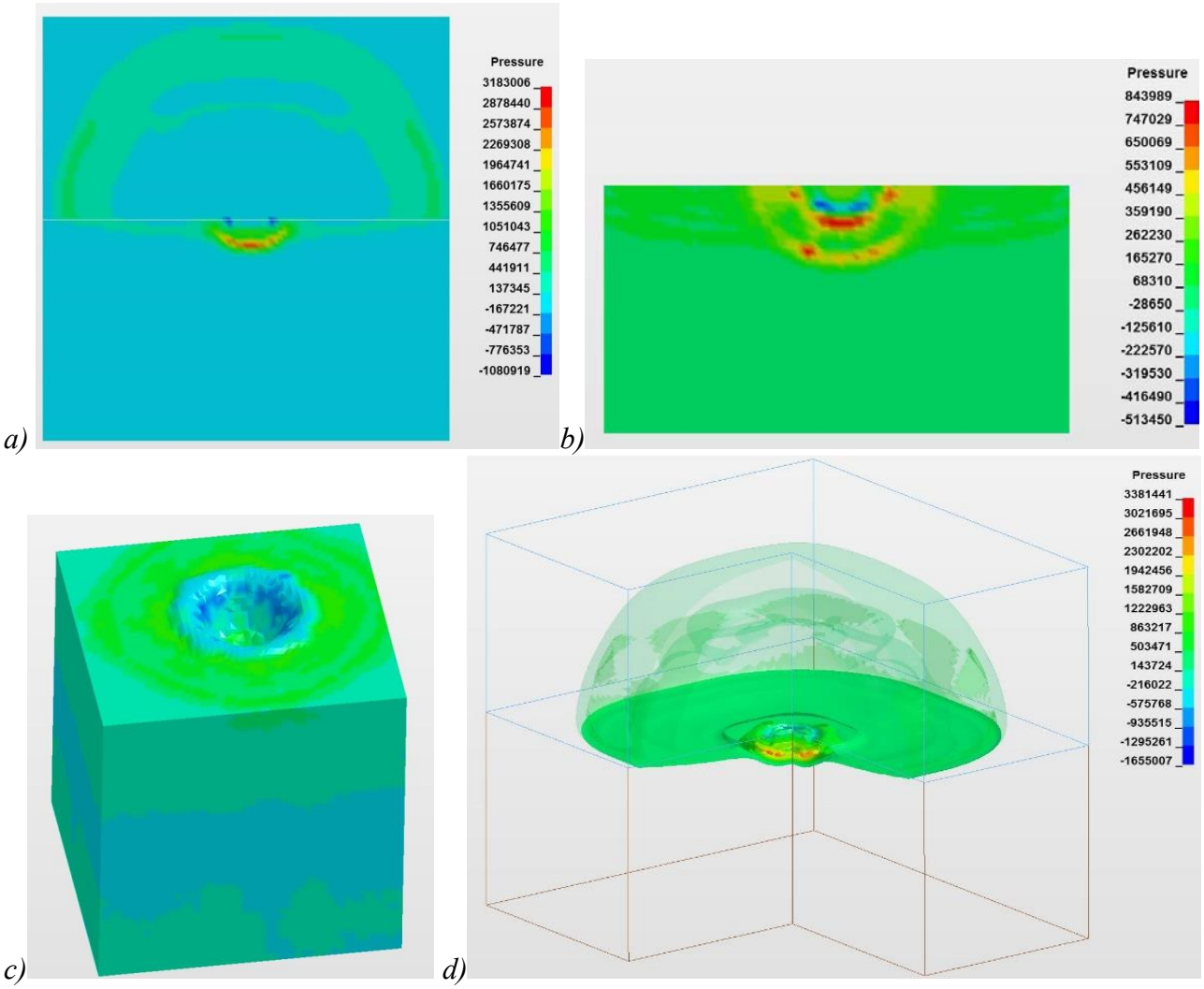


Figure 6. Isopoles of pressures at time points: a) 0,0077 s; b) 0,022 s; c) formation of explosive crater; d) propagation of air shock waves and compression wave.

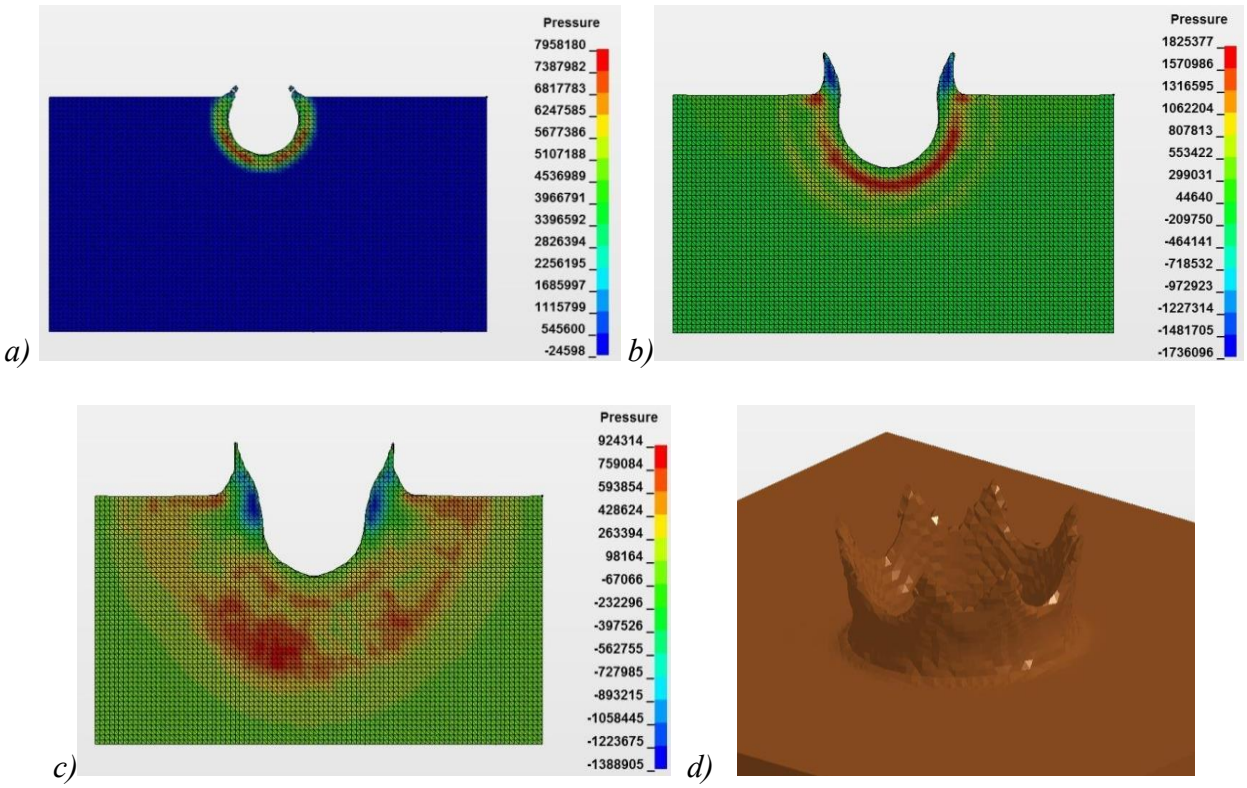


Figure 7. Isopoles of pressures at time points: a) 0,0077 s; b) 0,026 s; c) 0,056 s; d) formation of explosive crater.

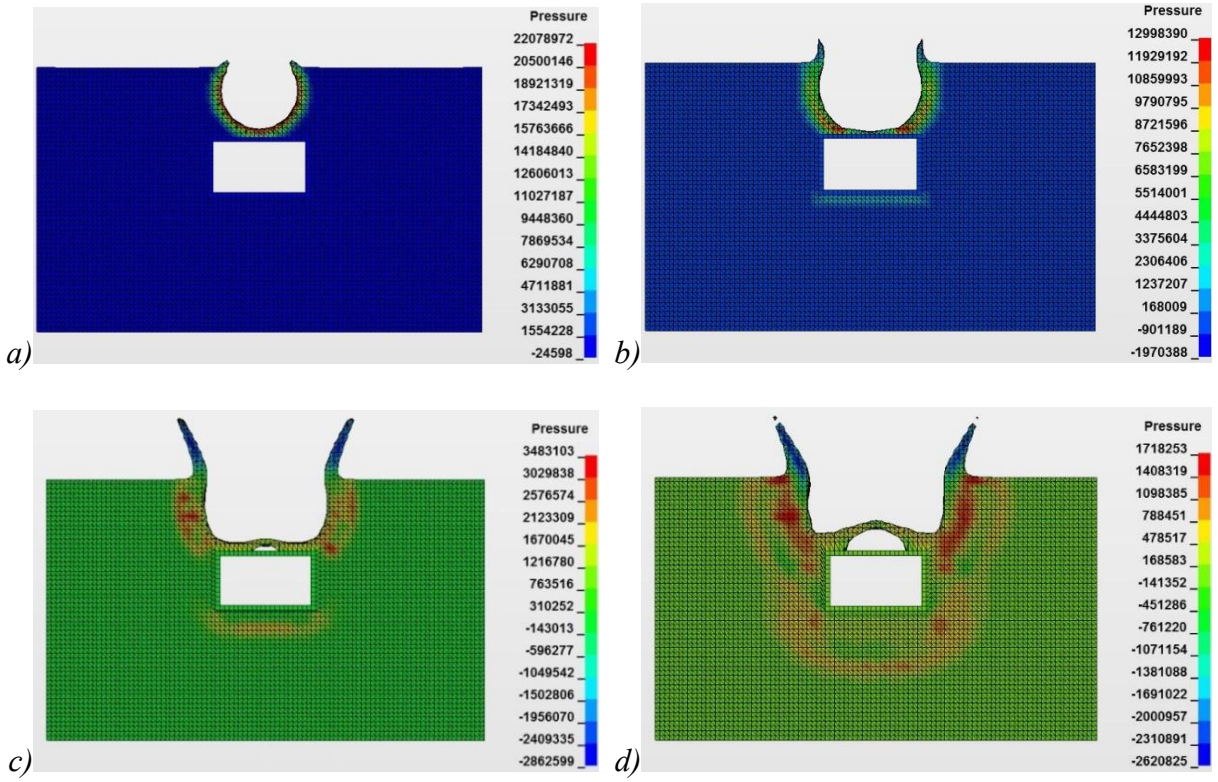


Figure 8. Isopoles of pressures at time points: a) 0,0077s; b) 0,01s; c) 0,022s; d) 0,05s.

3.1. Explosion on the ground surface.

The propagation of a shock wave during an explosion on the ground surface is considered (Figure 6), where it can be seen that immediately after detonation, spherical shock waves propagated in the air from the charge epicenter, which was on the ground surface. Shock waves penetrated the ground in the form of hemispherical waves, forming a crater in the ground, followed by the propagation of seismic waves.

3.2. The explosion at a depth of 1m.

Next, an explosion at a depth of 1 m from the ground surface was considered (Figure 7).

Taking into account the results of these two loading cases, it can be concluded that the most dangerous case is an explosion at a depth of 1 m, since the propagating seismic waves have a greater depth and blast pressure.

3.3. Impact of an explosion on an underground structure at a depth of 1 m.

Figure 8 shows the impact of an explosion on an underground structure at a depth of 1 m. The wave front reached the surface of the structure within 7 ms from the beginning of the explosion. The blast pressure was 1.7 MPa.

4. CONCLUSIONS

The parameters of the shock wave in an explosion on the surface and at a depth of 1 m were compared with empirical values using the formulas [19] and the calculation results with accuracy of 5-10% coincide, which proves the adequacy of the adopted numerical calculation methods. Solving the problem in a nonlinear dynamic formulation makes it possible to obtain the parameters of a shock wave at different depths from the explosion center, as well as to get a complete picture of the shock wave interaction with the underground structure during a surface and underground explosion.

REFERENCES

1. Federal'nyy zakon No. 68 ot 11.11.1994 “O zashchite naseleniya i territoriy ot chrezvychaynykh situatsiy prirodnogo i tekhnogennogo kharaktera” (in Russian).
2. Design Code of the Russian Federation SP 248.1325800.2016. Svod Pravil. Sooruzheniya podzemnyye. [Underground structures. Design principles] (In Russian).
3. Design Code of the Russian Federation SP 88.13330.2014. Svod Pravil. Zashhitnye sooruzheniya grazhdanskoj oborony. Aktualizirovannaya redaktsiya SNiP II-11-77* [The protective shelters of civil defense. Updated Version of SNiP II-11-77*] (in Russian).
4. Design Code of the Russian Federation SP 56.13330.2011. Svod Pravil. Proizvodstvennyye zdaniya. Aktualizirovannaya redaktsiya SNiP 31-03-2001 [Production buildings. Updated Version of SNiP 31-03-2001] (in Russian).
5. **Mkrtychev O.V., Dorozhinskiy V.B.** (2012). Analiz podkhodov k opredeleniyu parametrov vzryvnogo vozdeystviya [Analysis of approaches to determining the parameters of explosive exposure]. // *Vestnik MGSU*, 2012, No. 5, pp. 45-49 (in Russian).
6. **Mkrtychev O.V., Dorozhinskiy V.B., Lazarev O.V.** (2011). Raschet konstruktsiy zhelezobetonnogo zdaniya na vzryvnyye nagruzki v nelineynoy dinamicheskoy postanovke [Structural analysis of reinforced concrete buildings for explosive loads in a nonlinear dynamic formulation]. // *Vestnik MGSU*, 2011, No. 4, pp. 243-247 (in Russian).
7. **Mkrtychev O.V., Dorozhinskiy V.B., Sidorov D.S.** Nadezhnost' stroitel'nykh konstruktsiy pri vzryvakh i pozharakh [Reliability of building structures during explosions and fires]. Moscow, ASV Publishing House, 2016, 173 pages (in Russian).
8. **Mkrtychev O.V., Savenkov A.Y.** Chislennoye modelirovaniye fronta vozdushnoy

udarnoy volny pri vzryve v vozdukhe i nad zemley v programmnom komplekse LS-DYNA [Numerical simulation of the front of an air shock wave in a ground and air explosion in the software package LS-DYNA]. // *Structural mechanics of engineering constructions and buildings*, 2018, No. 14(6), pp. 467-474 (in Russian).

9. **Savenkov A.Y., Mkrtychev O.V.** Nelineynyy raschet zhelezobetonnogo sooruzheniya na vozdeystviye vozdushnoy udarnoy volny [Nonlinear calculation of reinforced concrete structure to the impact of the air shock wave]. // *Vestnik MGSU*, 2019, No. 14(1), pp. 33-45 (in Russian).
10. **Rastorguev B.S., Plotnikov A.I., Khusnutdinov D.Z.** Proektirovanie zdaniy i sooruzheniy pri avariynykh vzryvnykh vozdeystviyakh [Design of Buildings and Structures Exposed to Emergency Blast Effects]. Moscow, ASV Publishing House, 2007, 152 pages (in Russian).
11. **Pavlov A.S.** Chislennoye modelirovaniye vzryvnykh vozdeystviy na zdaniya i sooruzheniya proizvol'noy formy. [Numerical method of calculation of blast loads pressure to structures with complex geometry Shapes]. // *Academia. Architecture and construction*, 2017, No. 3, pp. 108-112 (in Russian).
12. **Boldyrev G.G., Aref'yev D.V., Muyzemnik A.Yu**. Identifikaciya parametrov modeley gruntov [Identification of soil model parameters]. URL: https://docplayer.ru/68796939-Identifikaciya-parametrov-modeley-gruntov-boldyrev-g-g-arefev-d-v-muyzemnik-a-yu-ooo-npp-geotek-annotaciya.html
13. Manual for LS-DYNA Soil Material Model 147 Evaluation / Report No FHWA-HRT-04-095. Lincoln, University of Nebraska, 77 pages.
14. **Huang Y., Willford M.R.** Validation of LS-DYNA® MMALE with Blast Experiments // 12th International LS-DYNA® Users Conference. 2012. URL: https://www.dynalook.com/12th-international-ls-dyna-conference/blast-impact20-c.pdf
15. **Goel M., Matsagar V., Gupta A.** An Abridged Review of Blast Wave Parameters. // *Defense Science Journal*, 2012, Volume 62, Issue 5, pp. 300-306.
16. **Bate K., Wilson E.** Chislennyye metody analiza i metod konechnykh elementov [Numerical analysis methods and the finite element method]. Moscow, Stroyizdat, 1982, 448 pages (in Russian).
17. **Van Leer B.J.** Towards the ultimate conservative difference scheme. Second-order sequel to Godunov's Method. // *Journal of Computational Physics*, 1979, Volume 32, Issue 1, pp. 101-136.
18. LS-DYNA. Keyword user's manual. 2017. Volume I. Version 971. Livermore Software Technology Corporation (LSTC). URL: https://www.dynasupport.com/manuals/ls-dyna-manuals/ls-dyna-manual-r-8.0-vol-iii
19. **Orlenko L.P., Andreev S.G., Babkin A.V., Baum F.A., Imhovik N.A., Kobylkin I.F., Kolpakov V.I., Ladov S.V., Odintsov V.A., Ohitin V.N., Selivanov V.V., Soloviev V.S., Stanyukovich K.P., Chelyshev V.P., Shehter B.I.** Fizika vzryva [Physics of a Blast]. Volume 2. Moscow, Fizmatlit Publ., 2004, 832 pages (in Russian).

СПИСОК ЛИТЕРАТУРЫ

1. Федеральный закон №68 от 11 ноября 1994 г. «О защите населения и территорий от чрезвычайных ситуаций природного и техногенного характера».
2. СП 248.1325800.2016. Свод правил. Сооружения подземные. Правила проектирования. Утв. Приказом Минрегиона России от 16.06.2016. №416/пр.
3. СП 88.13330.2014. Свод правил. Защитные сооружения гражданской обороны. Актуализированная редакция СНиП II-

11-77*. Утв. Приказом Минрегиона России от 18.02.2014. №59/пр.
4. СП 56.13330.2011 Свод правил. Производственные здания. Актуализированная редакция СНиП 31-03-2001. Утв. Приказом Минрегиона России от 30.12.2010. №850.
5. **Мкртычев О.В., Дорожинский *В.Б.*** Анализ подходов к определению параметров взрывного воздействия. // *Вестник МГСУ*, 2012, №5, с. 45-49.
6. **Мкртычев О.В., Дорожинский В.Б.**, Лазарев О.В. Расчет конструкций железобетонного здания на взрывные нагрузки в нелинейной динамической постановке. // *Вестник МГСУ*, 2011, №4, с. 243-247.
7. **Мкртычев О.В., Дорожинский В.Б.**, **Сидоров Д.С.** Надежность строительных конструкций при взрывах и пожарах. – М.: АСВ, 2016. – 173 с.
8. **Мкртычев О.В., Савенков А.Ю.** Численное моделирование фронта воздушной ударной волны при взрыве в воздухе и над землей в программном комплексе LS-DYNA. // *Строительная механика инженерных конструкций и сооружений*, 2018, Том 14, №6, с. 467-474.
9. **Савенков А.Ю., Мкртычев О.В.** Нелинейный расчет железобетонного сооружения на воздействие воздушной ударной волны. // *Вестник МГСУ*, 2019, Том 14, Выпуск 1, с. 33-45.
10. **Расторгуев Б.С., Плотников А.И., Хуснутдинов Д.З.** Проектирование зданий и сооружений при аварийных взрывных воздействиях. – М.: АСВ, 2007. – 152 с.
11. **Павлов А.С.** Численное моделирование взрывных воздействий на здания и сооружения произвольной формы // *Academia. Архитектура и строительство*, 2017, №3, с. 108-112.
12. **Болдырев Г.Г., Арефьев Д.В., Муйземник А.Ю.**, Идентификация параметров моделей грунтов. URL: https://docplayer.ru/68796939-Identifikaciya-parametrov-modeley-gruntov-boldyrev-g-g-arefev-d-v-muyzemnik-a-yu-ooo-npp-geotek-annotaciya.html
13. Manual for LS-DYNA Soil Material Model 147 Evaluation / Report No FHWA-HRT-04-095. Lincoln, University of Nebraska, 77 pages.
14. **Huang Y., Willford M.R.** Validation of LS-DYNA® MMALE with Blast Experiments // 12th International LS-DYNA® Users Conference. 2012. URL: https://www.dynalook.com/12th-international-ls-dyna-conference/blast-impact20-c.pdf
15. **Goel M., Matsagar V., Gupta A.** An Abridged Review of Blast Wave Parameters. // *Defense Science Journal*, 2012, Volume 62, Issue 5, pp. 300-306.
16. **Бате К., Вилсон Е.** Численные методы анализа и метод конечных элементов. – М.: Стройиздат. 1982. – 448 с.
17. **Van Leer B.J.** Towards the ultimate conservative difference scheme. Second-order sequel to Godunov's Method. // *Journal of Computational Physics*, 1979, Volume 32, Issue 1, pp. 101-136.
18. LS-DYNA. Keyword user's manual. 2017. Volume I. Version 971. Livermore Software Technology Corporation (LSTC). URL: https://www.dynasupport.com/manuals/ls-dyna-manuals/ls-dyna-manual-r-8.0-vol-iii
19. **Андреев С.Г., Бабкин А.В., Баум Ф.А., Имховик Н.А., Кобылкин И.Ф., Колпаков В.И., и др**. Физика взрыва. В 2 томах. – М.: ФИЗМАТЛИТ, 2004. – 832 с.

Oleg V. Mkrtychev, Professor, Dr.Sc., Department of Strength of Materials, National Research Moscow State University of Civil Engineering; 26, Yaroslavskoe Shosse, Moscow, 129337, Russia;
phone: +7(499)183-85-59;
E-mail: mkrtychev@yandex.ru.

Anton Y. Savenkov, Ph.D. student, Department of Strength of Materials, National Research Moscow State

University of Civil Engineering; 26, Yaroslavskoe Shosse, Moscow, 129337, Russia;
phone: +7(499)183-85-59;
E-mail: savenkov.asp@mail.ru.

Мкрытчев Олег Вартанович, профессор, доктор технических наук; профессор кафедры сопротивления материалов, Национальный исследовательский Московский государственный строительный университет; 129337, Россия, г. Москва, Ярославское шоссе, дом 26; тел. +7(499)183-85-59;
E-mail: savenkov.asp@mail.ru.

Савенков Антон Юрьевич, аспирант кафедры сопротивления материалов, Национальный исследовательский Московский государственный строительный университет; 129337, Россия, г. Москва, Ярославское шоссе, дом 26; тел. +7(499)183-85-59;
E-mail: savenkov.asp@mail.ru.

DOI:10.22337/2587-9618-2019-15-4-123-132

SUPERELEMENT SIMULATION TECHNIQUE OF DYNAMICS FOR LARGE-SIZE SYSTEMS "BASE – REINFORCED CONCRETE STRUCTURES – METAL STRUCTURES". VERIFICATION AND APPROBATION

Alexander I. Nagibovich
Scientific Research Center "StaDyO", Moscow, RUSSIA
National Research Moscow State University of Civil Engineering, Moscow, RUSSIA

Abstract: The distinctive paper presents short descriptions, verification and approbation of the developed technique of numerical (superelement) simulation of dynamics for large-size combined systems "base – reinforced concrete structures – metal structures".

Keywords: mathematical modeling, numerical methods, finite element method, superelement, component mode synthesis, stress-strain state, strain-stress state, dynamic characteristics, natural frequencies and modes, mechanical safety, large-size combined systems

МЕТОДИКА СУПЕРЭЛЕМЕНТНОГО МОДЕЛИРОВАНИЯ ДИНАМИКИ БОЛЬШЕРАЗМЕРНЫХ СИСТЕМ «ОСНОВАНИЕ – ЖЕЛЕЗОБЕТОННЫЕ КОНСТРУКЦИИ – МЕТАЛЛИЧЕСКИЕ КОНСТРУКЦИИ». ВЕРИФИКАЦИЯ И АПРОБАЦИЯ

А.И. Нагибович
Научно-исследовательский центр СтаДиО, г. Москва, РОССИЯ
Национальный исследовательский Московский государственный строительный университет, г. Москва, РОССИЯ

Аннотация: В настоящей статье представлены: краткое описание, верификация и апробация разработанной методики численного (суперэлеметного) моделирования динамики большеразмерных комбинированных систем «основание – железобетонные конструкции – металлические конструкции».

Ключевые слова: математическое моделирование, численные методы, метод конечных элементов, суперэлемент, метод динамического синтеза подконструкций, напряженно-деформированное состояние, динамические характеристики, собственные частоты и формы колебаний, механическая безопасность, большеразмерные комбинированные системы

INTRODUCTION

A key feature of the numerical simulation of the static and dynamic stress-strain state of unique construction objects: the development and optimization of related large-sized basic subsystems "base", "reinforced concrete structures", "metal structures of roof" are carried out independently various design organizations. The dimension of combined building systems can reach hundreds of thousands of different types of structural elements and, accordingly, tens of millions of degrees of freedom of their finite element models. It is not possible for such organizations to build an adequate computational model of a complete system, for example, modern football stadiums. Obstacles to this are various factors: from the incompatibility of file formats of computational models in various software systems and the large computational

dimension of such models to commercial secrets.

To solve this problem, it is necessary to develop and apply "advanced" methods of numerical simulation, which make it possible to justify the possibility of switching to investigations within the framework of individual subsystem models (the "organizational" aspect) and reduce the computational dimension of the problem.

It is convenient to build such a technique on the basis of superelement approaches. The superelement method or the substructure method is a procedure in which a group of finite elements is combined into one element, presented in the form of a matrix.

A single-matrix element is called a superelement and can be used in the calculation as a finite element.

For problems of static, a variant of the superelement method is used - static condensation (Guyan reduction) [1]. For dynamic problems, methods of dynamic synthesis of substructures (component mode synthesis) are used. Their advantage is that they allow you to correctly simulate the behavior of the structure under dynamic influences, by taking into account the truncated sets of generalized coordinates of the natural modes defined for each substructure of the system under study. The component mode synthesis, in turn, are divided into methods of fixed [2, 3], free [4, 5], mixed [6] and loaded boundaries [7].

1. DESCRIPTION OF THE TECHNIQUE

The developed superelement technique of numerical simulation of the dynamics of the systems "base - reinforced concrete structures - metal structures" is intended to determine the parameters of stress-strain state, strength, dynamics of these large-sized combined systems under the influence of various kinds of influences. The general block diagram of the technique is shown in Figure 1.

To realize the possibility of investigation the associated subsystems "base – reinforced concrete structures" and "metal structures", developed, as a rule, by various organizations, two ways are proposed. In the first case, comparing the dynamic characteristics of the complete system and subsystems, evaluate their mutual influence and thereby justify the possibility of switching to individual models (blocks 1-5). In the second, universal, case to use superelement technologies. With the superelement approach (blocks 6-14), each of the organizations develops a FE-model of its "own" subsystem (block 6), forms a superelement (SE) (blocks 8-11), which is a set of influence matrices. Further, the teams of investigators exchange these superelements and join "their" FE-model with a superelement developed and formed by colleagues (blocks 12). This ensures the transition from the study of the complete system to individual subsystems with the correct consideration of the dynamic characteristics of the subsystems developed by subcontractors.

The proposed methodology uses two versions of the dynamic synthesis method, which differ in the way of limiting the docking degrees of freedom – the fixed interface method and the free interface method. Docking degrees of freedom are called those by which the superelement is docked with the FE model of the subsystem or other superelements.

The technique is implemented on the basis of the ANSYS Mechanical software package and the author's own software development.

A more detailed description of the developed superelement technique is given in [8, 9].

2. VERIFICATION OF THE TECHNIQUE

To verify the developed technique, the following tasks were selected. The task from the original verification report of the ANSYS Mechanical was selected as the first verification example. In this test example, the dynamic characteristics of the tuning fork, obtained using a full FE-model and superelement models using various methods for taking into account the internal mode shapes of substructures, are determined and compared.

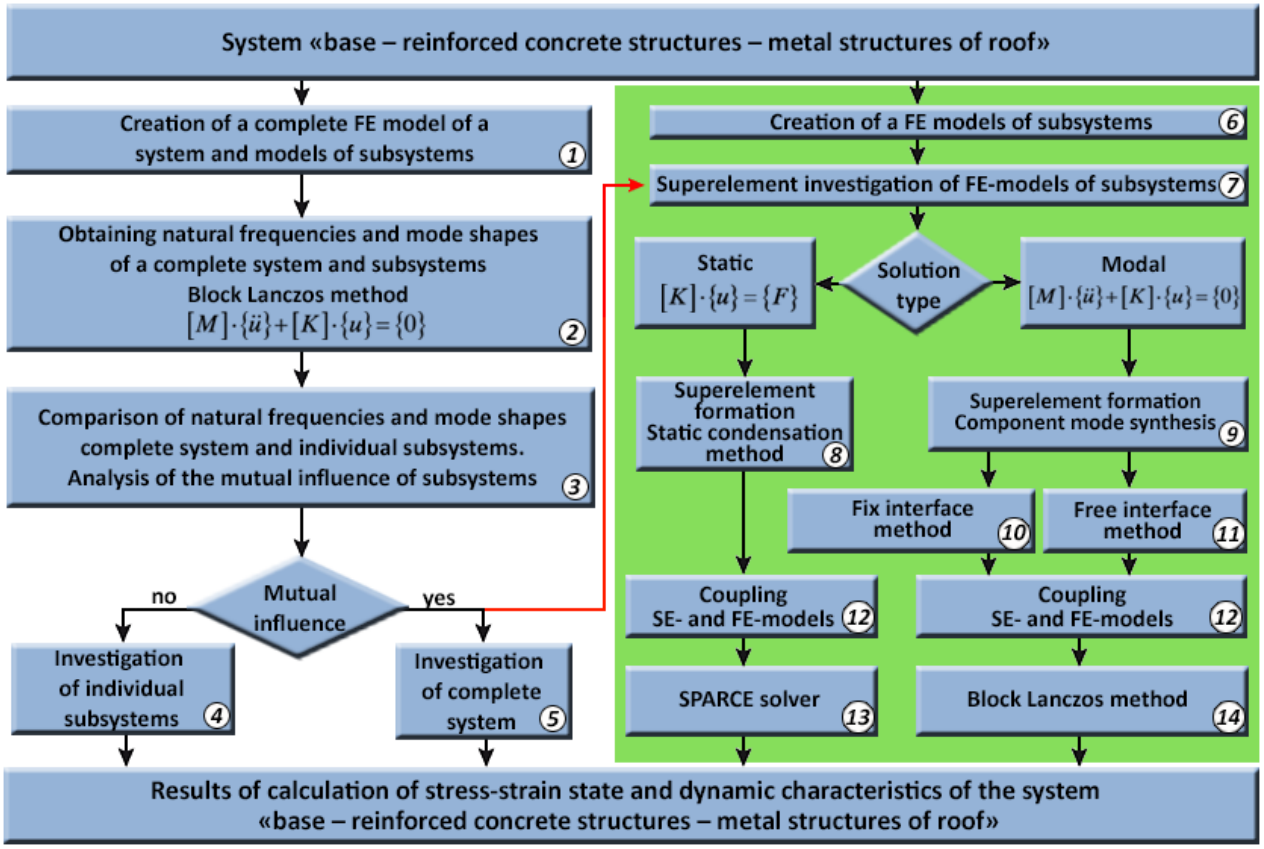


Figure 1. General block diagram of the developed technique of superelement simulation of dynamics of the systems "base - reinforced concrete structures - metal structures".

This example demonstrates the operability of the component mode synthesis of substructures. A comparative analysis of the obtained natural frequencies and mode shapes of the tuning fork for the mentioned models showed similar results for all the investigation options. The maximum difference between the obtained natural frequencies was 0.014%. The most effective and convenient, from the point of view of practical use and implementation in the PC used, have shown themselves to be fixed and free interface methods.

As a second example of pricing for a real object – the entrance block of the Volgamall shopping center in Volzhsky, having a design similar to the type investigated for large-sized systems. In this example, the analysis was carried out:

- the influence of the details of the FE-model (finite element mesh) on the accuracy of the obtained dynamic characteristics of the structure, as well as on the "machine" time spent on the obtaining;
- the possibility of transition to the investigation of the dynamic characteristics of subsystems within the framework of individual models "base - reinforced concrete structures" and "metal structures of the roof";
- the possibilities and features of the application of the component mode synthesis to the investigations of this kind of combined systems. The influence of the choice of the method of accounting for the internal mode shapes of the substructure and the number of internal frequencies and mode shapes of the substructure taken into account were analyzed.
- "organizational" and computational effectiveness of the proposed options developed by the superelement technique.

Comparison of the obtained natural frequencies and mode shapes of the entrance block of the Volgamall on FE models of various details showed that dividing the model by 3-4 finite el-

ements into one structural element of the structure (span of a plate, beam, column corresponds to optimal results and computational dimensions), element of the truss cover).

A comparative analysis of the obtained dynamic characteristics of the complete system "base – reinforced concrete structures – metal structures of the roof" and subsystems showed a significant effect of the compliance of the support subsystem on the behavior of the coating structure subsystem. This indicates the impossibility of conducting independent investigations of the subsystems "base – reinforced concrete structures" and "metal structures of the roof".

Comparison of the natural frequencies and mode shapes of a complete system modeled "head-on" by finite elements and subsystems with superelements (hereinafter, the subsystem with superelement for brevity denotes the complete system in which one of the subsystems is modeled by finite elements and the second is dynamic superelement) shows almost identical results. The difference in natural frequencies, taking into account a sufficient number of internal mode shapes of substructures for the fixed-interface method, was mainly no more than 0.007%, and for individual mode shapes up to 0.295%. For the free interface method, basically, no more than 0.005%, and for individual mode shapes, up to 0.038%.

The number of internal mode shapes of the substructures, which must be taken into account to obtain an adequate result, significantly depends on the stiff-bone and inertial characteristics of the construction itself. For constructions of the type under consideration, it is necessary to take into account the internal mode shapes of the substructure in the frequency range 1.5–2 times higher than the studied frequency range of the entire system [9, 10].

For the considered problem of "small" dimension (bearing in mind real unique structures), the factor of computational efficiency, as shown by a comparative analysis with full FE models, is expectedly not a strong point of the developed superelement technique.

Based on the presented and analyzed results of verification and computational studies, the applicability of superelement methods to simulating the dynamic characteristics of the investigated combined large-sized systems is substantiated.

Verification of the developed superelement technique in more detail is given in [8, 9].

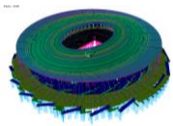
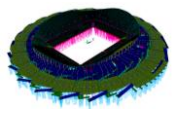
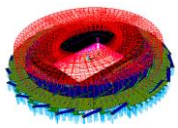
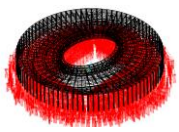
3. APPROBATION OF THE TECHNIQUE

To approbate the developed superelement technique as the research objects were selected designed and constructed for the 2018 World Cup 2018 are large-capacity stadiums (45,000 spectators): in Nizhny Novgorod and Rostov-on-Don, as illustrative examples of all branches of the technique.

Spatial shell-beam finite element and superelement models of stadium structures were developed and verified (Tables 1 and 2). For foundation slabs, walls, ceilings, stairwells and elevator shafts, folds of stands, beams under the folds of stands, SHELL181 type shells were used. Beams and columns are modeled by beam FEs of the BEAM188 type. MPC184 – an element of kinematic restrictions, was used at the junction of columns and floor slabs. LINK180 is a spatial core element working in tension or compression. Piles are modeled with special FEs of COMBIN14 type. The SURF154 element is used to assign various load effects. MATRIX50 – Superelement.

To obtain a significant part of the spectrum of natural frequencies and oscillation forms, the direct block Lanczos method was used. The investigations were carried out taking into account the masses only from the dead weight of supporting structures. For each system and subsystem, the frequencies and modes of natural vibrations in the range from 0 to 6 Hz were obtained. In the investigations using superelements, the internal mode shapes of the substructure were taken into account using the methods of a fixed boundary and a free boundary. The number of internal mode shapes of the substructure varied. The internal natural frequencies falling into the intervals were taken into account: up to 3 Hz, 6 Hz, 9 Hz, 12 Hz.

Table 1. Developed FE-models of the stadium in Nizhny Novgorod.

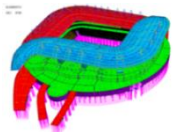
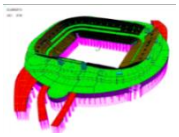
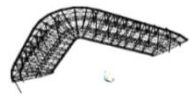
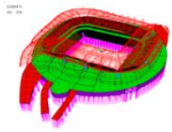
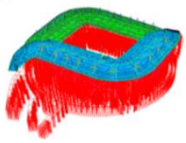
No.	FE-models of system / subsystem	Picture	Number of nodes	Number of elements	FE types
1.1	"base – reinforced concrete construction of foundations and stands – metal structures of the roof"		***633 461***	***699 383***	SHELL181, BEAM188, MPC184, SURF154, LINK180, COMBIN14
1.2	"base – reinforced concrete construction of foundations and stands "		***624 127***	***684 500***	SHELL181, BEAM188, MPC184, SURF154 COMBIN14
1.3	"metal structures of the roof"		***9 728***	***15 102***	BEAM188, MPC184, SURF154, LINK180
1.4	"base – reinforced concrete construction of foundations and stands" + superelement of the roof		***624 127***	***684 501***	SHELL181, BEAM188, MPC184, SURF154, COMBIN14, MATRIX50
1.5	"metal structures of the roof"+ superelement of of foundations and stands		***9 728***	***15 103***	BEAM188, MPC184, SURF154, LINK180, MATRIX50

A comparative analysis of the natural frequencies and mode shapes of the complete system "base - reinforced concrete structures of foundations and stands - metal structures of the roof" and subsystems of the stadium in Nizhny Novgorod revealed a weak effect of the flexibility of the support subsystem on the dynamic characteristics of the coating structure subsystem, which allows us to justify study of the latter in a separate model. In turn, the subsystem "metal structures of the roof" does not have a significant effect on the behavior of the support subsystem "base - reinforced concrete construction of foundations and tribunes", which also gives reason to carry out studies of the isolated subsystem.

A similar comparison of the natural frequencies and mode shapes of the complete system and subsystems of the stadium in Rostov-on-Don showed a significant mutual influence of the reference subsystem and the subsystem of the coating structures on the dynamic characteristics. This indicates the impossibility of conducting independent calculations of subsystems without taking into account the stiffness and mass characteristics of all elements of the complete system.

In Tables 3 and 4, the natural frequency of the complete system and subsystems on which the mode shapes coincide are marked with a green background. The red background marks those frequencies of subsystems at which the mode shapes do not correspond to the mode shapes of the complete system or are absent.

Table 2. Developed FE-models of the stadium in Rostov-on-Don.

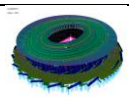
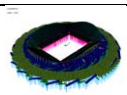
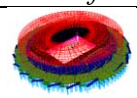
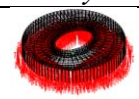
No.	FE-models of system/subsystem	Picture	Number of nodes	Number of elements	FE types
2.1	"base - reinforced concrete construction of foundations and stands – metal structures of the roof"		***621 048***	***604 358***	SHELL181, MPC184, BEAM188, SURF154, LINK180, COMBIN14
2.2	"base - reinforced concrete construction of foundations and stands "		***599 417***	***589 387***	SHELL181 BEAM188 MPC184 SURF154 COMBIN14
2.3	"metal structures of the north-east wing of the coating"		***9 185***	***6 304***	BEAM188 LINK180 SURF154
2.4	"metal structures of the south-western wing of the roof"		***12 446***	***8 667***	BEAM188 LINK180 SURF154
2.5	"base - reinforced concrete construction of foundations and stands "+ superelement of the roof		***599 417***	***589 388***	SHELL181, MPC184, BEAM188, SURF154, COMBIN14 MATRIX50
2.6	"metal structures of the roof"+ superelement of the reinforced concrete construction of foundations and stands		***21 651***	***14 972***	BEAM188 LINK180 SURF154 MATRIX50

A comparative analysis of the natural frequencies and mode shapes of the complete system "base - reinforced concrete structures of foundations and stands - metal structures of the roof" and subsystems of the stadium in Nizhny Novgorod revealed a weak effect of the flexibility of the support subsystem on the dynamic characteristics of the coating structure subsystem, which allows us to justify study of the latter in a separate model. In turn, the subsystem "metal structures of the roof" does not have a significant effect on the behavior of the support subsystem "base - reinforced concrete construction of foundations and tribunes", which also gives reason to carry out studies of the isolated subsystem.

A similar comparison of the natural frequencies and mode shapes of the complete system and subsystems of the stadium in Rostov-on-Don showed a significant mutual influence of the reference subsystem and the subsystem of the coating structures on the dynamic characteristics. This indicates the impossibility of conducting independent calculations of subsystems without taking into account the stiffness and mass characteristics of all elements of the complete system.

In Tables 3 and 4, the natural frequency of the complete system and subsystems on which the mode shapes coincide are marked with a green background. The red background marks those frequencies of subsystems at which the mode shapes do not correspond to the mode shapes of the complete system or are absent.

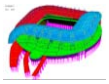
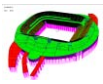
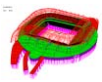
Table 3. Comparison of natural frequencies of the complete system and its constituent subsystems of the stadium in Nizhny Novgorod.

 Model 1.1		 Model 1.2		 Model 1.3		Δ, %	 Model 1.4		Δ_1, %	 Model 1.5		Δ_2, %
No.	Freq, H	No.	Freq, H	No.	Freq, H		No.	Freq, H		No.	Freq, H	
1	**0,4116**			1	**0,4381**	*6,040*	1	**0,4116**	*0,000*	1	**0,4116**	*0,000*
2	**0,4177**			2	**0,4447**	*6,069*	2	**0,4177**	*0,000*	2	**0,4177**	*0,000*
3	**0,4701**			3	**0,4906**	*4,174*	3	**0,4701**	*0,000*	3	**0,4701**	*0,000*
…	…	…	…	…	…	…	…	…		…	…	…
7	**0,9120**			7	**0,9359**	*2,550*	7	**0,9120**	*0,000*	7	**0,9120**	*0,000*
8	**0,9256**	1	**0,9299**			*0,462*	8	**0,9256**	*0,000*	8	**0,9256**	*0,000*
…	…	…	…	…	…	…	…	…		…	…	…
682	**5,0317**			369	**5,0325**	*0,015*	682	**5,0343**	***0,052***	682	**5,0322**	*0,010*
…	…	…	…	…	…	…	…	…		…	…	…
749	**5,2537**			415	**5,2532**	*0,010*	749	**5,2545**	0,015	749	**5,2553**	***0,030***
…	…	…	…	…	…	…	…	…		…	…	…
922	**5,7199**	287	**5,7239**			*0,070*	922	**5,7199**	*0,000*	922	**5,7199**	*0,000*
…	…	…	…	…	…	…	…	…		…	…	…
1021	**5,9895**			619	**5,9929**	*0,057*	1021	**5,9897**	*0,003*	1021	**5,9897**	*0,003*
…	…	…	…	…	…	…	…	…		…	…	…

A comparison of the natural frequencies and mode shapes of complete systems and subsystems taking into account superelements shows that obtaining of dynamic characteristics using the component mode synthesis give results close to those when investigating the complete system. The discrepancy between the values of the obtained natural frequencies for most mode shapes does not exceed 0.050%, and for individual modes, in the range under study, up to 0.900% depending on the frequency range considered, with a sufficient number of internal forms of vibration of the substructure taken into account.

Comparison of the dynamic characteristics, obtained by various versions of the component mode synthesis, allows us to formulate the following recommendations: for the formation of a superelement of the subsystem "base - reinforced concrete construction of foundations and tribunes", it is preferable to use the method of freedom boundaries, for the superelement of the subsystem "metal structures" – a fixed border method.

Table 4. Comparison of natural frequencies of the complete system and its constituent subsystems of the stadium in Rostov-on-Don.

 Model 2.1		 Model 2.2		 Model 2.3		 Model 2.4		Δ, %	 Model 2.5		Δ_1, %	 Model 2.6		Δ_2, %
№	Freq, Hz	№	Freq, H	№	Freq, H	№	Freq, H		№	Freq, H		№	Freq, H	
1	**1,2304**					1	**1,3157**	*6,483*	1	**1,2304**	*0,000*	1	**1,2323**	*0,154*
2	**1,4093**					2	**1,4253**	*1,123*	2	**1,4093**	*0,000*	2	**1,4095**	*0,014*
3	**1,5981**					3	**1,7469**	*8,518*	3	**1,5982**	*0,000*	3	**1,5987**	*0,031*
4	**1,6012**			1	**1,7369**			*7,813*	4	**1,6013**	*0,000*	4	**1,6014**	*0,006*
5	**1,6498**	1	**1,6504**					*0,036*	5	**1,6502**	*0,018*	5	**1,6501**	*0,024*
6	**1,6658**					4	**1,8129**	*8,114*	6	**1,6660**	*0,006*	6	**1,6668**	*0,054*
7	**1,7059**			2	**1,8215**			*6,346*	7	**1,7060**	*0,000*	7	**1,7068**	*0,047*
8	**1,7275**	2	**1,7790**						8	**1,7277**	*0,012*	8	**1,7339**	*0,369*
…	…	…	…	…	…	…	…	…	…	…	…	…	…	…
16	**1,9766**		**1,9773**						16	**1,9773**	***0,035***	16	**1,9763**	*0,015*
…	…	…	…	…	…	…	…	…	…	…	…	…	…	…
93	**3,0150**		**3,0377**		**3,0220**				93	**3,0151**	*0,003*	93	**3,0381**	***0,760***
…	…	…	…	…	…	…	…	…	…	…	…	…	…	…
350	**5,9914**								350	**5,9915**	*0,002*	350	**5,9915**	*0,002*
…	…	…	…	…	…	…	…	…	…	…	…	…	…	…

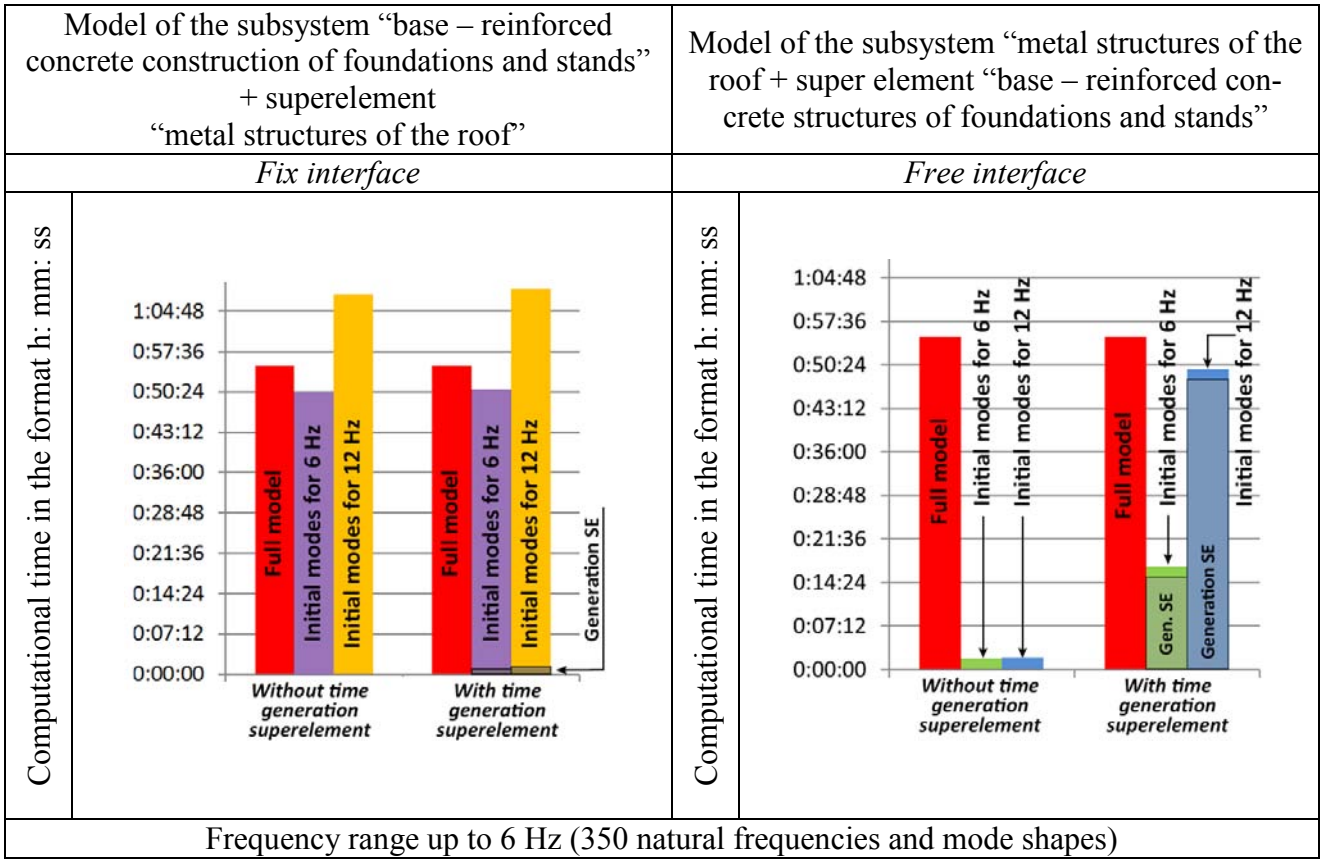


Figure 2. Comparison of the time for obtaining the dynamic characteristics of a complete system and subsystems with super elements of the stadium in Rostov-on-Don.

It is with this approach that the minimum discrepancy between the natural frequencies and mode shapes of the complete system and subsystems using superelements is achieved. Also, the recommendation was confirmed to hold for the substructure all mode shapes and natural frequencies of which are 1.5-2 times higher than the studied frequency range for the entire system [9, 10].

The total "machine" time for the formation of a superelement and obtain the dynamic characteristics of the subsystem with its application, taking into account a sufficient number of internal modes of the substructure, is comparable to the time spent on the investigation of the complete system. The time for investigation the subsystem "metal structures of the roof" taking into account the superelement "base - reinforced concrete structures" (not taking into account the spent "machine" time for the genegation of the superelement) is 15-30 times (for Rostov-on-Don. Figure 2) and 40-75 times (for Nizhny Novgorod) less than that spent on the investigation of the complete system. This gives a significant gain in computational efficiency when conducting multivariate computational investigations of the subsystem "metal structures of the roof" in order to optimize it, since it is not necessary to re-generate the superelement.

CONCLUSION

Summarizing the results presented in this article, we can draw the following conclusions:

1) An effective superelement technique of numerical simulation of dynamic characteristics of large-sized systems "base – reinforced concrete structures – metal structures of the roof" was developed, verified and approbated, which allows us to proceed to the investigation of subsystems "base",

"reinforced concrete structures" and "metal structures of the roof" as part of individual models.

2) Verification examples (including the entrance block of the Volgamall shopping center in Volzhsky) demonstrated the effectiveness and features of using the developed superelement technique to investigate the dynamic characteristics of combined systems of a similar type.

3) A comparative analysis of the natural frequencies and mode shapes of the complete system and subsystems of the stadium in Nizhny Novgorod revealed a weak effect of the compliance of the support subsystem on the dynamic characteristics of the coating structures, which allows us to justify the investigate of the latter within a separate model. In turn, the subsystem of coating structures does not significantly affect the behavior of the supporting subsystem, which also gives reason to perform its investigations in isolation.

4) On the contrary, a comparison of the natural frequencies and mode shapes of the complete system and the structural subsystems of the stadium in Rostov-on-Don showed a significant mutual influence of the subsystems on the dynamic characteristics. This indicates the impossibility of investigating subsystems for individual models without the use of superelements.

5) Analysis of natural frequencies and mode shapes of complete systems and subsystems with superelements of stadiums in Nizhny Novgorod and Rostov-on-Don show that the dynamic characteristics are almost identical when taking into account a sufficient number of internal natural frequencies and mode shapes of substructures.

6) The most valuable, "organizational" effectiveness of the developed technique for two real combined large-sized systems "foundation – reinforced concrete construction of foundations and stands – metal structures of the roof" with the use of superelement approaches was demonstrated. The computational competitiveness of the developed models with superelements was confirmed (compared to the full FE models).

7) The presented results allow us to recommend the developed superelemental technique for use for a wide class of computational investigations of combined large-sized systems of unique buildings and structures.

8) The development and application of the proposed superelement technique of numerical simulation of combined large-sized systems to solve problems in physical, geometrical, structural and genetically non-linear settings seems to be a prospect for further development of this topic.

REFERENCES

1. **Gayan R.** Privedenie Matric Zhestkosti I Massy [The Reduction of the Stiffness and Mass Matrices]. // *Raketnaya Tekhnika I Kosmonavtika*, 1965, Volume 3, Number 2, pp. 277-278 (in Russian).
2. **Craig R.R.,Jr., Bampton M.C.C.** Coupling of substructures for dynamic analysis. // *AIAA Journal*, 1968, Volume 6, No. 7, pp. 1313-1319.
3. **Hurty W.C.** Dynamic analysis of structural systems using component modes. // *AIAA Journal*, 1984, Volume 4, pp. 733-738.
4. **Zu-Qing Qu.** Model Order Reduction Techniques with Applications in Finite Element Analysis. Springer Publications, 2004 (Electronic book; ISBN 978-1-4471-3827-3).
5. **Craig R., Chang C.-J.** Free-interface methods of substructure coupling for dynamic analysis. // *AIAA Journal*, 1976, Volume 14, No. 11, pp. 1633-1635.
6. **MacNeal R.H.** A hybrid method of component mode synthesis. // *Computers and structures*, 1971, Volume 4, pp. 591-601.
7. **Curnier A.** On three modal synthesis variants. // *Journal of Sound and Vibration*, 1983, Volume 90, No. 4. pp. 527-540.
8. **Nagibovich A.I**. Metodika superelementnogo modelirovaniya dinamiki sistem "osnovaniye – konstruktsii fundamentov i tribun – kon-struktsii pokrytiya" stadionov chempionata mira po futbolu 2018 goda v Rossii. Opisaniye i verifikatsiya. // *International Journal for Computational Civil and Structural Engineering*, 2018, Volume 14, Issue 2, pp. 117-132 (in Russian).

9. **Nagibovich A.I**. Superelementnoye modelirovaniye dinamicheskikh kharakteristik bol'sherazmernykh kombinirovannykh sistem «osnovaniye – zhelezobetonnyye konstruktsii – metallicheskiye konstruktsii» // Dissertation of the Candidate Technical Sciences. Moscow, 2019, 161 pages.
10. **Rubin S.** Improved component-mode representation for structural dynamic analysis. // *AIAA Journal*, 1975, Volume 13, No. 8, pp. 995-1006.
11. **Nagibovich A.I**. Approbation of the developed technique of superelement simulation of dynamics for system "Basis–Foundations structures and stands – Structures of the roof" for stadiums for the 2018 FIFA World Cup in Russia. // *IOP Conference Series: Materials Science and Engineering*, 2018, Volume 456, 012121.

СПИСОК ЛИТЕРАТУРЫ

1. **Гайан Р.** Приведение матрицы жесткости и массы. // *Ракетная техника и космонавтика*, 1965, Том 3, № 2, с. 277-278.
2. **Craig R.R.,Jr., Bampton M.C.C.** Coupling of substructures for dynamic analysis. // *AIAA Journal*, 1968, Volume 6, No. 7, pp. 1313-1319.
3. **Hurty W.C.** Dynamic analysis of structural systems using component modes. // *AIAA Journal*, 1984, Volume 4, pp. 733-738.
4. **Zu-Qing Qu.** Model Order Reduction Techniques with Applications in Finite Element Analysis. Springer Publications, 2004 (Electronic book; ISBN 978-1-4471-3827-3).
5. **Craig R., Chang C.-J.** Free-interface methods of substructure coupling for dynamic analysis. // *AIAA Journal*, 1976, Volume 14, No. 11, pp. 1633-1635.
6. **MacNeal R.H.** A hybrid method of component mode synthesis. // *Computers and structures*, 1971, Volume 4, pp. 591-601.
7. **Curnier A.** On three modal synthesis variants. // *Journal of Sound and Vibration*, 1983, Volume 90, No. 4. pp. 527-540.
8. **Nagibovich A.I**. Metodika superelementnogo modelirovaniya dinamiki sistem "osnovaniye – konstruktsii fundamentov i tribun – kon-struktsii pokrytiya" stadionov chempionata mira po futbolu 2018 goda v Rossii. Opisaniye i verifikatsiya. // *International Journal for Computational Civil and Structural Engineering*, 2018, Volume 14, Issue 2, pp. 117-132.
9. **Нагибович А.И.** Суперэлементное моделирование динамических характеристик большеразмерных комбинированных систем «основание – железобетонные конструкции – металлические конструкции». Диссертация на соискание ученой степени кандидата технических наук по специальности 05.13.18 – «Математическое моделирование, численные методы и комплексы программ». – М.: НИУ МГСУ, 2019. – 161 с.
10. **Rubin S.** Improved component-mode representation for structural dynamic analysis. // *AIAA Journal*, 1975, Volume 13, No. 8, pp. 995-1006.
11. **Nagibovich A.I**. Approbation of the developed technique of superelement simulation of dynamics for system "Basis–Foundations structures and stands – Structures of the roof" for stadiums for the 2018 FIFA World Cup in Russia. // *IOP Conference Series: Materials Science and Engineering*, 2018, Volume 456, 012121.

Alexander I. Nagibovich, Senior Engineer of Scientific Research Center "StaDyO"; University teacher, Department of Applied Mathematics, National Research Moscow State University of Civil Engineering; office 810, 18, 3ya Ulitsa Yamskogo Polya, Moscow, 125040, Russia;
phone +7 (499) 706-88-10;
E-mail: nagibovich@yandex.ru.

Нагибович Александр Игоревич, ведущий инженер-расчетчик, ЗАО «Научно-исследовательский центр СтаДиО»; преподаватель кафедры прикладной математики, Национальный исследовательский Московский государственный строительный университет; 125040, Москва, ул. 3-я Ямского Поля, д.18, офис 810; тел. +7 (499) 706-88-10; e-mail: nagibovich@yandex.ru.

DOI:10.22337/2587-9618-2019-15-4-133-142

SOLUTION OF THE PROBLEM OF THERMOELASTICITY FOR NONLINEAR ELASTIC INHOMOGENEOUS THICK-WALL CYLINDRICAL SHELL

Lyudmila S. Polyakova, Vladimir I. Andreev
National Research Moscow State University of Civil Engineering, Moscow, RUSSIA

Abstract: The distinctive paper presents the calculation of a thick-walled cylindrical shell with hinged and free ends on the temperature effect. The shell consists of three layers: two layers of heat-resistant concrete and steel outer layer. The calculation takes into account the piecewise linear inhomogeneity of the shell due to its three-layer construction and the continuous inhomogeneity caused by the action of a stationary temperature field. To take into account the nonlinear nature of concrete deformation, the problem was solved using the method of successive approximations described in [1]. A comparative analysis of the results of the calculation of the shell with and without taking into account the continuous inhomogeneity and the nonlinear nature of the deformation of concrete is given. Comparison of the results showed a significant decrease in circumferential stresses in the most loaded concrete layers when calculating the shell with regard to physical nonlinearity and heterogeneity of materials.

Keywords: nonlinearity, inhomogeneity, concrete, elevated temperature, cylindrical shell

РЕШЕНИЕ ЗАДАЧИ ТЕРМОУПРУГОСТИ ДЛЯ НЕЛИНЕЙНО УПРУГОЙ НЕОДНОРОДНОЙ ТОЛСТОСТЕННОЙ ЦИЛИНДРИЧЕСКОЙ ОБОЛОЧКИ

Л.С. Полякова, В.И. Андреев
Национальный исследовательский Московский государственный строительный университет,
г. Москва, РОССИЯ

Аннотация: В настоящей статье приводится расчет толстостенной цилиндрической оболочки с шарнирно закрепленными и свободными торцами на температурное воздействие. Оболочка состоит из трех слоев: два слоя из жаростойкого бетона и стальной наружный слой. При расчете учитывается кусочно-линейная неоднородность оболочки, обусловленная ее трехслойной конструкцией и непрерывная неоднородность, вызванная воздействием стационарного температурного поля. Для учета нелинейного характера деформирования бетона задача решалась методом последовательных приближений, описанном в [1]. Приведен сравнительный анализ результатов расчета оболочки с учетом и без учета непрерывной неоднородности и нелинейного характера деформирования бетона. Сравнение результатов показало значительное снижение окружных напряжений в наиболее нагруженных слоях бетона при расчете оболочки с учетом физической нелинейности и неоднородности материалов.

Ключевые слова: нелинейно упругий материал, неоднородность, бетон, повышенные температуры, цилиндрическая оболочка

INTRODUCTION

Structural elements in the form of hollow cylinders are widely used in technological equipment of the chemical and energy industries. Such structures often work in conditions of elevated and high temperatures, aggressive environments (reactors and regenerators for many catalytic processes). In order to protect the steel casing of the apparatus, it is lined inside with heat-resistant concrete, which is coated by a corrosion-resistant layer.

This design of the reactor allows to protect the metal against corrosion, reduce the metal con-

sumption of the apparatus and reduce heat loss. Modern building standards [2] require taking into account changes in the mechanical and elastoplastic properties of concrete depending on the temperature of exposure, and suggest using a two-line or three-line deformation diagram for assessing the stress-strain state of compressed concrete. This article proposes a solution to the problem of thermoelasticity taking into account changes in the properties of concrete depending on temperature and using experimental deformation diagrams.

1. FORMULATION OF THE PROBLEM

The problem of calculating a three-layer cylindrical shell on the temperature effect is considered. Shell materials are: internal corrosion-resistant layer of heat-resistant concrete made of alumina cement (concrete No. 1) of 50 mm thick, the middle layer of heat-resistant concrete made of Portland cement (concrete No. 2) - of 100 mm, the outer layer made of steel - of 40 mm. A constant temperature of 500 ° C is maintained inside.

Two solutions are considered: with hinged end of the cylinder and with a free end (Figure 1 a, b).
The temperature distribution inside the multi-layer wall is determined by solving the heat equation. The following initial data are used in the solution: $T_i = 500\,^\circ\mathrm{C}$ is temperature inside the shell; $T_o = 20\,^\circ\mathrm{C}$ is the temperature of the outside air; $\alpha_1 = 162{,}8\ \mathrm{W/m^2{\cdot}^\circ C}$ is heat transfer coefficient from the internal area to the concrete wall; $\lambda_1 = 0{,}8\ \mathrm{W/m{\cdot}^\circ C}$ is the thermal conductivity of the first concrete layer; $\lambda_2 = 0{,}85\ \mathrm{W/m{\cdot}^\circ C}$ is the thermal conductivity of the second concrete layer; $\lambda_3 = 25\ \mathrm{W/m{\cdot}^\circ C}$ - coefficient of thermal conductivity of steel; $\alpha_2 = 7{,}6\ \mathrm{W/m^2{\cdot}^\circ C}$ - heat transfer coefficient from the outer surface of the shell to the air; $r_1 = 0{,}55\ \mathrm{m}$, $r_2 = 0{,}6\ \mathrm{m}$, $r_3 = 0{,}7\ \mathrm{m}$, $r_4 = 0{,}74\ \mathrm{m}$. The temperature distribution in the three-layer wall is shown in Figure 1: $T_i = 500\,^\circ\mathrm{C}$, $T_1 = 488{,}9\,^\circ\mathrm{C}$, $T_2 = 380{,}4\,^\circ\mathrm{C}$, $T_3 = 199{,}5\,^\circ\mathrm{C}$, $T_4 = 197{,}3\,^\circ\mathrm{C}$, $T_o = 20\,^\circ\mathrm{C}$.

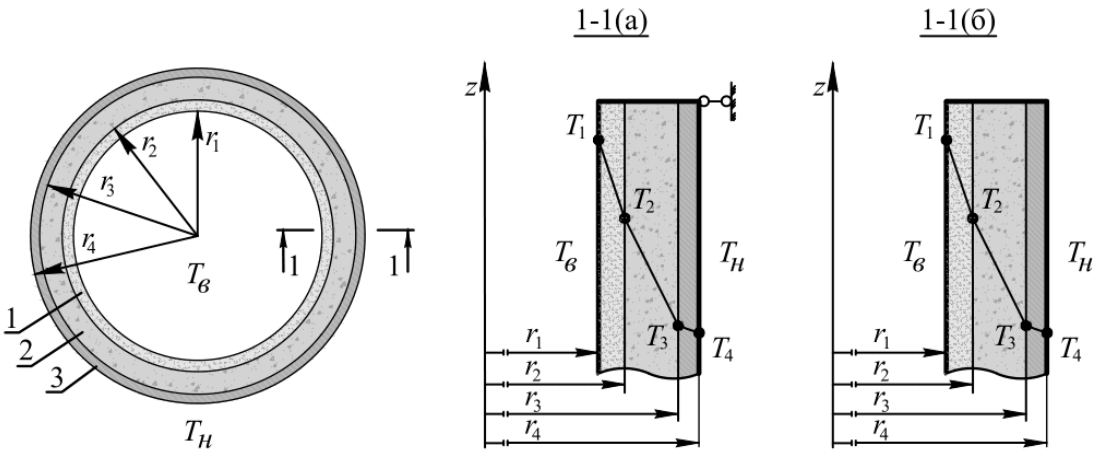


Figure 1. Distribution of temperature into a three-layer shell: 1 – concrete No. 1; 2 - concrete No. 2; 3 – steel.

Function of the temperature changes through the radius of each layer takes the form:

$$T_j\ r = \ln\ r/a\ \frac{T_{j+1}-T_j}{\ln(r_{j+1}/r_j)} + \frac{T_j \ln\ r_{j+1}/a\ - T_{j+1}\ln\ r_j/a}{\ln(r_{j+1}/r_j)}, \quad (1)$$

where j is layer number (1, 2, …, n), a = 1 m.
Thus, the following temperature distribution functions were obtained for the first and second concrete layers:

$$T_1\ r\ = -1247 \ln\ r\ - 256,4\,,$$
$$T_2\ r\ = -1173 \ln\ r\ - 218,9\,. \qquad (2)$$

The change in temperature over the thickness of the steel layer is not taken into account in the solution, the average temperature value $T_3 = 198,4\ ^\circ\mathrm{C}.$ is taken instead it.

In order to describe the nonlinear nature of concrete deformation, the experimental deformation diagrams of heat-resistant concrete given in [3] are used. The solution uses a diagram $\sigma_i - \varepsilon_i$ that is described by a dependence with three constants, proposed in [4]:

$$\sigma_i = E\varepsilon_i - A\varepsilon_i^{\alpha}, \qquad (3)$$

The heterogeneity of concrete resulting from exposure under elevated temperatures is taken into account by replacing the constants *E*, *A*, and α with the functions *E* (*T*), *A* (*T*), and α (*T*). In order to describe the deformation diagrams of heat-resistant concrete made of Portland cement, the following functions were used:

$$E_1(T) = E_{01} + k_{E1}\left(\frac{\Delta T}{T_0}\right)^{0,5} + m_{E1}\left(\frac{\Delta T}{T_0}\right)^{2,5},$$
$$A_1(T) = A_{01} + k_{A1}\left(\frac{\Delta T}{T_0}\right)^{0,8} + m_{A1}\left(\frac{\Delta T}{T_0}\right)^{1,5}, \qquad (4)$$
$$\alpha_1(T) = \alpha_{01} + k_{\alpha 1}\left(\frac{\Delta T}{T_0}\right)^{1,2} + m_{\alpha 1}\left(\frac{\Delta T}{T_0}\right)^{1,5}.$$

The following functions were used to describe the deformation diagrams of heat-resistant concrete on alumina cement:

$$E_2(T) = E_{02}\cdot\exp\left[k_{E2}\left(\frac{\Delta T}{T_0}\right)^{0,9} + m_{E2}\left(\frac{\Delta T}{T_0}\right)^{0,2}\right],$$
$$A_2(T) = A_{02}\cdot\exp\left[k_{A2}\left(\frac{\Delta T}{T_0}\right)^{0,7} + m_{A2}\left(\frac{\Delta T}{T_0}\right)^{0,3}\right], \qquad (5)$$
$$\alpha_2(T) = \alpha_{02}\cdot\exp\left[k_{\alpha 2}\left(\frac{\Delta T}{T_0}\right)^{0,9} + m_{\alpha 2}\left(\frac{\Delta T}{T_0}\right)^{0,15}\right].$$

We accept the following designations in formulas (4) and (5): $\Delta T = T - T_0$, where $T_0 = 20°C$ is the normal temperature of concrete; E_0, A_0, α_0, k_E, k_A, k_α, m_E, m_A, m_α are the coefficients obtained by approximating the experimental deformation diagrams.

The work [2] presents the values of the coefficient of linear temperature deformation of concretes of various compositions depending on temperature. We accepted the values α_b that correspond to the continuous heating mode upon repeated exposure to temperature. To approximate the data from [2], the following functions were used:

$$\alpha_{b1}(T) = k_1\left(\frac{\Delta T}{T_0}\right) + k_2\left(\frac{\Delta T}{T_0}\right)^{1,5} + k_3\left(\frac{\Delta T}{T_0}\right)^{2},$$
$$\alpha_{b2}(T) = \alpha_t + k_4\left(\frac{\Delta T}{T_0}\right)^{1,1} + k_5\left(\frac{\Delta T}{T_0}\right)^{1,2} + k_6\left(\frac{\Delta T}{T_0}\right)^{1,5}, \qquad (6)$$

Where α_{b1} is the coefficient of linear temperature deformation of concrete No. 1; α_{b2} is coefficient of linear temperature deformation of concrete No. 2; $k_1 \ldots k_6$ are the coefficients obtained by approximating the data from [2].

The values of the coefficients from formulas (4), (5), (6), as well as the diagram $\sigma_i - \varepsilon_i$ of the deformation of concrete of two different compositions are given in [5], where a solution to a similar problem for an infinite cylindrical shell was considered.

2. METHOD OF ANALYSIS

Based on the method of successive approximations, we developed a numerical method for solving plane axisymmetric and centrally symmetric problems for thick-walled shells made of physically nonlinear radially inhomogeneous

material with arbitrary dependences of mechanical characteristics through the radius. We obtained numerical solutions to test problems. A comparison of the results of numerical and analytical solutions showed sufficient accuracy of the developed method [6]. The solution for the condition of a planar deformed state assumes that the cylinder is very long and stresses arising at a sufficient distance from the ends are considered. This article proposes a solution to the problem taking into account local disturbances near the ends of the cylinder.

The solution obtained for the conditions of planar deformable state requires that normal stresses σ_z^* be distributed at the ends of the cylinder. The work [7] proposed determining the stresses in the final cylindrical shell by summing up the solution for the planar deformable state condition and the solution for the cylindrical shell, at the ends of which forces, that are equal in value and opposite in sign to the stresses σ_z^*, are applied.

In order to determine the stresses caused by these forces $(-\sigma_z^*)$, we consider a longitudinal strip of unit width cut from a cylindrical shell. Such a strip can be considered as a beam on an elastic base, for which the equation of deflection has the form:

$$D\frac{d^4u}{dz^4} + Ku = p(z), \qquad (7)$$

where $p(z) = 0$ is the intensity of the radial axisymmetric load;

$$D = \frac{Eh^3}{12(1-\nu^2)}$$

is the flexural stiffness of the cylindrical shell, replacing the flexural stiffness of the rod *EI*;

$$K = \frac{Eh}{R^2}$$

is the stiffness of the shell in tension-compression in the circumferential direction, replacing the stiffness coefficient of the elastic base.

In the case of a radially inhomogeneous shell, the equation takes the form:

$$\frac{d^4u}{dz^4}\frac{h^2}{12}\int_{r_1}^{r_4}\frac{E(r)dr}{1-\nu\ r^2} + u\int_{r_1}^{r_4}\frac{E(r)dr}{r^2} = 0, \qquad (8)$$

where *h* is the thickness of the shell.

For the convenience of integrating equation (8), we introduce the dimensionless variable: $\xi = \lambda z$, where

$$\lambda = \sqrt[4]{\frac{K_1}{4D_1}}.$$

The parameter λ depends on the flexural stiffness of the shell and on the stiffness of the shell in tension-compression in the circumferential direction. Derivatives with respect to variables ξ and *z* are related by the ratio:

$$\frac{d^n}{dz^n} = \lambda^n \cdot \frac{d^n}{d\xi^n}. \qquad (9)$$

After replacing the variable, the differential equation takes the form:

$$\frac{d^4u(\xi)}{dz^4} + 4u(\xi) = 0. \qquad (10)$$

Solution to the homogeneous equation:

$$u(\xi) = \sin\ \xi\ \ c_1\exp\ \xi + c_3\exp\ -\xi\ + \\ +\cos\ \xi\ \ c_2\exp\ \xi + c_4\exp\ -\xi\ , \qquad (11)$$

where

$$\xi = z\sqrt[4]{\frac{K_1}{4D_1}}.$$

Stresses arising near the ends of the cylinder quickly descend with increasing distance from the end *z*, and already at a distance of 1.5 m from the edge tend to zero, therefore, with a cylinder length of more than $L = 3$ m, the beam can be considered as semi-infinite, on the end of which stresses $-\sigma_z^*$ are attached. Then, assuming that the integration constants C_1 and C_2 equal to zero, we obtain the equation:

$$u(\xi) = c_3 \exp(-\xi)\sin(\xi) + c_4 \exp(-\xi)\cos(\xi). \quad (12)$$

The constants C_3 and C_4 are determined from the boundary conditions. Let us consider the case of hinge supporting and free edge.
For hinge supporting it is

$$u(0) = 0,$$

then $c_4 = 0$. Also it is known normal stresses σ_z distributed over the ends of the cylinder, which are equal to the stresses calculated in the planar deformable state condition, taken with the opposite sign:

$$\sigma_z(0) = -\sigma_z^*.$$

Stresses σ_z are determined through displacements:

$$\sigma_z = -\frac{E}{1-\nu^2}\left(r - \frac{r_1 + r_4}{2}\right)\frac{d^2u}{dz^2}. \quad (13)$$

From the condition $\sigma_z(0) = -\sigma_z^*$, we get:

$$c_3 = \frac{1}{2\lambda^2}\frac{\int_{r_1}^{r_4}\sigma_z^*(r)dr}{\int_{r_1}^{r_4}\frac{E(r)}{1-\nu r^2}\left(r - \frac{r_1 + r_4}{2}\right)dr}. \quad (14)$$

The final expression for the displacement:

$$u(z) = \frac{1}{2\lambda^2}\frac{\int_{r_1}^{r_4}\sigma_z^*(r)dr}{\int_{r_1}^{r_4}\frac{E(r)}{1-\nu r^2}\left(r - \frac{r_1 + r_4}{2}\right)dr} \times \quad (15)$$
$$\times \exp(-\lambda z)\sin(\lambda z).$$

For the condition of a free edge, the conditions

$$\varphi(0) = 0,\ \varphi = \frac{du}{dz}$$

are satisfied, then $c_4 = -c_3$, the expression for the displacements takes the form:

$$u(z) = \frac{1}{2\lambda^2}\frac{\int_{r_1}^{r_4}\sigma_z^*(r)dr}{\int_{r_1}^{r_4}\frac{E(r)}{1-\nu r^2}\left(r - \frac{r_1 + r_4}{2}\right)dr} \times \quad (16)$$
$$\times\left[\exp(-\lambda z)\cos(\lambda z) - \exp(-\lambda z)\sin(\lambda z)\right].$$

Since we have a formula for the deflection curve, it is possible to calculate the corresponding bending stresses σ_z^u and tangential stresses σ_θ^u for any value of *z*. The component of deformation in the tangential direction is equal for each layer:

$$\varepsilon_\theta^u = \frac{u}{r}.$$

The component of stresses in the tangential direction is determined from Hooke's law:

$$\sigma_\theta^u = E\varepsilon_\theta^u + \nu\sigma_z^u =$$
$$= E\frac{u}{r} + \nu\frac{E}{1-\nu^2}\left(\frac{r_1 + r_4}{2} - r\right)\frac{d^2u}{dz^2}. \quad (17)$$

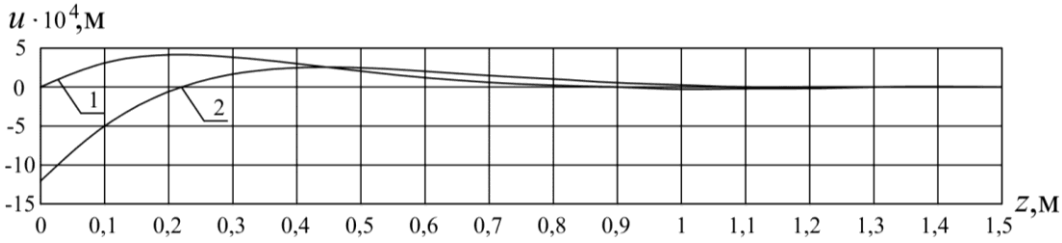


Figure 2. Curvature of deflections caused by acting of $-\sigma_z^*$.

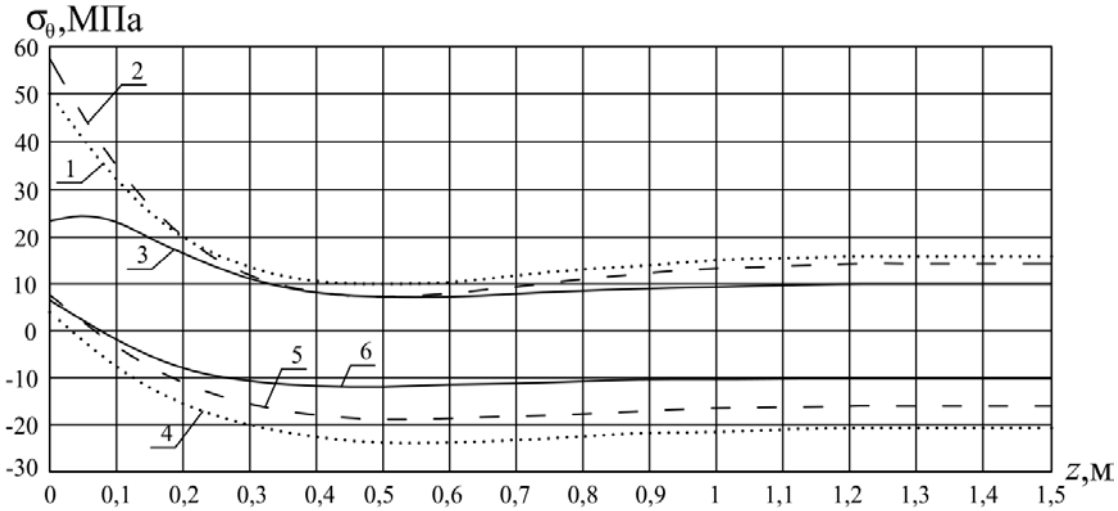


Figure 3. Stresses σ_θ *near the free end of cylinder for* $r = 0,55$ *m and* $r = 0,7$ *m.*

The final stresses in the cylinder are obtained by summing the stresses obtained assuming that stress-strain state is $\sigma_z^*, \sigma_\theta^*, \sigma_r^*$, and the stresses arising due to the action of the force $-\sigma_z^*$ attached at the ends of the cylinder are $\sigma_z^u, \sigma_\theta^u$.

3. RESULTS

Figure 2 shows the curve of the deflections that occur near the end of the cylinder: 1 - deflection for hinge supporting case, 2 - for the free end.

Figures 3-6 show stresses σ_θ calculated both for homogeneous materials and in comparison with the linear calculation. In the solution for homogeneous materials, the influence of elevated temperature on the properties of concrete was taken into account, but the values of the basic elastic characteristics of concrete were adopted for average temperature over the layer.

Figure 3 shows stresses σ_θ near the free end of the cylinder in the most stressed annular concrete layers $r = 0,55$m and $r = 0,7$ m: 1 - linear homogeneous material, $r = 0,7$ m; 2 - linear heterogeneous material, $r = 0,7$ m; 3 - nonlinear heterogeneous material, $r = 0,7$ m; 4 - linear homogeneous material, $r = 0,55$m; 5 - linear heterogeneous material, $r = 0,55$m; 6 - nonlinear inhomogeneous material, $r = 0,55$m.

Figure 4 shows the stresses σ_θ near the hinged end of the cylinder in the most stressed annular concrete layers $r = 0,55$m and $r = 0,7$ m: 1 - linear homogeneous material, $r = 0,7$ m; 2 - linear heterogeneous material, $r = 0,7$ m; 3 - nonlinear heterogeneous material, $r = 0,7$ m; 4 - linear homogeneous material, $r = 0,55$m; 5 - linear heterogeneous material, $r = 0,55$m; 6 - nonlinear inhomogeneous material, $r = 0,55$m.

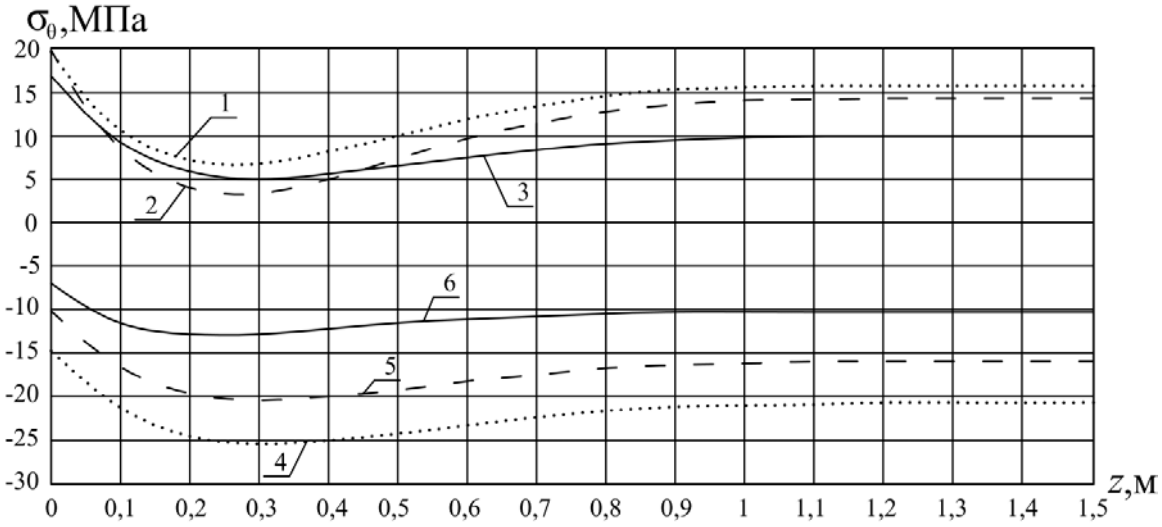


Figure 4. Stresses σ_θ *near the hinged end of cylinder for* $r = 0,55\,m$ *and* $r = 0,7\,m$.

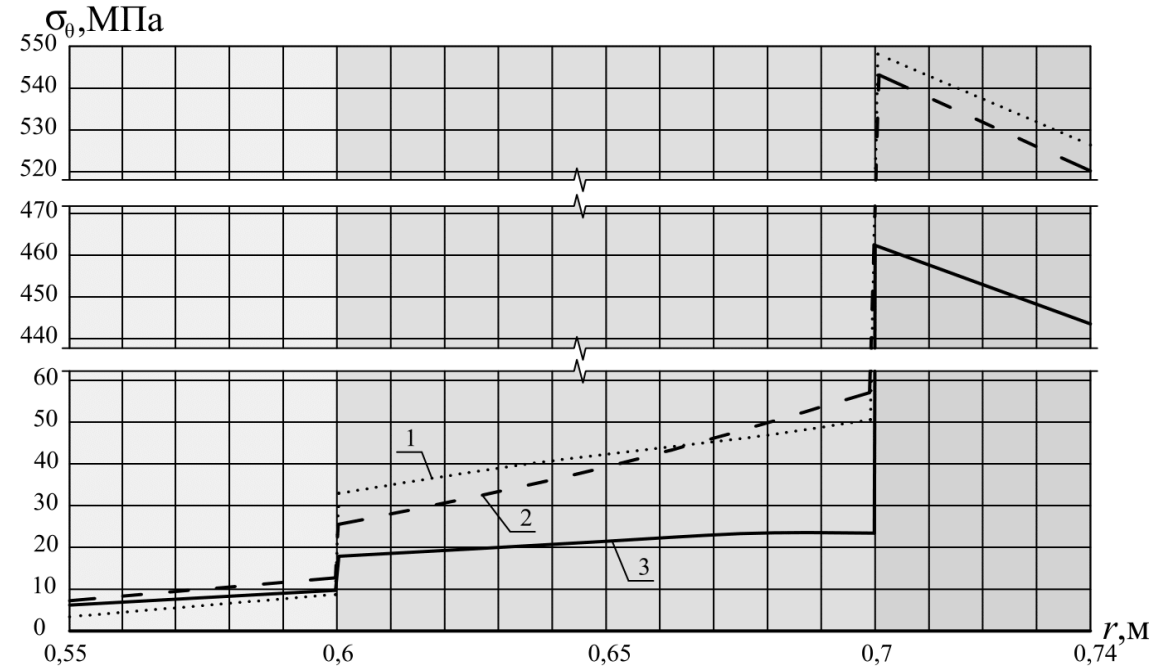


Figure 5. Stresses σ_θ *for* $z = 0\,m$.

Figures 5 and 6 show the stresses σ_θ over the entire wall thickness, at the free ends of the cylinder, at distances $z = 0\,\text{m}$ and $z = 0,55\,\text{m}$: 1 - linear homogeneous material; 2 - linear heterogeneous material; 3 - nonlinear heterogeneous material.

Figures 7 and 8 show stresses σ_θ over the entire wall thickness, with cylinder ends pivotally attached, at distances $z = 0\,m$ and $z = 0,32\,\text{m}$: 1 – linear homogeneous material; 2 - linear heterogeneous material; 3 - nonlinear heterogeneous material.

CONCLUSIONS

When analyzing the results stresses in the compressed zone of concrete are of greatest interest, since tensile stresses on the outside of the lining should be perceived by steel reinforcement.

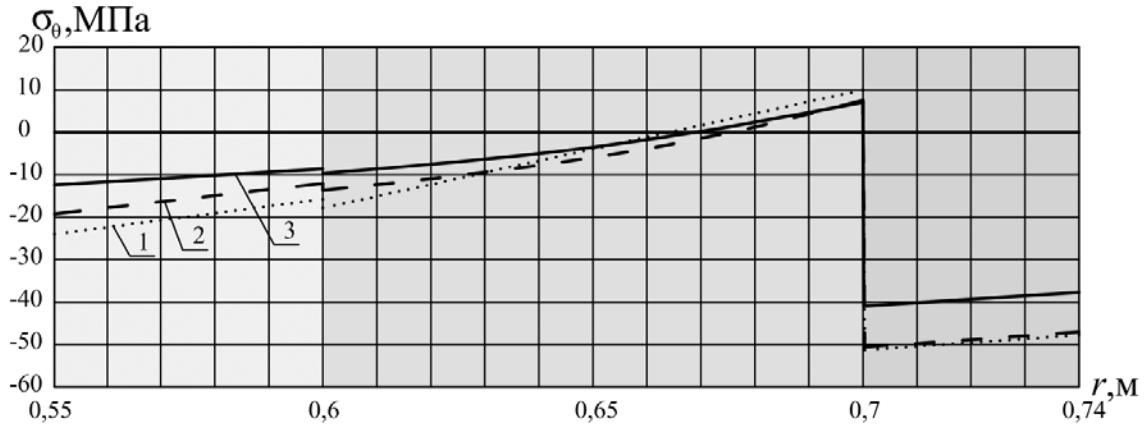


Figure 6. Stresses σ_θ *for* $z = 0,55\,m.$

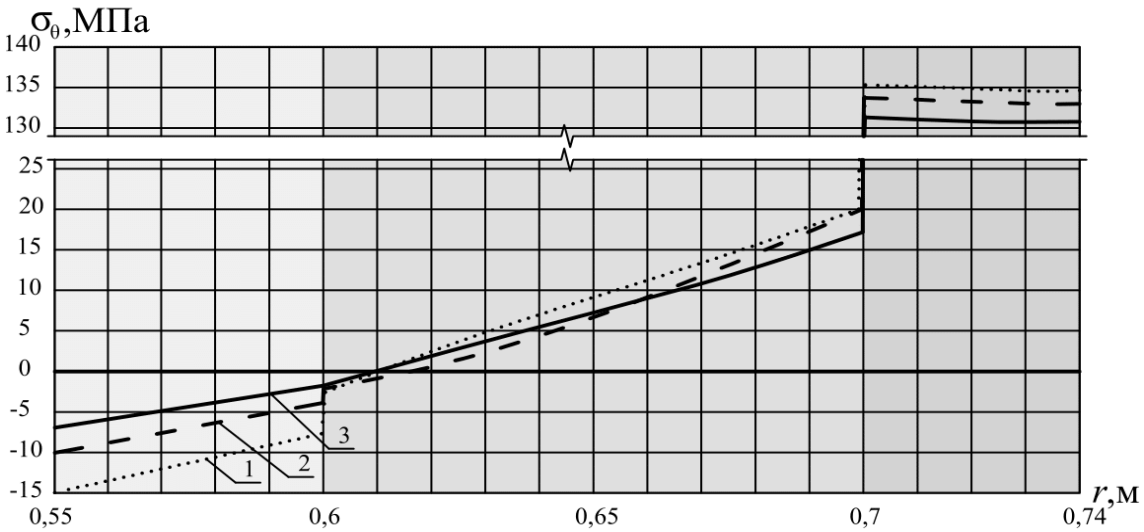


Figure 7. Stresses σ_θ *for* $z = 0\,m.$

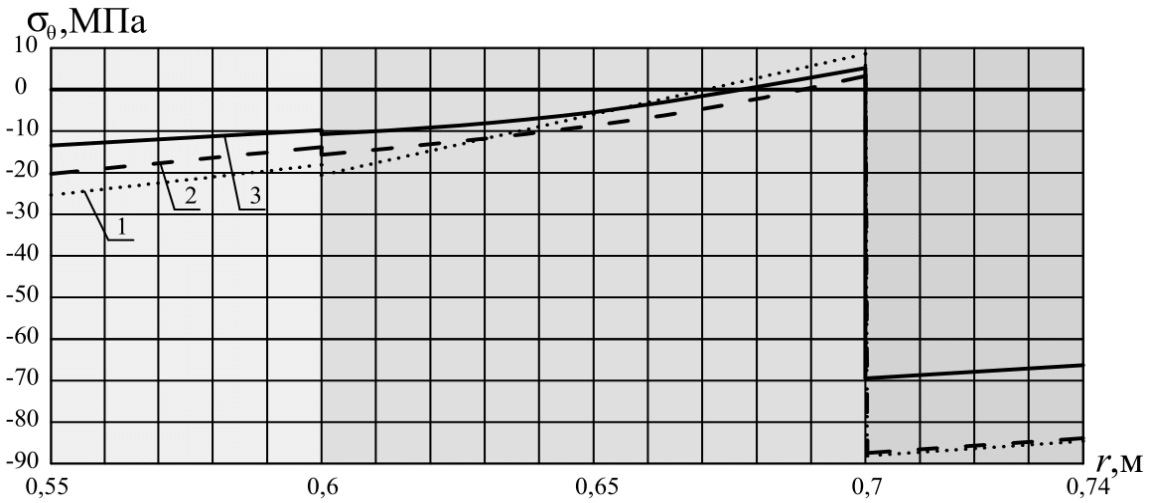


Figure 8. Stresses σ_θ *for* $z = 0,32\,m.$

Taking into account only the heterogeneity of concrete gives a reduction in circumferential stresses of about 20% in the compressed zone. When taking into account the heterogeneity and physical nonlinearity of concrete, the maximum circumferential stresses are significantly reduced in both the stretched and compressed zones, by about 2 times.

REFERENCES

1. **Andreev V.I.** Nekotoryye zadachi i metody mekhaniki neodnorodnykh tel [Some problems and methods of mechanics of heterogeneous bodies]. Moscow, Izdatel'stvo ASV, 2002, 288 pages (in Russian).
2. Building Code of Russia SP 27.13330.2011. Betonnyye i zhelezobetonnyye konstruktsii, prednaznachennyye dlya raboty v usloviyakh vozdeystviya povyshennykh i vysokikh temperature [Concrete and reinforced concrete structures designed to work in conditions of exposure to elevated and high temperatures]. Moscow, 2011, 116 pages (in Russian).
3. **Ushakov A.V.** Osnovnyye zakonomernosti deformirovaniya obychnogo i zharostoykikh betonov pri nagreve. Diss. kand. tekhnicheskikh nauk [The main laws of deformation of ordinary and heat-resistant concrete during heating. Diss. Cand. technical sciences]. Volgograd, 2006, 212 pages (in Russian).
4. **Lukash P.A.** Osnovy nelineynoy stroitel'noy mekhaniki [Fundamentals of nonlinear structural mechanics]. Moscow, Stroyizdat, 1978. 208 pages (in Russian).
5. **Polyakova L.S., Andreev V.I.** Calculation of a nonlinearly elastic three-layer cylindrical shell taking into account the continuous inhomogeneity caused by the temperature field. // *IOP Conference Series: Materials Science and Engineering*, 2018, Volume 456, 012124.
6. **Andreyev V.I., Polyakova L.S.** Fizicheski nelineynyye zadachi dlya neodnorodnykh tolstostennykh obolochek [Physically nonlinear problems for heterogeneous thick-walled shells]. // *International Journal for Computational Civil and Structural Engineering*, 2016, Volume 12, Issue 4, pp. 36-40 (in Russian).
7. **Timoshenko S.P., Goodier J.** Teoriya uprugosti [Theory of elasticity]. Moscow, Nauka, 1975, 576 pages (in Russian).

СПИСОК ЛИТЕРАТУРЫ

1. **Андреев В.И.** Некоторые задачи и методы механики неоднородных тел. – М.: Издательство АСВ, 2002. – 288 с.
2. СП 27.13330.2011. Свод правил. Бетонные и железобетонные конструкции, предназначенные для работы в условиях воздействия повышенных и высоких температур. Актуализированная редакция СНиП 2.03.04-84. – М., 2011. – 116 с.
3. **Ушаков А.В.** Основные закономерности деформирования обычного и жаростойких бетонов при нагреве. Диссертация на соискание ученой степени кандидата технических наук по специальности 05.23.05 – «Строительные материалы и изделия». – Волгоград: Волгоградский государственный архитектурно-строительный университет, 2006. – 212 с.
4. **Лукаш П.А.** Основы нелинейной строительной механики. – М.: Стройиздат, 1978 с. – 208 с.
5. **Polyakova L.S., Andreev V.I.** Calculation of a nonlinearly elastic three-layer cylindrical shell taking into account the continuous inhomogeneity caused by the temperature field. // *IOP Conference Series: Materials Science and Engineering*, 2018, Volume 456, 012124.
6. **Андреев В.И., Полякова Л.С.** Физически нелинейные задачи для неоднородных толстостенных оболочек. // *International Journal for Computational Civil and*

Structural Engineering, 2016, Volume 12, Issue 4, pp. 36-40.
7. **Тимошенко С.П., Гудьер Дж.** Теория упругости. – М.: Наука, 1975. – 576 с.

Андреев Владимир Игоревич, академик Российской академии архитектуры и строительных наук (РААСН), профессор, доктор технических наук, заведующий кафедрой сопротивления материалов, Национальный исследовательский Московский государственный строительный университет; Россия, 129337, г. Москва, Ярославское шоссе, д. 26;
E-mail: asv@mgsu.ru.

Полякова Людмила Сергеевна, магистр кафедры сопротивление материалов, Национальный исследовательский Московский государственный строительный университет; Россия, 129337, г. Москва, Ярославское шоссе, д. 26; e-mail: l.poliakova@inbox.ru.

Vladimir I. Andreev, Full Member of the Russian Academy of Architecture and Construction Sciences (RAACS), Professor, Doctor of Technical Sciences, Head of the Department of Strength of Materials, National Research Moscow State University of Civil Engineering; 26, Yaroslavskoye shosse, Moscow, 129337, Russia;
E-mail: asv@mgsu.ru.

Lyudmila S. Polyakova, Master student, Department of Strength of Materials, National Research Moscow State University of Civil Engineering; 26, Yaroslavskoye shosse, Moscow, 129337, Russia;
E-mail: l.poliakova@inbox.ru.

DOI:10.22337/2587-9618-2019-15-4-143-149

DESIGN AND CONSTRUCTION OF FOOTINGS OF BUILDINGS AND STRUCTURES ON PERMAFROST SOILS IN CONJUNCTION WITH ENVIRONMENTAL REQUIREMENTS

Igor I. Sakharov [1], Nadezda S. Nikitina [2], S. Nyamdorzh [3], E.S. Shin [4]

[1] Saint-Petersburg State Architecture and Construction University, Saint-Petersburg, RUSSIA
[2] National Research Moscow State University of Civil Engineering, Moscow, RUSSIA
[3] Mongolian University of Science and Technology, Ulaanbaatar, MONGOLIA
[4] University of Incheon, Republic of Korea, Incheon , SOUTH KOREA

Abstract: The article describes features of design and construction of footings of buildings and structures on permafrost soils. Examples of failures of objects were given. It was shown that the available calculation tools, in particular the "Termoground" program, allow to estimate many situations connected not only with temperature problems, but also with the stress-strain state of the "base – structure system". This allows carrying out design of arbitrary objects operating without failures during a long time. Consequently, the impact of such objects to ecology of surrounded environment is minimum.

Keywords: experimental studies, permafrost, freezing, thawing, bearing capacity, frost heaving

ПРОЕКТИРОВАНИЕ И СТРОИТЕЛЬСТВО ФУНДАМЕНТОВ ЗДАНИЙ И СООРУЖЕНИЙ НА ВЕЧНОМЕРЗЛЫХ ГРУНТАХ В УВЯЗКЕ С ТРЕБОВАНИЯМИ ЭКОЛОГИИ

И.И. Сахаров [1], Н.С. Никитина [2], С. Нямдорж [3], Е.С. Шин [4]

[1] Санкт-Петербургский государственный архитектурно-строительный университет, г. Санкт-Петербург, РОССИЯ
[2] Национальный исследовательский Московский государственный строительный университет, г. Москва, РОССИЯ
[3] Mongolian University of Science and Technology, Улан-Батор, МОНГОЛИЯ
[4] University of Incheon, Republic of Korea, Город, Инчеон, ЮЖНАЯ КОРЕЯ

Аннотация: В статье рассматриваются особенности проектирования и строительства фундаментов зданий и сооружений на вечномерзлых грунтах. Приведены примеры аварий объектов. Показано, что имеющиеся расчетные средства, в частности программа «Termoground», позволяют оценивать многие ситуации, связанные не только с температурными задачами, но и с напряженно-деформированным состоянием системы «основание – сооружение». Это позволяет осуществлять проектирование любых объектов, эксплуатирующихся безаварийно в течение длительного времени, что оказывает минимальную нагрузку на экологию окружающей среды.

Ключевые слова: экспериментальные исследования, вечномерзлый грунт, промерзание, оттаивание, морозное пучение, несущая способность

The construction of buildings and structures of any purpose on permafrost soils presents great difficulties. Objects in some cases are deformed, and sometimes accidents also happen. In addition, construction in northern conditions often

causes damage to the environment and, thus, negatively affects the environment.

The greatest damage to the frozen state of the base is caused by its heating. So, the heat spreading from heated buildings penetrates the frozen ground, which causes its degradation due to thawing. Oil and gas pipelines for any purpose at a temperature of the transported product from 25 to 60 ° C also cause thawing of the surrounding soil. Railways and roads transfer heat to the base, transferred by filtered water through the embankment, as well as heat caused by the action of the transport vibrodynamic load. Some noted problems are illustrated in Figures 1, 2, 3, 4.



Figure 1. Failure of parts of buildings constructed on permafrost soils when ice of permafrost soils thaw.



Figure 2. Failure of pipeline due to thawing of the foundation.



Figure 3. Bending of railway caused by thawing of the foundation.



Figure 4. Subsidence of the roadway when the foundation thaw locally.

The successful construction of buildings and structures on permafrost soils in accordance with applicable standards is ensured by the implementation of one of two principles - with conservation (principle I) and without conservation (principle II) of the frozen state of the base. For heated buildings, principle I is most often used. The most rational in this case is the installation of a ventilated underground (Figures 5, 6). This method is widely used in the North of Russia and in a number of cases gives good results. However, the underground is ineffective with a high height of snow, which has a warming effect on the base. In addition, when building on high-temperature soils, the underground device should be preceded by preliminary cooling of the base.



Figure 5. Construction of ventilated underground on metal piles.



Figure 6. Construction of ventilated underground on reinforced concrete piles.

Principle II, being significantly cheaper, is often used for linear structures such as embankments of railways and roads. For the Baikal-Amur Railway (BAR), whose length in the zone of high-temperature permafrost is about 2000 km, this principle is fundamental. However, the practice of exploitation of BAR has shown that further use of principle II is ineffective. Permafrost degradation occurs at the base of the embankments, which is accompanied by precipitation reaching 20 cm / year. Thawing processes at the base of one of the BAR mounds are shown in Figures 7-9.

Deformations of the railways lead to work on their repair and straightening. In addition to annual costs, repair work has a negative impact on the environment. At the same time, the passageways of the equipment are accompanied by damage to the natural thermal insulation - the moss carpet, which leads to complete degradation of the territory (Figure 10). Thus, attempts to use the cheaper principle II often leads to accidents of objects and degradation of frozen soils not only at the construction site, but at a considerable distance from it.

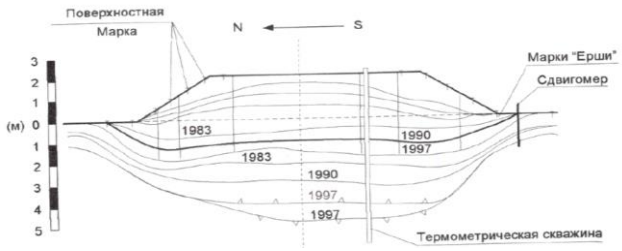


Figure 7. Dynamic of thawing process in the one of the BAR mounds. Numbers on isolines corresponds to years.

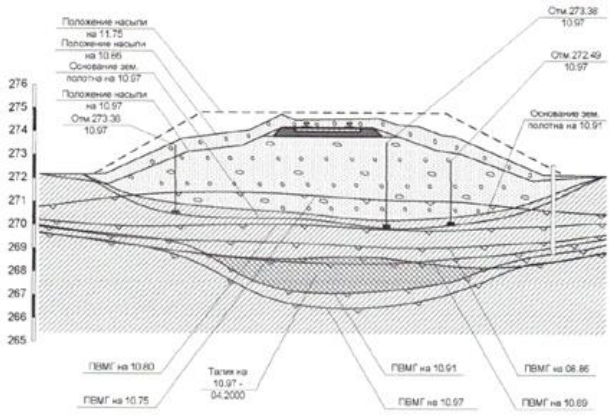


Figure 8. The dynamics of thawing of the base with the formation of talik (shaded area).

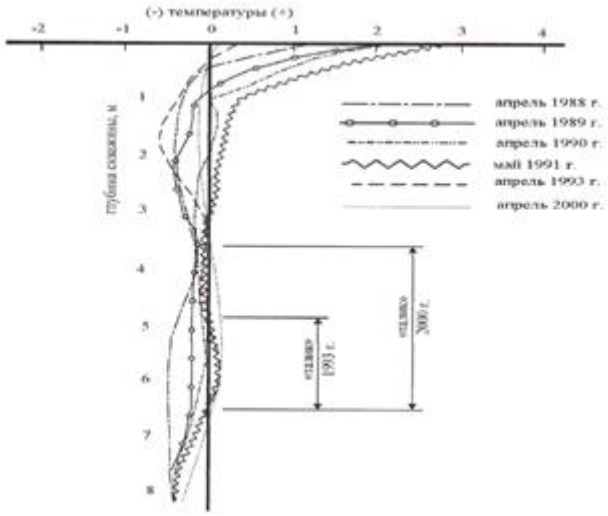


Figure 9. Graphs of temperature measured in the well. The formation of talik not freezing in the annual cycle. Numbers on isolines corresponds to years.



Figure 10. Degradation of frozen soils when moss carpet is damaged

In connection with the aforementioned facts, in order to minimize the influence of buildings and structures on the surrounding Arctic environment, it is necessary to build so that the object retains its operational properties without repairs for many years. For buildings, this is usually achieved using principle I, implemented with the help of modern cooling systems, and first of all, seasonal cooling devices (SCD) (Figure 11). Relatively more rarely are thermo supports used primarily for bridges or pipelines (Figures 12, 13).



Figure 11. The location of the capacitor parts of the SCD at the wall of the building.



Figure 12. Bridge support on stilts with natural air cooling (thermal supports).



Figure 13. Oil pipeline on stilts equipped with SCD.

If principle II is used in construction, then a gap should usually be provided between the sole of the structure and the base, while pile or post

supports should be buried in frozen ground, substantially greater than the depth of the expected thawing. For highways, in this case, overpasses will be effective, which will bring the speed to 300 km / h. In this case, the influence of objects on the environment will be minimal (Figures 14, 15).



Figure 14. The device of the railway track on the low overpass.



Figure 15. Arrangement of the railway track on a high overpass

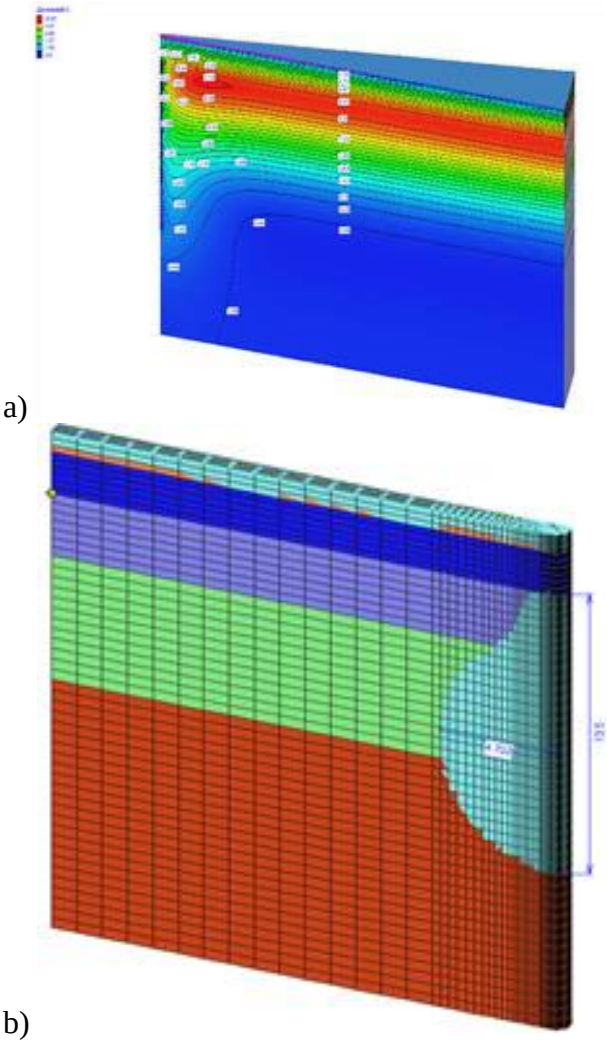
Note that the arrangement of roads on overpasses has a number of advantages. Among them, simplicity of design due to specific extremely stringent requirements for maximum precipitation (20 - 30 mm) and profile fracture angle (1 ° / °°) [1,2], which forces designers to resort to powerful, relatively deeply laid supports. The construction of overpasses allows you to abandon the large volume of inert materials delivered from quarries on temporary roads. In addition, overpasses practically do not affect the environmental situation and, with proper design and construction, guarantee the road's maintenance-free existence for many years.

The design support for the construction of footings on permafrost soils should primarily include an assessment of the temperature fields in the base. Due to the layering of the base, the frequent presence of thermal insulation, etc. effective temperature calculations can be performed only by numerical methods. There are many programs that allow you to evaluate temperature fields. However, when calculating temperatures in freezing or thawing clay soils, it is necessary to take into account that, due to the large amount of non-freezing bound water, phase transitions occur in the so-called "negative temperature spectrum", which leads to significant computational difficulties. However, the greatest difficulty is the assessment of deformations initiated by freezing and thawing processes. At the same time, if thawing strains can be relatively easily calculated using the two-term norm formula (Lapkin - Tsytovich), then defining frost heaving strains is a difficult task.

In order to establish deformations of frost heaving, the calculation method proposed in [3] may turn out to be quite effective. The method allows you to set all the components of frost heaving - deformation, as well as tangential and normal forces. Based on the "Termoground" program [4], the proposed method allows, in addition to deformations of raising and lowering, to evaluate the stability of structures against the action of tangential forces of frost heaving. In the case of thawing, the "Termoground" program quite simply allows you to set the negative friction forces acting, for example, on piles or pillars.

Below Figure 16 shows a number of examples of calculations of temperature fields around a single SCD (Figure 16) and groups of SCD at the base of a building (Figure 17).

Figure 18 shows the lifting deformations of the building frame elements under the action of frost heaving forces. Figure 19 shows the effect of negative friction on the pile foundation of a building with possible thawing of the base.



a)

b)

Figure 16. Temperature contours (a) and contours of the frozen ground zone (b) around a single SCD.



Figure 17. Temperature plots in the base, cooled by group SCD (horizontal and vertical).

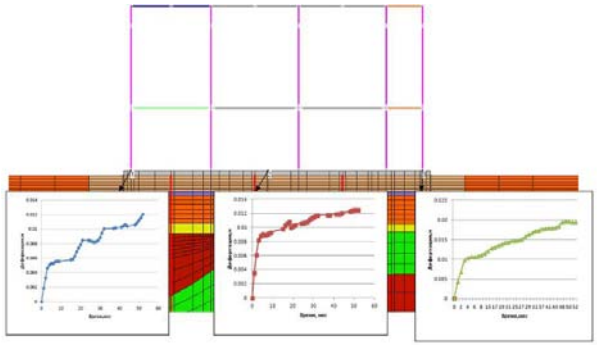


Figure 18. Lift deformations of building frame elements under the action of frost heaving forces.

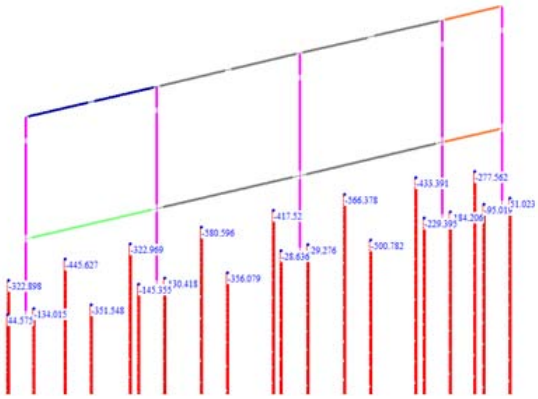


Figure 19. Increased loads on piles with negative friction caused by possible thawing.

Thus, the available settlement tools allow you to implement a fairly reliable and durable design solutions. This allows the construction of buildings and structures, trouble-free operation of which is possible for a long time. This approach minimizes the environmental impact of the construction and operation of buildings and structures, which is important in light of stricter environmental requirements, especially relevant in the northern regions.

REFERENCES

1. California High-Speed Train Project: Design Criteria: Book 3, Part C, Subpart 1. California High-Speed Rail Authority. – Sacramento: California High-Speed Rail Authority Publ., 2012, 1279 pages.

2. Code for Design of High-Speed Railway: Professional standard of the People's Republic of China: (Trial)/Ministry of Railways of the PRC. Beijing: China Railway Publishing House, 2010, 217 pages.
3. **Sakharov I.I.** Computational method for soil frost heaving characteristics determination. // Proceedings of the international conference on geotechnics fundamenals … (grac 2019), Saint Petersburg, Russia, 6-8 February 2019. Geotechnics Fundamentals and Applications in Construction: New Materials, Structures, Technologies and Calculations. Volume 2 CRC Press/Balkema 2019, pp. 307-312.
4. **Ulitskii V.M. Sakharov I.I., Paramonov V.N., Kudryavtsev S.A.** Bed – Structure System Analysis for Soil Freezing and Thawing Using the Termoground Program. // *Soil Mechanics and Foundation Engineering*, 2014, No. 52(5), pp. 240-246.

СПИСОК ЛИТЕРАТУРЫ

1. California High-Speed Train Project: Design Criteria: Book 3, Part C, Subpart 1. California High-Speed Rail Authority. – Sacramento: California High-Speed Rail Authority Publ., 2012, 1279 pages.
2. Code for Design of High-Speed Railway: Professional standard of the People's Republic of China: (Trial)/Ministry of Railways of the PRC. Beijing: China Railway Publishing House, 2010, 217 pages
3. **Sakharov I.I.** Computational method for soil frost heaving characteristics determination. // Proceedings of the international conference on geotechnics fundamenals … (grac 2019), Saint Petersburg, Russia, 6-8 February 2019. Geotechnics Fundamentals and Applications in Construction: New Materials, Structures, Technologies and Calculations. Volume 2 CRC Press/Balkema 2019, pp. 307-312.
4. **Улицкий В.М., Сахаров И.И., Парамонов В.Н., Кудрявцев С.А.** Расчет системы «основание – сооружение» при промерзании и оттаивании грунтов с помощью программы «Termoground». // *Основания, фундаменты и механика грунтов*, 2015, №5.

Сахаров Игорь Игоревич, доктор технических наук, профессор кафедры геотехники Санкт-Петербургского государственного архитектурно-строительного университета; г. Санкт-Петербург, Россия, 198005, 2-я Красноармейская ул., д. 4, тел./факс +7(812) 316-03-41;
E-mail: i.sakharov2014@yandex.ru.

Никитина Надежда Сергеевна, старший научный сотрудник кафедры «Механики грунтов и геотехники» Московский государственный строительный университет, г. Москва, Россия, 129337, Ярославское шоссе, д.26,тел./факс: +7(495) 287-49-14;
E-mail: nsnikitina@mail.ru.

Тугчин Нямдорж Сетев, Ph.D, профессор кафедры «Промышленно-гражданского строительства» Монгольского государственного университета науки и технологии. г.Уланбатор, Монголия 14191, Бага тойруу-34.Тел/факс: +(976-11) 323619;
E-mail: nyamdorj_999@yahoo.com.

Ёон Чул Шин,Ph.D, профессор кафедры «Инженеринга гражданского строительства и окружающей среды» Национального университета Инчеона. г. Инчеон 22012, Южная Корея, 119 Академия-ро, Сонгдо-дон, Иеонсу-гу. Тел: +82-32-835-8466,
E-mail: ecshin@inu.ac.kr.

Igor Igorevich Sakharov, PhD CEng. Doctor of Science and Technology, professor, Department of Geotechnial, St-Petersburg State University of Civil Engineering, 4, 2-Krasnoarmeiskaya str. Saint-Petersburg, 198005, Russia, phone/fax: +7(812) 316-03-41;
E-mail: i.sakharov2014@yandex.ru

Nadezda Sergeevna. Nikitina, PhD, Department of "Soil Mechanics and Geotechnical", Moscow State University of Civil Engineering (National Research University), 26, Yaroslavskoe Shosse, Moscow, 129337, Russia; phone/fax: +7(495) 287-49-14;
E-mail: nsnikitina@mail.ru.

Nyamdorj Setev Tugchin, Ph.D, professor Department "Civil engineering" of Mongolian State University of Science and Technology. Ulaanbaatar 14191 .Mongolia, Bagatoiruu-34, phone/fax: +(976-11)323619;
E-mail: nyamdorj_999@yahoo.com.

Eun Chul Shin Ph.D, professor Department "Civil and Environmental engineering" Incheon National University, 119 Academy-ro. Songdo-dong. Yeonsu-gu. Incheon. 22012. Respublic of Korea; phone/fax:+82-32-835-8466;
E-mail: ecshin@inu.ac.kr.

DOI:10.22337/2587-9618-2019-15-4-150-163

DETERMINATION OF STRAIN-STRESS PARAMETERS OF A MULTI-STOREY REINFORCED CONCRETE BUILDING ON AN ELASTIC FOUNDATION WITH ALLOWANCE FOR DIFFERENT RESISTANTANCE OF MATERIALS AND CRACKING

Alexander A. Treschev, Victor G. Telichko, Nikita V. Zolotov
Tula State University, Tula, RUSSIA

Abstract: In this paper, we consider the construction of a finite-element model for determining the stress-strain state of a multi-storey building made of monolithic reinforced concrete on an elastic foundation. This takes into account the dependence of the mechanical characteristics of concrete on the form of the stressed state, the development of plastic deformation in the reinforcement, cracking. Confirmed that the account of the complicated properties of the material is necessary for obtaining correct estimates of the stress-strain state of reinforced concrete structures under conditions of progressive cracking.

Keywords: finite element method, reinforced concrete, multi-storey building, multimodulus behavior, cracking, hybrid finite element, elastic foundation

ОПРЕДЕЛЕНИЕ ПАРАМЕТРОВ НАПРЯЖЕННО-ДЕФОРМИРОВАННОГО СОСТОЯНИЯ МНОГОЭТАЖНОГО ЖЕЛЕЗОБЕТОННОГО ЗДАНИЯ НА УПРУГОМ ОСНОВАНИИ С УЧЕТОМ РАЗНОСОПРОТИВЛЯЕМОСТИ И ТРЕЩИНООБРАЗОВАНИЯ

А.А. Трещев, В.Г. Теличко, Н.В. Золотов
Тульский государственный университет, г. Тула, РОССИЯ

Аннотация: В данной статье, рассмотрено построение конечно-элементной модели для определения напряженно-деформированного состояния многоэтажного здания из монолитного железобетона на упругом основании. При этом учитывалась зависимость механических характеристик бетона от вида напряженного состояния, развитие пластических деформации в арматуре, трещинообразование. Подтверждено, что учёт усложнённых свойств материала необходим для получения корректных оценок напряженно-деформированного состояния железобетонных конструкций в условиях прогрессирующего трещинообразования.

Ключевые слова: метод конечных элементов, железобетон, многоэтажное здание, разносопротивляемость, трещинообразование, гибридный конечный элемент, упругое основание

INTRODUCTION

The intensive development of technology and the science of materials in the last decade, as well as the ever increasing demands on the economy and reliability of building structures, make serious demands on the development of construction mechanics. With a detailed study of the deformation of some materials widely used in engineering practice, such as concrete, it was found that their behavior is significantly different from the usual representations. The de-

formation and strength characteristics of such materials show sensitivity to the form of the stress state realized at the point, and under operational loads the dependences between stresses and deformations are essentially nonlinear. To determine the stress-strain state of nonlinear multimodulus materials, a number of defining relations were proposed [1-6]. However, almost all of these models have significant drawbacks, limiting their application for the calculation of structures in a complex stress state [2]. Therefore, in this paper, we use a version of the equations of state of isotropic, multimodulus materials, based on the method of normalized stress spaces [1].

It is important to bear in mind the fact that in order to take into account the entire complex of effects associated with modeling the behavior of nonlinear multimodulus materials, fracture of material in the form of cracking, plastic deformations in the armature, it is necessary to improve the corresponding calculation base, since existing software packages, as well as known mathematical models do not always satisfy the requirements for carrying out calculations with the necessary accuracy [1, 2, 7-11]. Therefore, in this study, a variant of a hybrid finite element (FE) is proposed, taking into account the physically nonlinear behavior of the material and its destruction in the form of cracks [7]. The creation of new mathematical models for describing the mechanical behavior of reinforced concrete structures with the most complete account of complicated properties, as well as the improvement of the corresponding design models, is undoubtedly an actual task of the construction industry and mechanics of a deformable solid [9].

As shown in [2, 9, 10], hybrid modifications of hybrid FE with three degrees of freedom at the node are quite effective for the calculation of reinforced concrete structures [12]. The direct application of R.Kuk's finite elements to the calculation of reinforced concrete spatial structures showed that they do not take into account longitudinal forces and displacements in the middle surface, and also do not allow to determine the generalized forces vector in the center of the FE quite simply and accurately [2, 8]. Therefore, a modification of the hybrid FE with five degrees of freedom in the node and a stiffness matrix obtained directly for an arbitrary plane triangular element was developed. On the basis of the chosen defining relations, the model of a hybrid flexural triangular finite element with 5 degrees of freedom in a node, taking into account the longitudinal forces and deformations of the transverse shear, allowing simple and effective study of stress-strain state of the construction of arbitrary geometry is considered. The procedures associated with obtaining the stiffness matrix of the hybrid finite element are described in detail in [2, 12, 13].

1. FINITE ELEMENT FORMULATION

To describe the connection between deformations and displacements, the following relations are used in the framework of S.P. Timoshenko's hypotheses:

$$\begin{gathered} e_{11} = u_{1,1} + x_3\psi_{2,1};\ e_{22} = u_{2,2} - x_3\psi_{1,2}; \\ e_{33} = 0; \gamma_{12} = u_{1,2} + u_{2,1} + x_3\left(\psi_{2,2} - \psi_{1,1}\right); \\ \gamma_{13} = \psi_2 + w_1;\ \gamma_{23} = -\psi_1 + w_2, \end{gathered} \quad (1)$$

where u_k - horizontal displacements; x_3 - coordinate in thickness; ψ_k - angles of rotation of the middle surface; γ_k - deformation of transverse shear; w_k - the derivative of the deflection.

Equilibrium equations are written in the traditional form:

$$\begin{gathered} N_{11,1} + N_{12,2} = 0; N_{12,1} + N_{22,2} = 0; \\ M_{11,1} + M_{12,2} = Q_1; M_{12,1} + M_{22,2} = Q_2; \\ Q_{1,1} + Q_{2,2} = q. \end{gathered} \quad (2)$$

The relationship between strains and stresses, which follows from the potential W_1 [1] looks like following:

$$\{e\} = [A]\{\sigma\}, \qquad (3)$$

where

$$\{\sigma\} = \begin{Bmatrix} \sigma_{11} \\ \sigma_{22} \\ \tau_{12} \\ \tau_{13} \\ \tau_{23} \end{Bmatrix}; \ \{e\} = \begin{Bmatrix} e_{11} \\ e_{22} \\ \gamma_{12} \\ \gamma_{13} \\ \gamma_{23} \end{Bmatrix};$$

$$[A] = \begin{bmatrix} A_{11} & A_{12} & A_{16} & A_{14} & A_{15} \\ & A_{22} & A_{26} & A_{24} & A_{25} \\ & & A_{66} & A_{64} & A_{65} \\ & sim & & A_{44} & A_{45} \\ & & & & A_{55} \end{bmatrix}.$$

Here A_{11}, A_{12}, A_{16}, A_{14}, A_{15}, A_{22}, A_{26}, A_{24}, A_{26}, A_{66}, A_{64}, A_{65}, A_{44}; A_{45}, A_{55} are the components of a symmetric matrix $[A]$ including the functions and potential constants W_1, denoted by R_k [1].

The relationship between stresses and strains can be represented in the form [2]:

$$\{\sigma\} = [B]\{e\}, \qquad (4)$$

where $[B] = [A]^{-1}$.

Then the forces in the section of the element defined as follows [2]:

$$N_{ij} = \int_{-h/2}^{h/2} \sigma_{ij} dx_3; \ M_{ij} = \int_{-h/2}^{h/2} \sigma_{ij} x_3 dx_3; \qquad (5)$$
$$Q_i = \int_{-h/2}^{h/2} \tau_{i3} dx_3, \ (i, j = 1, 2)$$

The connection between the vector of generalized forces and the vector of generalized deformations of the middle surface takes the form:

$$\{M\} = [D]\{\varepsilon\},$$

where

$$M = \begin{Bmatrix} M_{11} \\ M_{22} \\ M_{12} \\ Q_1 \\ Q_2 \\ N_{11} \\ N_{22} \\ N_{12} \end{Bmatrix}; \{\varepsilon\} = \begin{Bmatrix} \psi_{2,1} \\ -\psi_{1,2} \\ \psi_{2,2} - \psi_{1,1} \\ \gamma_{13} \\ \gamma_{23} \\ u_{1,1} \\ u_{2,2} \\ u_{1,2} + u_{2,1} \end{Bmatrix};$$

$$[D] = \begin{bmatrix} D_{11} & D_{12} & D_{16} & K_{14} & K_{15} & K_{11} & K_{12} & K_{16} \\ & D_{22} & D_{26} & K_{24} & K_{25} & K_{12} & K_{22} & K_{26} \\ & & D_{66} & K_{64} & K_{65} & K_{16} & K_{26} & K_{66} \\ & & & C_{44} & C_{45} & C_{14} & C_{24} & C_{46} \\ & & & & C_{55} & C_{15} & C_{25} & C_{65} \\ & Sim & & & & C_{11} & C_{12} & C_{16} \\ & & & & & & C_{22} & C_{26} \\ & & & & & & & C_{66} \end{bmatrix}; \qquad (6)$$

$$C_{km} = \int_{-h/2}^{h/2} B_{km} dx_3; \ K_{km} = \int_{-h/2}^{h/2} B_{km} x_3 dx_3;$$
$$D_{km} = \int_{-h/2}^{h/2} B_{km} x_3^2 dx_3$$

are the integral stiffness parameters obtained as a result of numerical integration over the thickness of the element and depending on the stress state.

It is obvious that the mathematical model for determining the stress-strain state of reinforced slabs of which the building consists should take into account the specific features of the interaction of the complex environment "concrete-reinforcement" at various stages, be quite foreseeable and practically realizable. This model can not be completely free from additional technical hypotheses, in particular, the following is considered fair [8, 9]: 1) the loading is simple, the deformation is active, creep deformations of concrete are not considered; 2) the dimensions of the slabs of the structure in plan are large in comparison with the average distance between reinforcing bars, the reinforcement is modeled

by a smeared layer, taking into account the coefficient of layer reinforcement; 3) in view of the structural heterogeneity in thickness, the plates are broken up into a series of fictitious layers: a) non-reinforced (concrete) layers without cracks; b) reinforced (reinforced) layers without cracks; c) non-reinforced (concrete) layers with cracks; d) reinforced (reinforced) layers with cracks; e) reinforced (reinforced) layers with intersecting cracks. 4) The stresses within the reinforced layers of the element are defined as the sum of the stresses in the concrete and reinforcement, and the condition for compatibility of concrete and reinforcement assumes the equality of deformations of these two materials; 5) the middle surface of the plate is represented by a network of hybrid finite elements, taking into account the thickness partitioning into a number of fictitious layers; 6) the stiffness characteristics calculated for the center of the fictitious layer of this finite element extend to the entire layer; 7) the criterion for the strength of concrete in each fictitious layer is adopted according to P.P. Balandin's condition [8]; 8) cracks in the region of the cracked fictitious layer within the finite element are considered to be continuous and parallel to each other. The effect of stretched concrete is taken into account by the coefficient of V.I. Murashev and the characteristic of concrete damage [8, 15]; 9) in the presence of cracks, concrete within the fictitious layer is modeled by a transversely isotropic body with an isotropic plane parallel to the plane of cracks.

2. FICTITIOUS LAYERS

Non-reinforced (concrete) layers without cracks. The relationship between strains and stresses is:

$$\{e\} = [A]\{\sigma\}, \qquad (7)$$

where $[A]$ the symmetrical square matrix is 5 × 5 (neglecting voltages in the calculation σ_{33}).

$$A_{11} = \{2\left(R_1 + 2R_2\right)/3 + R_3\xi\left(3 - 2\xi^2\right)/3 + R_4 \times$$
$$\times[\xi\left(2 - \eta^2\right) + 4\left(\sigma_{11} - 2\sigma_{22}\right)/9S_0] + R_5[\eta \times$$
$$\times\cos 3\varphi\left(1 + \xi^2\right) + 2\sqrt{2}\xi - 2\cos 3\varphi - \sqrt{2}\frac{\sigma_{22}}{S_0}]\}/3;$$
$$A_{12} = \{2\left(R_1 - R_2\right)/3 + \left(R_3 + R_4/3\right)\xi + R_5[\cos 3\varphi \times$$
$$\times\left(1 - \xi\right) - \sqrt{2}\xi]\}/3;$$
$$A_{16} = \left(2R_4/3 + \sqrt{2}R_5\right)\tau_{12}/3S_0;\ A_{26} = A_{16};$$
$$A_{14} = \left(2R_4/3 + \sqrt{2}R_5\right)\tau_{13}/3S_0;$$
$$A_{15} = 2\left(R_4/3 - \sqrt{2}R_5\right)\tau_{23}/3S_0;$$
$$A_{22} = \{2\left(R_1 + 2R_2\right)/3 + R_3[\xi\left(3 - 2\xi^2\right)/3 + R_4[\xi \times$$
$$\times\left(2 - \eta^2\right) + 4\left(\sigma_{22} - 2\sigma_{11}\right)/9S_0] + R_5[\eta\cos 3\varphi \times$$
$$\times\left(1 + \xi^2\right) + 2\sqrt{2}\xi - 2\cos 3\varphi - \sqrt{2}\sigma_{11}/S_0]\}/3;$$
$$A_{24} = 2\left(R_4/3 - \sqrt{2}R_5\right)\tau_{13}/3S_0;'$$
$$A_{25} = \left(2R_4/3 + \sqrt{2}R_5\right)\tau_{23}/3S_0;$$
$$A_{66} = 2\{2R_2 - R_3\xi^3 + R_4[\xi\left(2 - \eta^2\right) - \left(\sigma_{11} + \sigma_{22}\right)/$$
$$/3S_0] + R_5[\sqrt{2}\eta\left(\sigma_{11} - \sigma_{22}\right)/2 - \eta^3\cos 3\varphi]\}/3;$$
$$A_{64} = \sqrt{2}R_5\tau_{23}/S_0;\quad A_{65} = \sqrt{2}R_5\tau_{13}/S_0;$$
$$A_{44} = 2\{2R_2 - R_3\eta^3 + R_4[\xi\left(2 - \eta^2\right) - \left(\sigma_{11} + \sigma_{22}\right)/$$
$$/3S_0] + R_5[\sqrt{2}\eta\left(\sigma_{11} - 2\sigma_{22}\right)/2 - \eta^3\cos 3\varphi]\}/3;$$
$$A_{45} = \sqrt{2}R_5\tau_{12}/S_0;$$
$$A_{55} = 2\{2R_2 - R_3\eta^3 + R_4[\xi\left(2 - \eta^2\right) - \left(\sigma_{11} + \sigma_{22}\right)/$$
$$/3S_0] + R_5[\sqrt{2}\eta\left(\sigma_{22} - 2\sigma_{11}\right)/2 - \eta^3\cos 3\varphi]\}/3.$$

Here: $\xi = \sigma/S_0$, $\eta = \tau/S_0$ - normalized normal and shear stresses on the octahedral platform; $S_0 = \sqrt{\sigma^2 + \tau^2}$ - module of the total voltage vector on the octahedral platform; $\sigma = \delta_{ij}\sigma_{ij}/3$ and $\tau = \sqrt{S_{ij}S_{ij}/3}$ - normal and tangential stresses; $Cos3\varphi = \sqrt{2}\det(S_{ij})/\tau^3$; φ - phase of stresses; $S_{ij} = \sigma_{ij} - \delta_{ij}\sigma$.

The matrix of "elasticity" $[B]$ for each of the unreinforced layers of the FE is expressed through the matrix of compliance:

$$[B]=[A]^{-1}. \quad (8)$$

Reinforced layers without cracks. Taking into account the accepted hypotheses, the stresses in the reinforced concrete layer are taken as the sum of the stresses in concrete and reinforcement, from which the matrix of "elasticity" for reinforced layers without cracks follows:

$$[B]=[A]^{-1}+[B_S], \quad (9)$$

where

$$[B_S]=\begin{bmatrix} \frac{\mu_{11}E_s}{1-\nu_s^2\mu_{11}} & \frac{\mu_{11}E_s\nu_s}{1-\nu_s^2\mu_{11}} & 0 & 0 & 0 \\ \frac{\mu_{22}E_s\nu_s}{1-\nu_s^2\mu_{22}} & \frac{\mu_{22}E_s}{1-\nu_s^2\mu_{22}} & 0 & 0 & 0 \\ 0 & 0 & B_{S3,3} & 0 & 0 \\ 0 & 0 & 0 & \frac{\mu_{22}E_s}{1+\nu_s\mu_{22}} & 0 \\ 0 & 0 & 0 & 0 & \frac{\mu_{11}E_s}{1+\nu_s\mu_{11}} \end{bmatrix};$$

$$B_{s3,3}=\frac{\mu_{11}E_s}{1+\nu_s\mu_{11}}+\frac{\mu_{22}E_s}{1+\nu_s\mu_{22}};$$

E_S - modulus of elasticity of reinforcement, ν_s - Poisson's ratio of reinforcement;

$$\mu_{11}=A_{Si}/S_{i11}h_S,\ \mu_{22}=A_{si}/S_{i22}h_S$$

- the reinforcement factors in the direction of the axes X_1 and X_2 the initial coordinate system, respectively; A_{si} - cross-sectional area of the reinforcing bar; S_{i11}, S_{i22} - the pitch of the rods parallel to the axes X_1 and X_2; h_S - total thickness of reinforced layers. Note that the matrix components $[A]^{-1}$ in the expression (9) are determined by the formulas in which instead of the total stresses σ_{ij} the stresses in the concrete σ_{Bij} should be used.

Not reinforced (concrete) layers with a crack. According to the hypothesis No. 7 cracks will be formed if the following condition is fulfilled:

$$\sigma_{11}^2+\sigma_{22}^2+3\cdot\left(\tau_{12}^2+\tau_{23}^2+\tau_{13}^2\right)-\left(\sigma_{11}\sigma_{22}\right)- -\left(R_{bt}-R_b\right)\left(\sigma_{11}+\sigma_{22}\right)-R_{bt}R_b>0, \quad (10)$$

where $\sigma_{11},\sigma_{22},\tau_{12},\tau_{13},\tau_{23}$ - stresses in concrete at the time of crack formation, calculated for the center of the fictitious layer. Here R_{bt}, R_b - the ultimate strength of concrete for axial tension and compression, respectively.

When inequality (10) is satisfied, a crack is formed in the concrete layer along the areas orthogonal to the direction of the greatest of the principal tensile stresses, calculated from the formula for a plane stress state:

$$\sigma_{1t}=[\sigma_{11}+\sigma_{22}+\sqrt{(\sigma_{11}-\sigma_{22})^2+4\tau_{12}^2}]/2.$$

The direction of the development of cracks is determined by the magnitude of the angle between the normal to the crack and the axis x_1:

$$\chi_1=arctg[(\sigma_{1t}-\sigma_{11})/\tau_{12}].$$

We note that when parallel cracks arise in the region of the layer of a given finite element, the initially isotropic concrete acquires the properties of orthotropy. In this regard, the acceptability of potential defining relationships is lost, oriented to a nonlinear dilatable, mutually resisting isotropic material. We assume that the validity of the selected potential relationships is only valid for directions along the cracks, where the integrity of the concrete is not violated. In the indicated direction, the physically nonlinear properties of concrete will be approximated by the secant modulus of elasticity E_B and the secant coefficient of transverse deformations ν_B determined from equation

$$e_{22}^{*} = A_{12}^{*}\sigma_{11}^{*} + A_{22}^{*}\sigma_{22}^{*} = \left(\sigma_{22}^{*} - \nu_B \sigma_{11}^{*}\right)/E_B,$$

i.e.

$$E_B = 1/A_{22}^{*};\ \nu_B = -A_{12}^{*}/A_{22}^{*},$$

where A_{12}^{*}, A_{22}^{*} are the components of the compliance matrix, calculated from the formulas for concrete layers without cracks; σ_{ij}^{*} - stresses in concrete, calculated in an orthogonal coordinate system $X_1^{*}OX_2^{*}$, rotated relative to the initial system X_1OX_2 by an angle χ_1.

Taking into account the foregoing, the relationship between strains and stresses in a rotated coordinate system can be represented as:\

$$\left\{e^{*}\right\} = \left[A^{*}\right]\left\{\sigma_B^{*}\right\},$$

where

$$\left\{e^{*}\right\} = \begin{Bmatrix} e_{11}^{*} \\ e_{22}^{*} \\ \gamma_{12}^{*} \\ \gamma_{13}^{*} \\ \gamma_{23}^{*} \end{Bmatrix}; \left\{\sigma_B^{*}\right\} = \begin{Bmatrix} \sigma_{B11}^{*} \\ \sigma_{B22}^{*} \\ \tau_{B12}^{*} \\ \tau_{B13}^{*} \\ \tau_{B23}^{*} \end{Bmatrix};$$

$$\left[A^{*}\right] = \begin{bmatrix} A_{11}^{*} & A_{12}^{*} & 0 & 0 & 0 \\ & A_{22}^{*} & 0 & 0 & 0 \\ & & A_{66}^{*} & 0 & 0 \\ & Sim & & A_{44}^{*} & 0 \\ & & & & A_{55}^{*} \end{bmatrix};$$

or for the case with a crack in the direction of the axis X_1^{*}:

$$\left[B^{*}\right] = \left[A^{*}\right]^{-1} = \begin{bmatrix} B_{11}^{*} & B_{12}^{*} & 0 & 0 & 0 \\ & B_{22}^{*} & 0 & 0 & 0 \\ & & B_{66}^{*} & 0 & 0 \\ & Sim & & B_{44}^{*} & 0 \\ & & & & B_{55}^{*} \end{bmatrix};$$

where

$$B_{11}^{*} = 0;\ B_{12}^{*} = 0;\ B_{22}^{*} = E_B; B_{44}^{*} = B_{66}^{*} = 0;$$
$$B_{55}^{*} = E_B/\left[2\left(1+\nu\right)\right].$$

Then, having carried out the transformation of coordinates from the system $X_1^{*}OX_2^{*}$ to the initial one, we obtain a stiffness matrix for the cracked concrete $\left[B^{c}\right]$:

$$\left[A^{c}\right]^{-1} = \left[B^{c}\right] = \begin{bmatrix} B_{11}^{c} & B_{12}^{c} & B_{16}^{c} & 0 & 0 \\ & B_{22}^{c} & B_{26}^{c} & 0 & 0 \\ & & B_{66}^{c} & 0 & 0 \\ & \text{sim} & & B_{44}^{c} & 0 \\ & & & & B_{55}^{c} \end{bmatrix}.$$

where

$$B_{11}^{c} = B_{22}^{*}Sin^4\chi_1;\ B_{22}^{c} = B_{22}^{*}Cos^4\chi_1;$$
$$B_{12}^{c} = B_{22}^{*}Sin^2\chi_1Cos^2\chi_1;$$
$$B_{16}^{c} = B_{22}^{*}Cos\chi_1Sin^3\chi_1;\ B_{26}^{c} = B_{22}^{*}Cos^3\chi_1Sin\chi_1;$$
$$B_{66}^{c} = 4B_{22}^{*}Sin^2\chi_1Cos^2\chi_1;\ B_{44}^{c} = B_{55}^{*}Sin^2\chi_1;$$
$$B_{55}^{c} = B_{55}^{*}Cos^2\chi_1.$$

Reinforced (reinforced) layers with a crack. The appearance of cracks is determined by the triggering of the Balandin condition within the fictitious FE layer:

$$\sigma_{B11}^2 + \sigma_{B22}^2 + 3\cdot\left(\tau_{12}^2 + \tau_{23}^2 + \tau_{13}^2\right) - \\ -\left(\sigma_{B11}\sigma_{B22}\right) - \left(R_{bt} - R_b\right)\left(\sigma_{B11} + \sigma_{B22}\right) - \\ -R_{bt}R_b > 0 \quad (11)$$

where σ_{Bij} - stresses in reinforced concrete.

The direction of the development of cracks is determined by the magnitude of the angle χ_1 between the normal to the crack and the axis X_1 of the original system:

$$\chi_1 = arctg\left[\frac{(\sigma_{1t} - \sigma_{B11})}{\tau_{12}}\right],$$

where σ_{1t} - the largest of the main tensile stresses in the carrier layer (concrete). Further, taking into account the arguments given above, we have:

$$\begin{aligned} e^*_{22} &= A^*_{12}\sigma^*_{B11} + A^*_{22}\sigma^*_{B22} = \\ &= \left(\sigma^*_{B22} - \nu_B\sigma^*_{B11}\right)/E_B \end{aligned} \quad (12)$$

ie,

$$E_B = 1/A^*_{22};\ \nu_B = -A^*_{12}/A^*_{22},$$

where A^*_{12}, A^*_{22} are the components of the compliance matrix, calculated from the formulas in which σ_{11} and σ_{22} it is necessary to replace by the stresses calculated in the orthogonal coordinate system $X^*_1OX^*_2$ rotated relative to the initial system X_1OX_2 by an angle χ_1; σ^*_{B11}, σ^*_{B22} - respectively, the stresses in concrete in this coordinate system.

Then the dependencies between strains and stresses in the rotated coordinate system will take the form:

$$\left\{e^*\right\} = \left[A^*\right]\left\{\sigma^*_B\right\}, \quad (13)$$

where

$$\left\{e^*\right\} = \begin{Bmatrix} e^*_{11} \\ e^*_{22} \\ \gamma^*_{12} \\ \gamma^*_{13} \\ \gamma^*_{23} \end{Bmatrix};\ \left\{\sigma^*_B\right\} = \begin{Bmatrix} \sigma^*_{B11} \\ \sigma^*_{B22} \\ \tau^*_{B12} \\ \tau^*_{B13} \\ \tau^*_{B23} \end{Bmatrix};$$

$$\left[A^*\right] = \begin{bmatrix} A^*_{11} & A^*_{12} & 0 & 0 & 0 \\ & A^*_{22} & 0 & 0 & 0 \\ & & A^*_{66} & 0 & 0 \\ & Sim & & A^*_{44} & 0 \\ & & & & A^*_{55} \end{bmatrix};$$

$$A^*_{11,} = 1/\left(E_B\omega\right);\ A^*_{12} = -\nu_B/E_B;\ A^*_{22} = 1/E_B;$$
$$A^*_{44} = A^*_{66} = 2\left(1+\nu_B\right)/\left(E_B\omega\right);$$
$$A^*_{55} = 2\left(1+\nu\right)/E_B,$$

where in the direction of the axis X^*_1 the secant modulus of elasticity (modulus of deformation of concrete) is determined by the value $E_B\omega$ (ω - the function by which the degree of concrete damage is taken into account $0 < \omega \le 1$). Then in the initial coordinate system, the compliance matrix for the cracked concrete takes the form $\left[A^C\right]$:

$$\left[A^c\right] = \begin{bmatrix} A^c_{11} & A^c_{12} & A^c_{16} & 0 & 0 \\ & A^c_{22} & A^c_{26} & 0 & 0 \\ & & A^c_{66} & 0 & 0 \\ & sim & & A^c_{44} & 0 \\ & & & & A^c_{55} \end{bmatrix}. \quad (14)$$

The matrix of "elasticity" for the reinforcement of a cracked reinforced layer in the original orthogonal coordinate system X_1OX_2 has the form:

$$\left[B^C_S\right] = \begin{bmatrix} B^C_{S1,1} & B^C_{S1,2} & 0 & 0 & 0 \\ B^C_{S2,1} & B^C_{S2,2} & 0 & 0 & 0 \\ 0 & 0 & B^C_{S3,3} & 0 & 0 \\ 0 & 0 & 0 & B^C_{S4,4} & 0 \\ 0 & 0 & 0 & 0 & B^C_{S5,5} \end{bmatrix}, \quad (15)$$

where

$$B^C_{S1,1} = \frac{\mu_{11}E_{s11}\chi_{11}}{\left(1-\nu^2_{s11}\mu_{11}\right)\lambda_{11}},\ B^C_{S1,2} = \frac{\mu_{11}E_{s11}\nu_{s11}\chi_{11}}{\left(1-\nu^2_{s11}\mu_{11}\right)\lambda_{11}},$$

$$B^C_{S2,1} = \frac{\mu_{22}E_{s22}\nu_{s22}\chi_{22}}{\left(1-\nu^2_{s22}\mu_{22}\right)\lambda_{22}},\ B^C_{S2,2} = \frac{\mu_{22}E_{s22}\chi_{22}}{\left(1-\nu^2_{s22}\mu_{22}\right)\lambda_{22}}$$

$$B^C_{S\,3,3} = \frac{E_{s11}\chi^k_{11}}{\left(1+\nu_{s11}\mu_{11}\right)\lambda_{11}\mathrm{ctg}^2\chi_1} + \frac{E_{s22}\chi^k_{22}}{\left(1+\nu_{s22}\mu_{22}\right)\lambda_{22}\mathrm{tg}^2\chi_1};$$

$$B^C_{S\,4,4} = \frac{E_{s11}\chi^k_{11}}{\left(1+\nu_{s11}\mu_{11}\right)\lambda_{11}\mathrm{ctg}^2\chi_1};$$
$$B^C_{S\,5,5} = \frac{E_{s22}\chi^k_{22}}{\left(1+\nu_{s22}\mu_{22}\right)\lambda_{22}\mathrm{tg}^2\chi_1},$$

where E_{skk} - the secant modulus of deformation of the reinforcement located along the axes X_1 and X_2, ν_{skk} - the secant coefficient of transverse deformation of the reinforcement (k = 1,2).

$$\chi^k_{11} = 1+\frac{\mu_{11}\left(1-\lambda_{11}\psi_s\right)E_{s11}\cos^2\chi_1}{E_B},$$
$$\chi^k_{22} = 1+\frac{\mu_{22}\left(1-\lambda_{22}\psi_s\right)E_{s22}\sin^2\chi_1}{E_B},$$
$$\lambda_{11} = \frac{\eta_\tau\mu_{11}}{\eta_\tau\mu_{11}+\mu_{22}\mathrm{ctg}^2\chi_1},\ \lambda_{22} = \frac{\eta_\tau\mu_{22}}{\eta_\tau\mu_{22}+\mu_{11}\mathrm{tg}^2\chi_1},$$

η_τ – coefficient taking into account the increased flexibility of reinforcing bars to tangential movements in concrete near a crack $\eta_\tau \approx 16$ [19].

In order to take into account the development of plastic deformations in the reinforcement, we will calculate their values by the formulas:

$$E_{S\,kk} = \begin{cases} E_S & npu\ \ \sigma_{Skk} < \sigma_p\mu_{kk} \\ \sigma_p / e_{kk} & npu\ \ \sigma_{Skk} \ge \sigma_p\mu_{kk} \end{cases}, k = 1,2,$$

where σ_p is the yield stress of the reinforcing material.

The matrix of "elasticity" of the reinforced layer represented in the form

$$\left[B\right] = \left[B^C_B\right] + \left[B^C_S\right], \qquad (16)$$

where

$$\left[B^C_B\right] = \left[A^C\right]^{-1}.$$

To specify the model of a cracked reinforced layer, a damage function ω is defined, defined with the help of the parameter of V. I. Murashev ψ_S, which takes into account the work of stretched concrete in the areas between the cracks:

$$\psi_S = E_{sn} / \left(E_B\omega + E_{sn}\right), \qquad (17)$$

where E_{sn} is the elastic modulus of the reinforcement in the direction along the normal to the crack,

$$E_{sn} = E_{S11}\mu_{11}\cos^4\chi_1 + E_{S22}\mu_{22}\sin^4\chi_1. \qquad (18)$$

Solving jointly equations (17) and (18) with respect to the damage function, we obtain an expression of the form:

$$\omega = \left(E_{S11}\mu_{11}\cos^4\chi_1 + E_{S22}\mu_{22}\sin^4\chi_1\right)\times \\ \times\left(1/\psi_s - 1\right)/E_B. \qquad (19)$$

The parameter ψ_S is calculated using the empirical formula recommended in the works of G.A. Geniev, V.N. Kissyuk. and Tyupin G.A. [15]:

$$\psi_S = 1 - 0,7R_{bt} / \sigma^*_{11}, \qquad (20)$$

where it is assumed that

$$\sigma^*_{B11} = 0,7R_{bt},$$

$\sigma^*_{11}, \sigma^*_{B11}$ - the normal stresses in reinforced concrete and concrete on sites coinciding with the crack.

Expression for σ^*_{B11} taking into account the rules of transformation of coordinates for stresses σ_{Bij} we obtain a nonlinear equation with respect to ω:

$$\left(B^C_{B11}e_{11} + B^C_{B12}e_{22} + B^C_{B16}\gamma_{12}\right)\cos^2\chi_1 + \\ +\left(B^C_{B12}e_{12} + B^C_{B22}e_{22} + B^C_{26}\gamma_{12}\right)\sin^2\chi_1 + \\ +\left(B^C_{B16}e_{11} + B^C_{B26}e_{26} + B^C_{B66}\gamma_{12}\right)\sin 2\chi_1 = 0,7R_{bt}. \qquad (21)$$

The solution of this equation constructed in the framework of the method of successive approximations. Thus, the matrix $\left[A^C\right]$ and components of the "elasticity" matrix $\left[B\right]$ are determined from the calculated damage function and the parameter of V.I. Murashev.

Reinforced layers with intersecting cracks. Taking into account the accepted model of the reinforced layer with cracks and the hypotheses introduced earlier, the matrix of "elasticity" within the fictitious layer is obtained in the form:

$$\left[B\right]=\left[B_S^C\right], \qquad (22)$$

where the matrix $\left[B_S^C\right]$ is determined according to condition (15).

3. MODEL TESTING

To demonstrate the features developed by the authors of the model, the problem solved on determining the stress-strain state of a building on an elastic foundation. The building contains 12 floors with the same layout (Figure 1), the exterior of the building in the form of a 3D model is shown in Figure 2.

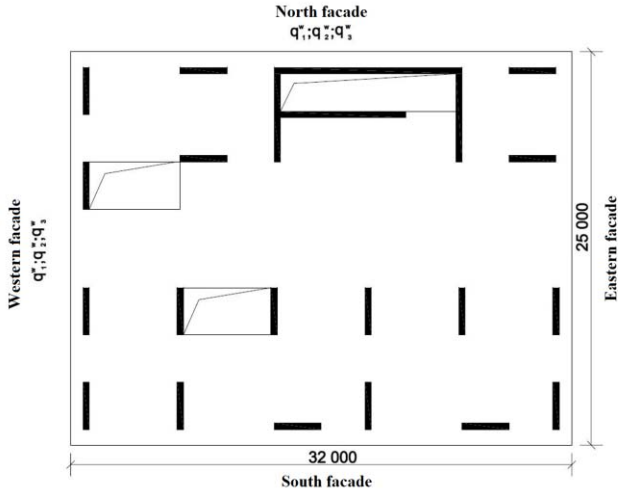


Figure 1. Plane plan of the building scheme.

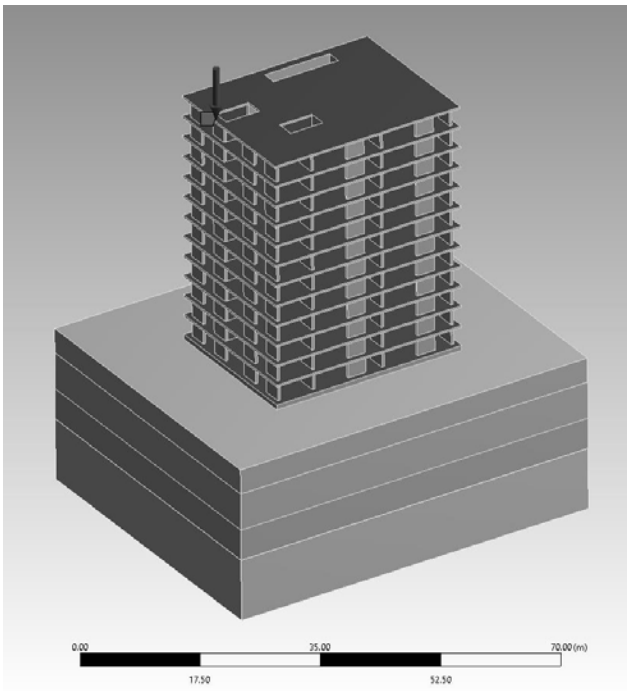


Figure 2. General view of the building (model in ANSYS Workbench 2019 R1).

The following assumptions were made: 1) the design model of the building consists only of horizontal and vertical load-bearing elements of a monolithic reinforced concrete skeleton, respectively - interfloor ceilings and pylons; 2) the thickness of all the inter-floor ceilings is the same and equal to 300 mm (the thickness of the foundation slab is 800 mm); 3) the thickness of all pylons assumed to be the same and equal to 400 mm; 4) all the interface nodes of the elements of the supporting skeleton between themselves are taken rigid; 5) the deformation of the horizontal and vertical elements of the supporting skeleton takes into account the destruction processes, 6) the elastic base is modeled in accordance with [16-18], based on the defining relations for anisotropic differently resisting materials [3]. As the main material of the building was used concrete with a compressive strength $R^- = 28,4$ MPa [1, 2]. Foundation slab reinforcement adopted by A400 rods with a diameter of 16 mm in the form of a grid symmetrically disposed in the cross-section of the plate (protective layer 50 mm, yield strength

Table 1. Characteristics of soil layers.

Layer number	Mechanical characteristics (all deformation and shear moduli are given in MPa, Poisson's ratios in fractions of a unit)								
1	E_1^+	E_1^-	E_2^+	E_2^-	E_3^+	E_3^-	G_{12}	G_{13}	G_{23}
	31,05	27,95	29,74	24,16	26,35	19,12	10,72	9,39	10,1
	ν_{12}^+	ν_{12}^-	ν_{13}^+	ν_{13}^-	ν_{23}^+	ν_{23}^-	–	–	–
	0,38	0,32	0,37	0,32	0,37	0,32	–	–	–
2	E_1^+	E_1^-	E_2^+	E_2^-	E_3^+	E_3^-	G_{12}	G_{13}	G_{23}
	40,55	32,42	42,01	29,42	25,35	20,24	14,33	10,6	11,14
	ν_{12}^+	ν_{12}^-	ν_{13}^+	ν_{13}^-	ν_{23}^+	ν_{23}^-	–	–	–
	0,33	0,25	0,33	0,25	0,33	0,25	–	–	–
3	E_1^+	E_1^-	E_2^+	E_2^-	E_3^+	E_3^-	G_{12}	G_{13}	G_{23}
	80,00	64,15	70,9	55,3	60,0	35,0	27,36	23,81	25,64
	ν_{12}^+	ν_{12}^-	ν_{13}^+	ν_{13}^-	ν_{23}^+	ν_{23}^-	–	–	–
	0,27	0,2	0,27	0,2	0,22	0,17	–	–	–
4	E_1^+	E_1^-	E_2^+	E_2^-	E_3^+	E_3^-	G_{12}	G_{13}	G_{23}
	10,05	7,5	12,25	9,12	10,35	8,28	3,83	3,92	3,55
	ν_{12}^+	ν_{12}^-	ν_{13}^+	ν_{13}^-	ν_{23}^+	ν_{23}^-	–	–	–
	0,27	0,23	0,27	0,23	0,25	0,25	–	–	–

$\sigma_p = 400$ MPa), reinforcement of the slabs is adopted by A400 rods with a diameter of 14 mm in the form of a grid symmetrically disposed in the cross-section of the plate (protective layer 35 mm, yield strength $\sigma_p = 400$ MPa), pylon reinforcement adopted by A400 rods with a diameter of 12 mm in the form of two nets symmetrically located in the cross-section of the pylon (protective layer 30 mm, yield strength $\sigma_p = 400$ MPa). The characteristics of the soil base layers given in Table 1.

In our study, we took into account the vertical, evenly distributed load on the slabs (on all floor slabs and the foundation slab), as well as the horizontal wind load. Loads are given in Table 2.

Figures 5-6 show the results of calculating the vertical deflections (m) in the floors of the building, at characteristic points - the floors of the 12th and 6th floors (maximum deflections are shown). Deflections are presented in comparison with a similar calculation performed in ANSYS Workbench \ ANSYS APDL.

Table 2. Loads.

Load	Load step		Maximum load	
Units:	kPa	kN/m	kPa	kN/m
Cover - q_{rf}	1,5	-	30	-
Floor slab – q_{fl}	1,5	-	30	-
Wind - q_{w1}	0,5	0,152	10	3,04
Wind 2 - q_{w2}	0,7	0,212	14	4,24
Wind 3 - q_{w3}	0,45	0,136	8	2,42

Three calculation options presented: 1) the model proposed by the authors of the work based on Treschev A.A. theory for concrete model; 2) calculation in ANSYS 2019 taking into account the nonlinear strain-stress diagram for concrete $R^- = 28,4$ MPa [8]; 3) calculation in ANSYS 2019 taking into account the linear strain-stress diagram for $R^- = 28,4$ MPa concrete.

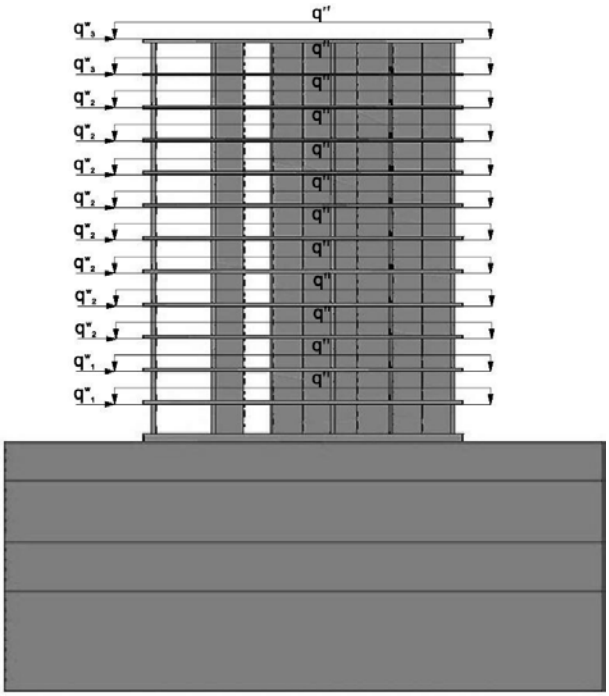


Figure 3. South façade.

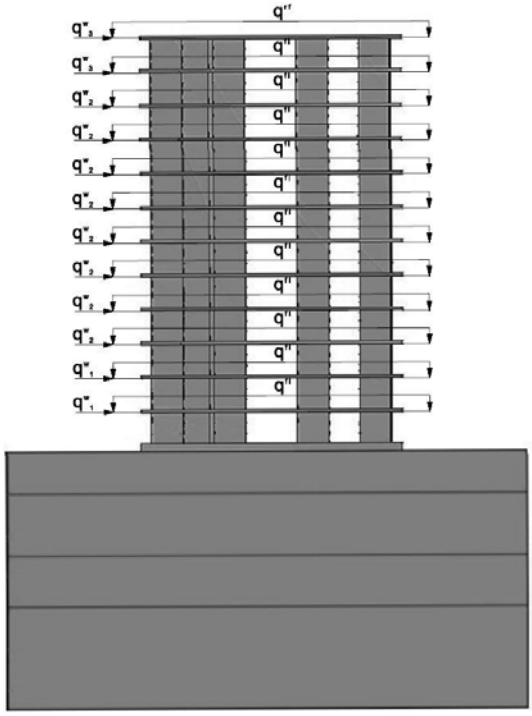


Figure 4. Western acade.

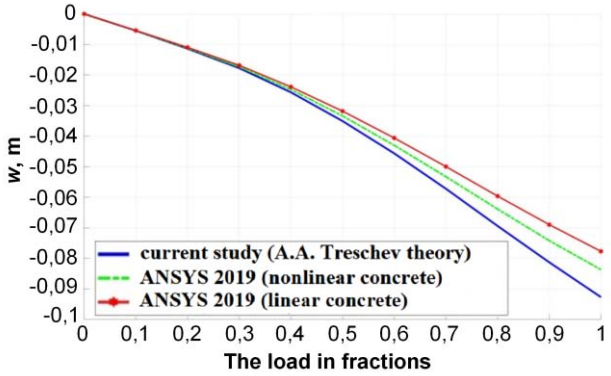


Figure 5. Maximum vertical movement at a point (12th floor).

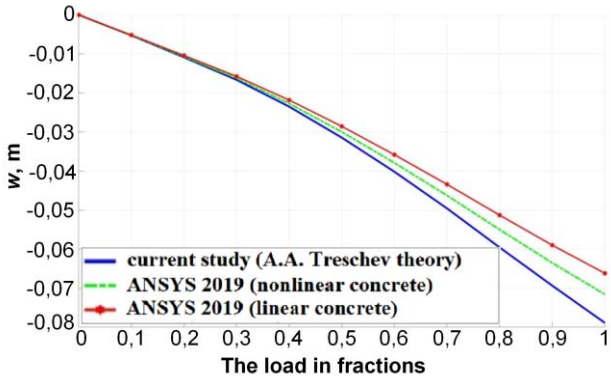


Figure 6. Maximum vertical movement at a point (6th floor).

4. CONCLUSION

Based on the results obtained, the following conclusions can be drawn:

1. The model of different resistance, adopted in accordance with the work of [2, 3, 8], showed good results in terms of determining displacements, the results differ from those obtained as a result of nonlinear calculation in the ANSYS program, at the extremum point by 24 %.
2. A numerical experiment to solve the problem of determining the stress-strain state of a building allows us objectively state that this model has several advantages over existing ones implemented in popular CAD systems. The model allows one to take into account the material's different resistance, cracking, plastic deformations in the reinforcement, the final element constructed is obtained in the form convenient for its software implementation, which was demonstrated in this work, it is also possible to take into account the work

of the elastic state for calculating combined structures.

Failure to take into account the phenomenon of different resistance, as well as the effects associated with crack formation in reinforced concrete structures, leads to significant errors in the calculation of the main characteristics of the stress-strain state of structures. To obtain reliable results of engineering calculations and to prevent the occurrence of emergency conditions of structural elements and structures, it is necessary to take into account the influence of the complicated properties of materials in full.

REFERENCES

1. **Green A.E., Mkrtichian J.Z.** Elastic Solids with Different Moduli in Tension and Compression. // *Journal of Elasticity*, 1977, Volume 7, No. 4, pp. 369-368.
2. **Telichko V.G., Treschev A.A.** Gibridnyj konechnyj jelement dlja rascheta plit i obolochek s uslozhnennymi svojstvami [Hybrid finite element for calculation of slabs and shells with complicated properties]. // *News of universities. Building*, 2003, No. 5, pp. 17-23 (in Russian).
3. **Treschev A.A.** Teorija deformirovanija i prochnosti materialov s iznachal'noj i navedennoj chuvstvitel'nost'ju k vidu naprjazhennogo sostojanija. Opredeljajushhie sootnoshenija [The theory of deformation and strength of materials with initial and induced sensitivity to the form of a stressed state. Defining relations]. Moscow, Tula, RAACS, TulGU, 2016, 326 pages (in Russian).
4. **Ambartsumyan S.A.** Raznomodul'naja teorija uprugosti [Multimodular theory of elasticity]. Moscow, Nauka, 1982, 320 pages (in Russian).
5. **Jones R.M.** Stress-Strain Relations for Materials with Different Moduli in Tension and Compression. // *AIAA Journal*, 1977, Volume 15, No. 1, pp. 16-25.
6. **Reddy J.N., Bert C.W., Hsu Y.S.** Thermal bending of thick rectangular plates of bimodulus composite materials. // *Journal of Mechanical Engineering Science*, 1980, Volume 22, No. 6, pp. 297-304.
7. **Karpenko N.I.** Teorija deformirovanija zhelezobetona s treshhinami [Theory of deformation of reinforced concrete with cracks]. Moscow, Stroyizdat, 1976, 208 pages (in Russian).
8. **Artemov A.N., Treschev A.A.** Poperechnyj izgib zhelezobetonnyh plit s uchetom treshhin [Transverse bending of reinforced concrete slabs taking into account cracks]. // *News of universities. Building*, 1994, No. 9-10, pp. 7-12 (in Russian).
9. **Jendele L, Cervenka J.** On the solution of multi-point constraints – application to FE analysis of reinforced concrete structures. // *Computers & Structures*, 2009, Volume 87, pp. 970-980.
10. **Bathe K.J., Walczak J., Welch A., Mistry N.** Nonlinear analysis of concrete structures. // *Computers & Structures*, 1989, Volume 32, pp. 563-590.
11. **Bathe K.J.** Finite Element Procedures. New Jersey, Prentice Hall, 1996, 1037 pages.
12. **Cook R.D.** Two hybrid elements for analysis of thick thin and sandwich plates. // *International Journal for Numerical Methods in Engineering*, 1972, Volume 5, pp. 277-288.
13. **Tong P.A., Pian T.H.H.** Variation principle and the convergence of a finite-element method based on assumed stress distribution. // *International Journal of Solids and Structures*, 1969, pp. 463-472.
14. **Zienkiewicz O.C., Taylor R.L., Zhu J.Z.** The Finite Element Method: Its Basis and Fundamentals. 7th Edition. Butterworth-Heinemann, 2013, 756 pages.
15. **Geniev G.A., Kissyuk V.N., Tyupin G.A.** Teorija plastichnosti betona i zhelezobetona [Theory of plasticity of concrete and rein-

forced concrete]. Moscow, Stroiizdat, 1974, 316 pages (in Russian).
16. **Lade P.V.** Overview and evalution of constitutive models. // Soil Constitutive Models: Evaluation, Selection, and Calibration. Ed. J.A. Yamamuro, V.N. Kaliakin, American Society of Civil Engineers, 2005, Volume 128, pp. 1-34.
17. **Brinkgreve R.B.J.** Selection of soil models and parameters for geotechnical engineering application. // Soil Constitutive Models: Evaluation, Selection, and Calibration. Ed. J.A. Yamamuro, V.N. Kaliakin, American Society of Civil Engineers, 2005, Volume 128, pp. 69-98.
18. **Treschev A.A., Telichko V.G., Khodorovich P.Yu.** K zadache o davlenie na gruntovoe osnovanie [To the problem of pressure on a soil foundation]. // Bulletin of the Department of Construction Sciences RAACS, 2014, Issue 18, pp. 95-99 (in Russian).
19. **Zaitsev Yu.V.** Mehanika razrushenija dlja stroitelej [The mechanics of destruction for builders]. Moscow, Vysshaya Shkola, 1991, 288 pages (in Russian).
20. **Karpenko N.I., Karpenko S.N., Petrov A.N., Palyuvina S.N.** Model' deformirovanija zhelezobetona v prirashhenijah i raschet balok-stenok i izgibaemyh plit s treshhinami [Reinforced concrete deformation model in increments and calculation of wall beams and bending plates with cracks]. Petrozavodsk, Publishing House of PetrSU, 2013, 156 pages (in Russian).

СПИСОК ЛИТЕРАТУРЫ

1. **Green A.E., Mkrtichian J.Z.** Elastic Solids with Different Moduli in Tension and Compression. // *Journal of Elasticity*, 1977, Volume 7, No. 4, pp. 369-368.
2. **Теличко В.Г., Трещев А.А.** Гибридный конечный элемент для расчета плит и оболочек с усложненными свойствами. // Известия вузов. Строительство, 2003, №5, с. 17-23.
3. **Трещев А.А.** Теория деформирования и прочности материалов с изначальной и наведенной чувствительностью к виду напряженного состояния. Определяющие соотношения. – М.: Тула: РААСН, ТулГУ, 2016. − 326 с.
4. **Амбарцумян С.А.** Разномодульная теория упругости. – М.: Наука, 1982. – 320с.
5. **Jones R.M.** Stress-Strain Relations for Materials with Different Moduli in Tension and Compression. // *AIAA Journal*, 1977, Volume 15, No. 1, pp. 16-25.
6. **Reddy J.N., Bert C.W., Hsu Y.S.** Thermal bending of thick rectangular plates of bimodulus composite materials. // *Journal of Mechanical Engineering Science*, 1980, Volume 22, No. 6, pp. 297-304.
7. **Карпенко Н.И.** Теория деформирования железобетона с трещинами. – М.: Стройиздат, 1976. – 208 с.
8. **Артемов А.Н., Трещев А.А.** Поперечный изгиб железобетонных плит с учетом трещин. // *Известия вузов. Строительство*, 1994, №9-10, с. 7-12.
9. **Jendele L, Cervenka J.** On the solution of multi-point constraints – application to FE analysis of reinforced concrete structures. // *Computers & Structures*, 2009, Volume 87, pp. 970-980.
10. **Bathe K.J., Walczak J., Welch A., Mistry N.** Nonlinear analysis of concrete structures. // *Computers & Structures*, 1989, Volume 32, pp. 563-590.
11. **Bathe K.J.** Finite Element Procedures. New Jersey, Prentice Hall, 1996, 1037 pages.
12. **Cook R.D.** Two hybrid elements for analysis of thick thin and sandwich plates. // *International Journal for Numerical Methods in Engineering*, 1972, Volume 5, pp. 277-288.
13. **Tong P.A., Pian T.H.H.** Variation principle and the convergence of a finite-element method based on assumed stress distribu-

tion. // *International Journal of Solids and Structures*, 1969, pp. 463-472.
14. **Zienkiewicz O.C., Taylor R.L., Zhu J.Z.** The Finite Element Method: Its Basis and Fundamentals. 7th Edition. Butterworth-Heinemann, 2013, 756 pages.
15. **Гениев Г.А., Киссюк В.Н., Тюпин Г.А.** Теория пластичности бетона и железобетона. – М.: Стройиздат, 1974. – 316 с.
16. **Lade P.V.** Overview and evalution of constitutive models. // Soil Constitutive Models: Evaluation, Selection, and Calibration. Ed. J.A. Yamamuro, V.N. Kaliakin, American Society of Civil Engineers, 2005, Volume 128, pp. 1-34.
17. **Brinkgreve R.B.J.** Selection of soil models and parameters for geotechnical engineering application. // Soil Constitutive Models: Evaluation, Selection, and Calibration. Ed. J.A. Yamamuro, V.N. Kaliakin, American Society of Civil Engineers, 2005, Volume 128, pp. 69-98.
18. **Трещев А.А., Теличко В.Г., Ходорович П.Ю.** К задаче о давление на грунтовое основание. // Вестник отделения строительных наук РААСН, 2014, Выпуск 18, с. 95-99.
19. **Зайцев Ю.В.** Механика разрушения для строителей. – М.: Высшая школа, 1991. – 288 с.
20. **Карпенко Н.И., Карпенко С.Н., Петров А.Н., Палювина С.Н.** Модель деформирования железобетона в приращениях и расчет балок-стенок и изгибаемых плит с трещинами. – Петрозаводск: Изд-во ПетрГУ, 2013. – 156 с.

Alexander A. Treschev, corresponding member of the Russian Academy of Architecture and Construction Sciences (RAACS), Doctor of Technical Sciences, Professor, Head of Department of Construction, building materials and structures, Tula State University; 92, Lenin Ave., Tula, 300012, Russia; phone +7(4872)257108;
E-mail: taa58@yandex.ru.

Victor G. Telichko, Candidate of Technical Sciences, Associate Professor, Department of Construction, building materials and structures, Tula State University; 92, Lenin Ave., Tula, 300012, Russia; phone +7(4872)257108;
E-mail: katranv@yandex.ru.

Nikita V. Zolotov, graduate student, Department of Construction, building materials and structures, Tula State University; 92, Lenin Ave., Tula, 300012, Russia;
phone +7(4872)257108;
E-mail: nikita.v.zolotov@gmail.com.

Трещев Александр Анатольевич, член-корреспондент Российской академии архитектуры и строительных наук (РААСН), доктор технических наук, профессор, заведующий кафедрой «Строительства, строительных материалов и конструкций», Тульский государственный университет; 300012, Россия, г. Тула, проспект Ленина, д. 92; тел. +7(4872)257108;
E-mail: taa58@yandex.ru.

Теличко Виктор Григорьевич, кандидат технических наук, доцент, кафедра «Строительства, строительных материалов и конструкций», Тульский государственный университет; 300012, Россия, г. Тула, проспект Ленина, д. 92; тел. +7(4872)257108;
E-mail: katranv@yandex.ru.

Золотов Никита Владимирович, аспирант, кафедра «Строительства, строительных материалов и конструкций», Тульский государственный университет; 300012, Россия, г. Тула, проспект Ленина, д. 92; тел. +7(4872)257108; E-mail: nikita.v.zolotov@gmail.com.

DOI:10.22337/2587-9618-2019-15-4-164-169

STRESS-STRAIN RELATION FOR CONCRETE IN NONUNIFORM TENSION

Michael L. Zak
Ariel University, Ariel, ISRAEL

Abstract: Discrepancy between reported in the literature tensile stress-strain relations for concrete is addressed. A conclusion is reached that in the post-peak (softening) range of deformation the stress-strain relation is not unique and depends on the gradient of stress. A simplified variant of such a relation, intended for analysis of concrete beams with regard to the effect of size (the depth of section), is proposed.

Keywords: concrete, stress-strain relation, tension, size effect

СООТНОШЕНИЕ «НАПРЯЖЕНИЯ-ДЕФОРМАЦИИ» ДЛЯ БЕТОНА ПРИ НЕОДНОРОДНОМ РАСТЯЖЕНИИ

М.Л. Зак
Университет Ариэль, г. Ариэль, ИЗРАИЛЬ

Аннотация: Рассмотрено несоответствие между приводимыми в литературе соотношениями «напряжения-деформации» для бетона. Делается вывод, что в постпиковом (смягчающем) диапазоне деформирования соотношение «напряжения-деформации» не является единственным и зависит от градиента напряжения. Предложен упрощенный вариант такого соотношения, предназначенный для анализа бетонных балок с учетом размерного эффекта (глубины сечения).

Ключевые слова: бетон, соотношение «напряжения-деформации», растяжение, размерный эффект

INTRODUCTION

The tensile stress (σ)-strain (ε) relation is one of principal characteristics of concrete behavior. Unfortunately, there is a considerable uncertainty with regard to the choice of its appropriate variant for nonlinear analysis of concrete and reinforced concrete structures. In particular, (a) reported in the literature (e.g. [1-5]) relations differ essentially from each other (see Figure 1), and (b) in deformation-controlled direct tension tests on standard concrete specimens the deformation localizes when the ultimate load is attained and, therefore, the descending branches of diagrams, like those in Figure 1, are unrealizable (see [6, 7]).

The aim of this paper is to consider this issue and formulate a new σ-ε relation for concrete in tension. The paper is organized as follows. Firstly, a ratio $m=f_{t,fl,15}/f_t$ is shown to be a

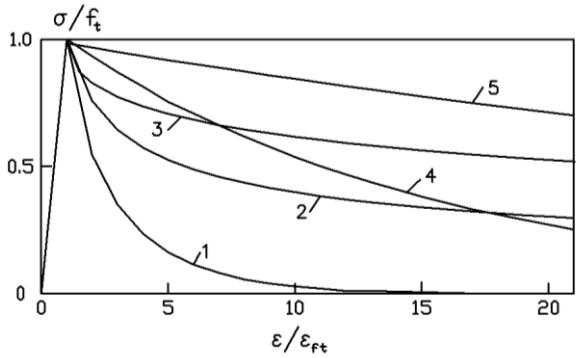


Figure 1. Tensile σ-ε diagrams for concrete: 1 – [1], 2 – [2], 3 – [3], 4 – [4], 5 – [5].

suitable calibration parameter. Here, f_t=the strength of concrete in direct tension, $f_{t,fl,15}$=the flexural tensile strength of concrete determined

in tests on standard 15×15×60 cm concrete beams with the third-point loading. Then, a calibrated relation is presented and an example given illustrating the accuracy of results obtainable with the use of this relation in analysis of relatively small elements. Finally, an extended version of the same relation, intended for analysis of bending elements of any depth, is proposed and its applicability range discussed.

The compressive σ-ε relation [8]

$$\frac{\sigma}{f_c} = \frac{k(\varepsilon/\varepsilon_{fc}) - (\varepsilon/\varepsilon_{fc})^2}{1 + (k-2)(\varepsilon/\varepsilon_{fc})}, \qquad (1)$$

where f_c is the concrete compressive strength, ε_{fc} is the strain corresponding to f_c, $k=E_{c0}\varepsilon_{fc}/f_c$, E_{c0} is the tangent modulus of elasticity at the origin of the σ-ε diagram, and a conventional plane sections hypothesis are adopted in this work for analysis of concrete elements acted upon by the bending moment, M, and longitudinal load, P, applied at $x=x_p$, using the equilibrium equations

$$b\int_0^d \sigma(\varepsilon)x\,dx = M + Px_p, \quad b\int_0^d \sigma(\varepsilon)\,dx = P. \qquad (2)$$

Here b, d are the width and depth of section, respectively.

1. COMPARISON OF DIAGRAMS IN FIGURE 1

See Figure 2.

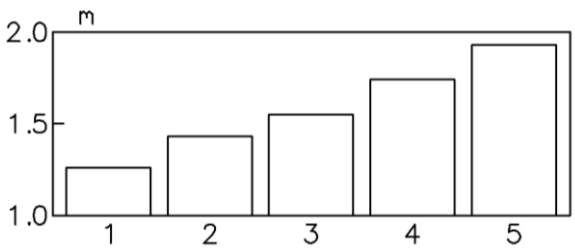


Figure 2. m-ratios for concrete of grade C30 [8] (f_c=2.9MPa , E_{c0}=33.6GPa, ε_{fc}=2.04 f_c/ E_{c0}) according to diagrams in Figure 1.

2. PROPOSED RELATION

The tensile σ-ε relation for concrete is taken in the form similar to that adopted in [9]

$$\sigma = E_{c0}\varepsilon \;\; if \;\; \varepsilon \le \varepsilon_{ft} = f_t / E_{c0},$$
$$\sigma = f_t \frac{\gamma(\varepsilon/\varepsilon_{ft})}{1 + (\gamma-1)(\varepsilon/\varepsilon_{ft})^{\gamma/(\gamma-1)}} \quad if \;\; \varepsilon > \varepsilon_{ft}. \qquad (3)$$

Here $\gamma=\gamma_{15}$ is a parameter indicating steepness of the descending branch of the diagram (see Figure 3) and obtainable, as a function of the m-ratio, from a graph in Figure 4.

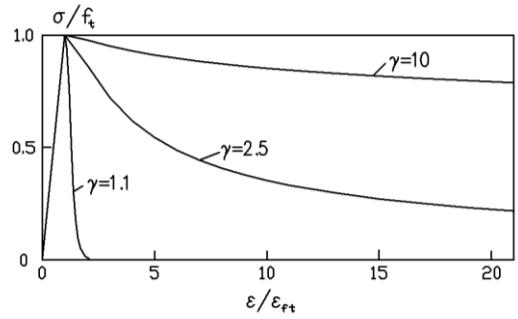


Figure 3. Proposed diagram depending on γ.

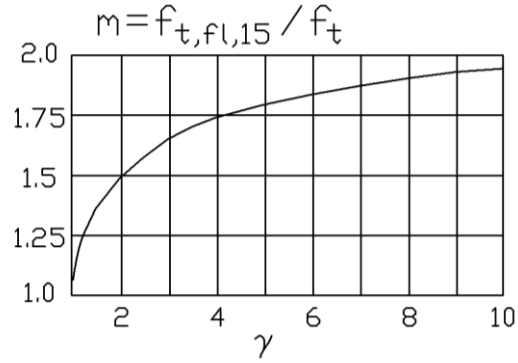


Figure 4. m versus $\gamma=\gamma_{15}$.

In absence of experimental values of $f_{t,fl,15}$ and f_t, this ratio can be assessed as follows

$$m = 2.17 - 0.02 f_c[MPa] \quad for \; f_c \le 25.5MPa,$$
$$m = 1.66 \;\; for \; f_c > 25.5MPa. \qquad (4)$$

See Figure 5.

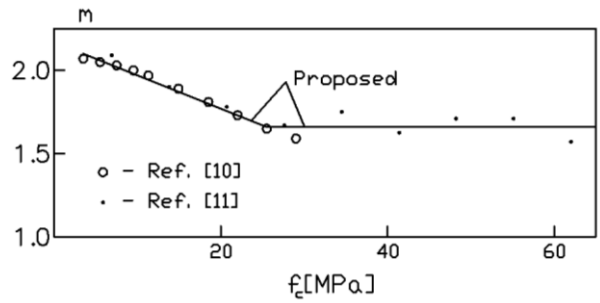


Figure 5. m versus f_c.

Values of $f_{t,fl,15}$ and m for standard concrete beams tested with the third-point loading are lower than the corresponding values, $f_{t,fl,15}^{CP}$ and m^{CP}, for identical beams tested with the center-point loading. According to [11], $m = m^{CP}/1.09$.

3. EXAMPLE

In tests [12], shown schematically in Figure 6,

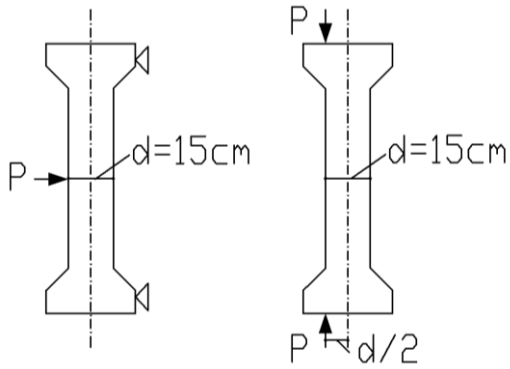


Figure 6. Schemes of tests [12].

the following data have been obtained: f_{cube}=350*kgf/cm*^{2}, f_t=15.2*kgf/cm*^{2}, m^{CP}=1.9, $P_{ult}^{\exp} = 3.19P_0$, where $P_0 = f_t bd$. Here $P_{ult}^{\exp}$ is the mean experimental value of ultimate loads for eccentrically loaded plain concrete specimens. From the graph in Figure 4, $\gamma = 4.0$ for $m = m^{CP}/1.09 = 1.74$. $f_c \approx 0.8\ f_{cube}$, $k \approx 2.1$. The calculated ultimate load $P_{ult}^{num} = 3.08P_0$ deviates from $P_{ult}^{\exp}$ by 3.4%. Note that shrinkage of the concrete in the considered tests [12] was prevented.

4. PROPOSED RELATION: EXTENDED VERSION

When the concrete shrinkage is prevented, f_t is practically independent of the specimen's cross-sectional dimensions. See Appendix and Ref. [12]. Unlike f_t, the concrete flexural tensile strength $f_{t,fl} = 6M_{ult}/(bd^2)$, where M_{ult} is the ultimate bending moment for a plain concrete beam of rectangular ($b \times d$) section, depends essentially on d. In order to reflect this size effect, parameter γ in the proposed relation is taken as a function of d

$$\gamma = \gamma_{15}\ if\ 10 \le d \le 20cm,$$
$$\gamma = \max[1.01; 1 + (\gamma_{15} - 1)0.1^{\alpha}]\ if\ d > 20cm, \quad (5)$$

where α=(*d*[*cm*]-20)/30. See Figure 7.

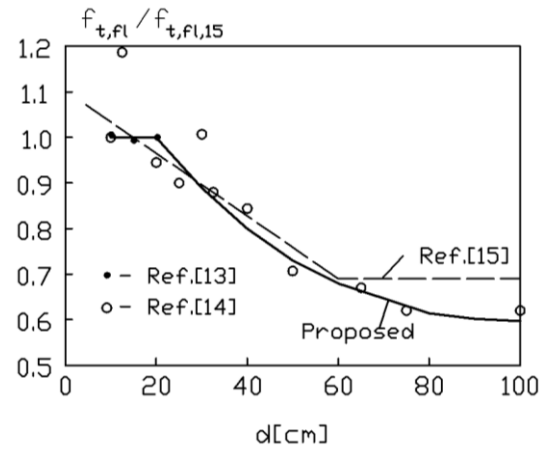


Figure 7. $f_{t,fl}/f_{t,fl,15}$ versus d.

5. DISCUSSION

Irrespective of the cross-sectional dimensions, the behavior of concrete in uniform tension is similar to that in flexural tension when $d \to \infty$. Therefore, the shape of the tensile σ-ε diagram depends on the stress gradient. In the proposed simplified relation, intended for analyses of bending elements, this dependence is taken into account implicitly.

CONCLUSIONS

1. A new σ-ε relation for tensile concrete is proposed.
2. The proposed relation models ductile and brittle modes of the concrete behavior in shallow and deep bending elements, respectively.
3. Based on tests of relatively small laboratory specimens, empirical formulas, like that in Ref. [16] for reinforced concrete beams' deflections, may be unsafe in application to large elements.

APPENDIX

Figure 8 presents the averaged data obtained in direct tension tests [17] on concrete specimens with dimensions of the working parts 10x10x30, 20x20x70 and 50x50x110 cm. In series 1 of the tests, the specimens were sealed in order to prevent shrinkage of the concrete. In series 2, the specimens were not sealed. It is seen that sealing the specimens reduces the size effect to the level predicted by the "weakest link" theory (e.g. [18])

$$\frac{f_t(L)}{f_t(L_0)} = 1 - v\sqrt{\ln(\frac{L}{L_0})}, \qquad (6)$$

where $f_t(L)$ is the strength of specimen of length L, L_0=30cm, v is the variability of $f_t(L_0)$ assumed to be in the interval (0.05, 0.1).

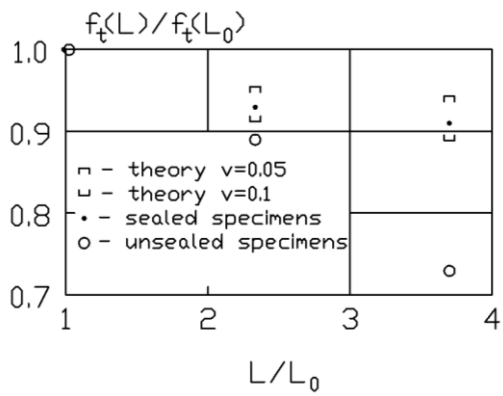


Figure 8. $f_t(L)/f_t(L_0)$ versus L/L_0.

It can be concluded, therefore, that – when shrinkage of the concrete is prevented – f_t depends moderately on L, but is practically independent of the cross-sectional dimensions.

REFERENCES

1. **Dere Y., Koroglu M.A.** Nonlinear FE Modeling of Reinforced Concrete. // *International Journal of Structural and Civil Engineering Research*, 2017, Volume 6, No. 1, pp. 71-74.
2. **Hsu T.T., Zhang S.J.** Tension Stiffening in Reinforced Concrete Membrane Elements. // *ACI Structural Journal*, 1996, Volume 93, No. 1, pp. 108-115.
3. **Bentz E.C., Veccio F.J., Collins M.P.** Simplified Modified Compression Field Theory for Calculating Shear Strength of Reinforced Concrete Elements. // *ACI Structural Journal*, 2006, Volume 103, No. 4, pp. 614-624.
4. **Fields K., Bischoff P.** Tension-Stiffening and Cracking of High-Strength Reinforced Concrete Tension Members. // *ACI Structural Journal*, 2014, Volume 101, No.4, pp. 447-456.
5. **Stramandinoli R.S.B., Rovere H.L.** An Efficient Tension-Stiffening Model for Nonlinear Analysis of Reinforced Concrete Members. // *Engineering Structures*, 2008, Volume 30, No.7, pp. 2069-2080.
6. **Reinhardt H.W.** Factors Influencing the Tensile Properties of Concrete. In "Understanding the Tensile Properties of Concrete", Ed. J. Weerheim, Oxford, 2013, pp. 19-51.
7. **Zak M.L.** On Modeling of Concrete Behavior in Post-Peak Range of Deformation. In "The Optimization of the Composition, Structure and Properties of Metals, Oxides, Composites, Nano- and Amorphous Materials", Proc. of the Sixteenth Bi-National Workshop Russia-

Israel, Ariel University, Ariel, 28-31 August 2017, pp. 237-246.
8. Model Code 2010. Final Draft. Vol. 1. fib Bull. No. 65, 2012, 311 pages.
9. **Prakhya G.K.V., Morley C.T.** Tension-Stiffening and Moment-Curvature Relations of Reinforced Concrete Elements. // ACI Structural Journal, 1990, Volume 87, No.5, pp. 597-605.
10. ACI Committee 224. Cracking of Concrete in Direct Tension, 1997, 12 pages.
11. **Heilmann H.G.** Beziehungen zwischen Zug- und Druckfestigkeit de Betons. // *Beton*, 1969, No. 2, pp. 68-70.
12. **Mal'cov K.A.** Fizicheskoe znachenie predela prochnosti betona na razryv pri izgibe [Physical Significance of Flexural Tensile Strength of Concrete]. // *Beton i Zhelezobeton*, 1958, No. 3, pp. 107-111 (in Russian).
13. **Nielsen K.E.C.** Effect of Various Factors on the Flexural Strength of Concrete Test Beams. // *Magazine of Concrete Research*, 1954, No. 3, pp. 105-114.
14. **Mal'cov K., Karavaev A.** "Abhangigkeit der Festigkeit des Betons auf Zug bei Biegung und aussmittiger Belastung von den Querschnittsabmessungen", Wiss. Z. Univers. Dresden, Vol. 17, H. 6, 1968, pp. 1545-1547.
15. Eurocode 2: Design of Concrete Structures – Part 1-1: General Rules and Rules for Buildings, Brussels, 2014, 225 pages.
16. ACI Committee 318. Building Code Requirements for Structural Concrete (ACI 318-14) and Commentary (ACI 318R-14), American Concrete Institute, Farmington Hills, MI, 2014, 503 pages.
17. **Vorob'eva V.I., Simakov G.K., Sudakov V.B.** Masshtabnyj faktor pri ispytanii obrazcov na osevoe rastjazhenie [Scale Factor in Direct Tensile Tests]. In "Effect of Concrete Properties on Its Cracking Strength". Works of Coordination Meetings on Hydraulic Structures, 1976, No. 112, Leningrad, pp. 154-161 (in Russian).
18. Bolotin V.V. Statistical Methods in Structural Mechanics. Holden-Day, 1969, 240 pp.

СПИСОК ЛИТЕРАТУРЫ

1. **Dere Y., Koroglu M.A.** Nonlinear FE Modeling of Reinforced Concrete. // *International Journal of Structural and Civil Engineering Research*, 2017, Volume 6, No. 1, pp. 71-74.
2. **Hsu T.T., Zhang S.J.** Tension Stiffening in Reinforced Concrete Membrane Elements. // *ACI Structural Journal*, 1996, Volume 93, No. 1, pp. 108-115.
3. **Bentz E.C., Veccio F.J., Collins M.P.** Simplified Modified Compression Field Theory for Calculating Shear Strength of Reinforced Concrete Elements. // *ACI Structural Journal*, 2006, Volume 103, No. 4, pp. 614-624.
4. **Fields K., Bischoff P.** Tension-Stiffening and Cracking of High-Strength Reinforced Concrete Tension Members. // *ACI Structural Journal*, 2014, Volume 101, No.4, pp. 447-456.
5. **Stramandinoli R.S.B., Rovere H.L.** An Efficient Tension-Stiffening Model for Nonlinear Analysis of Reinforced Concrete Members. // *Engineering Structures*, 2008, Volume 30, No.7, pp. 2069-2080.
6. **Reinhardt H.W.** Factors Influencing the Tensile Properties of Concrete. In "Understanding the Tensile Properties of Concrete", Ed. J. Weerheim, Oxford, 2013, pp. 19-51.
7. **Zak M.L.** On Modeling of Concrete Behavior in Post-Peak Range of Deformation. In "The Optimization of the Composition, Structure and Properties of Metals, Oxides, Composites, Nano- and Amorphous Materials", Proc. of the Sixteenth Bi-National Workshop Russia-Israel, Ariel University, Ariel, 28-31 August 2017, pp. 237-246.

8. Model Code 2010. Final Draft. Vol. 1. fib Bull. No. 65, 2012, 311 pages.
9. **Prakhya G.K.V., Morley C.T.** Tension-Stiffening and Moment-Curvature Relations of Reinforced Concrete Elements. // ACI Structural Journal, 1990, Volume 87, No.5, pp. 597-605.
10. ACI Committee 224. Cracking of Concrete in Direct Tension, 1997, 12 pages.
11. **Heilmann H.G.** Beziehungen zwischen Zug- und Druckfestigkeit de Betons. // *Beton*, 1969, No. 2, pp. 68-70.
12. **Мальков К.А.** Физическое значение предела прочности бетона на разрыв при изгибе. // *Бетон и железобетон*, №3, 1958, с. 107-111.
13. **Nielsen K.E.C.** Effect of Various Factors on the Flexural Strength of Concrete Test Beams. // *Magazine of Concrete Research*, 1954, No. 3, pp. 105-114.
14. **Mal'cov K., Karavaev A.** "Abhangigkeit der Festigkeit des Betons auf Zug bei Biegung und aussmittiger Belastung von den Querschnittsabmessungen", Wiss. Z. Univers. Dresden, Vol. 17, H. 6, 1968, pp. 1545-1547.
15. Eurocode 2: Design of Concrete Structures – Part 1-1: General Rules and Rules for Buildings, Brussels, 2014, 225 pages.
16. ACI Committee 318. Building Code Requirements for Structural Concrete (ACI 318-14) and Commentary (ACI 318R-14), American Concrete Institute, Farmington Hills, MI, 2014, 503 pages.
17. **Воробьева В.И., Симаков Г.К., Судаков В.Б.** Масштабный фактор при испытании образцов на осевое растяжение. // Труды координационного совещания по гидротехническим сооружениям, 1976, Выпуск 112, с. 154-157.
18. **Bolotin V.V.** Statistical Methods in Structural Mechanics. Holden-Day, 1969, 240 pages.

Michael L. Zak, PhD, Lecturer, Civil Engineering Department, Ariel University, Ariel 40700, Israel,
E-mail: m.l.zak@012.net.il

Майкл Л. Зак, доктор наук (PhD), Университет Ариэль; Ариэль 40700, Израиль;
E-mail: m.l.zak@012.net.il.

Рецензия

на учебник «Технология возведения высотных, большепролетных зданий и сооружений».

Авторы: А. И. Гныря - заведующий кафедрой «ТСП» ТГАСУ, доктор технических наук, профессор.

А. П. Бояринцев - заслуженный строитель, доцент кафедры «ТСП».

В. И. Теличенко - академик РААСН.

Учебник предназначен для изучения курса «Возведение высотных и большепролетных зданий и сооружений». В соответствии с требованиями государственного образовательного стандарта высшего профессионального образования по направлению подготовки 08.05.01 «Строительство уникальных зданий и сооружений».

Профиль подготовки 08.04.01.24. «Строительство высотных и большепролетных зданий и сооружений».
Квалификация(степень)выпускник – специалист.
Вид профессиональной деятельности выпускника - производственно-технологическая.
Форма обучения – очная.

Учебник состоит из четырех разделов и содержит более 700 страниц.

Раздел первый. Строительные технологии возведения высотных, большепролетных и специальных зданий и сооружений.

Раздел второй. Технология возведения жилых и общественных зданий повышенной этажности.

Раздел третий. Технология возведения многофункциональных высотных зданий.

Раздел четвертый. Технология возведения большепролетных и специальных зданий и сооружений.

В первый раздел «Строительные технологии возведения высотных, большепролетных и специальных зданий и сооружений» входит:

Глава 1. Организационно-техническая подготовка строительства высотных, большепролетных и специальных зданий и сооружений.

Данная глава содержит: классификацию промышленных, гражданских и жилых зданий по конструктивным решениям и особенностям технологии строительно-монтажных работ. Технологическое проектирование, где рассматриваются вопросы содержания организационно-технической документации, принципы возведения высотных зданий, календарное и сетевое планирование и проект производства работ.

Глава 2. Инженерная подготовка строительной площадки возведения высотных, большепролетных и специальных зданий и сооружений.

Благоустройство, организация поверхностного стока, водоотвод и водопонижение. Разработка выемок, снос существующих зданий и сооружений, вертикальная планировка. Земляные работы в особых условиях, взрывные работы, свайные фундаменты, шпунтовые ограждения и анкеры. Устройство водонепроницаемых преград в ограждениях котлованов. Возведение подземных частей высотных зданий и защита их от агрессивных воздействий.

Глава 3. Система мониторинга высотных, большепролетных и специальных зданий и сооружений.

В данной главе рассматриваются вопросы: геодезическое обеспечение строительства, проект производства геодезических работ (ППРГ). Научно-техническое сопровождение и мониторинг высотных зданий на стадии строительства. Инструментальные обследования конструкций и грунтов оснований и сейсмометрический мониторинг.

Во второй раздел «Технология возведения жилых и общественных зданий повышенной этажности» входит:

Глава 4. Строительно-конструктивные системы многоэтажных жилых и общественных зданий.

Строительно-конструктивные системы жилых зданий и их элементы (крупнопанельные системы, каркасно-сборные и сборно-монолитные системы, блочные системы, конструктивные системы жилых зданий из монолитного железобетона, жилые здания из кирпича и керамических камней, системы навесных ограждающих конструкций). Отечественный опыт строительства многоэтажных жилых домов и общественных зданий.

Глава 5. Технология возведения жилых и общественных зданий повышенной этажности со сборно-монолитным каркасом.

Особенности технологии производства работ. Возведение сборных и монолитных железобетонных колон и диафрагм жесткости. Технология опалубочных, арматурных и бетонных работ. Бетонирование монолитных конструкций при отрицательных температурах. Технология возведения наиболее распространённых сборно-монолитных конструктивных систем (система «КУБ - каркас универсальный безбалочный», каркас системы «АРКОС», каркас системы «РЕКОН»).

Глава 6. Технология возведения жилых и общественных зданий повышенной этажности с монолитным железобетонным каркасом.

В этой главе рассмотрены: опалубочные работы (особенности технологического проектирования опалубочных работ, устройство опалубки для монолитных колон, перекрытий, возведение стен, лифтовых шахт, лестничных маршей, балконов и лоджий), арматурные, бетонные работы. Технология производства монолитных

конструкций при отрицательных температурах, режимы телеобработки и обеспечение набора прочности. Распалубка монолитных конструкций.

В третий раздел «Технология возведения многофункциональных высотных зданий» входит:

Глава 7. Конструктивное решение высотных зданий.

Общие сведения о высотных зданиях. Конструктивное решение высотных зданий. Конструктивные решения фундаментов. Конструктивные особенности и схемы надземных частей высотных зданий. Несущие конструкции высотных зданий.

Глава 8. Организация технологии строительства многофункциональных высотных комплексов.

Технологические особенности возведения высотных зданий. Средства механизации и строительное оборудование при возведении высотных зданий. Технологические особенности работы нулевого цикла. Технология возведения надземной части здания (технология производства бетонных работ, опалубочных работ, устройство сталежелезобетонных конструкций между этажных перекрытий, возведение наружных стен, устройство навесных фасадных систем, подъёмно-транспортное и вспомогательное оборудование для высотного строительства). Методы строительства подземных и заглубленных сооружений (строительство подземных сооружений открытым методом, «островной» метод строительства, декельный метод возведения высотных зданий, комбинированный метод разработки грунта, возведение междуэтажных перекрытий, возведение ядер жесткости заглубленной части, возведение надземной части).

В четвертый раздел «Технология возведения большепролетных и специальных зданий и сооружений» входит:

Глава 9. Технология возведения большепролетных зданий и сооружений.

Классификация большепролетных конструкций и методы их монтажа. Технология монтажа балочных покрытий, покрытий зданий рамных конструкций и арочных покрытий. Монтаж структурных плит, оболочек и куполов. Возведение большепролетных зданий и сооружений. Монтаж шатровых покрытий, тентовых покрытий.

Глава 10. Технология возведения специальных зданий и сооружений.

Технология возведения подземных и заглубленных сооружений, башенно-мачтовых сооружений, промышленных дымовых труб. Технология монтажа буровых вышек, платформ, градирен и водонапорных башен. Возведение металлических резервуаров, газгольдеров и сооружений для хранения сыпучих веществ.

К учебнику даны приложения:

1. Методика расчета параметров ранней распалубки перекрытия.

2. Технология возведения подземной части «Лахта центра».

3.Бетоносмесительные узлы, бетононасосы и распределительные стрелы.

4. Характеристики специальных опалубочных систем.

5. Подъёмники.

6. Технология предварительного напряжения монолитного железобетона.

7. Технология монтажа арочного покрытия ледового дворца « Уфа- Арена».

8. Технология монтажа купольного покрытия цирка в г. Москве.

9. Технология монтажа вантового покрытия спортивно - развлекательного комплекса «Минск - Арена» в г. Минск.

10. Возведение мембранного покрытия пролетом 228м. Олимпийского стадиона в г. Москве.

11. Монтаж пространственного покрытия спортивного зала «Дружба» г. Москва.

ЗАКЛЮЧЕНИЕ

Авторский коллектив проделал большую работу при подготовке учебника, состоящего из четырех разделов и содержащего более 700 страниц. Учебник предназначен для изучения курса «Возведение высотных и большепролетных зданий и сооружений.» В соответствии с требованиями государственного образовательного стандарта высшего профессионального образования по направлению подготовки 08.05.01 «Строительство уникальных зданий и сооружений»

Учебник, представленный на рецензирование, так же будет способствовать углублению и расширению знаний, лучшему усвоению магистрантами и аспирантами теоретического материала по специальности 05.23.08 «Технология и организация строительства»

Учебник будет полезен бакалаврам и выпускникам специалистам по профилю подготовки 08.04.01.24. «Строительство высотных и большепролетных зданий и сооружений» при проведении научно-исследовательской работы.

Считаю, что учебник подготовленный А.И. Гныря, А.П. Бояринцев, В.И. Теличенко «Технология возведения высотных, большепролетных зданий и сооружений» может быть рекомендован к опубликованию

Академик РААСН В. И. Травуш